NASA SP-113

# DYNAMIC STABILITY OF ROTOR-BEARING SYSTEMS



GUNTER




NATIONAL AERONAUTICS AND SPACE ADMINISTRATION

NASA SP-113

# DYNAMIC STABILITY OF ROTOR-BEARING SYSTEMS

**Edgar J. Gunter, Jr.**

**Department of Mechanical Engineering**
**University of Virginia**

Prepared under contract
for Lewis Research Center
Cleveland, Ohio
by The Franklin Institute Research Laboratories
Philadelphia, Pennsylvania


*Scientific and Technical Information Division*
OFFICE OF TECHNOLOGY UTILIZATION 1966
NATIONAL AERONAUTICS AND SPACE ADMINISTRATION
*Washington, D.C.*

For Sale by the Superintendent of Documents
U.S. Government Printing Office, Washington, D.C. 20402
**Price $1.00**
*Library of Congress Catalog Card Number 66–60091*

# Contents

# Preface

The objective of this investigation has been to examine in general the conditions which can lead to nonsynchronous precession in a rotor system. Nonsynchronous precession, which has often been referred to as shaft whirling, oil film whirl, resonance whip, half-frequency whirl, is a self-excited motion which can be caused by several factors such as internal rotor friction and fluid film bearings. In the analysis, general equations of motion of the extended Jeffcott rotor are developed to include rotor and foundation flexibility, internal and external damping, rotor and bearing mass, and fluid film bearings. The rotor threshold of stability is determined for the system by Routh's criterion. The various stability charts developed in the thesis reveal that a considerable improvement in the rotor stability characteristics can be obtained by proper foundation design.

To represent the rotor motion above and below the threshold of stability, the equations of motion were programed on the analog computer and traces of the rotor orbits were obtained for a number of runs. The theoretical results were compared to various experimental observations on rotor whirl.

Chapter 1 contains the introduction and description of the system. Chapter 2 discusses the background and state of the art in rotor dynamics as related to rotor stability. Some of the major contributions of Jeffcott, Newkirk, Hagg, Poritsky, Pinkus, and others are discussed.

Chapter 3 presents an analysis of the single-mass Jeffcott rotor considered as a conservative and nonconservative system. The results are compared to the analysis of Kane on rotor whirling and also to the work of Soderberg on secondary critical speeds. Chapter 3 shows that even light damping forces can considerably alter the motion of the system and shows also that the problem of nonsynchronous rotor whirling cannot be analyzed from the standpoint of a conservative system.

In Chapter 4 the general equations of motion of the extended Jeffcott rotor are developed to include rotor and foundation flexibility, foundation damping, internal and external rotor damping, bearing mass and rotor unbalance. Chapter 4 discusses and explains some of the early work by Newkirk on rotor instability in 1924. The results of Chapter 4 are also compared to the experimental findings of Kushul' on instability caused by internal rotor friction.

Chapter 5 discusses in general the conditions required for stability in linear system. The hydrodynamic fluid film characteristics for small displacements are related to the general stability criterion. The influence of lubricant compressibility and nonlinear bearing forces on stability are also discussed.

Chapter 6 presents an analysis of the extended Jeffcott model to include fluid film bearing characteristics. Chapter 6 shows that the one-dimensional planar analysis approach for critical speeds is inadequate.

Chapter 7 contains a discussion of the major assumptions and conclusions of the investigation.

This is a report of research performed under Contract NAS 3–6473, administered by Lewis Research Center.

# Chapter 1

# Introduction and Statement of the Problem

## 1.1 INTRODUCTION

With the increase in performance of high-speed rotating machinery in various fields such as process equipment, auxiliary power machinery, and space applications, the engineer is faced with the problem of designing a unit capable of smooth operation under various conditions of speed and load. As an example, turborotors in the auxiliary power systems of space applications must be designed to perform satisfactorily under adverse load conditions ranging from the high acceleration forces encountered at takeoff to the zero-gravity load condition encountered in orbit. In many of these applications the design operating range may be well above the rotor first critical speed.[1] Under these circumstances the problem of insuring that a turbomachine will perform with a stable, low-level amplitude of vibration is extremely difficult.

Under certain conditions of high speed and light loading, a situation can arise in which the rotor system is capable of orbiting or precessing in its bearings at a rate less than the total rotor angular speed. This nonsynchronous precessive motion, which has often been referred to in the literature as whirling or whipping, can lead to destruction of the rotor if the whirl threshold speed is exceeded.[2] This whirl motion is considerably unlike the orbiting obtained at a rotor critical speed. If the rotor damping and balancing requirements are met, it is possible to safely pass through a rotor critical speed,[3] whereas the occurrence of nonsynchronous precession will limit the operating speed of a rotor.

Nonsynchronous rotor precession is a self-induced vibration[4] and has sometimes been described as "sustained transient motion." In general, a self-excited or self-induced vibration is defined as a phenomenon in

[1] See Secs. 2.3 and 3.21 for discussion and definition of rotor critical speed.

[2] Fig. 44 of Ch. 5 is an illustration of rotor behavior below and above the whirl threshold speed. A further increase in speed above the threshold would lead to bearing failure.

[3] See Fig. 5.

[4] See J. G. Baker, "Self-Induced Vibrations," *Trans. ASME*, Vol. 55, pp. 5–13.

which the excitation forces inducing the vibration are controlled by the motion. This is in contrast to a forced vibration in which the external excitation is a function of time only. There are several very common examples of vibration which may be considered under the classification of self-excited motion. Some of these are:

1. Aerodynamic wing flutter.
2. Vibration of transmission lines.
3. Sway or nosing of streetcars and locomotives.
4. String or blown musical instruments.
5. Pneumatic hammer of valves in air or water lines.
6. Vacuum tube oscillations.

With respect to the last item, the instances of self-excited motion are of greater familiarity to the electrical engineer; hence the subject has received considerable attention in that field. In the field of mechanical engineering, particularly with respect to rotating machinery or mechanical vibrations, the phenomenon has received less attention. As an example, the excitation forces usually associated with rotating machinery are alternating and impulse forces such as caused by unbalance and shock. These force systems are expressed as explicit functions of time and are unaltered by the mode of vibration of the system.

Examination of Eqs. (2.5) and (2.6), which apply to an unbalanced flexible rotor with a single mass, reveals that as the unbalance is reduced ($\epsilon \rightarrow 0$), the rotor deflection will approach zero and hence the forces transmitted to the bearings will be zero. Thus, by properly balancing a rotor, it is possible to run through the first critical speed with little noticeable change in the rotor amplitudes. For large turbines, where good balancing can be achieved, this has been observed. In some instances it was found necessary to add additional unbalance in order to excite the critical speeds.

With a self-excited whirl instability, unbalance is of minor importance. (It will, however, affect the whirl threshold speed by changing the dynamic loads exerted on the bearings and hence the bearing characteristics.) At the onset of whirl, the rotor behavior is unlike a critical speed resonance where the amplitude of motion builds up to a maximum value and then decreases. At the inception of nonsynchronous whirling, the rotor motion will continually build up with speed, since the self-excitation increases the energy transfer into the system with increased speed. If the rotor speed is increased appreciably above the whirl threshold speed, the large orbiting obtained will usually result in rotor or bearing failure. Thus, the problem of maintaining smooth rotor performance and satisfactory operation can be of a much more serious nature when encountering self-excited whirling than with a critical speed resonance.

Rotor whirling can be caused by several mechanisms such as hydrodynamic fluid film bearings, internal rotor friction, magnetic fields, and

turbine torques. The most common case of self-excited whirling is that caused by the fluid film bearings. Bearing specialists have given various titles to this phenomenon such as half-frequency whirl, oil-film whirl, resonant whip, or oil whip. The instability caused by internal friction damping or rotary damping is very similar in nature to that caused by the oil-film bearings.[5] This phenomenon has been variously labeled as "shaft whirling" or "whip." The instabilities caused by each of the above cases occur at speeds only above first-system resonance frequency. Therefore, we shall consider a high-speed rotor as one which operates above the first critical speed.

Dr. Newkirk in 1924 was the first person to demonstrate that nonsynchronous, unstable motion could exist in a high-speed rotor. (For a more detailed discussion on the work of Dr. Newkirk and other investigators, see Ch. 2.) His methods used to observe the rotor motion were crude, since at that time electronic capacitance or inductance probes were not available. Today considerable interest has developed in the field of high-speed rotor systems. This is due not only to higher unit speeds but also to better electronic instrumentation which allows the researcher to observe the actual rotor behavior. For example, the rotor oscilloscope trace of Fig. 47 shows that at 19 000 rpm, a component of self-excited whirling is created in addition to the steady-state synchronous orbit. The resulting whirl orbit may be viewed as the combination of the two rotating vectorial components. The occurrence of this typical oscilloscope pattern is an indication that the whirl threshold speed has been reached. If the speed were increased much above this instability threshold, rotor destruction would have resulted.

The above discussion serves to illustrate some of the fundamental differences between stable and unstable rotor motion. It also points out several mechanisms which can cause unstable motion. The designer is deeply concerned with the problem of rotor stability and also with the closely allied problems of rotor critical speeds and bearing force transmission.

## 1.2 DESCRIPTION OF THE SYSTEM

The usual high-speed rotor may be considered as a continuous elastic body with variable mass and inertia properties along its length as shown in Fig. 1A. The shaft usually has attached to it such components as turbine wheels, impeller disks, etc. If the axial dimension of each rotor component is small in comparison to the overall length of the rotor, then these components may be treated as concentrated masses with a polar moment of inertia equivalent to that of the original component.

---

[5] See Sec. 2.4, *Nonsynchronous Precession—Internal Friction Damping*, of Ch. 2 for further discussion.

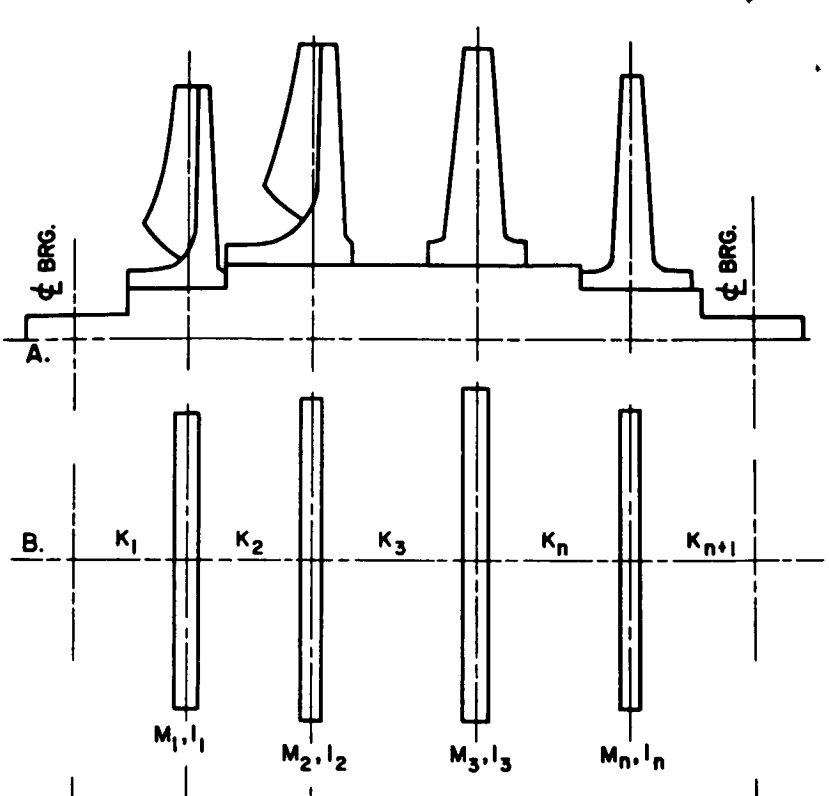


FIGURE 1.—Schematic diagram of a typical turbo rotor.

If, in addition, the mass of the attachment is large in comparison to the shaft mass between two adjacent stations, then the shaft weight may be considered as also concentrated at the weight stations. The rotor may then be represented as a massless elastic shaft to which is attached $n$-mass stations as shown in Fig. 1B. If the polar moment of inertia of each section is ignored, then the stations may be considered as concentrated masses (Fig. 1C), rather than as masses distributed in the plane of the rotor element perpendicular to the shaft axis of rotation.

Figure 2 represents a typical cross section of the idealized rotor taken at the $n$th mass station. The position vector of the $n$th mass center is given by

$$\vec{P}_n = \vec{\delta_b} + \vec{\delta_j} + \vec{\delta_r^{(n)}} + \vec{e^{(n)}}$$

where

$\vec{\delta_b}$ = vectorial foundation or bearing housing deflection

$\vec{\delta_j}$ = vectorial journal deflection

$\vec{\delta_r^{(n)}}$ = vectorial rotor deflection at the $n$th station

$\vec{e^{(n)}}$ = displacement vector of the mass center from the rotor elastic center

The total angular velocity of the system is given by the time rate of change of a line fixed in the disk and will be represented by $\omega$. By examination of the configuration of Fig. 2, the following definitions of whirl ratio may be stated:

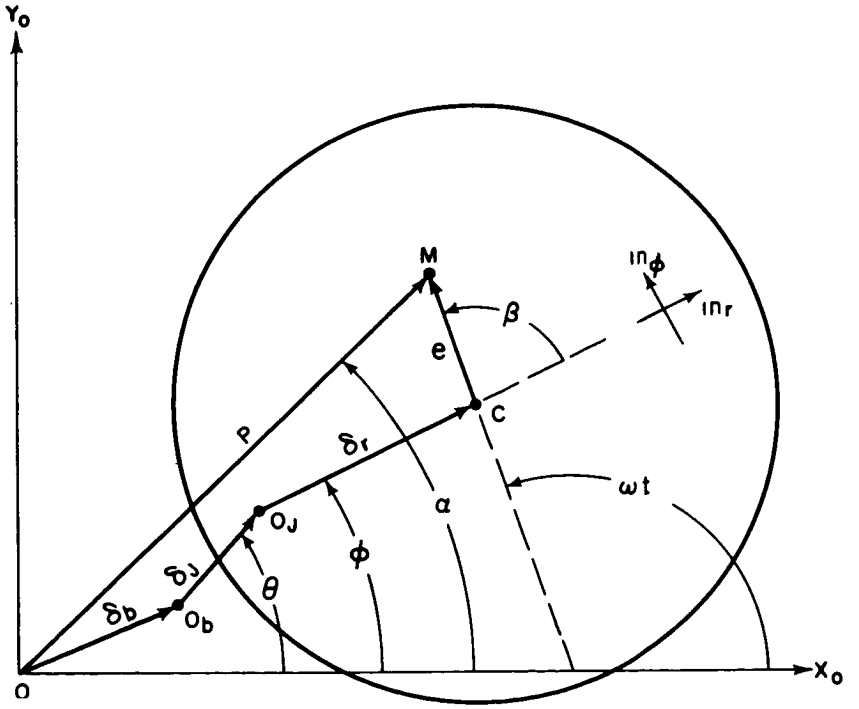


FIGURE 2.—Vectorial representation of a cross section of a deflected rotor.

$\dot{\phi}/\omega$ = shaft whirl or "whip" ratio

$\frac{\dot{\theta}}{\omega}$ = journal whirl ratio

$\frac{\dot{\alpha}}{\omega}$ = system whirl or precession ratio.

For the case of steady-state synchronous precession investigated by Tang and Trumpler,[102] the configuration formed by $O$, $O_b$, $O_j$, $C$, $M$ is constant and precesses with an angular velocity equal to the rotor angular velocity $\omega$.

## 1.3 STATEMENT OF THE PROBLEM

The problem of the present investigation is to determine under what conditions nonsynchronous precession can develop in a rotor system depicted by Fig. 2 and also to determine the approximate characteristics of the rotor motion.

# Chapter 2

# Background and State of the Art

## BACKGROUND

To illustrate the important areas of investigation that need to be undertaken in this field, a brief summary of the advances of some of the major investigations will be discussed.

### 2.1 INDIFFERENT EQUILIBRIUM

The first recorded article on the subject of rotor dynamics was presented in 1869 by Rankine,[78] who introduced the elementary conception of indifferent rotor equilibrium. Rankine examined the equilibrium conditions of a frictionless, uniform shaft disturbed from its initial position. Because he neglected the influence of the Coriolis force, he concluded that: motion is stable below the first critical speed, is neutral or in "indifferent" equilibrium at the critical speed, and unstable above the critical speed.[1] During the next half century, this analysis led engineers to believe that operation above the first critical speed was impossible. It was not until 1895 that DeLaval demonstrated experimentally that a steam turbine was capable of sustained operation above first critical speed. Investigators remained at a loss to explain why they were able to achieve high-speed operation in certain cases. Rotating equipment manufacturers were unable to explain why successful operation could be attained with some units but not with others of similar construction.

With the advent of the steam turbine in the last century and the gradual transition from low-speed reciprocating powerplants to higher speed rotary-type units, it soon became apparent to manufacturers that an understanding of the dynamic behavior of these systems was necessary to insure satisfactory rotor performance. As the steam turbine progressed in efficiency around the turn of the century and the design operational speeds were increased, these problems became

[1] The neglect of the Coriolis term has caused several writers to deduce a fictitious critical condition at $1/\sqrt{2}$ times the critical speed.

greatly accentuated. It became much more difficult to design a rotor to run smoothly under all operating conditions.

## 2.2 ROTOR CRITICAL SPEED—NATURAL LATERAL FREQUENCY

To understand why some units would operate successfully while others of similar design would fail, some of the leading scientists of England were engaged to investigate the problem. Starting with the work of Rankine[78] in 1869, the extensive studies by Dunkerley[13] in 1894, and Chree[9] in 1904, it was shown that a rotor has certain speed ranges in which vibrations of large amplitude could develop. These speed ranges, which became known as "critical speeds," could cause the unit to run roughly, transmitting large forces to the bearings and producing large deflections of the rotor. If the running speed of a unit happened to coincide with the rotor critical speed, the large forces transmitted through the bearings quite often caused bearing failure, or the resulting excessive rotor deflections would wipe out the internal labyrinth seals causing rotor failure, or at least a reduction in the unit efficiency due to the increase in internal leakage across the seals.

Dunkerley, who made the major contribution at the time, analyzed the rotor dynamic behavior by considering the rotor as a flexible elastic body and the bearings as simple supports. (During this period, the hydrodynamic theory of lubrication was just beginning to be developed.) By neglecting rotor unbalance and damping, he showed that the problem of a whirling rotor could be replaced by the problem of finding the natural lateral frequencies of vibration of an equivalent beam on simple supports. Under the above assumptions, these natural lateral frequencies would correspond to the rotor critical speeds. He then postulated that if the rotor had any unbalance (which is unavoidable), it would excite these natural frequencies causing high vibrational amplitudes if the operating range should correspond to any of these values. As a result of his investigation, manufacturers attempted to construct their rotors sufficiently stiff so that the first natural lateral frequency of vibration would be sufficiently above the operating range. In this way the unit would operate as a stiff[2] rotor; that is, below the first critical speed. As the design speed of machinery was continually increased to gain economic advantage, it was found that it was difficult to design a rotor with the operating range below the first critical speed. Accomplishing this entailed the construction of heavier rotors which meant larger shaft diameters. This in turn caused higher bearing loads, necessitating an increase in the accuracy of rotor balancing.

[2] A unit that operates below the first critical speed is commonly referred to as a "stiff" rotor, and one that operates above first critical is referred to as a "flexible" rotor. This nomenclature used in past literature has caused some confusion, since an unbalanced rotor will deflect at any speed due to centrifugal forces.

## 2.3 SYNCHRONOUS WHIRLING OF A SINGLE-MASS ROTOR—JEFFCOTT MODEL

In 1919, H. H. Jeffcott,[40] a noted English dynamicist, was asked to engage in the problem of rotor dynamics, in particular to examine the effect of unbalance on the whirl amplitudes and forces transmitted to the bearings. He too, like Dunkerley, neglected the effect of the bearings on the system, but considered a general two-dimensional problem including damping on the rotor. To further explain what is meant by critical speed and as a subsequent introduction to the terminology of "whirl instability," we shall briefly examine Jeffcott's model and his conclusions. Figure 3 represents a flexible rotor composed of a centrally located unbalanced disk attached to a massless elastic shaft. The elastic restoring force acting at $C$ is given by

$$F = \delta K \tag{2.1}$$

where

$K$ = shaft stiffness coefficient
$\delta$ = deflection of the shaft centerline $C$ from the bearing line of centers $O$.

The angular speed $\omega$ of the rotor is assumed to be constant and is represented by the time derivative of angle formed by the line CM fixed in the disk with respect to the fixed reference axis OX. At this point no assumption can be made concerning the angular speed of the rotor centerline OC. Jeffcott arrived at the conclusion that the center of the rotor also revolves or precesses at the same angular velocity as the disk. That is, for a particular speed, the rotor center moves at a constant angular velocity $\omega$, describing a circle of radius $\delta$. This condition of the rotor centerline moving with the same angular speed as the mass center is defined as "synchronous precession."

From the examination of this simple model, we are now in a position to define "whirling" in general. It is defined as the angular velocity of the rotor center, or the time derivative of angle $\phi$. The whirl ratio will be defined as the ratio of $\dot{\phi}$ to the total angular speed of the rotor $\omega$. We will refer to nonsynchronous precession as the condition when $\dot{\phi} \neq \omega$. With the assumptions that Jeffcott used, it is not possible to arrive at a steady-state condition where $\dot{\phi} \neq \omega$; that is, synchronous precession is the only possible solution. He did point out, however, the important conclusion that the position of the mass center is not stationary with respect to the rotating reference frame $R$, but is dependent upon

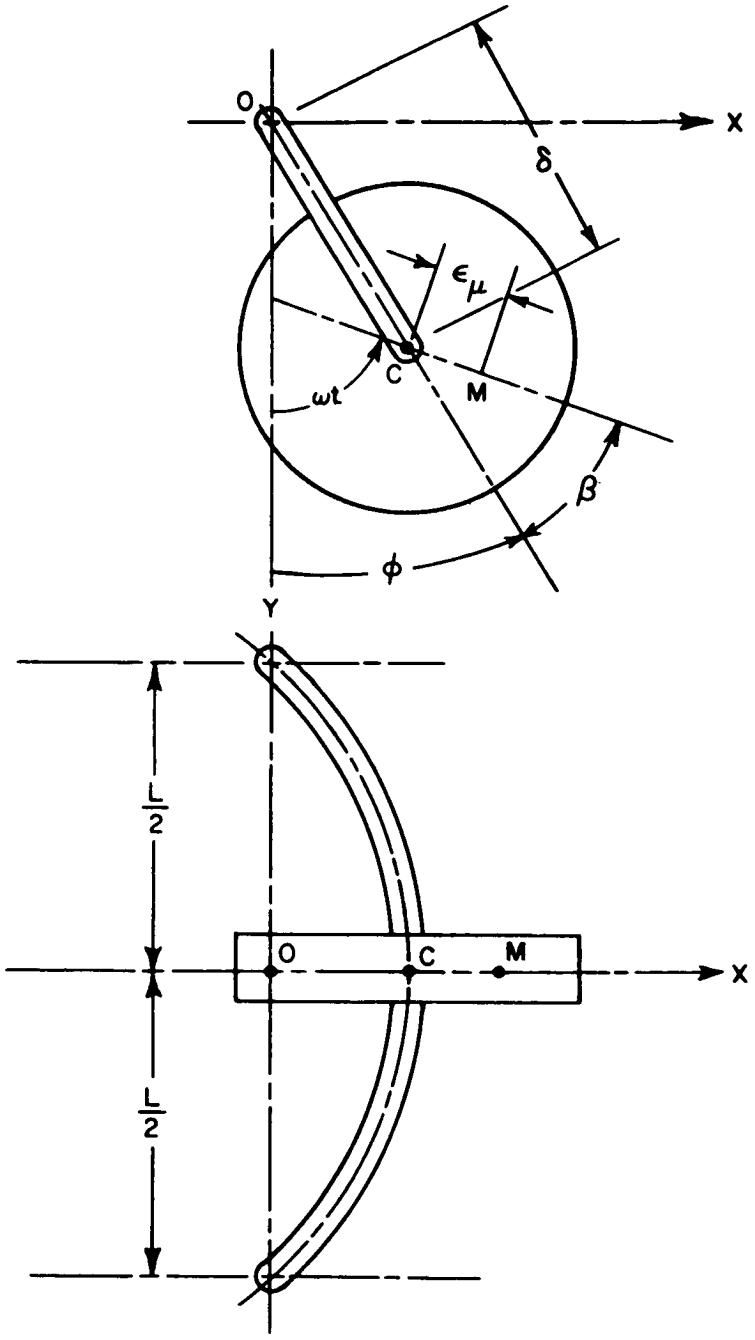


FIGURE 3. – Single-mass flexible rotor.

the ratio of rotor critical speed and the damping on the rotor. This phase angle relationship is given by (see Sec. 3.21).

$$\beta = \tan^{-1}\left[\frac{\frac{C}{M\omega}}{\left(\frac{\omega_{CR}}{\omega}\right)^2 - 1}\right] \tag{2.2}$$

where

$\beta$ = phase angle, degrees
$M$ = rotor mass, lb-sec$^2$/in.
$\omega$ = angular speed of rotor rad/sec
$\omega_{CR}$ = rotor critical speed = $\sqrt{K/M}$, rad/sec
$C$ = damping coefficient, lb-sec/in

Upon the examination of the phase relationship equation for various speeds, we can arrive at three important limiting conditions (see Fig. 4):

First,

$$\omega \ll \omega_{CR} \qquad \beta \to 0$$

The mass center is in phase with and rotates about the rotor centerline.

Second,

$$\omega = \omega_{CR} \qquad \beta = \frac{\pi}{2}$$

The mass center is leading the rotor centerline.

Third,

$$\omega \gg \omega_{CR} \qquad \beta \to \pi$$

The mass center is 180° out of phase with the rotor center and the point C rotates about the mass center.

If we examine the steady-state radial forces acting on the shaft elastic centerline at point C, that is, equate the centrifugal forces to the elastic restraining forces (neglecting damping), we arrive at the following equation

$$M\omega^2(\delta + e_\mu \cos \beta) = K\delta \tag{2.3}$$

where $e_\mu$ = displacement of rotor mass center from shaft elastic centerline (see fig. 4). At the critical speed, when $\omega = \omega_{CR}$, then $\beta = \pi/2$ and the above equation reduces to

$$M\omega_{CR}^2\delta = K\delta \tag{2.4}$$

From the above equation, we arrive at the conclusion that at $\omega = \omega_{CR}$, the deflection of the rotor centerline is indeterminate, or that for any given value of deflection $\delta$, the elastic restoring forces will exactly bal-

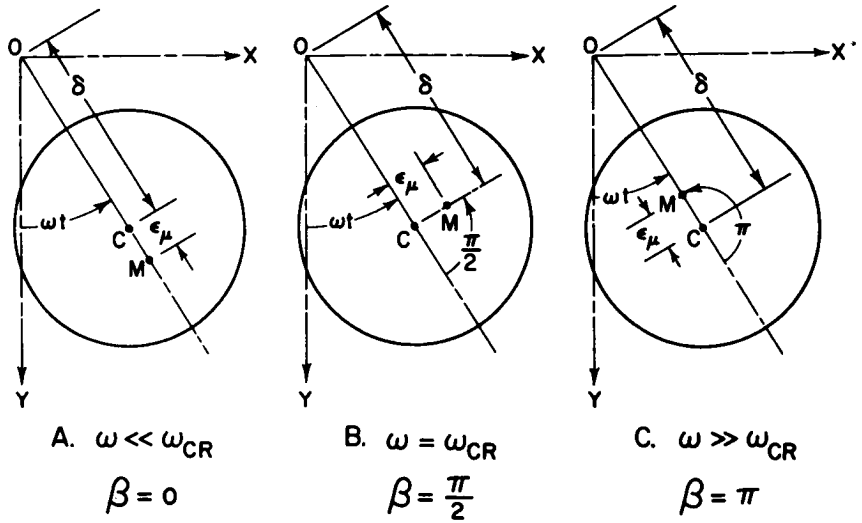


FIGURE 4.—Phase relationships.

ance the centrifugal forces. This had led to the concept of "indifferent equilibrium" for the calculation of rotor critical speeds. This concept is equivalent to Dunkerley's original postulation that the rotor critical speeds are exactly equal to the natural lateral frequencies of vibration. Since, in the physical system, damping is always present, the deflection $\delta$ and thus the forces transmitted to the bearings remain bounded. Hence the concept of "indifferent equilibrium" yields the correct value of the critical speed only for the limiting condition when the rotor damping approaches a very small value (see Eq. (3.21)). When damping of the motion of the volume center is considered, the deflection is given by

$$\delta = \frac{e_\mu}{\sqrt{\left[\left(\frac{\omega_{CR}}{\omega}\right)^2 - 1\right]^2 + \left(\frac{C}{M\omega}\right)^2}} \tag{2.5}$$

and the force transmitted to each bearing is given by

$$F = \frac{Ke_\mu}{2}\left\{\frac{1}{\sqrt{\left[\left(\frac{\omega_{CR}}{\omega}\right)^2 - 1\right]^2 + \left(\frac{C}{M\omega}\right)^2}}\right\} \tag{2.6}$$

If we plot this function, we see that the transmitted bearing forces increase with speed and reach a maximum value and then diminish.

A dimensionless plot of the force function is given in Fig. 5. We are now able to define the true critical speed of the rotor as the speed at

which the force amplitude transmitted to the bearings is a maximum. This is mathematically expressed as the speed corresponding to the point where $dF/d\omega$ is zero. Of particular interest is that as the rotational speed increases above the rotor critical speed, the bearing forces diminish to a constant value of $Ke_\mu/2$, which is a function of only the rotor stiffness and the displacement of the mass center from the volume center (a measure of the rotor unbalance).

As a result of Jeffcott's splendid analysis of a relatively simple model, it became apparent to turbomachinery designers that it was possible, and in many ways even desirable, to operate above the first critical speed. By examination of this simple model, a designer gains considerable insight into the behavior of more complex systems. For example, examination of the rotor response curves of Fig. 5 shows why operation near a critical speed should be avoided if the rotor is lightly damped. It also demonstrates that if the system is critically damped, it is possible to pass through the critical-speed region without encountering excessive rotor amplitudes.[3]

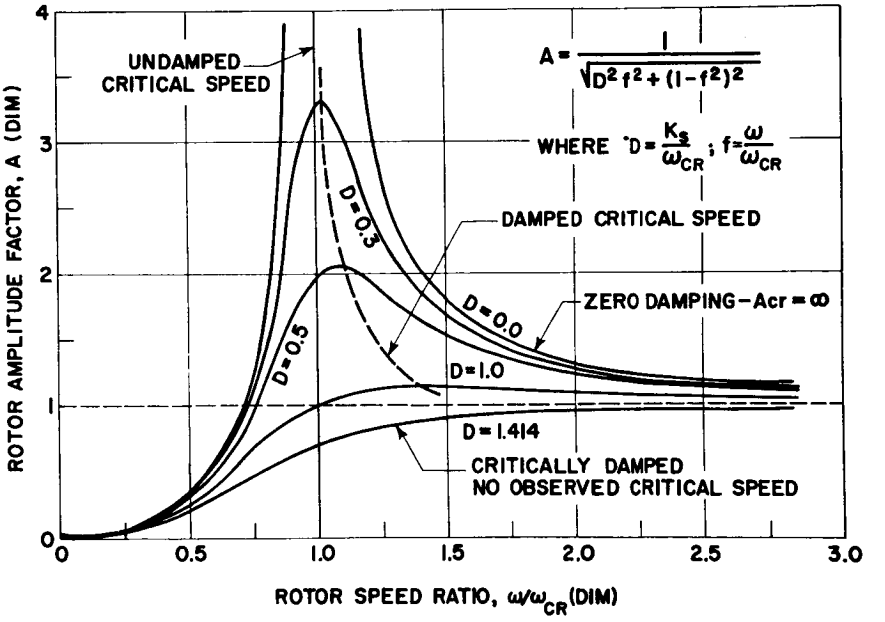


FIGURE 5. – Rotor amplitude for various damping values.

[3] To speak of a rotor as "vibrating" or having high vibrational amplitudes is misleading because the rotor motion is not confined in a plane. Only in the limiting case as the unbalance goes to zero is it possible for the rotor to vibrate in a plane.

It is of interest to note that the behavior of this simple model has not been fully explored. In Chapter 3 are presented the complete governing equations of motion of the Jeffcott model. An investigation of these equations has been undertaken to analyze transient behavior and the problem of whirling in general.

Robertson[85] in 1935 conducted an experimental and theoretical investigation on the transient whirling of the single-mass Jeffcott rotor. Robertson observed that the rotor elastic centerline could possess both forward and backward precessive motion depending upon the initial conditions. The influence of external damping caused the transient motion to die out until only the steady-state synchronous motion caused by rotor unbalance remained. He observed that only in the case where the deflection of the rotor was sufficient to cause it to strike the guard ring was it possible to develop a sustained transient motion.

## 2.4 NONSYNCHRONOUS PRECESSION—INTERNAL FRICTION DAMPING

The 1920's saw a trend reversing the rotor-design concepts of the previous decade. Turbine and particularly compressor and pump manufacturers were beginning to construct lighter weight rotors with lower critical speeds designed to operate well above the first critical speed. As more manufacturers went to the "flexible" rotor design, several encountered severe operating difficulties when operating well above the first critical speed. These problems at first were attributed to the lack of proper balancing. In the United States at this time, General Electric encountered a series of failures of blast furnace compressors designed to operate above the first critical speed. These machines were subject to occasional fits of more or less violent vibration of unknown origin. During these disturbances the shaft would vibrate at a low frequency which in some cases could be visually observed. The phenomenon was therefore called by shop men and engineers "shaft whipping."

Dr. B. L. Newkirk of the General Electric Research Laboratory was called in to investigate the nature of the failures. He set up a series of experiments with several units to observe the rotor dynamic behavior. It was observed that at speeds above the first critical speed, these units would enter into a violent whirling in which the rotor centerline precessed at a rate equal to the first critical speed. If the unit rotational speed were increased above its initial whirl speed, the whirl amplitude would increase, leading to eventual rotor failure. To further investigate all aspects and contributing factors to this problem, an experimental test rotor was constructed to simulate a typical compressor unit. Upon extensive testing of this unit, the following important facts were uncovered concerning this phenomenon:[63]

1. The onset speed of whirling or whirl amplitude was unaffected by refinement in rotor balance.
2. Whirling always occurred above the first critical speed, never below it.
3. The whirl threshold speed could vary widely between machines of similar construction.
4. The precession (or whirl) speed was constant regardless of the unit rotational speed.
5. Whirling was encountered only with built-up rotors.
6. Increasing the foundation flexibility would increase the whirl threshold speed.
7. Distortion or misalinement of the bearing housing would increase stability.
8. Introducing damping into the foundation would increase the whirl threshold speed.
9. Increasing the axial thrust bearing load would increase the whirl threshold speed.
10. A small disturbance was sometimes required to initiate the whirl motion in a well-balanced rotor.

It became clear to Dr. Newkirk that the rotor dynamic behavior could not be attributed to a critical-speed resonance, since the high vibrations encountered always occurred above the first critical speed and refinement of balance had no effect upon diminishing the whirl amplitudes. There was nothing in the literature at that time to indicate that any mode of motion, other than synchronous whirl, was possible. During the course of the investigation, a theory of the cause of the vibration was postulated by A. L. Kimball.[47] Kimball suggested that forces normal to the plane of the deflected rotor could be produced by the hysteresis of the metal undergoing alternate stress reversal cycles. (See App. A.) Newkirk concluded that these out-of-phase[4] forces could also be developed by a disk shrunk on a shaft. Upon reexamination of Jeffcott's model and introduction of an additional force normal to the deflected rotor, he was able to demonstrate that the rotor was indeed unstable above the first critical speed, and thus was partially able to explain some of his experimental findings. Since Newkirk made no attempt to extend Jeffcott's model by considering a flexible foundation with damping, he was unable to explain theoretically several of the key points of his experimental investigations, particularly as to why increased bearing or foundation flexibility and damping will improve the whirl stability.

[4] When a force vector produced by a given displacement or velocity vector is noncollinear, the component of the force vector normal to the line of action of the displacement or velocity vector is referred to as the out-of-phase component. Also see Ch. 5.

Dr. Newkirk's observations became known as whirling above the first critical speed or shaft whirling. Its nature is completely different from the vibrations encountered when operating in the vicinity of a critical speed. Whirling is in general a self-excited phenomenon, while a critical-speed vibration requires external excitation such as provided by rotor unbalance. The exciting force for the case of shaft whirling, as described above, is provided by the frictional forces developed between two mating surfaces when undergoing relative sliding. This frictional force will henceforth be referred to as rotating or rotary damping and can be expressed in the form[5]

$$\vec{F} = -C_r {}^{R'}\vec{V}^{C/O} = -C_r[{}^{R}\vec{V}^{C/O} - {}^{R}\vec{\omega}^{R'} \times \vec{\delta}] \tag{2.7}$$

where

$C_r$ = Rotary damping coefficient
$R'$ = Rotating reference frame with angular velocity $\omega$
$R$ = Fixed reference frame
${}^{R'}\vec{V}^{C/O}$ = Velocity of rotor center $C$ relative to $O$ in the rotating reference frame.

For the case where the rotor centerline deflection in $R'$ is invariant with time, the above relationship reduces to

$$F = -C_r\delta(\dot{\phi} - \omega) \tag{2.8}$$

It is seen that this force is developed only if the whirl speed $\dot{\phi}$ is different than the rotational speed $\omega$. When the motion of the system is such that $\dot{\phi} > \omega$ (which occurs below the first critical speed), the whirl motion is damped out and the system is stable. When the precession rate is smaller than the rotational speed $\omega$, the rotary damping force becomes a source of excitation; that is, energy is added to the system causing the whirl amplitudes to increase.

An analysis is presented in Chapter 4 which includes the effects of foundation flexibility and damping on the whirl threshold speed for a flexible rotor subjected to rotary damping. From this analysis, it is now possible to obtain theoretically all of the conclusions that Dr. Newkirk arrived at experimentally.

Stability charts of the rotor performance in Chapter 4 show the effects of the ratio of rotor flexibility to foundation flexibility and of the ratio of stationary damping to rotational damping on the whirl threshold speed.

## 2.5 NONSYNCHRONOUS PRECESSION—OIL FILM WHIRL

In Dr. Newkirk's continuing research of the problem of shaft whipping, he encountered in his experimental investigations cases of shaft whirling

[5] See Ch. 4 and App. A for additional discussion and derivation.

in which the frictional effects of a shrink-fit disk could not possibly have caused rotor instability.[65] He labeled this particular case of rotor instability "oil whip" to distinguish it from the whirl motion encountered with built-up rotors or rotors with shrink fits. His investigations of this phenomenon showed that this form of rotor instability also occurred only above the system critical speed. Newkirk found that under certain conditions a rotor shaft mounted in sleeve bearings whipped when the rotor was running at a speed greater than twice the first critical. He observed that the whipping occurred only when the bearings were flooded and the unstable motion could be stopped by reducing the oil flow to the bearings.[6]

The action of the oil bearings in promoting whirl instability was obscure at the time and Newkirk was at a particular loss to explain why oil whip did not commence until a speed range greater than twice the critical speed was attained. Especially confusing to Newkirk was the influence of foundation flexibility on rotor stability. In the case of shaft whirling due to internal friction, Newkirk found that he was able to totally eliminate the rotor instability by means of a flexibly mounted bearing housing (he employed ball bearings with the test rotors with internal friction). When this was tried with the oil film bearings, it caused the rotor to develop a violent whip motion. Only after external damping was added to the flexible bearing mount was it possible to control the rotor instability.[7]

In an attempt to analyze Newkirk's findings on oil-film whirl, Robertson[82] in 1933 investigated the stability of the ideal 360° infinitely long journal bearing. Using the film forces derived by Harrison[31] in 1913, Robertson concluded that the rotor will be unstable at all speeds rather than at speeds above twice the critical speed. This is because the steady-state bearing forces derived by Harrison have a 90° attitude angle between the applied load and journal displacement; hence the system has no radial bearing stiffness. Chapter 5 shows that if the bearing radial stiffness, or in general the system principal stiffness coefficients vanish, the system will be inherently unstable.

The reason for the discrepancy in Robertson's analysis is that the Sommerfeld-Harrison treatment of the hydrodynamic pressure profile predicts a negative film pressure of the same order as the positive pressure. Simons[91] showed that only for small displacements from the origin is it possible for the hydrodynamic film force to be normal to the displacement. For larger bearing loads, the oil film cavitates causing a

[6] An explanation for this is given in Ch. 5.

[7] The explanation of why only foundation flexibility (see Fig. 7 and Fig. D.2) should improve rotor stability for the case of internal shaft friction but not for oil whip is given in Sec. 4.10.3. Also explained is the reason why external damping is necessary in certain cases. See Figs. 39–41.

steady-state bearing attitude angle of $0 \leq \phi \leq \pi/2$. It is this cavitation of the fluid film which introduces a radial bearing force into the system.

Poritsky[75] in 1952, using small displacement theory, extended Robertson's analysis by introducing a radial bearing stiffness term into the equations of motion. Thus by doing this he was able to demonstrate that the rotor is indeed stable below twice the rotor critical speed. Poritsky extended his analysis to include rotor flexibility and arrived at the following stability criterion

$$M\omega^2\left[\frac{1}{K_r}+\frac{1}{K_b}\right]<4 \tag{2.9}$$

where

$K_r$ = rotor stiffness
$K_b$ = bearing stiffness

The system critical speed is approximated by

$$\omega_{CR}=\sqrt{\frac{K_r+K_b}{MK_rK_b}} \tag{2.10}$$

Thus

$$\omega < 2\omega_{CR} \qquad \text{for stability}$$

The Poritsky analysis indicates that the introduction of rotor flexibility will lower the system critical speed and hence will reduce the threshold of stability.[8] Extension of the Poritsky analysis to include foundation flexibility predicts a reduction in the threshold of stability. Hence at first glance, this would appear to answer Newkirk's question of why foundation flexibility should reduce stability.

In 1955, Pinkus[73] conducted an extensive experimental investigation on oil-film whirl with various bearing arrangements. Some of the major conclusions that Pinkus states are—

1. Rotor unbalance has little effect on the bearing stability.
2. Rotor whip, when developed, occurred at speeds equal to about twice the first natural critical frequency of the shaft.
3. The frequency of vibration in the unstable range is constant and equal to the first natural critical frequency of the shaft.
4. Whip motion stopped at speeds nearly three times the first critical with a heavy shaft.
5. With a light shaft, the whip motion could not be stopped.
6. High loads, high viscosities, and flexible mountings promote stability.

---

[8] A similar conclusion was reached by Hagg and Warner in their paper "Oil Whip in Flexible Rotors," *ASME Trans.*, Oct. 1953, pp. 1339–1344.

7. The order of bearing stability, starting with the most stable, is the three-lobe, tilting pad, pressure, elliptical, three-groove, and plain circular.
8. Bearing asymmetry favors stability.

Pinkus' experimental conclusion that bearing flexibility will improve stability is directly opposite to Newkirk's findings and to the theoretical conclusions of Poritsky, and Hagg and Warner. Recently, Tondl[107] in Czechoslovakia conducted an experimental investigation on a test rotor similar to Fig. 7 of Chapter 4 with various bearing arrangements. He concludes that "bearings with a flexible-element loose bushing are of all the bearings tested undisputably the most resistant to the initiation of self-excited vibrations . . . ." This apparent discrepancy between the theoretical and experimental findings on the effects of flexibly mounted bearings is explained in Chapter 4.

## 2.6 HYDRODYNAMIC BEARING CHARACTERISTICS

Many articles have been published on whirling since Newkirk's original investigation. Such articles as those written by Hagg,[29] Poritsky,[75] Hori,[33] Boeker and Sternlicht,[4] and Reddi and Trumpler[79] are a considerable aid in the understanding of the mechanism of whirl as caused by fluid film bearings.

The equation necessary to describe the characteristics of the hydrodynamic fluid film bearing is the Reynolds equation[9]

$$\frac{\partial}{\partial\theta}\left[H^3\rho\frac{\partial P}{\partial\theta}\right]+\left(\frac{R}{L}\right)^2\frac{\partial}{\partial Z}\left[H^3\rho\frac{\partial P}{\partial z}\right]=\Lambda\left[1-\frac{2\dot{\phi}}{\omega}\right]\frac{\partial}{\partial\theta}[\rho H]+\frac{\partial}{\partial t}[\rho H] \qquad (2.11)$$

where

$H=1+\epsilon\cos\theta=$ dimensionless film thickness
$R=$ bearing radius
$P=$ dimensionless pressure
$\rho=$ fluid density
$\dot{\phi}=$ journal precession rate
$\omega=$ total journal angular speed
$\Lambda=\dfrac{6\mu\omega}{P_a}\left(\dfrac{R}{C}\right)^2$

For the case of a compressible fluid, the above equation is a nonlinear partial differential equation with variable coefficients. As such, it is almost impossible to obtain closed-form solutions except in a certain limiting cases of high or low $\Lambda$ values. This has made it necessary to

[9] See App. D for discussion and derivation of the general Reynolds equation.

resort to the digital computer to obtain the bearing load-carrying capacity. In past analytical work on rotor stability (where the rotor is treated as a point mass), the Reynolds equation would be coupled with the dynamical equations, the system stability would be determined by first obtaining the perturbated equations of motion about an equilibrium configuration, integrating the unknown pressure profile, and evaluating the threshold of stability. The drawbacks to this approach are that the results are not general and cannot be easily extended to a more realistic situation where rotor flexibility, foundation deflection, and bearing mass are considered.

The total fluid film forces for both the compressible and incompressible cases can be shown to be represented in the form

$$F_r = -\Lambda f_r(\Lambda, \epsilon, \dot{\epsilon}, L/D)\left|\left(1-\frac{2\dot{\phi}}{\omega}\right)\right| \tag{2.12}$$

$$F_t = \Lambda f_t(\Lambda, \epsilon, \dot{\epsilon}, L/D)\left(1-\frac{2\dot{\phi}}{\omega}\right) \tag{2.13}$$

where the radial and tangential bearing coefficients $f_r$ and $f_t$ are complex functions of eccentricity and its time derivative, bearing aspect ratio, and $\Lambda$ value.

The forces developed in a hydrodynamic journal bearing have the following important characteristics:

1. The resultant journal displacement does not lie along the line of the applied bearing load. This gives rise to force components acting along and normal to the journal eccentricity vector. These force components are referred to as the radial and out-of-phase bearing forces, respectively
2. The radial and out-of-phase bearing forces are nonlinear functions of the eccentricity ratio
3. The magnitude and direction of action of the out-of-phase bearing component is dependent upon the journal precession rate.

If the bearing lubricant is incompressible, then $\rho =$ constant and the Reynolds equation is linear. In this case, closed form expressions for $f_r$ and $f_t$ can be obtained for such bearings as the ideal 360° and "cavitated" 360° (180° bearing).[10] For small perturbations from an equilibrium position, the fluid film bearing forces are represented by

$$F_r = -\omega[C_d(e_0, L/D)|(1-2\dot{\phi}/\omega)|+D_d\mathscr{D}]\delta e \tag{2.14}$$

[10] See Eqs. (6.1) and (6.2).

$$F_t = -\omega \left[ C_s(e_0, L/D)\left(\frac{2\dot{\phi}}{\omega} - 1\right) + D_s \mathscr{D} \right] \delta e \tag{2.15}$$

where

$C_d$ = radial film stiffness factor
$C_s$ = tangential film stiffness factor
$D_d$ = radial damping factor
$D_s$ = tangential damping factor
$\mathscr{D} = d/dt$
$\delta e$ = small displacement from equilibrium

Examination of Eq. (2.12) reveals that the tangential hydrodynamic bearing component is very similar in nature to rotary damping (see Eq. (2.8)), except with the appearance of $2\dot{\phi}$ instead of $\dot{\phi}$. Because of this similarity, many of the conclusions of Chapter 4 concerning the rotor stability characteristics with respect to rotary damping may be equally applied to the rotor stability problem caused by fluid film bearings.

Thus, in the fluid film bearing, it is the out-of-phase bearing component that generates the force required to initiate whirl instability. The shaft-attitude angle at equilibrium then is a direct measure of the ratio of the out of phase to radial bearing forces and hence is a measure of the degree of stability of the system.

## 2.7 PRESENT STATE OF THE ART

Of the numerous articles written on the subject of rotor behavior, a complete theory to explain whirl has not been developed. These many expositions on whirl vary according to whether the investigator is essentially a rotor dynamicist or a bearing specialist. Since the bearing behavior is rather complex, the rotor dynamicist has approached the problem by either ignoring the action of the bearings altogether, or replacing the bearings by linear springs and dashpots. The recent article by Dr. Kane[45] of Stanford is an example of the first type of approach. He examined the conditions for general whirling of a flexible unbalanced rotor by trying to extend Jeffcott's model. Since he did not include the effects of bearing displacements or any form of damping (stationary or rotating), his results are inconclusive. This is as expected, since the forces required to initiate self-excited whirling have not been included in his analysis. However, an extension of Dr. Kane's analysis to include stationary damping has been accomplished (Ch. 3). This analysis shows that the only possible whirl ratio that satisfies the differential equations of motion for both the transient and steady-state conditions is the value of $\dot{\phi}/\omega = 1/3$. When the system speed reaches three times the value of the first critical speed, the rotor center will precess at a rate equal to the first critical speed. At a recent gas-bearing conference in England, it was reported that one-third whirl

was observed with an externally pressurized gas bearing rotor.[21] This gas-bearing rotor is closely approximated by the extended Jeffcott model.

The other typical approach applied by rotor dynamicists is to consider the bearings as one-dimensional linear springs and dashpots, neglecting the bearing out-of-phase force components. The one-dimensional bearing representation will not even furnish an accurate evaluation of the system critical speeds (eigenvalues) and bearing attenuation characteristics. This deviation is accentuated as the effective bearing attitude angle increases.

Such an assumption was the basis of analysis by Smith[93] and Linn and Prohl[57]. Prohl makes no attempt to discuss stability (since it is impossible with his model), but elaborates rather on how the action of the oil-film elasticity reduces the overall system critical speed. For bearings with large attitude angles, the critical speed as predicted by Prohl's method, which utilizes a one-dimensional spring rate, can be in considerable error due to the neglect of the large out-of-phase film stiffness factor.

In Ch. 6 the equations of motion of the Jeffcott model are developed based on the work by Tang and Trumpler with the inclusion of bearing characteristics and foundation flexibility. The equations show that a hydrodynamic bearing requires a minimum of two orthogonal stiffness coefficients or spring rates to represent the film characteristics. Hence, the bearings require a two-dimensional representation to completely describe their behavior. Any attempts to examine system stability while excluding the effects of the cross-coupling or out-of-phase bearing coefficient(s) are meaningless. In general, eight quantities are necessary to describe the characteristics of a fluid film bearing—four film stiffness rates and four damping terms.[71]

## 2.8 STABILITY OF THE RIGID BEARING—POINT-MASS ROTOR

Another method of approach that has been frequently used is to examine the rotor stability problem from the viewpoint of the fluid dynamicist. In this approach the stability problem is considered as being mainly a problem of the characteristics of fluid film bearings and the rotor is treated either as a rigid body or as a point mass. Such a method of approach was the basis of the work performed by Reddi and Trumpler[79] in a stability analysis of the 360° and 180° incompressible fluid film bearing, and by Cheng and Trumpler[7] and Castelli and Elrod[5] in the analysis of the stability characteristics of the infinitely long gas-lubricated 360° journal bearing. Because of the complexity of the highly nonlinear dynamical equations involved, all previous investigations have been concerned only with the determination of the inception of unstable motion, or the threshold of stability. This is essentially

done by linearizing the equations of motion about an equilibrium position and applying the well-known Routh stability criterion for linear systems.

Trumpler pointed out to Poritsky [75] in 1952 that the rotor forces and displacements do not increase without limit, as predicted by the linear system, but remain bounded due to the nonlinear characteristics of the film and that the "factors which maintain the rotor forces within limits are very important and should be included in a more comprehensive analysis." He states that the magnitude of the oscillatory motion above the stability threshold is all-important to the engineer.

Poritsky, in reply, states that—

> unless the nonlinear theory predicts low limits for the whirl amplitudes, the integration of these nonlinear equations is only of academic interest. For steady operation, a rotor should be free from large scale whirling . . . . Therefore, what is of more interest from the practical point of view is the study of the stability of small oscillations about the positions of steady operations.

He further states that "while the effect of nonlinearity of the oil-film forces may limit the whirl amplitude to a finite value, . . . nonlinearity by itself can never restore complete stability in a range where the linear theory indicates instability."

The author has found that such is not the case. From analog computer studies of an unbalanced rotor, it was found that the addition of a small nonlinear radial force creates a finite limit cycle, and also, depending upon the rotor unbalance, bearing attitude angle, a small nonlinear component can restore the motion of the system to stable synchronous precession. Nonlinear analysis is difficult to apply to even the simplest system of a rigid point mass rotor in a journal bearing. Therefore the main concern of this thesis will be the determination of the inception speed of unstable motion.

As Newkirk demonstrated experimentally, the conditions that determine stable rotor operation are dependent upon several system parameters such as the bearing characteristics, the rotor flexibility, the bearing support foundation, and also the external forces and torques acting on the system. These external forces and torques exerted on the system by means of the drive mechanism, the rotor unbalance, and the damping, as furnished by rotor windage losses and through axial thrust bearings, can have a pronounced effect on the range of stable operation.

The present state of the art does not adequately cover the general problem of rotor stability even for small perturbations. As such, the present literature is unable to theoretically verify and explain several important and contradictory aspects of the experimental investigations of Newkirk,[63,65] Pinkus,[73] Wildmann,[111] and others, on whirl instability. It is the purpose of this thesis to help shed light on this

problem to explain some of the conflicting experimental evidence gathered on these phenomena.

The work presented herein represents an attempt to treat the problem of rotor instability in general in order to develop a useful stability criteria that may be employed by the design engineer so as to avoid or minimize the problem of self-excited whirl instability.

# Chapter 3

# Whirling of a Single-Mass Flexible Unbalanced Rotor

*Nomenclature*

$C$ – rotor volume center
$M$ – rotor mass
$I$ – rotor polar moment of inertia about CG
$O$ – undeflected rotor position
$R$ – fixed reference frame
$R'$ – relative reference frame
$M$ – rotor mass center
$\omega$ – total angular velocity of system $= \dot{\beta} + \dot{\phi}$
$\vec{n}_x, \vec{n}_y$ – unit vector set fixed in $R$
$\vec{n}_r, \vec{n}_\phi$ – unit vector set fixed in $R'$

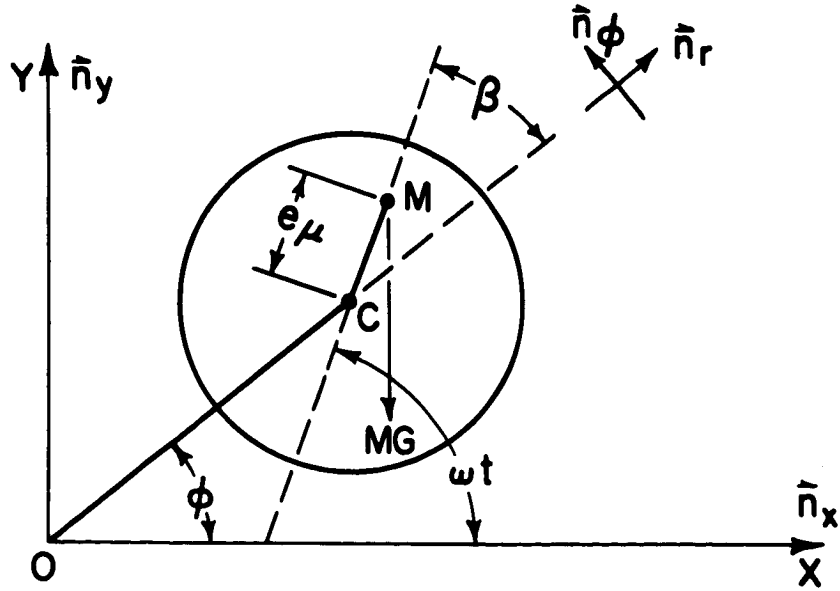


FIGURE 6. – Section $A$–$A'$ of rotor.

## 3.1 WHIRLING OF A SINGLE-MASS FLEXIBLE ROTOR—EQUATIONS OF MOTION

The system under consideration possesses three degrees of freedom. The generalized coordinates employed to describe this system are:

(a) $\delta$ —deflection of rotor center from origin $O$
$\phi$ —precession angle
$\beta$ —phase angle

(b) $X$, $Y$—Cartesian coordinates of the displaced rotor center
$\beta$ —phase angle

The equations of motion may be expressed in either set of coordinates. Since the system has three degrees of freedom, there will be three equations of motion, one for each generalized coordinate.

### 3.1.1 Kinetic Energy of System

$$T = 1/2\ MV_m^2 + 1/2\ \omega_i \omega_j \phi_{ij} \tag{3.1}$$

$V_m$ = velocity of mass center

A position vector to the rotor mass center $M$ from the fixed point $O$ is given by

$$\vec{P}^{M/O} = [\delta + e\ \cos\ \beta]\vec{n}_r + e\ \sin\ \beta\ \vec{n}_\phi \tag{3.2}$$

The velocity of the mass center $M$ is given by

$$^R\vec{V}^{M/O} = \frac{^Rd}{dt}[\vec{P}^{M/O}] = \frac{^{R'}d}{dt}[\vec{P}^{M/O}] + {}^R\vec{\omega}^{R'} \times \vec{P}^{M/O} \tag{3.3}$$

where:

$\frac{^Rd}{dt}$ = time rate of change in fixed reference frame $R$

$\frac{^{R'}d}{dt}$ = time rate of change in relative reference frame $R'$

$^R\vec{\omega}^{R'}$ = angular velocity vector of relative reference frame $R'$ in $R = \dot{\phi}\vec{n}_z$

$$^R\vec{V}^{M/O} = [\dot{\delta} - e\ \sin\ \beta\omega]\vec{n}_R + [\delta\dot{\phi} + e\ \cos\ \beta\omega]\vec{n}_\phi$$

The total kinetic energy of the system is given by

$$T = \tfrac{1}{2} m[^R\vec{V}^{M/O} \cdot {}^R\vec{V}^{M/O}] + \tfrac{1}{2}\omega \cdot \omega I$$

$$= \tfrac{1}{2}\{m[\dot{\delta} - e\omega\ \sin\ \beta]^2 + m[\delta\dot{\phi} + e\omega\ \cos\ \beta]^2 + I\omega^2\} \tag{3.4}$$

### 3.1.2 Potential Energy—V

The potential energy of the rotor is composed of the strain energy of deformation of the rotor and the vertical position of the rotor mass center.

$$V = \tfrac{1}{2} K_r \delta^2 + mgh \tag{3.5}$$

where

$$K_r = \text{rotor stiffness coefficient}$$

$$h = \vec{P}^{M/O} \cdot \vec{n}_y = \delta \sin \phi + e \sin (\beta + \phi)$$

$$\therefore V = \tfrac{1}{2} K_r \delta^2 + mg[\delta \sin \phi + e \sin (\beta + \phi)] \tag{3.6}$$

### 3.1.3 Generalized Forces

The external forces and torques acting on the system which have not been taken into consideration is the rotor damping force acting at $C$ and the rotor drive torque $T$.

The damping force acting at $C$ is given by

$$\vec{F}^c_{ext} = -[C\dot{\delta}\vec{n}_r + C\delta\dot{\phi}\vec{n}_\phi] \tag{3.7}$$

The generalized forces for each of the coordinates are given by

$$F_{gr} = \sum_{i=1}^{N} \vec{F}^i_{ext} \cdot \frac{\partial \vec{V}}{\partial \dot{g}_r} \qquad \vec{V}^c = \dot{\delta}\vec{n}_r + \delta\dot{\phi}\vec{n}_\phi \tag{3.8}$$

(a) $\delta_j$; $F_\delta = -[C\dot{\delta}\vec{n}_r + C\delta\dot{\phi}\vec{n}_\phi] \cdot \vec{n}_R = -C\dot{\delta}$

(b) $\beta$; $F_\beta = -\vec{T} \cdot \dfrac{\partial \vec{\omega}}{\partial \dot{\beta}} = -T$

(c) $\phi$; $F_\phi = -[C\dot{\delta}\vec{n}_r + C\delta\dot{\phi}\vec{n}_\phi] \cdot \delta\vec{n}_\phi - \vec{T} \cdot \dfrac{\partial \vec{\omega}}{\partial \dot{\phi}}$

$$= -C\delta^2\dot{\phi} - T \tag{3.9}$$

### 3.1.4 Lagrange's Equations of Motion

The equations of motion will be derived by means of Lagrange's equations which state:

$$\frac{d}{dt}\left(\frac{\partial L}{\partial \dot{g}_r}\right) - \frac{\partial L}{\partial g_r} = F_{gr} \tag{3.10}$$

Where:

$L$ = Lagrangian = $T - V$

$F_{gr}$ = Generalized force for the $g_r$ coordinate

$$L_{1,2}=\frac{m}{2}\{[\dot{\delta}-e\omega\sin\beta]^2+[\delta\dot{\phi}+e\omega\cos\beta]^2+k^2\omega^2+ -2g(\dot{\delta}\sin\phi+e\sin[\beta+\phi])\}-\tfrac{1}{2}K\delta^2 \quad (3.11)$$

$k$ = radius of gyration

(a) $\delta$; $\dfrac{d}{dt}\{m[\dot{\delta}-e\sin\beta\omega]\}+m[g\sin\phi-\delta\dot{\phi}^2-e\omega\cos\beta]+K\delta=-C\dot{\delta}$

(b) $\beta$; $\dfrac{d}{dt}\left\{me\left[\omega e\left[1+\left(\dfrac{k}{e}\right)^2\right]-\dot{\delta}\sin\beta+\delta\dot{\phi}\cos\beta\right]\right\}$
$+me[\omega(\dot{\delta}\cos\beta+\delta\phi\sin\beta)+g\cos(\beta+\phi)]=-T$

(c) $\phi$; $\dfrac{md}{dt}[\delta^2\dot{\phi}-e\dot{\delta}\sin\beta+e^2\omega+e\delta\cos\beta(\omega+\dot{\phi})+K^2\omega]$
$+mg[\delta\cos\phi+e\cos(\beta+\phi)]=-C\delta^2\dot{\phi}-T$

Assume the total angular velocity $\omega$ of the system is constant,

$$\omega=\dot{\phi}+\dot{\beta}=\text{constant}$$

Hence $\dot{\omega}=0$; and $\ddot{\beta}=-\ddot{\phi}$

The equations of motion of the system reduce to:

(a) $\delta$; $\ddot{\delta}+\dfrac{C}{m}\dot{\delta}+(\omega_{CR}^2-\dot{\phi}^2)\delta=e\omega^2\cos\beta-g\sin\phi$

(b) $\beta$; $e\{[\delta\ddot{\phi}+2\dot{\delta}\dot{\phi}]\cos\beta-[\ddot{\delta}-\delta\dot{\phi}^2]\sin\beta\}=-eg\cos(\beta+\phi)-\dfrac{T}{m}$

(c) $\phi$; $\delta^2\ddot{\phi}+\left[\dfrac{C}{m}\delta+2\dot{\delta}\right]\delta\dot{\phi}+e[(\delta\ddot{\phi}+2\dot{\delta}\dot{\phi})\cos\beta-\sin\beta(\ddot{\delta}+\delta[\omega^2-\dot{\phi}])]$
$=-g[\delta\cos\phi+e\cos(\beta+\phi)]-\dfrac{T}{m}$ (3.12)

The torque $T$ will be eliminated between Eq. 3.12 (b) and (c) to yield the system:

(a) $\ddot{\delta}+K_s\dot{\delta}+(\omega_{CR}^2-\dot{\phi}^2)\delta=e\omega^2\cos\beta-g\sin\phi$
(b) $\delta\ddot{\phi}+(K_s\delta+2\dot{\delta})\dot{\phi}=e\omega^2\sin\beta-g\cos\phi$ (3.13)

where:

$K_s$ = damping factor $= C/m$
$\omega_{CR}^2$ = (Natural lateral rotor frequency)$^2 = K/m$ (for case of light damping)

## 3.2 ANALYSIS OF ROTOR MOTION

Specific cases for the governing equations of motion will be considered:

### 3.2.1 Case I—Synchronous Precession

Synchronous precession implies that the precession rate $\dot{\phi}$ of the rotor is equal to the total angular velocity of the system $\omega$.

The equations of motion are:

$$\text{(a)}\quad \ddot{\delta}+K_s\dot{\delta}+(\omega_{CR}^2-\omega^2)\delta=e\omega^2\cos\beta-g\sin\phi \tag{3.14}$$

$$\text{(b)}\quad \delta\ddot{\phi}+(K_s\delta+2\dot{\delta})\dot{\phi}=e\omega^2\sin\beta-g\cos\phi \tag{3.15}$$

Assume a condition of steady-state whirling of a vertical rotor. This condition implies:

$\delta=$ constant
$\beta=$ constant
$\dot{\phi}=\omega=$ constant
$g=0$

The governing Eqs. (3.14) and (3.15) reduce to:

$$\begin{aligned}&\text{(a)}\quad (\omega_{CR}^2-\omega^2)\delta=me\omega^2\cos\beta\\&\text{(b)}\quad K_s\delta\omega=e\omega^2\sin\beta\end{aligned} \tag{3.16}$$

Solving for the phase angle $\beta$:

$$\tan\beta=\frac{K_s\omega}{\omega_{CR}^2-\omega^2};\qquad K_s=\frac{C}{m};\qquad \omega_{CR}^2=\frac{K}{m} \tag{3.17}$$

Solve for the rotor deflection $\delta$:

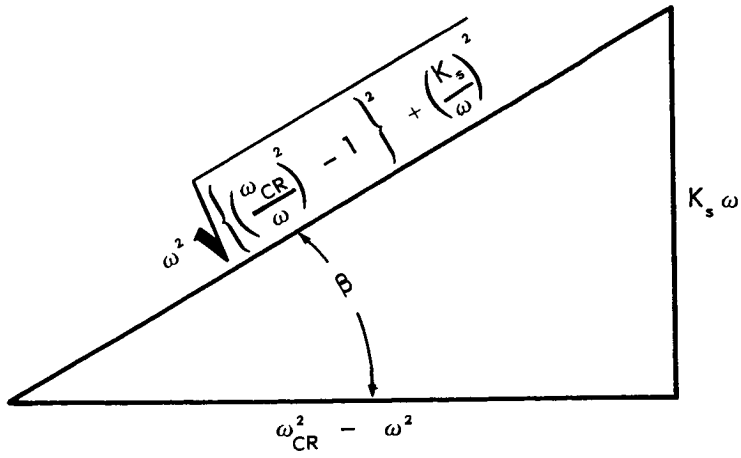


$$\delta=\frac{e\omega^2\sin\beta}{K_s\omega}=\frac{e}{\sqrt{\left\{\left(\frac{\omega_{CR}}{\omega}\right)^2-1\right\}^2+\left(\frac{K_s}{\omega}\right)^2}} \tag{3.18}$$

The force transmitted to each bearing is given by

$$F = (\tfrac{1}{2} Ke)A$$

where $A$ = amplitude factor

$$A = \frac{1}{\sqrt{\left\{\left(\frac{\omega_{CR}}{\omega}\right)^2 - 1\right\}^2 + \left(\frac{K_s}{\omega}\right)^2}} \tag{3.19}$$

The critical speed is defined as the speed at which

$$\frac{dF}{d\omega} = 0 = \frac{Ke}{2}\left\{\frac{2\omega}{\sqrt{K_s^2\omega^2 + (\omega_{CR}^2 - \omega^2)^2}} - \frac{\omega^2[2\omega K_s^2 - 4\omega(\omega_{CR}^2 - \omega^2)]}{2[K_s^2\omega^2 + (\omega_{CR}^2 - \omega^2)^2]^{3/2}}\right\}$$

$$= \frac{Ke}{2[K_s^2\omega^2 + (\omega_{CR}^2 - \omega^2)^2]^{3/2}}\{K_s\omega^2 + 2(\omega_{CR}^2 - \omega^2)\omega_{CR}^2\} = 0 \tag{3.20}$$

If we assume that the denominator will be nonzero, we have the following relationship:

$$\omega_s = \omega_{CR}\sqrt{\frac{1}{1 - \frac{1}{2}\left(\frac{K_s}{\omega_{CR}}\right)^2}} \tag{3.21}$$

Where:

$\omega_{CR}$ = free natural lateral resonance frequency = $\sqrt{K/m}$

$\omega_s$ = actual system resonance frequency

From the above equation, it can be seen that only for the case of zero damping ($K_s = 0$) will the system resonance frequency (critical speed) correspond to the natural lateral frequency $\omega_{CR}$. In general, the effects of damping will increase the system resonance frequency.

The maximum force transmitted to the bearings during the system resonance is given by

$$F_{max} = \frac{Ke\omega_{CR}}{2K_s\sqrt{1 - \frac{1}{2}\left(\frac{K_s}{\omega_{CR}}\right)^2}} \tag{3.22}$$

In general, the ratio $\omega_{CR}/K_s \gg 1.0$. In this case the maximum force transmitted may be expressed by

$$F_{max} = \frac{e\omega_{CR}}{2}\left(\frac{K}{K_s}\right) \tag{3.23}$$

Thus, it is seen that with the perfectly balanced rotor ($e=0$), the force transmitted to the bearings will be zero. In actuality, a finite value will exist for $e$ depending upon the rotor-balancing equipment used. For a particular rotor, the value of $e$ and $K$, the rotor stiffness, is fixed or may be varied only slightly. The only other two variables at our disposal to adjust are $\omega_{CR}$ and the damping factor $K_s$. The damping factor is greatly affected by the choice of bearings in the system. The inherent damping as furnished by fluid film bearings greatly exceeds the damping characteristics of rolling element bearings. For a given rotor it is possible to greatly reduce the forces transmitted during system resonance by reducing the natural lateral frequency of the system. This is accomplished by having the bearings elastically mounted. The equations presented apply rigorously only to the case of a simply supported rotor. The simple performance criterion developed may be viewed as a guide to predict the total system behavior when including the effects of simple bearings, etc.

### 3.2.2 Case II—Zero Precession

The condition of zero precession implies that the rotor vibrates in a plane. This is given by the precessional angular velocity.

$$\dot{\phi}=0$$

$$\text{(a)}\quad \ddot{\delta}+K_s\dot{\delta}+\omega_{CR}^2\delta \underset{(3.13)}{=} e\omega^2\cos\beta-g\sin\phi$$

$$\text{(b)}\quad 0 \underset{(3.13)}{=} e\omega^2\sin\beta-g\cos\phi \tag{3.24}$$

The above condition is possible only if the eccentricity $e$ (unbalance) or the total angular velocity $\omega$ is zero. In either case the resulting equation of motion is

$$\ddot{\delta}+K_s\dot{\delta}+\omega_{CR}^2\delta=0 \tag{3.25}$$

which is the equation of free, damped lateral vibrations. It is important to note that all of the present methods of calculating critical speeds are based upon finding the natural lateral frequencies of undamped motion. From this simple model it is seen that the normal unbalanced rotor does not vibrate in a plane but revolves or precesses to form an orbit.

### 3.2.3 Case III—Secondary Critical Speed (Effect of Gravity)

Assume rotor synchronous precession

$$\dot{\phi}=\omega$$

$$\phi=\omega t-\beta$$

$$\text{(a)}\quad \ddot{\delta}+K_s\dot{\delta}+(\omega_{CR}^2-\omega^2)\delta=e\omega^2\cos\beta-g\sin(\omega t-\beta)$$

$$\text{(b)}\quad 2\omega\dot{\delta}+K_s\omega\delta=e\omega^2\sin\beta-g\cos(\omega t-\beta) \tag{3.26}$$

Solving Eq. (3.26(b)) for a particular solution; we obtain

$$\delta=\frac{e}{2D}\sin\beta-\frac{g}{2\omega^2[1+D^2]}[\sin(\omega t-\beta)+D\cos(\omega t-\beta)] \tag{3.26.1}$$

where

$$D=\frac{K_s}{2\omega}$$

Equation (3.26.1) must also represent a particular solution of Eq. (3.26(a)). Substitution of the above into the first equation of motion results in the following conditions to be met in order that $\delta$ be a valid solution.

$$\left.\begin{aligned}
&\text{(1)}\quad \sin\beta-\frac{2D}{\left(\frac{\omega_{CR}}{\omega}\right)^2-1}\cos\beta=0\\
&\text{(2)}\quad \frac{g}{2[1+D^2]}\left[3+\frac{5}{2}D^2+\left(\frac{\omega^2-\omega_{CR}^2}{\omega^2}\right)\right]\sin(\omega t-\beta)=0\\
&\text{(3)}\quad \frac{gD}{2[1+D^2]}\left[\frac{1}{2}+\left(\frac{\omega^2-\omega_{CR}^2}{\omega^2}\right)\right]\cos(\omega t-\beta)=0
\end{aligned}\right\} \tag{3.27}$$

The first condition, Eq. (3.27.1), is satisfied by the requirement that the rotor phase angle $\beta$ be given by

$$\beta=\tan^{-1}\frac{K_s\omega}{\omega_{CR}^2-\omega^2} \tag{3.27.4}$$

the above is identical to Eq. (3.17) obtained for synchronous precession in general. The second relationship requires that

$$3+\frac{5}{2}D^2+\frac{\omega^2-\omega_{CR}^2}{\omega^2}=0$$

or

$$\boxed{\omega=\frac{1}{2}\omega_{CR}\sqrt{1-\frac{5}{8}\left(\frac{K_s}{\omega_{CR}}\right)^2}} \tag{3.27.5}$$

The above condition represents the system secondary critical speed. Note that the last two conditions are identically satisfied if $g=0$ and $\omega$ may be any speed.

Equation (3.27.3) requires that either

(A) $\frac{1}{2}+\frac{\omega^2-\omega_{CR}^2}{\omega^2}=0$

or

(B) $$\frac{gD}{2[1+D^2]}=0 \tag{3.27.6}$$

The first condition leads to the contradictory statement that

$$\omega=\sqrt{\frac{2}{3}}\,\omega_{CR}$$

which is in conflict with Eq. (3.27.5). Thus it is necessary that

$$\frac{gD}{2[1+D^2]}\rightarrow 0$$

substitute $\delta_{st}$ = rotor static deflection = $Mg/K$ and

$$D=\frac{K_s}{2\omega}=\frac{C}{2M\omega}$$

$$\therefore \left(\frac{\omega_{CR}}{2\omega}\right)^2 \frac{\omega K_s\delta_{st}}{[1+D^2]} \underset{(3.27.5)}{\approx} \frac{C\omega\delta_{st}}{m} \tag{3.28}$$

The third condition implies that the rotor damping force $C\cdot\omega\delta$ divided by the bearing mass $M$ must be a small quantity or

$$\frac{F_{\text{damping}}}{M}\rightarrow 0$$

in order to observe a secondary system critical speed. This criterion may help to explain why secondary critical speeds have sometimes been observed with heavy, massive low-speed turborotors, but seldom with lightweight high-speed rotors. If the system damping characteristics are too high, this phenomenon is completely suppressed.

The rotor deflection at the secondary critical speed ($\omega=\omega_{CR}/2$ for light damping) is given by

$$\delta_{(3.26.1)}=_{(3.27.4)} \frac{e}{\sqrt{1+\left(\frac{2}{3}D\right)^2}}-\frac{2\delta_{st}}{[1+D^2]}\left[\sin\left(\frac{\omega_{CR}}{2}t-\beta\right)+D\cos\left(\frac{\omega_{CR}}{2}t-\beta\right)\right] \tag{3.29}$$

Hence we conclude that when the rotor angular velocity is equal to one-half the first critical speed, a horizontal rotor is capable of possessing a secondary critical speed. The radius of the whirl orbit is equal to twice the static deflection (or initial rotor sag). Note that gravity is not the only cause of secondary critical speeds. Rotors with unsymmetric shaft properties can cause excessive rotor deflection.

The investigation of the possible occurrence of subcritical resonance vibrations has been discussed by several authors. Rankine,[78] in his early publications on vibrations of rotors, stated that a resonance vibration at $1/2\omega_{CR}$ was possible. This value was later shown to be erroneous, since Rankine neglected the Coriolis acceleration term in his equations of motion. Stodola[100] was the first to demonstrate that the disk weights of a horizontal shaft can create disturbing forces which at a certain speed can produce considerable shaft vibration. Timoshenko gives a simplified explanation of the secondary critical-speed effect, developed along the lines of Stodola, in his text *Vibration Problems in Engineering.*[105] The actual observation of the secondary critical-speed phenomenon was reported as early as 1919 by Toppl.[99]

An extensive article on the subcritical speeds of a rotating shaft was presented by Soderberg[94] in the past decade. Soderberg examines and compares the resonance amplitudes at the critical speed to the rotor subcritical vibrations caused by gravity and by variable rotor elasticity for an undamped rotor. In his investigation of the secondary critical speed due to gravity, he arrives at the following equation

$$\frac{d^2r}{dt^2}+(\omega_{CR}^2-\omega^2+2\mu\omega^2 \sin \omega t)r=\omega_{CR}^2 e \qquad [28]$$

where $r$ is the displacement of the rotor mass center from the steady-state position.

Equation [28] of Ref. 94 is a nonhomogeneous Mathieu equation of the form

$$\frac{d^2W}{dz^2}+[\delta+\epsilon \cos z]W=C$$

and its solutions and regions of stability are discussed in detail in Stoker.[101] Soderberg approximates the solution by solving the equation considering the term $(2\mu r\omega^2) \sin \omega t$ as a forcing function independent of $r$, which results in

$$r=\frac{e\omega_{CR}^2}{\omega_{CR}^2-\omega^2}\left[1+\frac{2\epsilon\omega^2(\omega_{CR}^2-\omega^2)}{\omega_{CR}^2(\omega_{CR}^2-4\omega^2)} \sin \omega t\right] \qquad [34]$$

He then concluded that since $r$ becomes unbounded when the rotor speed is exactly one-half the rotor critical speed, then the rotor precession angle must be of the form

$$\theta = \omega t + \chi \omega t \sin \omega t \qquad [37]$$

which leads to a higher order Mathieu equation. The solution he obtains when $\omega = \omega_{CR}/2$ is given by

$$r = \frac{4}{3} e[1 - 3/8\epsilon(2 \sin \omega t + \omega t \cos \omega t)] \qquad [49]$$

where

$$\epsilon = e\gamma_0 \left(\frac{\omega_c}{\rho\omega}\right)^2; \qquad \rho = \text{radius of gyration}$$

Even though the term $\epsilon$ is a small quantity, Soderberg predicts that the vibration amplitudes of an undamped rotor will become unbounded if operated continuously at one-half the rotor critical speed. This finding is in contrast to Eq. (3.29), which shows that the subcritical vibration amplitude of an undamped rotor is bounded and also that the inclusion of sufficient rotor damping will suppress this phenomenon.

### 3.2.4 Case IV—General Whirling (Nonsynchronous Precession)

Let

$$\dot{\beta} = n\omega$$
$$\beta = n\omega t + \beta_0$$
$$\dot{\beta} + \dot{\phi} = \omega$$

The equations of motion (neglecting gravity) are

$$\begin{aligned} &\text{(a)}\ \ddot{\delta} + K_s\dot{\delta} + [\omega_{CR}^2 + (1-n)^2\omega^2]\delta = e\omega^2 \cos(n\omega t + \beta_0) \\ &\text{(b)}\ [2\dot{\delta} + K_s\delta]\omega[1-n] = e\omega^2 \sin(n\omega t + \beta_0) \end{aligned} \qquad (3.30)$$

Solving for $\delta$

$$\delta = A\left(e^{-\frac{K_s}{2}t}\right) - \frac{e\omega \cos(\beta - \alpha)}{2[1-n]\left[\left(\frac{K_s}{2}\right)^2 + n^2\omega^2\right]^{1/2}} \qquad (3.31)$$

where

$$\beta - \alpha = n\omega t + \beta_0 - \tan^{-1}\left(\frac{K_s}{2n\omega}\right)$$

Applying the initial condition of

$$\delta(0)=\delta_0$$

$$\delta_0=A-R\cos(\beta_0-\alpha) \tag{3.32}$$

where

$$R=\frac{e\omega}{2[1-n]\left[\left(\frac{K_s}{2}\right)^2+n^2\omega^2\right]^{1/2}}$$

Hence

$$e^{-\frac{K_s}{2}t}\left\{\left[\omega_{CR}^2-(1-n)^2\omega^2-\frac{K_s}{4}\right][\delta_0+R\cos(\beta_0-\alpha)]\right\}+R\cos(\beta-\alpha)[n^2\omega^2$$
$$-\omega_{CR}^2+(1-n)^2\omega^2]+n\omega K_sR\sin(\beta-\alpha)-e\omega^2\cos\beta=0 \tag{3.33}$$

(Equation (3.33) represents an extension of the work of Dr. T. R. Kane in "An Addition to the Theory of Whirling," *J. Appl. Mech.*, Vol. 83, 1961. Dr. Kane neglected the effects of damping in his equations. It will be seen that even for the case of light damping, the nature of the solutions is considerably altered.)

*Problem:*

Do any values of $n$ exist such that the above equation is satisfied for all time $t$?

If we consider light damping, then

$$\frac{K_s}{2n\omega}\to 0; \qquad R\to\frac{e}{2n[1-n]}$$

$$e^{-\frac{K_s}{2}t}[\omega_{CR}^2-(1-n)^2\omega^2]\left[\delta_0+\frac{e}{2n[1-n]}\cos(\beta_0-\alpha)\right]$$
$$+\frac{e}{2n[1-n]}[(2n-1)^2\omega^2-\omega_{CR}^2]\cos\beta=0 \tag{3.34}$$

Consider values of $n$ (other than 0 or 1) which will make Eq. (3.34) identically vanish. Let

$$\omega_{CR}^2-(1-n)^2\omega^2=0$$

and

$$[2n-1]^2\omega^2-\omega_{CR}^2=0 \tag{3.35}$$

Solving for $n$

$$n=2/3$$

Hence,

$$\omega = 3\omega_{CR} \qquad \text{and} \qquad \dot{\phi} = \omega_{CR} \tag{3.36}$$

The above condition implies that if the rotor angular velocity $\omega$ of the system is three times the natural lateral critical frequency $\omega_{CR}$, one possible motion is for the system to precess at a rate equal to the critical speed. This has been reported to occur with an externally pressurized gas bearing rotor and has been referred to as "fractional frequency whirl." (Although the single-mass Jeffcott model is physically unlike a rigid rotor or externally pressurized bearings, the equations of cylindrical precession are similar.)

As a second case, consider the less-stringent condition that the transient whirl dies out. The steady-state equation ($t \to \infty$) is

$$\frac{e}{2n(1-n)} \cos\beta \left[ (2n-1)^2 - \left(\frac{\omega_{CR}}{\omega}\right)^2 \right] \omega^2 = 0 \tag{3.37}$$

Consider the case where $\omega \gg \omega_{CR}$ or the angular velocity is much higher than the first critical speed. In this case, Eq. (3.37) reduces to

$$(2n-1)^2 = 0 \tag{3.38}$$

or

$$n = 1/2$$

Hence

$$\dot{\phi} = \omega/2$$

Thus, we have demonstrated that half-frequency whirling is possible only in the limiting case as the rotor approaches speeds considerably greater than the first critical. Note that it is impossible to obtain this conclusion unless damping is retained in the equations of motion.

Half-frequency whirling is usually associated with hydrodynamic fluid-film bearings. At least two bearing coefficients are required to represent the bearing stiffness characteristics: a radial "spring" rate and a tangential spring rate. It is the presence of the tangential or out-of-phase bearing force which causes self-excited half-frequency whirl to occur at approximately twice the rotor critical speed. In the absence of this force, half-frequency whirling cannot occur.

## 3.3 SUMMARY AND CONCLUSIONS

In Table 1 are presented a summary of the various forms of rotor whirling. For each particular case there are three subsections which represent various degrees of rotor damping. Line A, which represents the rotor behavior with zero damping, was obtained from Ref. 45. Line B represents the rotor performance with nonzero damping forces.

TABLE 1.—*Description of various modes of rotor motion*

| | Rotor speed | Damping | Precession rate, $\dot{\phi}$ | Rotor deflection, $\delta$ | Rotor phase angle, $\beta$ |
|---|---|---|---|---|---|
| Case 1: | | | | | |
| A | | $K_s = 0$* | $\dot{\phi} = \pm\omega_{CR}$ | $\delta = \delta_0 \pm e\omega_{CR}/2t$ | $\pm\pi/2$ |
| B | $\omega = \omega_{CR}$ | $K_s \to 0$ | $\dot{\phi} = \omega_{CR}$ | $\delta = \delta_0 + e\omega_{CR}/2t$ | $+\pi/2$ |
| C | | $K_s \neq 0$ | $\dot{\phi} = \omega_{CR}$ | $\delta = e\omega_{CR}/K_s$ | $+\pi/2$ |
| Case 2: | | | | | |
| A | | $K_s = 0$* | $\pm\omega$ | $\pm e\omega^2/(\omega^2 - \omega_{CR}^2)$ | $(1 \pm 1)\pi/2$ |
| B | $\omega \neq \omega_{CR}$ | $K_s \to 0$ | $\omega$ | $e\omega^2/\sqrt{(\omega^2 - \omega_{CR}^2)^2}$ | 0 if $\omega < \omega_{CR}$<br>$\pi$ if $\omega > \omega_{CR}$ |
| C | | $K_s \neq 0$ | $\omega$ | $e\omega^2/\sqrt{(\omega^2 - \omega_{CR}^2)^2 + (K_s\omega)^2}$ | $\mathrm{Tan}^{-1}[K_s\omega/(\omega_{CR}^2 - \omega^2)]$ |
| Case 3: | | | | | |
| A | | $K_s = 0$* | $\pm\omega$ | $\delta_0 + 9/4e\ [\cos\beta_0 - \cos(\beta_0 \pm 2\omega_{CR}t)]$ | Unrestricted |
| B | $\omega = 3\omega_{CR}$ | $K_s \to 0$ | $\omega_{CR}$ | $\delta_0 + 9/4e\ [\cos(\beta_0 + 2\omega_{CR}t) - \cos\beta_0]$ | Unrestricted |
| C | | $K_s \neq 0$** | $\omega_{CR}$ | $\delta_0 e^{-K_s/2t} + e\omega/2(1-n)((K_s/2)^2 + n^2\omega^2)^{-1/2}$ $\times [\cos(\beta_0 + 2\omega_{CR}t + \tan^{-1}(K_s/2\omega_{CR}))$ $- e^{-K_s/2t}(\cos(\beta_0 + \tan^{-1}(K_s/2\omega_{CR})))]$** | Unrestricted |
| Case 4: | | | | | |
| A | | $K_s = 0$* | $(\omega + \omega_{CR})/2$ | $2e\omega^2/(\omega_{CR}^2 - \omega^2)\cos[\beta_0 + 1/2(\omega \pm \omega_{CR})t]$ | $\mathrm{Cos}^{-1}(\delta_0(\omega_{CR}^2 - \omega^2)/2e\omega^2)$ |
| B | $\omega \neq \pm\omega_{CR}$ | $K_s \to 0$ | $(\omega + \omega_{CR})/2 = \omega$ | Same as 1B | Same as 1B |
| C | | $K_s \neq 0$ | $(\omega + \omega_{CR})/2 = \omega$ | Same as 1C | Same as 1C |

| | | | | | |
|---|---|---|---|---|---|
| Case 5: | | | | | |
| A..... | ..... | $K_s = 0$* | $\pm\omega_{CR}$ | $-9/4e \cos(\beta_0 \pm 2\omega_{CR}t)$ | $\cos^{-1}(-4\delta_0/9e)$ |
| B..... | $\omega = 3\omega_{CR}$ | $K_s \to 0$ | ..... | Suppressed transient | |
| C..... | ..... | $K_s \neq 0$ | ..... | Suppressed transient | |
| Case 6: | | | | | |
| A..... | $\omega \gg \omega_{CR}$ | $K_s = 0$ | Nonexistent | Nonexistent | |
| B..... | ..... | $K_s = 0$** | $t \to \infty$, $\phi^0 = \omega/2$ | $-2e \cos \omega/2t$ | Unrestricted |
| Case 7: | | | | | |
| A..... | $\omega = 1/2\omega_{CR}$ | $K_s = 0$ | $\omega$ | $-2\delta_{ST} \sin(\omega_{CR}t/2) + e/3$*** | 0 |
| B..... | $\omega = 1/2 \times \sqrt{\omega_{CR}^2 - 5/8K_s^2}$ | $K_s \neq 0$** | $\omega$ | $-2\delta_{ST}/(1+D^2)[\sin(\omega_{CR}t/2 - \beta) + D\cos(\omega_{CR}t/2 - \beta)] + e/3\sqrt{1+(2/3D)^2}$ | Same as 2C |

*Ref. (45).

**$K_s/2\omega \ll 1$.

***$\delta_{ST} = MG/K$.

It is important to note the influence of even small damping on the rotor characteristics. For example, in the first two cases which represent synchronous rotor precession, the introduction of damping eliminates the possibility of backward synchronous motion and also causes the rotor-phase relationship to be single valued. In case 1A and 1B, we see that if the rotor is running at the critical speed or resonance frequency, then the rotor amplitude will increase continuously with time. If the rotor damping is nonzero (1C), then the rotor amplitude will be bounded. The rotor deflection at the critical speed will be some multiple of the rotor unbalance $e$. This amplitude factor will be referred to as the rotor critical amplification factor, $A_{CR}=\omega_{CR}/K$ for a simple system, and we shall see later that it will be an important parameter in the study of rotor stability. Case 2 represents rotor synchronous precession in general. The rotor deflection given in 2C is identical to the results stated by Jeffcott[40] and Fig. 5 represents a plot of this function. Notice in 2C that damping causes the rotor-phase angle to be zero at low speed and increase smoothly with speed to a maximum value of $\pi$. This rotor-phase relationship is depicted in Fig. 4. For a single-mass rotor in which the motion is confined in a plane, there is only one phase angle. At the rotor critical speed of this system, the rotor-phase angle is 90° and the eccentricity vector is orthogonal to the rotor deflection. If additional degrees of freedom such as conical modes or multi-masses are introduced into the system, there will be additional rotor phase angles corresponding to each mode.

From the examination of Cases 1, 2, and 7, the following characteristics concerning rotor synchronous precession are summarized as follows:

1. For small values of the damping parameter and (or) $\omega \ll \omega_{CR}$, the phase angle $\beta$ is zero. Thus, for small damping and speeds below the first critical speed, the unbalance is in phase with the maximum deflection and the mass center rotates about the volume center.
2. As the rotor speed $\omega$ approaches the critical speed $\omega_{CR}$, the phase angle $\beta$ approaches $\pi/2$. At this speed, if no damping is present, amplitudes of vibration of dangerous proportions can result.
3. For the condition where $\omega \gg \omega_{CR}$ and low damping, the phase angle approaches $\pi$ as a limit. In this situation the volume center is revolving around the mass center and the force transmitted to the bearings reaches an asymptote equal to $Ke/2$.
4. If large amounts of damping are present in the system, a peak vibration is not observed at the system critical speed. The rotor deflection increases smoothly from 0 to $e$ as the rotor speed $\omega$ increases from 0 to $\omega \gg \omega_{CR}$.

5. The system critical speed increases slightly with an increase in viscous damping. The system critical corresponds to the natural lateral frequency of vibration $\omega$ only for the case when the damping is zero or the damping forces are proportionate to the velocity squared.[1]
6. The rotor phase angle is a single-valued and continuous function in a damped system.
7. Synchronous backward precession is not possible even in a lightly damped rotor.
8. A lightly damped horizontal rotor may exhibit a secondary critical speed effect when operating at one-half the rotor first critical speed. The rotor whirl orbit will be approximately twice the rotor static deflection (Case 7).

The Cases 3 through 6 represent various modes of whirling or nonsynchronous precession. For example, Case 3 shows that when the rotor speed reaches three times the rotor critical speed, the rotor is capable of forward or backward precession equal to the rotor critical speed $\omega_{CR}$. The inclusion of damping, however minute, eliminates the possibility of backward precession. If finite damping is considered, this motion is possible only if the system damping is light; i.e., if $K_s/2\omega_{CR} \ll 1.0$.

In all of the above cases of whirling in general, it was found that the inclusion of sufficient damping will suppress all whirl tendency and permit only synchronous forward rotor precession. The inclusion of damping into the equations of motion considerably changes the fundamental nature of the motion as described in Ref. 45. For example, Case 4 reduces to Case 1, and Case 5 vanishes altogether when damping is considered. Thus the only two distinct cases of whirling are Cases 3 and 6. Case 6 states that the rotor is capable of half-frequency whirling ($\phi^\circ = \omega/2$) when the rotor speed becomes infinitely high for a lightly damped system. Note that this conclusion, although unrealistic, cannot be obtained from a system in which the damping is excluded.

In conclusion, we find that it is impossible to examine or explain the occurrence of rotor whirling by means of a conservative system. It is impossible with this system to explain the rotor whirling as observed by Newkirk, Stodola, Pinkus, and others.

It will be shown later that whirling can occur only in nonconservative systems in which the system dissipation function possesses special characteristics. In the next chapter the early experimental findings

[1] See discussion by E. J. Gunter of "Dynamics of Synchronous-Precessing Turborotors . . . ," by T. M. Tang and P. R. Trumpler, *J. of Applied Mech.*, Mar. 1965, pp. 223–226.

of Newkirk will be evaluated and verified by including into the rotor equations of motion the influence of internal rotor friction damping. In subsequent chapters, the influence of hydrodynamic fluid-film bearings on self-excited whirling will be examined.

# Chapter 4

# Rotor Whirling Induced by Internal Friction Damping

It is clear from the analysis of Chapter 3 that the evaluation of the single-mass Jeffcott model does not lead to an explanation of the rotor whirl motion observed by Dr. Newkirk in 1924. In Chapter 3 the Jeffcott model was examined for whirling in general, with and without the influence of external viscous damping. Table 1 shows that the introduction of external damping into the system suppresses the transient rotor motion and allows only synchronous precessive motion due to rotor unbalance. To analyze the rotor whirl motion observed by Dr. Newkirk, the Jeffcott model will be extended to include the foundation characteristics, the bearing mass, and internal rotor friction.

## 4.1 DISCUSSION OF INTERNAL FRICTION DAMPING

As previously mentioned in Sec. 2.4, Kimball [47] in 1924 suggested that internal shaft friction could be responsible for shaft whirling. He postulated that below the rotor critical speed the internal friction would damp out the whirl motion, while above the critical speed the internal rotor friction would sustain the whirl. Later in 1925, Kimball and Lovell [51] performed extensive tests of the internal friction characteristics of various metallic and nonmetallic materials. (Additional discussion of the work of Kimball and Lovell and other investigators on hysteresis damping is given in App. A.) The experimental technique used to evaluate the magnitude of the internal friction was by measurements of the deflection characteristics of a vertically loaded, horizontal rotating shaft. If the shaft material were perfectly elastic, the application of a vertical load should cause only a corresponding vertical displacement. The presence of material hysteresis in the rotating, deflected shaft as its segments undergo alternate stress reversal cycles of compression and tension cause the shaft to deflect sideways. Kimball, by measurement of the shaft vertical inclination angle, was able to determine the ratio of the internal friction forces to the elastic shaft forces. His measurements showed that this ratio for most ferrous and nonferrous materials is between $(1 \text{ to } 2) \times 10^{-3}$.



219-720 O-66--4

## 4.2 EFFECT OF SHRINK FITS ON ROTOR INTERNAL FRICTION

Because of the small order of magnitude of the friction forces observed by Kimball, Newkirk concluded that the internal friction created by shrink fits of the impellers and spacers was the predominate cause of the observed whirl instability. He had observed that when all shrink fits were removed from his experimental rotor, no whirl instability could develop. Kimball, at Newkirk's suggestion, constructed a special test rotor with rings on hubs shrunk on the shaft.[48] He did indeed confirm Newkirk's conclusion that the frictional effect of shrink fits is a more active cause of shaft whirling than the internal friction within the shaft itself. Measurements showed that, even with the rather light shrinkages used in the tests, the effective internal friction may be increased from two to five times its original value. In fact, Kimball found that long clamping fits always lead to trouble with high-speed[1] rotors.[49]

For the case of a hub or a sleeve which is fastened to a shaft which is afterward deflected, either the surface fibers of the shaft must slip inside the sleeve as they alternately elongate and contract, or the sleeve itself must bend along with the shaft. Usually both actions occur simultaneously to an extent which depends upon the tightness of the shrink fit and the relative stiffness of the two parts. H. D. Taylor, after conducting numerous tests with various hub configurations, concluded that the axial contact length of shrink fits should be as short as permissible and as tight as possible without exceeding the yield strength of the material. Robertson[85] reports that even short, highly stressed shrink fits are not entirely devoid of problems. He states that even small, tight shrink fits may develop whirl instability, provided the rotor is given a sufficiently large initial disturbance or displacement to initiate relative internal slippage in the fit. If long shrink fits such as compressor wheels and impeller spacers must be employed, it is important that these pieces be undercut along the central region of the inner bore so that the contact area is restricted to the ends of the shrink fit. Robertson shows several designs of hubs and bosses which have been found to be beneficial in reducing internal friction effects.

Robertson also concludes that a similar effect can be produced by any friction which opposes a change of the deflection of the shaft, such as the friction which exists at the connections of flexible couplings, and even in "rigid" couplings. He referred to this group of friction forces as "hysteretic forces."

[1] A rotor is termed "high speed" if it operates above its first critical speed.

## 4.3 DISCUSSION OF THE EXPERIMENTAL INVESTIGATION AND CONCLUSIONS OF DR. NEWKIRK

The major conclusions that Dr. Newkirk stated on the behavior of shaft whirling due to internal rotor friction are summarized in Sec. 2.4. Of these conclusions, statement 6, concerning the influence of foundation flexibility, was the most perplexing to him. He remained at a loss to explain why foundation flexibility alone should improve the rotor stability.

In the early phase of his experimental investigation, his assistant, H. D. Taylor, discovered that any looseness in the bearing support or clamps which held the test model to the floor had a strong tendency to prevent whipping. Tests were conducted to determine whether bearing-support flexibility alone would prevent whipping or whether additional bearing damping was also required. Conclusions of the experiments indicated that bearing flexibility could prevent rotor whipping even without external bearing damping. Newkirk states in Ref. 63: "It is perhaps difficult to accept the view that flexibility only of the bearing support without any attendant damping or energy absorption in the bearing prevents whipping."

Following these experiments, special spring bearings were designed for the unstable turbocompressors, which incorporated flexibility and damping. Tests were conducted with this bearing arrangement on a three-bearing turbocompressor rotor, using a wide range of stiffness and damping values. In no case could the compressor be made to whip with the flexible bearing support. It was also found that the bearing damping was not necessary to suppress the whip.

It would appear that the introduction of foundation flexibility will lower the rotor first critical speed, as demonstrated by Linn and Prohl,[2] and hence reduce the whirl threshold speed in the absence of external damping. Instead, in all cases the rotor stability was improved! This question of foundation flexibility became even more of an enigma to Newkirk, when in 1925 he investigated shaft whirling caused by fluid film bearings.[65] When a spring-mounted bearing which was designed to avoid inherent damping was used on the rotor which exhibited oil-film whirl, instead of suppressing the instability it permitted a violent whipping to take place. In this case it was found that friction damping in the spring-mounted bearing was essential in stopping the whip motion.[3]

---

[2] F. C. Linn and M. A. Prohl, "The Effect of Flexibility of Support Upon the Critical Speeds of High-Speed Rotors," *Trans. SNAME*, Vol. 59, pp. 536–553.

[3] Further discussion of Newkirk's investigations on oil-film whirl is given in Ch. 6.

## 4.4. EQUATIONS OF MOTION FOR LIGHT DAMPING

### 4.4.1 Discussion of System and Assumptions

The system to be analyzed is shown in Fig. 7. Figure 7 represents the extended Jeffcott rotor to include foundation flexibility and bearing mass. The mass of the rotor is contained in a plane normal to line 0'0"

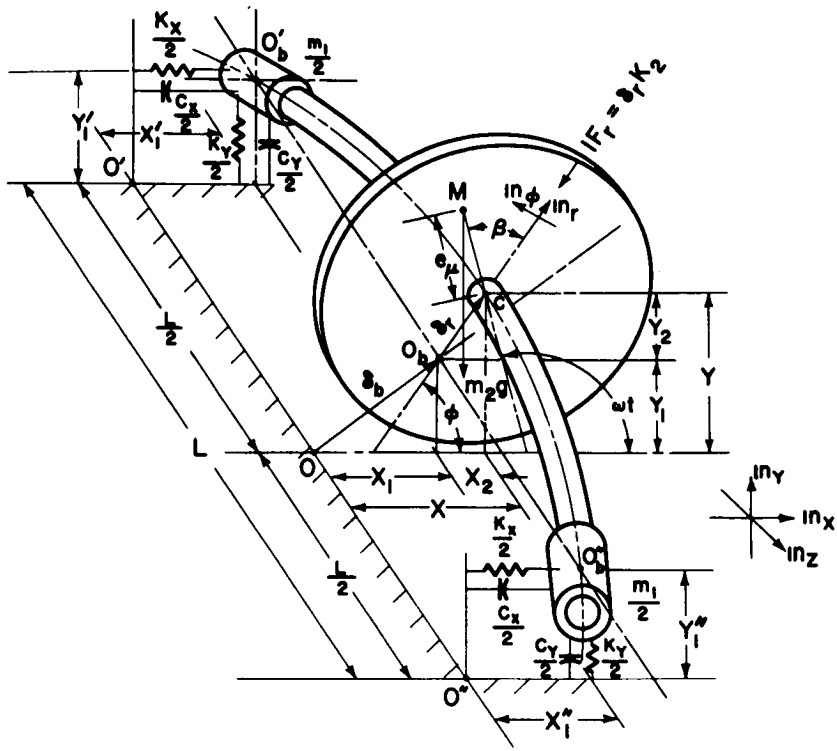


FIGURE 7.—General single-mass rotor on an elastic foundation.

which is situated midway between the two bearing locations. The major assumptions which will be employed in the simplified analysis are:

1. Zero bearing mass.
2. No gyroscopic forces.
3. The damping forces are small in comparison to the elastic forces.
4. The characteristics and displacements at both bearings are identical.
5. The rotor total angular velocity is constant.

If rotor unbalance is included, then Fig. 7 represents a system of five degrees of freedom.[4] If gyroscopic forces are included, the system would require seven degrees of freedom to represent it.

The assumption of constant angular rotor speed reduces the five degrees of freedom system to four. The assumption of zero bearing mass and light damping forces further reduces the system to two coupled second-order differential equations. The assumption that the rotor hysteresis damping forces are small in comparison to the elastic forces is in line with Kimball's experimental measurements.[5] This restriction will be removed in the general derivation.

### 4.4.2 Deflection Analysis

The displacement of the journal center is given by the position vector (see Fig. 8)

$$\vec{oP}_{O_b} = \vec{\delta}_b = X_1\vec{n}_x + Y_1\vec{n}_y \tag{4.1}$$

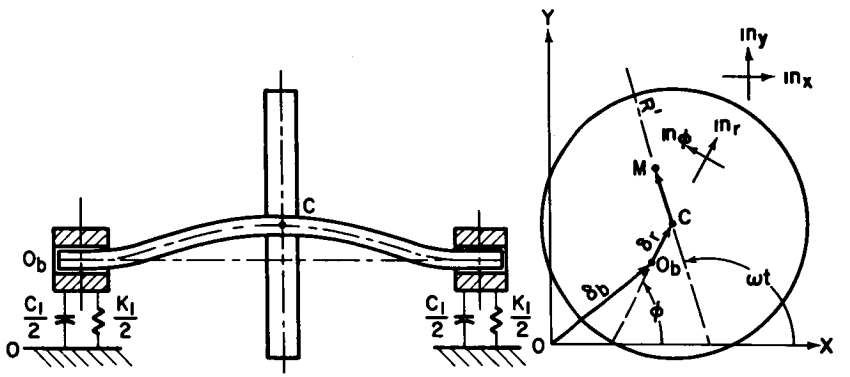


FIGURE 8.—Schematic representation of the Jeffcott rotor on an isotropic elastic foundation.

where $X_1$ and $Y_1$ are the Cartesian coordinates of point $O_b$ relative to point $O$, and the displacement of the rotor centerline at point $C_1$ is given by:

$$\vec{oP}_C = \vec{\delta}_r = X_2\vec{n}_x + Y_2\vec{n}_y \tag{4.2}$$

where $X_2$ and $Y_2$ are the Cartesian coordinates of point $C$ relative to point $O_b$ and $\vec{n}_x$, $\vec{n}_y$, and $\vec{n}_z$ represent a set of fixed unit vectors.

---

[4] The general five degrees of freedom system is given in Sec. 4.9.

[5] A. L. Kimball, Jr., "Measurement of Internal Friction in a Revolving Deflected Shaft," *G.E. Review*, vol. 28, No. 8, Aug. 1925, pp. 554–558.

The total displacement of the rotor center is given by

$$\vec{oP}_C = X\vec{n}_x + Y\vec{n}_y \tag{4.3}$$

where

$$\left.\begin{aligned} &\text{(a) } X = X_1 + X_2 \\ &\text{(b) } Y = Y_1 + Y_2 \end{aligned}\right\} \tag{4.4}$$

In general, the mass center of the rotor will not correspond to the rotor elastic axis at $C$. Only for the case of perfect balance will point $M$ correspond to point $C$. In this case $\vec{oP}_C = \vec{oP}_M$ and the equations of motion of the rotor will be given by

$$M\ddot{X} - F_x = 0 \qquad M\ddot{Y} - F_y = 0 \tag{4.5}$$

### 4.4.3 Bearing Forces

The forces exerted at the bearing or foundation at $O_b$ are assumed to be of the form

$$\left.\begin{aligned} F_x &= -C_x\dot{X}_1 - K_xX_1 \\ F_y &= -C_y\dot{Y}_1 - K_yY_1 \end{aligned}\right\} \tag{4.6}$$

For the case of a symmetric bearing support, the elastic and damping characteristics are uniform in all directions. The bearing force is given by

$$\vec{F}_b = -C_1\vec{V}_{o_b} - K_1\vec{\delta}_b \tag{4.7}$$

### 4.4.4 Shaft Characteristics

The forces acting on the shaft are the elastic restoring forces and the damping forces. Of importance in the calculation of rotor stability is the inclusion of rotary damping on the shaft caused by internal rotor friction. This will be defined as the damping which resists a change of strain of the flexible members.

Consider a rotating reference frame $R'$ which is revolving with an angular velocity of $\omega$. The rotor forces will be expressed in this system, since damping in the shaft is brought about by a change in configuration of the rotating shaft.

The forces acting at $C$ are given by (see App. A)

$$\vec{F}_c = -[C_2^{R'}\vec{V}_{C/o_b} + K_2\vec{\delta}_r] \tag{4.8}$$

where ${}^{R'}\vec{V}^{C/O_b}$ = velocity of point $C$ relative to $O$ in reference frame $R'$ or

$$ {}^{R'}\vec{V}^{C/O_b} = {}^{R}\vec{V}^{C/O_b} - \vec{\omega}\times\vec{\delta} = \dot{\phi}\delta\vec{n}_\phi + \dot{\delta}\vec{n}_r - \omega\delta\vec{n}_\phi \tag{4.9} $$

$$ \vec{F}_c = -[(C_2\dot{\delta}_r + K_2\delta_r)\vec{n}_r + C_2\delta_r(\dot{\phi}-\omega)\vec{n}_\phi] \tag{4.10} $$

The equations of transformation between the $\vec{n}_r$, $\vec{n}_\phi$ and the fixed Cartesian unit vector set $\vec{n}_x$ and $\vec{n}_y$ are given by

$$ \begin{pmatrix} \vec{n}_r \\ \vec{n}_\phi \end{pmatrix} = \begin{pmatrix} \cos\phi & \sin\phi \\ -\sin\phi & \cos\phi \end{pmatrix} \begin{pmatrix} \vec{n}_x \\ \vec{n}_y \end{pmatrix} \tag{4.11} $$

By taking the dot product of Eq. (4.10) with $\vec{n}_x$ and $\vec{n}_y$, the horizontal and vertical components are obtained

$$ \begin{aligned} &\text{(a)}\ F_x = \vec{F}_c\cdot\vec{n}_x = -[(C_2\dot{\delta}_r + K_2\delta_r)\cos\phi - C_2\delta_r(\dot{\phi}-\omega)\sin\phi] \\ &\text{(b)}\ F_y = \vec{F}_c\cdot\vec{n}_y = -[(C_2\dot{\delta}_r + K_2\delta_r)\sin\phi + C_2\delta_r(\dot{\phi}-\omega)\cos\phi] \end{aligned} \tag{4.12} $$

Since

$$ X_2 = \delta_r\cos\phi \qquad Y_2 = \delta_r\sin\phi $$

and

$$ \dot{X}_2 = \dot{\delta}_r\cos\phi - \delta_r\dot{\phi}\sin\phi \qquad \dot{Y}_2 = \dot{\delta}_r\sin\phi + \delta_r\dot{\phi}\cos\phi \tag{4.13} $$

Hence,

$$ \begin{aligned} &\text{(a)}\ F_x \underset{(4.12,\,13)}{=} -[C_2(\dot{X}_2 + \omega Y_2) + K_2X_2] \\ &\qquad F_y \underset{(4.12,\,13)}{=} -[C_2(\dot{Y}_2 - \omega X_2) + K_2Y_2] \end{aligned} \tag{4.14} $$

Combining Eqs. (4.4), (4.6), and (4.8) yields

$$ \left.\begin{aligned} &\text{(a)}\ F_x = -\frac{C_2K_x}{K_x+K_2}(X_2+\omega Y_2) - \frac{K_2C_1}{K_x+K_2}\dot{X}_1 - \frac{K_xK_2}{K_x+K_2}X \\ &\text{(b)}\ F_y = -\frac{C_2K_y}{K_y+K_2}(\dot{Y}_2-\omega X_2) - \frac{K_2C_1}{K_y+K_2}\dot{Y}_1 - \frac{K_yK_2}{K_1+K_2}Y \end{aligned}\right\} \tag{4.15} $$

If it is assumed that the damping forces are much smaller than the elastic forces, then Eqs. (4.15(a), (b)) become

$$\left.\begin{aligned}
&\text{(a) } F_x = -C_1\left(\frac{K_2}{K_x+K_2}\right)^2 \dot{X} - C_2\left(\frac{K_x}{K_x+K_2}\right)^2 (\dot{X}+\omega Y) - \frac{K_x K_2}{K_x+K_2} X \\
&\text{(b) } F_y = -C\left(\frac{K_2}{K_x+K_2}\right)^2 \dot{Y} - C_2\left(\frac{K_y}{K_y+K_2}\right)^2 (\dot{Y}-\omega X) - \frac{K_y K_2}{K_y+K_2} Y
\end{aligned}\right\} \quad (4.16)$$

### 4.4.5 Governing Equations

The equations of motion of the system including rotor unbalance and gravity are given by

$$\left.\begin{aligned}
&\ddot{X} + (\mu_x + \nu_x)\dot{X} + \omega\sqrt{\mu_x \mu_y}\, Y + \omega_{cx}^2 X = e_\mu \omega^2 \cos \omega t \\
&\ddot{Y} + (\mu_y + \nu_y)\dot{Y} - \omega\sqrt{\mu_x \mu_y}\, X + \omega_{cy}^2 Y = e_\mu \omega^2 \sin \omega t + g
\end{aligned}\right\} \quad (4.17)$$

where

$$\mu_x = \frac{C_2}{M}\left(\frac{K_y}{K_x+K_2}\right)^2 = D_2\left(\frac{\alpha}{\alpha+R}\right)^2$$

$$\mu_y = \frac{C_2}{M}\left(\frac{K_y}{K_y+K_2}\right)^2 = D_2\left(\frac{1}{1+R}\right)^2$$

$$\nu_x = \frac{C_1}{M}\left(\frac{K_2}{K_x+K_2}\right)^2 = D_1\left(\frac{\alpha}{\alpha+R}\right)^2$$

$$\nu_y = \frac{C_1}{M}\left(\frac{K_2}{K_y+K_2}\right)^2 = D_1\left(\frac{R}{1+R}\right)^2$$

$$D_1 = \frac{C_1}{M}, \qquad D_2 = \frac{C_2}{M}, \qquad R = \frac{K_2}{K_y}, \qquad \alpha = \frac{K_x}{K_y}$$

$\omega_{cx}$ = natural system resonance frequency for the $X$ direction.

$$= \sqrt{\frac{K_2 K_x}{M(K_2+K_x)}} = \omega_{CR_0}\sqrt{\frac{\alpha}{R+\alpha}}$$

$\omega_{cy}$ = natural system resonance frequency for the $Y$ direction.

$$= \sqrt{\frac{K_2 K_y}{M(K_2+K_y)}} = \omega_{CR_0}\sqrt{\frac{1}{1+R}}$$

$\omega_{CR_0}$ = rotor natural resonance frequency on rigid supports.

## 4.5 ROTOR SYNCHRONOUS PRECESSION

The system equations of motion may be combined in complex form by the following representation.

$$Z = X + iY \tag{4.18}$$

The Eqs. (4.17) combine to yield the following

$$\ddot{Z} + \left(\frac{C_x + C_y}{2}\right)\dot{Z} + \left(\frac{C_x - C_y}{2}\right)\dot{\bar{Z}} + \left(\frac{\omega_{cx}^2 - \omega_{cy}^2}{2}\right)\bar{Z} + \left[\frac{\omega_{cx}^2 + \omega_{cy}^2}{2} - i\omega\sqrt{\mu_x \mu_y}\right] Z = e_\mu \omega^2 e^{i\omega t} + ig \tag{4.19}$$

where

$$C_x = \mu_x + \nu_x$$

$$C_y = \mu_y + \nu_y$$

The unsymmetric stiffness and damping terms of Eq. (4.17) lead to complex conjugate terms in $\bar{Z}$. The appearance of the complex conjugate term $\bar{Z}$ in the complex vector representation implies the existence of rotor backward precessive motion. The steady-state synchronous precessive motion may be expressed as

$$Z = fe^{i\omega t} + be^{-i\omega t} \tag{4.20}$$

where $f$ is the complex amplitude of the forward precessive motion and $b$ is the complex amplitude of the backward component. Rewriting Eq. (4.19) in the form

$$\ddot{Z} + D_f \dot{Z} + D_b \dot{\bar{Z}} + K_b \bar{Z} + [K_f - iS]Z = e_\mu \omega^2 e^{i\omega t} \tag{4.21}$$

Substitution of $Z$ and $\bar{Z}$ and derivatives yield the following two equations:

$$\begin{aligned} &\text{(a)}\ [(K_f - \omega^2) + i(D_f\omega - S)]f + [K_b + i\omega D_b]\bar{b} = e_\mu \omega^2 \\ &\text{(b)}\ [(K_f - \omega^2) - i(D_f\omega + S)]b + [K_b - i\omega D_b]\bar{f} = 0 \end{aligned} \tag{4.22}$$

Solving for the complex amplitudes $f$ and $b$

$$f = \frac{[(K_f - \omega^2) + i(D_f\omega + S)]e_\mu \omega^2}{(K_f - \omega^2)^2 + \omega^2(D_b^2 - D_f^2) + S^2 - K_b^2 + 2i\omega(D_f S(K_f - \omega^2) - D_f K_b)} \tag{4.23}$$

and

$$b=\frac{[K_b-i\omega D_b]\bar{f}}{[(K_f-\omega^2)-i(D_f\omega+S)]}$$

The functions $f$ and $b$ which represent the complex rotor may be converted into a real component and a phase angle by the following procedure:

$$f=\frac{A+iB}{C+iD}=\frac{AC-BD+i(CB+AD)}{C^2+D^2}$$

$$f=U+iV \tag{4.24}$$

$$Z_f=fe^{i\omega t}=A_fe^{i(\omega t-B_f)} \tag{4.25}$$

Expanding and grouping terms were obtained

$$A_f=\sqrt{U^2+V^2}, \qquad B_f=\tan^{-1}\frac{V}{U}$$

Thus the rotor displacement may be expressed in the real form

$$Z=A_fe^{i(\omega t-B_f)}+A_be^{-i(\omega t-B_b)} \tag{4.26}$$

Where the functions $A_f$ and $A_b$ are the rotor amplification factors for forward and backward synchronous precession, respectively. These components combine to form ellipses in which the principal axis will vary from the horizontal to the vertical position depending upon the bearing damping and stiffness parameters. Figure 9 illustrates typical rotor synchronous precession as given by Eq. (4.26). Notice that as the rotor speed $\omega$ increases, the semimajor and semiminor axes of the elliptic orbit reach a maximum value and then reduce. Examination of the functions $A_f$ and $A_b$ reveals that they are speed dependent and have a maximum value.

Differentiating the functions $A_f$ and $A_b$ by $\omega$ and setting the results equal to zero, we obtain for the case of light rotor damping

$$\left.\begin{aligned} A_{f\max}&=A_{cf}; \qquad \omega=\omega_{cf}\\ A_{b\max}&=A_{cb}; \qquad \omega=\omega_{cb}\end{aligned}\right\} \tag{4.27}$$

where $\omega_{cf}$ = critical speed for forward precession

$$=\sqrt{\frac{\omega_{cx}^2+\omega_{cy}^2}{2}}=\sqrt{\frac{K_2\{K_2(K_x+K_y)+2K_yK_y\}}{2M(K_2+K_x)(K_2+K_y)}}$$

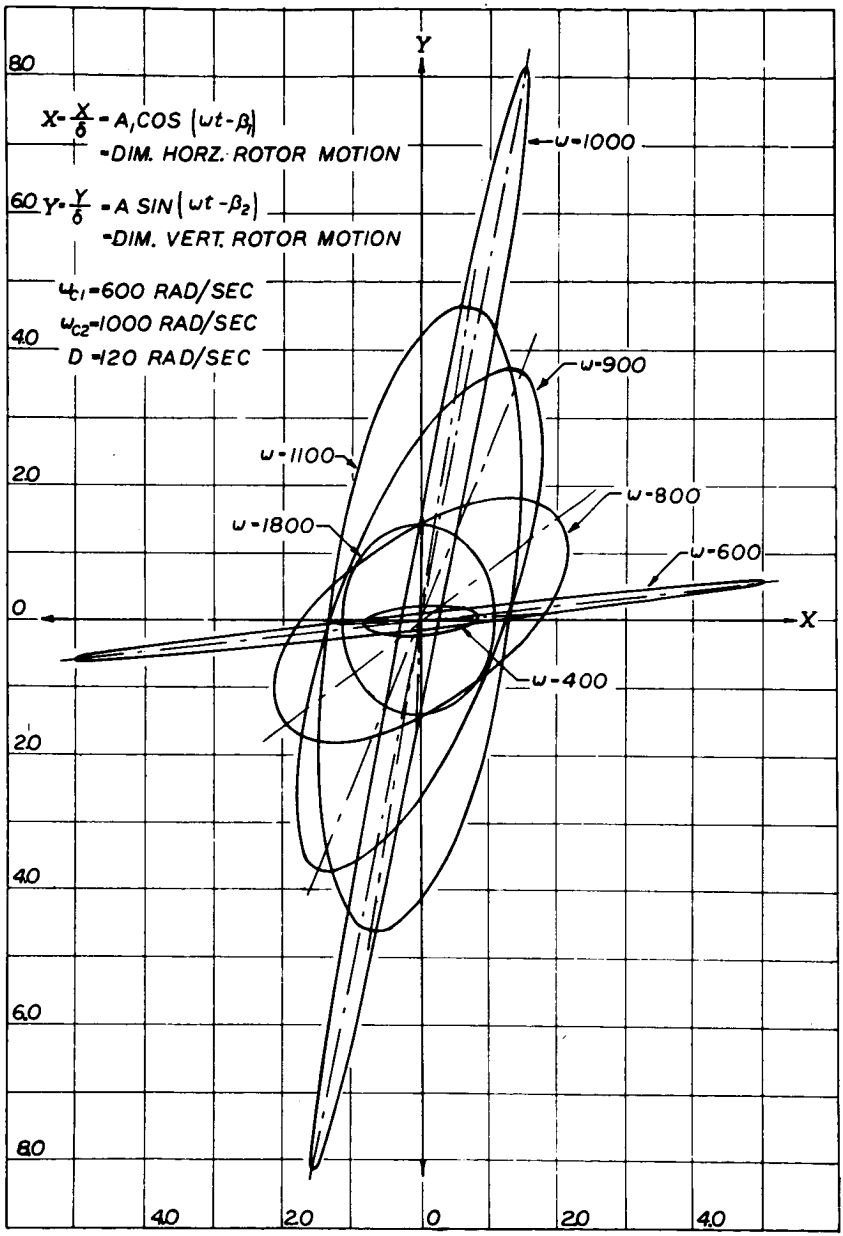


FIGURE 9.—Rotor orbit patterns for synchronous precession.

and

$$\omega_{cb} = \text{critical speed for backward precession}$$

$$= \sqrt{\frac{\omega_{cx}^2 - \omega_{cy}^2}{2}} = \sqrt{\frac{K_2^2(K_x - K_y)}{2M(K_2 + K_x)(K_2 + K_y)}}$$

When the rotor speed $\omega$ becomes very high such that

$$\omega \gg \omega_{cf};\ \omega_{cb}$$

the rotor amplification factors $A_f$ and $A_b$ reduce and approach $e_\mu$ as a limit. In Fig. 9, the rotor $X, Y$ displacements are made nondimensional with respect to the rotor unbalance $e_\mu$. At very high $\omega$, the rotor orbit becomes a circle of unity radius. This represents supercritical speed operation in which the mass center $M$ remains stationary and the elastic center $C$ traces out an orbit of radius $e_\mu$ about $M$.

In general, any rotor system which has nonsymmetric support flexibility will exhibit elliptic orbits. As an example, in Chapter 5 are presented oscilloscope traces of a high-speed rotor supported on air-lubricated pivoted pad bearings. Since this rotor has nonsymmetric bearing characteristics, it has distinct elliptic orbits.

## 4.6 NONSYNCHRONOUS ROTOR PRECESSION—SYMMETRIC BEARING SUPPORT

The rotor synchronous precessive motion given by Eq. (4.26) is caused by rotor unbalance. If the rotor were perfectly balanced ($e_\mu = 0$), then the rotor amplification factors $A_f$ and $A_b$ would both be identically zero. This implies that the steady-state synchronous motion is zero. This transient rotor motion under normal conditions dies out with time if damping is present in the system, leaving only the steady-state rotor motion. The influence of internal or hysteresis damping causes the motion to grow rather than die out at a particular threshold speed. Robertson[6] speaks of this as sustained transient motion. To investigate the transient rotor motion, the homogeneous Eqs. (4.17) are examined. The two second-order equations have displacement cross-coupling. By the elimination of one of the displacement variables, the two second-order equations may be combined into a single fourth-order equation in either $X$ or $Y$. For example, elimination of the $Y$ coordinate results in the following fourth-order equation in $X$:

$$\dddot{X} + [C_x + C_y]\ddot{X} + [\omega_{cx}^2 + \omega_{cy}^2 + C_x C_y]\dot{X} + [\omega_{cx}^2 C_y + \omega_{cy}^2 C_x]\dot{X} + [\omega_{cx}^2 \omega_{cy}^2 + \omega^2 \mu_x \mu_y]X = 0 \qquad (4.28)$$

[6] D. Robertson, "Hysteretic Influences on the Whirling of Rotors," *Phil. Mag.*, S. 7, Vol. 19, 1932, pp. 513–537.

The assumption of a solution of the form $X = ae^{\lambda t}$ leads to the following algebraic equation in $\lambda$

$$\sum_{K=0}^{N=4} A_{n-k}\lambda^K = 0 \tag{4.29}$$

### 4.6.1 Routh-Hurwitz Stability Criterion

Investigation of the stability of motion of Eq. (4.28) can be easily done if the characteristic equation has been solved and its roots are known. But equations of third order and higher are not readily solved without considerable labor, although with the high-speed digital computer at our disposal, this does not represent an overwhelming problem. The question of stability in linear systems can be resolved without solving the characteristic equation. The stability of the system is determined by the sign of the real components of the roots to the characteristic equation. The system will be stable and nonoscillatory in the steady state if all of the roots of the characteristic equation have negative real parts. It will be stable but oscillatory if the conjugate imaginary roots are all different. It will be unstable if there are roots with real positive terms or if there are repeated zero or conjugate imaginary roots.

Routh[88] presented a method to determine whether any root contains a real positive term by examination of the coefficients of the characteristic equation. This procedure was later generalized by Hurwitz[38] in 1895 in determinant form. The Routh-Hurwitz stability array for $N=4$ is given by

$$D = \begin{array}{c|cccc} & D_0 & D_1 & D_2 & D_3 \\ \hline & A_1 & A_0 & 0 & 0 \\ & A_3 & A_2 & A_1 & A_0 \\ & 0 & A_4 & A_3 & A_2 \\ & 0 & 0 & 0 & A_4 \end{array} \tag{4.30}$$

The condition of stability is that all of the $D_n$ determinants must be positive. For a fourth-order equation, these conditions are

$$
\left.
\begin{aligned}
D_0 &= A_1 = C_x + C_y > 0 \\
D_1 &= A_1 A_2 - A_0 A_3 > 0 \\
&= [C_x + C_y][\omega_{cx}^2 + \omega_{cy}^2 + C_x C_y] \\
&\quad - [\omega_{cx}^2 C_y + \omega_{cy}^2 C_x] \\
&= \omega_{cx}^2 C_x + \omega_{cy}^2 C_y + C_x C_y (C_x + C_y) > 0 \\
D_2 &= A_3[A_2 A_1 - A_0 A_3] - A_1^2 A_4 > 0 \\
&= A_3 D_1 - A_4 D_0^2 > 0 \\
D_3 &= A_4 D_2 > 0
\end{aligned}
\right\} \tag{4.31}
$$

The determinants $D_0$ and $D_1$ are always positive definite functions in the above example. The $D_2$ determinant leads to the stability criterion that:

$$
[\omega_{cx}^2 - \omega_{cy}^2] + [C_x + C_y][C_x \omega_{cy}^2 + C_y \omega_{cx}^2] > \frac{\omega^2 \mu_x \mu_y [C_x + C_y]^2}{C_x C_y} \tag{4.32}
$$

After some algebraic manipulation, the rotor threshold of stability is given by

$$
\omega_s = \omega_{\mathrm{CR}_0} \sqrt{F_1 + F_2} \tag{4.33}
$$

where

$$
F_1 = \left(\frac{\omega_{\mathrm{CR}_0}}{D_2}\right)^2 \frac{[R^2 + D][R^2 + D\alpha^2] R^2 (\alpha + R)^2 (1 + R)^2 (1 - \alpha)^2}{\{\alpha[(1 + R)^2 (R^2 + D\alpha^2) + (\alpha + R)^2 (R^2 + D)]\}^2}
$$

$$
F_2 = \frac{(R^2 + D)(R^2 + D\alpha^2)}{D^2 \alpha^2} \left[\frac{\alpha(R + \alpha)(R^2 + D) + (R + 1)(R^2 + D\alpha^2)}{(R + 1)^2 (R^2 + D\alpha^2) + (R + \alpha)^2 (R^2 + D)}\right]
$$

where

$$
R = \frac{K_2}{K_y} \qquad D = \frac{D_2}{D_1}
$$

$$
\alpha = \frac{K_x}{K_y} \qquad A = \frac{\omega_{\mathrm{CR}_0}}{D_2}
$$

### 4.6.2 Symmetric Bearing Support

For the case of a symmetric foundation, the horizontal and vertical bearing stiffness coefficients are equal

$$K_y = K_x = K_1$$

and hence $\alpha = 1$.

The stability criteria in this case reduces to

$$\omega_{s \lim \alpha \to 1} = \omega_{CR_0}\sqrt{F_2}$$

$$\omega < \omega_s = \omega_{CR_0}\sqrt{\frac{1}{1+R}\left(1+\frac{R^2}{D}\right)} \tag{4.34}$$

*Example 1*

As an illustration of Eq. (4.34), consider the following example

$$K_1 = K_2 = 250\,000 \text{ lb/in}, \quad R = 1$$

$$D_1 = D_2 = 200 \text{ rad/sec}, \quad D = 1$$

$$M = 0.25 \text{ lb-sec}^2/\text{in}$$

The rotor critical speed on rigid supports is

$$\omega_{CR_0} = \sqrt{\frac{K_2}{M}} = 1000 \text{ rad/sec}$$

The threshold of stability is given by

$$\omega_s = \omega_{CR_0}\sqrt{\frac{1}{1+R}}\left(1+\frac{R^2}{D}\right) = 1000\left(\frac{2}{\sqrt{2}}\right)$$

$$= 1414 \text{ rad/sec}$$

Figure 10 represents a plot of the stability criterion of Eq. (4.34). This simple relationship verifies a number of Newkirk's findings.[7]

[7] Recently C. Bellmot, apparently unaware of Newkirk and Kimball's early work, conducted experiments on internal friction whirling to determine the influence of external damping. He concludes that external damping forces favor stability and that the ratio of the two frictions to one another plays a far greater part than their absolute values. His experimental rotor is a close representation of the Jeffcott model. (See "The Effect of Friction on the Stability of a Rotating Shaft," *Brown Boveri Review*, Vol. 49, No. 12, pp. 48–55, 1962, for further details.)

For example, if the foundation is rigid, $R=0$ and the rotor is unstable above the critical speed. Figure 10 shows that, in general, the rotor stability threshold is always equal to or greater than the system critical

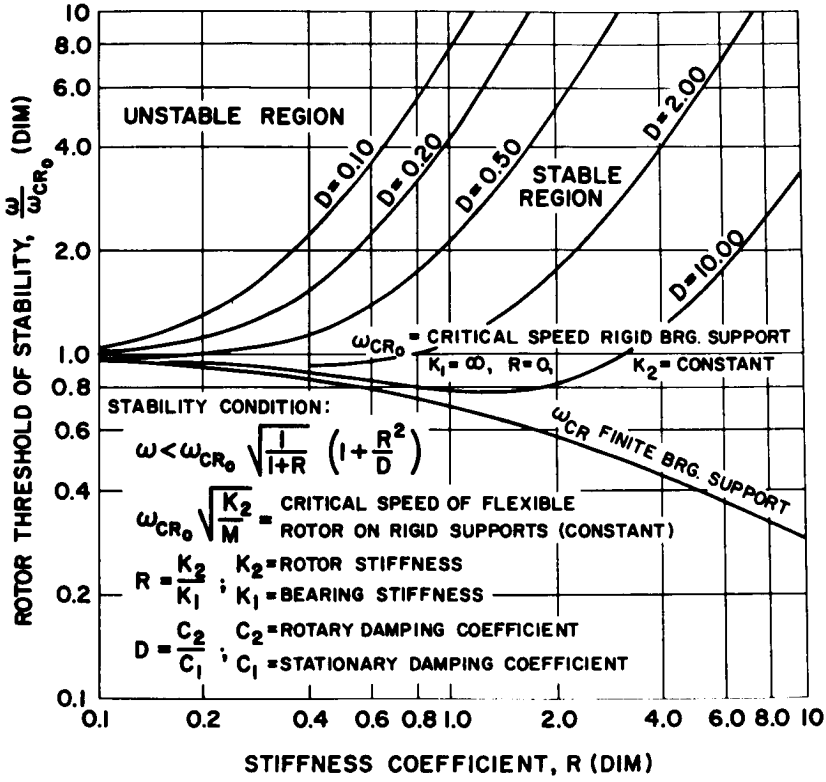


FIGURE 10.—Stability threshold of a flexible rotor with internal friction on a symmetric elastic bearing support.

speed and is a function of the ratio of the damping terms $C_1$ and $C_2$ and the stiffness coefficients $K_1$ and $K_2$. Note that if no damping is introduced into the foundation ($D_1=0$), the stability criterion reduces to

$$\omega_s=\omega_{CR_0}\sqrt{\frac{1}{1+R}}=\omega_{CR}$$

This implies that if we introduce bearing flexibility but no bearing damping, we will reduce the system critical speed and the whirl threshold speed. This does not seem to agree with Newkirk's findings that greater stability can be achieved by foundation flexibility alone. The stability criterion for a symmetric foundation states that both foundation flexi-

bility and damping must be incorporated to increase rotor stability. To resolve this question, it is necessary to examine the influence of foundation asymmetry on the rotor stability.

### 4.6.3 Rotor Precession Speed

The analysis of Sec. 4.6.1 does not furnish information on the behavior of the system such as the rotor precession speed and the growth rate of the unstable orbit. The Routh-Hurwitz stability criterion furnishes us only with the onset speed at which instability begins. We shall see in subsequent chapters that this criterion can give us misleading stability information in certain limiting cases, thus requiring the development of additional criteria.

To determine the rotor nonsynchronous precession rate, we proceed as follows:

For a symmetric, balanced rotor, Eq. (4.21) reduces to the following complex vector equation

$$\ddot{Z} + D_f\dot{Z} + [k_f - iS]Z = 0 \tag{4.36}$$

where

$$D_f = \frac{D_2}{(1+R)^2}\left[1+\frac{R^2}{D}\right]$$

$$D = \frac{D_2}{D_1}$$

$$k_f = \omega_{CR}^2 = \frac{K_2K_1}{M(K_2+K_1)} = \omega_{CR_0}^2\left(\frac{1}{1+R}\right)$$

$$S = \omega D_2\left(\frac{1}{1+R}\right)^2$$

Assume a solution of the form

$$Z = Ae^{\lambda t}$$

This results in the following frequency equation

$$\lambda^2 + D_f\lambda + k_f - iS = 0 \tag{4.37}$$

In general, the value of $\lambda$ is complex

$$\lambda = P + i\Omega$$

Substitution of the above into Eq. (4.37) and separating real and imaginary parts results in

$$\left.\begin{aligned} &\text{(a)}\ P^2-\Omega^2+D_fP+k_f=0 \\ &\text{(b)}\ 2P\Omega+D_f\Omega-S=0 \end{aligned}\right\} \tag{4.38}$$

By eliminating $\Omega$ from Eqs. (4.38(a), (b)), one obtains

$$4P^4+8D_fP^3+(5D_f^2+4k_f)P^2+(4D_fk_f+D_f^2)P+D_f^2k_f-S^2=0 \tag{4.39}$$

From the assumed form of the solution, it can be seen that if:

$P>0$ system is unstable (displacements will grow exponentially with time)
$P<0$ system is stable (motion is damped out)

at the threshold of stability we have the condition that $P=0$, which implies

$$D_f^2k_f-S^2=0$$

or expanding

$$\frac{D_2^2}{[1+R^2]^4}\left[-\omega^2+\frac{\omega_{CR_0}^2}{1+R}\left(1+\frac{R^2}{D}\right)^2\right]=0 \tag{4.40}$$

Close inspection reveals that the bracket expression is the Routh stability criterion of Eq. (4.34). If the hysteresis damping coefficient $D_2$ is nonzero, then the threshold speed is

$$\omega_s=\frac{\omega_{CR_0}}{\sqrt{1+R}}\left[1+\frac{R^2}{D}\right]$$

Notice that as $D_2$ approaches zero, Eq. (4.40) is identically satisfied and the Routh criterion is not applicable. We shall see later that application of Routh's criterion in such limiting cases can be misleading. An important parameter to examine is the rate of change of the real root $P$. Near the threshold of stability, $P$ is approximated by

$$P=\frac{S^2-D_f^2k_f}{D_f[4k_f+D_f^2]}=\frac{D_2^2[\omega^2-\omega_s^2]}{[1+R^2]^2[4\omega_{CR}^2+D_f^2][D_2+D_1R^2]} \tag{4.41}$$

Thus $P$ is negative when $\omega<\omega_s$ and positive when $\omega$ exceeds the threshold. In the limit as $D_2$ approaches zero, Routh's criterion will predict a threshold speed, but we see that in this case the real root $P$ also ap-

proaches zero. Hence the system is stable in this limiting case, since the orbital motion will not grow.

By eliminating $P$ from Eq. 4.38, we obtain

$$\Omega^4 + \left(\frac{D_f^2}{4} - k_f\right)\Omega^2 - \frac{S^2}{4} = 0 \tag{4.42}$$

solving for $\Omega^2$

$$\Omega^2 = \frac{\omega_{CR}^2 - \left(\frac{n_1+n_2}{2}\right)^2 \pm \sqrt{\left\{\left(\frac{n_1+n_2}{2}\right)^2 - \omega_{CR}^2\right\}^2 + (\omega n_2)^2}}{2} \tag{4.43}$$

where

$n_1 = D_1\left(\frac{R}{1+R}\right)^2$ = stationary damping coefficient of the bearing supports

$n_2 = D_2\left(\frac{1}{1+R}\right)^2$ = rotating damping coefficient of the shaft

From Eq. (4.34) it was found that at the threshold of instability $\omega = \omega_{CR}(1 + n_1/n_2)$. Introducing this conduction into the above, we obtain

$$\omega_P^2 = \frac{\omega_{CR}^2 - \left(\frac{n_1+n_2}{2}\right)^2 \pm \sqrt{\left(\frac{n_1+n_2}{2}\right)^4 + \frac{1}{2}\omega_{CR}^2(n_1+n_2)^2 + \omega_{CR}^4}}{2}$$

$$= \frac{\omega_{CR}^2 - \left(\frac{n_1+n_2}{2}\right)^2 \pm \left[\omega_{CR}^2 + \left(\frac{n_1+n_2}{2}\right)^2\right]}{2} \tag{4.44}$$

or

$$\omega_{p+}^2 = \omega_{CR}^2 \qquad \omega_{p-}^2 = -\tfrac{1}{2}(n_1+n_2)^2$$

Consider only the positive root or that

$$\boxed{\omega_P = \omega_{CR}} \qquad \text{when } \omega = \omega_s$$

The above statement implies that at the threshold of instability, the volume center $C$ of the rotor will precess in a forward direction at a rate equal to the first-system critical speed. Newkirk observed that the rotor precession rate was equal to the first critical speed and that it remained constant when the rotor speed was well above the threshold of stability. To illustrate this, consider the following example:

*Example 2*

Rotor conditions are identical to Example 1. The whirl precession rate is given by Eq. (4.43) in modified form as

$$\omega_P = \frac{\omega_{CR}}{2}\sqrt{1-\left(\frac{D}{4\omega_{CR}}\right)^2+\sqrt{\left\{1-\left(\frac{D}{4\omega_{CR}}\right)^2\right\}^2+\left(\frac{\omega}{\omega_{CR}}\right)^2\left(\frac{D}{4\omega_{CR}}\right)^2}}$$

note that

$$\left(\frac{D}{4\omega_{CR}}\right)^2=\left(\frac{200 \text{ rad/sec}}{4\times 706 \text{ rad/sec}}\right)^2=0.005 \ll 1$$

Hence, expanding in terms of $\left(\frac{D}{4\omega_{CR}}\right)^2$

$$\omega_P = \omega_{CR}\left[1+\frac{1}{8}\left(\frac{\omega}{\omega_{CR}}\right)^2\left(\frac{D}{4\omega_{CR}}\right)^2\right]$$

or

$$\underline{\underline{\omega_P = \omega_{CR} = \text{constant}}}$$

Thus, for all practical purposes we can say that the rotor precession rate is constant over a wide speed range.

### 4.6.4 Analog Computer Program—No. 1

In order to develop a better understanding of the rotor behavior and the transition from stable to unstable motion, the Eqs. (4.17) were programed on the 1631 R PACE analog computer. (See App. B.1 for the computer program and details.)

These equations were programed to include the effects of rotor unbalance and gravity.

### 4.6.5 Whirling of a Balanced Horizontal Rotor

The first conditions run on the analog computer were those corresponding to a balanced ($e_\mu = 0$) horizontal rotor. When the computer program was run for a number of speeds, including values well above the threshold of stability, absolutely nothing happened! Newkirk had observed that if the rotor system was well balanced, the rotor could maintain stability well above the threshold value. He found that in these cases it was necessary to give the system an initial disturbance to initiate whirling. Examination of Eqs. (4.17), including rotor unbalance, shows that they are satisfied by the following steady-state values

$$Y_0 = \frac{g}{\omega_{CR}^2\left[1+\left(\frac{\omega D_2}{\omega_{CR}}\left(\frac{1}{1+R}\right)^2\right)^2\right]}$$

$$Y_0 \approx \frac{g}{\omega_{CR}^2} = \frac{Mg}{K_T}$$

$$X_0 = \frac{\omega D_2}{\omega_{CR}^2(1+R)^2} \quad Y_0 = \frac{\omega D_2 g}{\omega_{CR}^2(1+R)^2} \tag{4.45}$$

Thus in order to observe whirl, the system must be given an initial displacement from the steady-state equilibrium position. The initial conditions used in the program were $X_0 = \dot{X}_0 = \dot{Y}_0 = 0$ and $Y_0 = Y_1(0)$. The last condition states that, initially, only the foundation deflects while the rotor is undeformed. Figure 11 represents the transient rotor

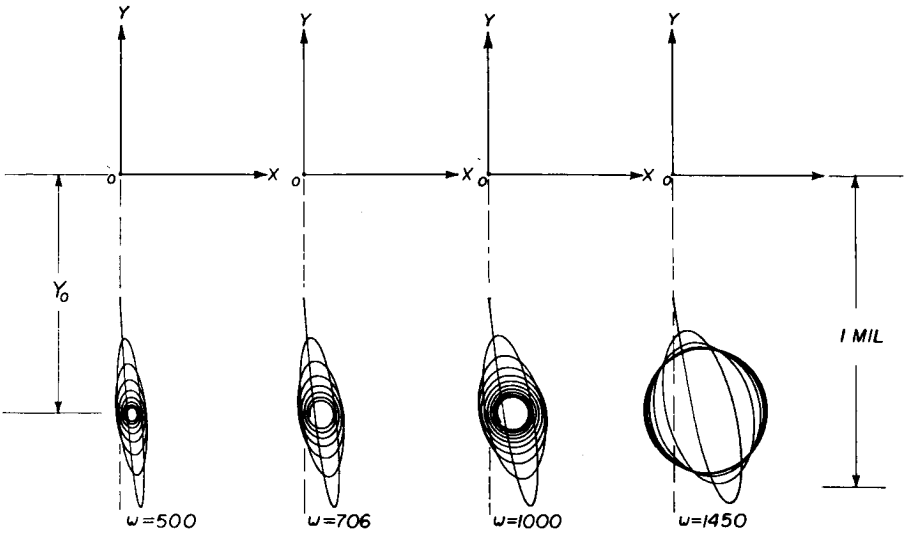


FIGURE 11.—Whirl orbits of a balanced horizontal rotor below the threshold of stability, $\omega < \omega_s$. Conditions: $M = 0.25$ lb sec²/in., $K_1 = K_2 = 250\,000$ lb/in., $D_1 = D_2 = 200$ rad/sec, $\omega_s = 1412$ rad/sec.

motion of a balanced horizontal rotor for various speeds up to the stability threshold. Note that when the undeflected rotor is released, it oscillates about the steady-state equilibrium position, as given by Eq. (4.45). As the rotor speed is increased, the hysteresis damping diminishes and the motion is not as rapidly damped out. At the threshold of stability $\omega = 1450$, a definite sustained orbit has developed which does not damp out. Figure 12 represents the motion of the system when the rotor speed is well above the whirl threshold speed. In this case, when the rotor is released, it deflects and then goes into a rapidly increasing spiral. At this speed the internal friction force has altered

its characteristic from a damping mechanism to a driving force. The rotor unstable precession rate is approximately equal to the rotor first critical speed as given by Eq. (4.44). The rotor precession speed is easily determined from examination of strip charts of the $X$–$Y$ motion of the system.

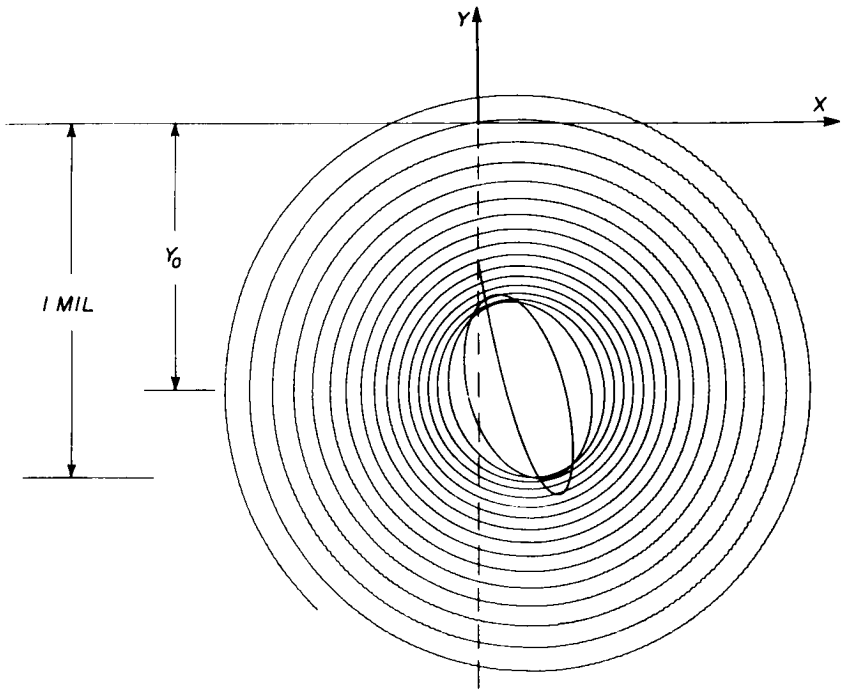


FIGURE 12.—Whirl orbit of a balanced horizontal rotor above the threshold of stability, $\omega > \omega_s$. Conditions: $\omega_{CR} = 706$ rad/sec, $\omega_s = 1412$ rad/sec, $\omega = 1700$ rad/sec.

Figure 13 represents the transient motion of a balanced horizontal rotor from the speed range of 500 to 750 rad/sec. The conditions are identical to the conditions stated in Fig. 11. In this figure, the top trace of each set is a reference sine wave to represent rotor speed. The next trace is the transient shaft $Y$ motion of point $C$ on the rotor, and the lower trace represents the shaft horizontal motion. In the four speed runs, it is seen that when the shaft is released, it oscillates about the steady-state equilibrium position at a frequency equal to the rotor first critical speed and is soon damped out. A change in running speed has little influence on the rotor frequency of oscillation.

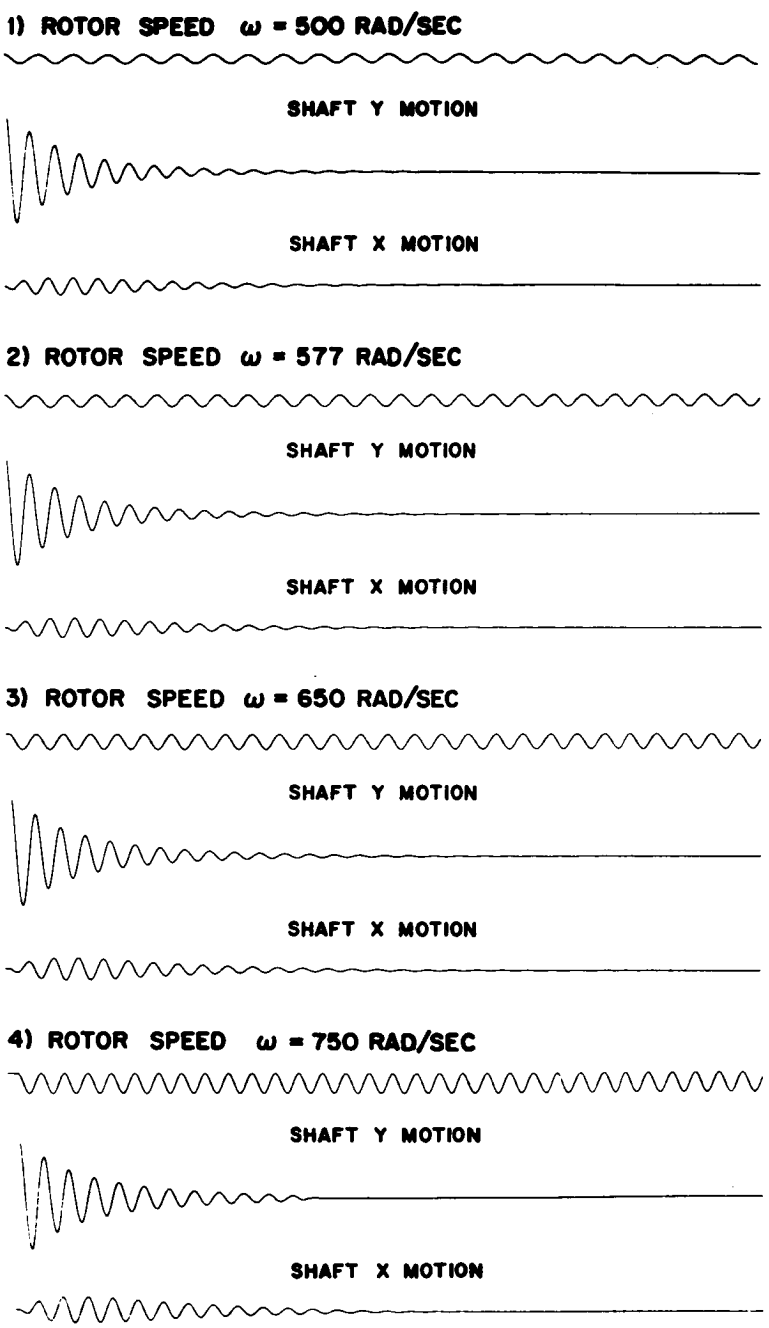


FIGURE 13.—Transient motion of a balanced horizontal rotor with internal friction damping, $\omega = 500$–$700$ rad/sec. Stability threshold, $\omega_s = 1412$ rad/sec.

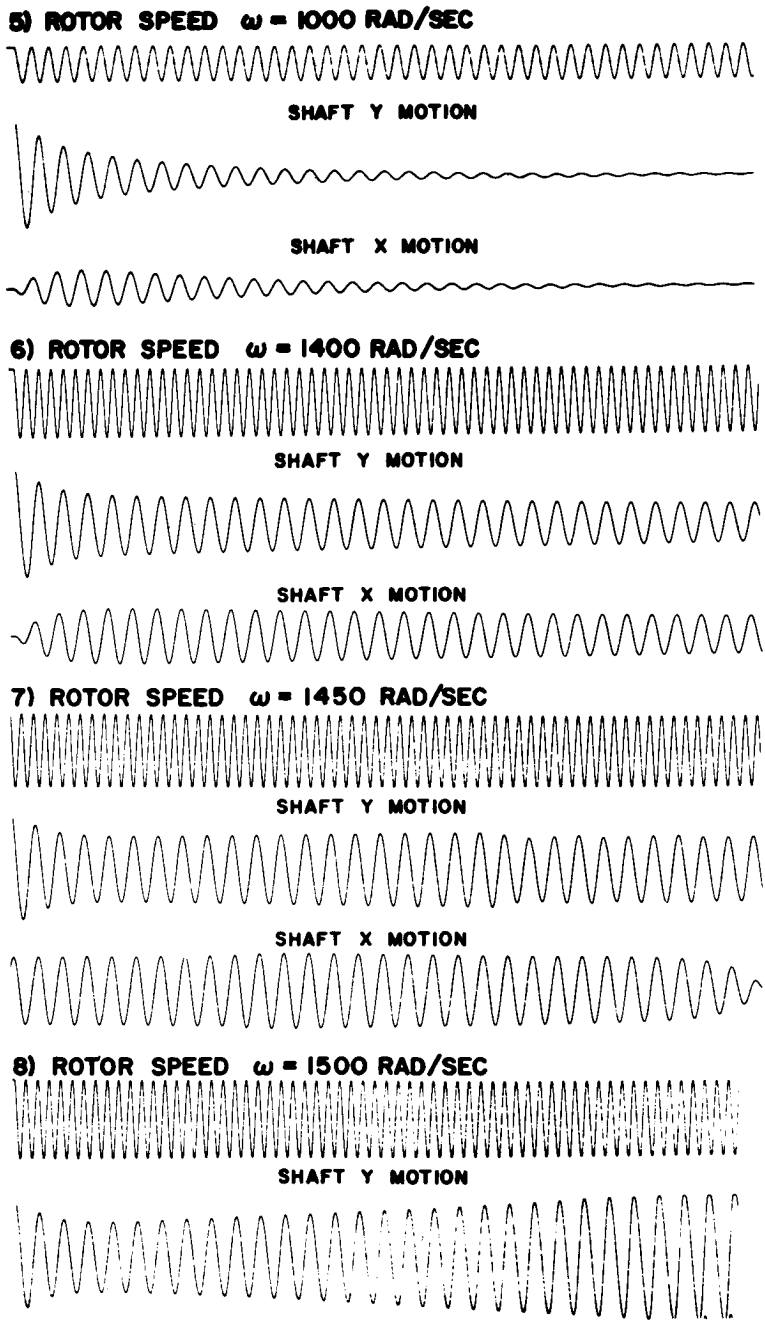


FIGURE 14.—Transient motion of a balanced horizontal rotor with internal friction damping, $\omega = 1000$–$1500$ rad/sec. Stability threshold, $\omega = 1412$ rad/sec.

Figure 14 represents the rotor behavior in the speed range of 1000 to 1500 rad/sec. In Run 5 where $\omega = 1000$ rad/sec, the frequency of oscillation remains unchanged but the time required to damp out the transient rotor motion has increased. As the rotor speed approaches the threshold speed, as shown in Run 6, the time required for the transient to diminish becomes extremely long. Once the threshold speed has been exceeded, the transient motion is sustained and increases as shown by Run 8 for $\omega = 1500$ rad/sec.

### 4.6.6 Whirling of an Unbalanced Rotor

A number of rotor orbits were obtained for conditions identical to Example 1, but with the addition of rotor unbalance. The effect of the rotor unbalance is to produce a steady-state rotor displacement similar to that shown in Fig. 5. The rotor motion below the threshold of stability is synchronous precession as shown by Fig. 15. When the rotor is released, the unbalance causes the rotor to spiral out and then settle down into a stable synchronous motion.

When the rotor angular speed exceeds the threshold speed $\omega_s$, the system develops an additional component of nonsynchronous precession as shown in Fig. 16. The nonsynchronous component greatly increases the total rotor orbit even at speeds close to the threshold. For example, the dashed circle about the origin represents the stable synchronous motion caused by unbalance alone. If the cross-coupling terms $\omega\sqrt{\mu_x\mu_y}\,X$ and $\omega\sqrt{\mu_x\mu_y}\,Y$ are removed from Eq. (4.17), this is the motion that would result. When the rotor is released, it spirals outward and returns to the vicinity of the steady-state synchronous orbit. The nonsynchronous component causes the total rotor orbit to form an internal loop. As time continues, the nonsynchronous component increases, causing the internal loop to change to a cusp. Eventually the motion becomes unbounded and the nonsynchronous precession predominates.

At speeds well above the threshold, the motion becomes rapidly unstable and the nonsynchronous component completely overshadows the synchronous motion to produce a divergent spiral similar to Fig. 12.

Figures 17 and 18 represent the $X$–$Y$ traces of the rotor motion equivalent to the rotor orbits of Figs. 15 and 16. In Fig. 17, the speed range is from 500 to 750 rad/sec, which includes the rotor critical speed. In Runs 1 to 5, the transient shaft motion quickly dies out and only stable synchronous precession remains. As the rotor speed increases, the size of the synchronous rotor motion increases and reaches a maximum at the rotor critical speed of $\omega_{CR} = 706$ rad/sec.

In Fig. 18, which illustrates the rotor motion in the speed range of 1000 to 1500, we see a sizable transient motion begin to develop. In

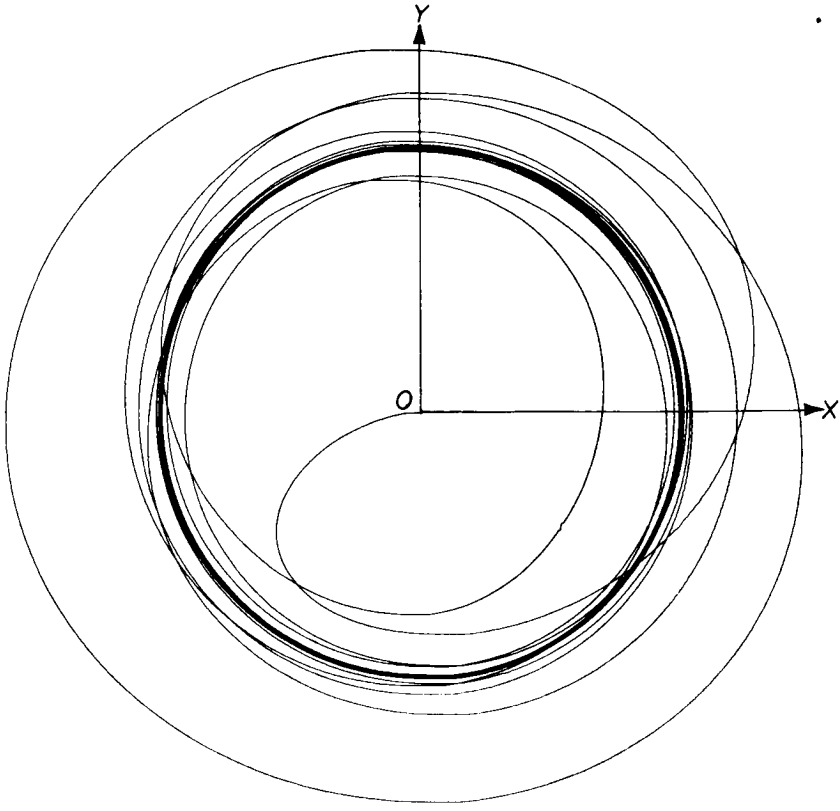


FIGURE 15.—Whirl orbit of an unbalanced rotor with internal friction damping below the threshold of stability, $\omega < \omega_s$. Conditions: unbalanced rotor, $M = 0.25$ lb-sec$^2$/in., $K_1 = K_2 = 250\,000$ lb/in., $D_1 = D_2 = 200$ rad/sec, $\omega_{CR} = 706$ rad/sec, $\omega_s = 1412$ rad/sec, $\omega = 500$ rad/sec, $G = 0$ (vertical rotor).

Run 6, a nonsynchronous transient motion is superimposed upon the rotor synchronous precession. After the transient motion is suppressed, the motion is stable synchronous precession as caused by unbalance. Notice that since we are above the rotor critical speed, the shaft $X$–$Y$ displacements are considerably smaller than those shown in Run 4. As the speed is increased, the nonsynchronous component becomes more predominant until it completely overshadows the synchronous component as shown by Run 8 for $\omega = 1500$ rad/sec.

## 4.7 WHIRLING OF AN UNBALANCED ROTOR—LIMIT CYCLES

Dr. Newkirk, in his investigations of rotor whirl behavior, observed that once the rotor whirl motion developed, the rotor orbit would continue

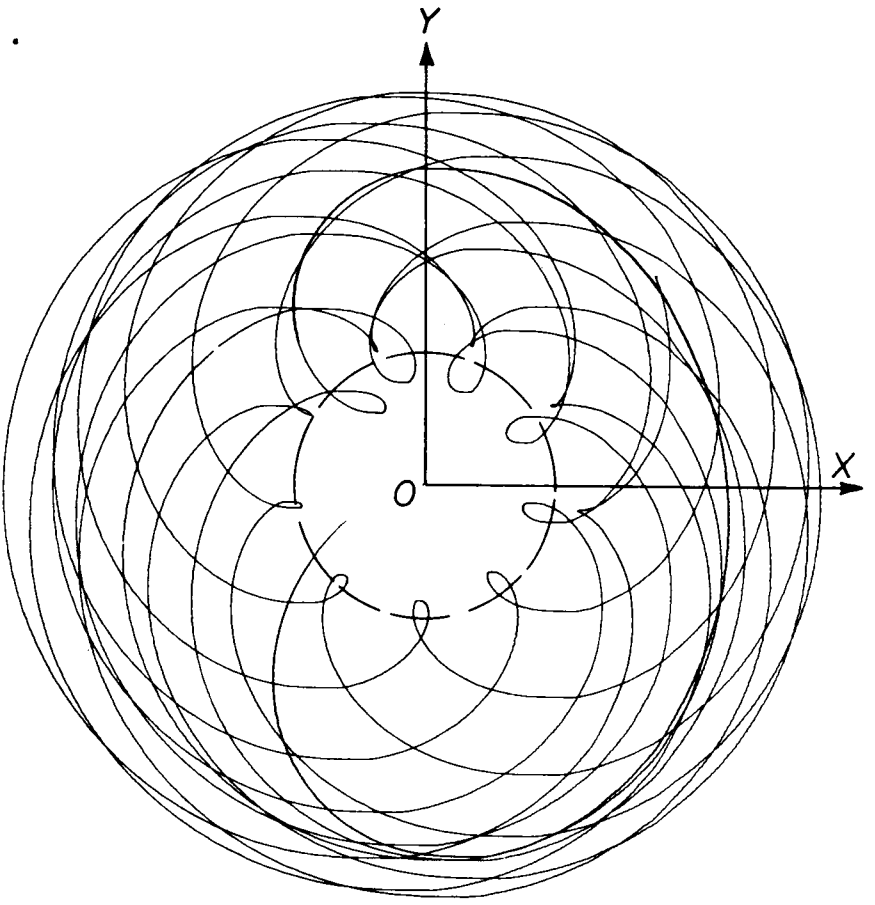


FIGURE 16.—Whirl orbit of an unbalanced rotor above the whirl threshold speed, $\omega > \omega_s$. Conditions: unbalanced rotor, $M = 0.25$ lb-sec$^2$/in., $K_1 = K_2 = 250\,000$ lb/in., $D_1 = D_2 = 200$ rad/sec, $\omega_{CR} = 706$ rad/sec, $\omega_s = 1412$ rad/sec, $\omega = 1500$ rad/sec, $G = 0$ (vertical rotor).

to grow until it was stopped by the protective guard ring surrounding the shaft. He observed that this spiral motion would be very gentle or extremely abrupt, depending upon rotor speed, type of shrink fit, etc. Occasionally he noticed that instead of the rotor orbit becoming unbounded, a finite quasi-steady-state whirl pattern would develop. When this occurred, the orbit would increase when the speed was increased, but the motion would still remain bounded. Closer investigation of the system revealed that these phenomena occurred only when the shaft deflection was large enough to cause the shaft to clamp the bearings (rolling element) at the edge, reducing the effective rotor span and thus changing the shaft stiffness characteristics.

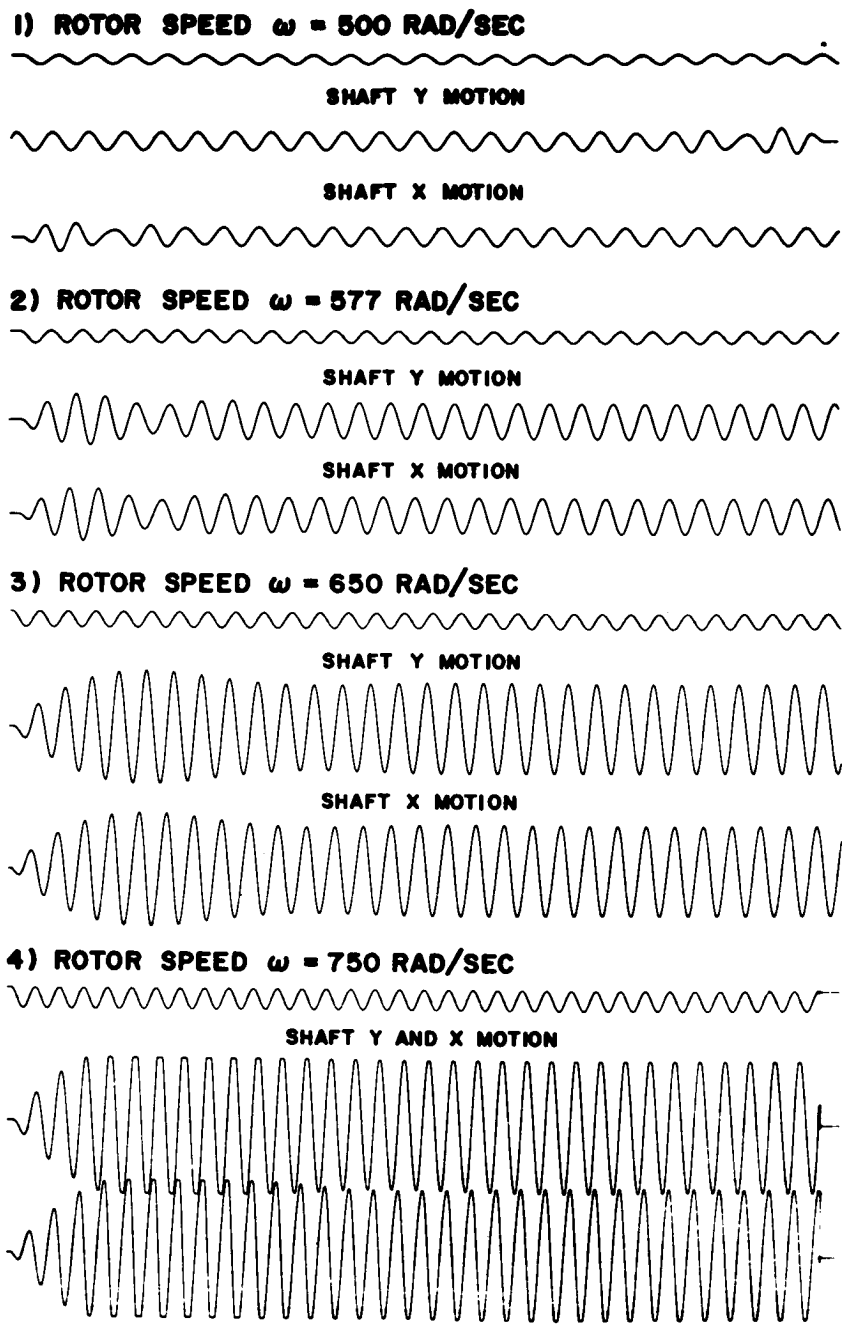


FIGURE 17.—Transient motion of an unbalanced rotor with internal friction damping, $\omega = 500-750$ rad/sec. Stability threshold, $\omega_s = 1412$ rad/sec.

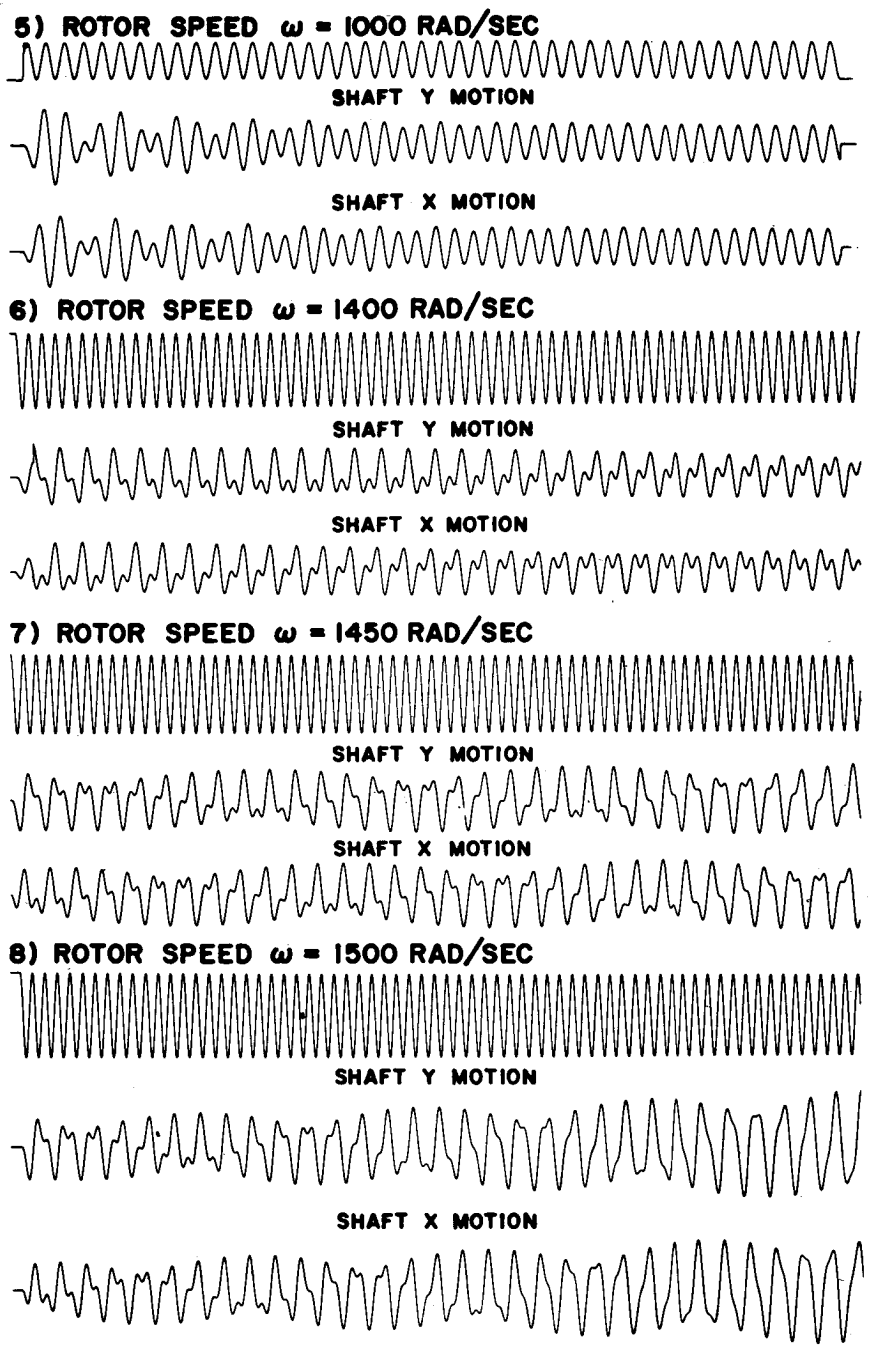


FIGURE 18.—Transient motion of an unbalanced rotor with internal friction damping, $\omega = 1000–1500$ rad/sec. Stability threshold, $\omega_s = 1412$ rad/sec.

The observations of Dr. Newkirk suggest that nonlinear shaft stiffness characteristics could produce limit cycles. In the investigation of the linear Eqs. (4.28), the transient motion of the system was found to be either stable or unstable; that is, at any given speed the motion either increased or reduced exponentially. In certain cases, the rotor motion near the threshold of stability appears to produce bounded orbits as shown in the last figure of Fig. 11 for $\omega = 1450$. When the rotor speed exceeds the threshold speed, the rotor motion diverges in all cases for the linear system.

The system equations of motion were modified to include nonlinear stiffness characteristics. The governing equations in complex vector form are

$$\ddot{Z} + D_f \dot{Z} + [k_f(1 + \delta Z\bar{Z}) - iS]Z = \omega^2 e^{i\omega t} + iG \tag{4.46}$$

These equations were programed on the analog computer to include the nonlinear effect. The analog computer program is given in Appendix B.2. This program was run over a wide range of speeds for various values of the nonlinear parameter $\delta$. It was found that only several percent change in radial stiffness characteristic was necessary to produce a limit cycle at the threshold of stability. Figure 19 represents the rotor motion slightly above the threshold speed. In the linear case, the total rotor orbit forms a slowly divergent spiral. The introduction of the nonlinear component ($\delta = 0.01$ and 0.04) causes a finite orbit to develop. When the rotor speed is increased above the threshold speed, the orbit grows but remains bounded.

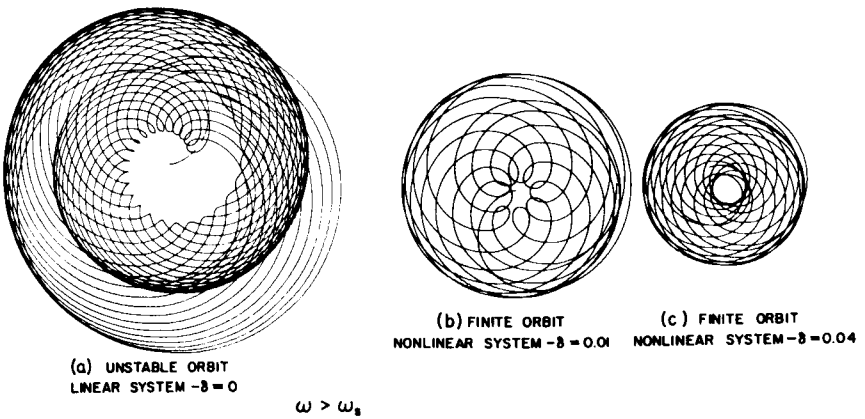


FIGURE 19.—The effect of nonlinearity on rotor motion above the threshold of stability. Conditions: $\omega_{CR} = 706$ rad/sec, $\omega_s = 1412$ rad/sec, $\omega = 1500$ rad/sec.

To date, all stability analyses of rotor-bearing systems have been based on the Routh-Hurwitz criterion which utilizes the small perturbation approach. The previous figure illustrates the fact that the introduction of even small nonlinear effects can greatly influence the rotor behavior at the stability threshold. Little attempts have been made to analyze the magnitude of the nonlinear orbits or limit cycles. The formation of limit cycles will also be discussed in a later section on fluid film bearings. It shall be seen that the nature of the limit cycle plays an important role in the concept of rotor stability.

For the situation represented by Eq. (4.46), where the degree of the nonlinearity is small, a close approximation to the size of the limit cycle can be obtained by the following procedure.

Assume a particular solution to the homogeneous Eq. (4.26) of the form

$$Z_L = Ae^{i\omega Pt}$$

where

$\omega_P$ = rotor precession rate $\approx$ constant
$A$ = complex amplitude of limit cycle

Substitution of the above into Eq. (4.28) and upon separation of real and imaginary components results in the following conditions to be satisfied

$$\omega_P D_f - S = 0$$

$$k_f(1 + \delta A\bar{A}) - \omega_P^2 = 0 \tag{4.46.1}$$

Solving for the amplitude of the limit cycle

$$|A| = \sqrt{\left[\left(\frac{S^2}{D_f^2 k_f}\right) - 1\right]\frac{1}{\delta}} \tag{4.46.2}$$

From the linear analysis

$$\omega_s = \frac{\omega\omega_{CR}D_f}{S}$$

Hence

$$|A| = \sqrt{\left[\left(\frac{\omega}{\omega_s}\right)^2 - 1\right]\frac{1}{\delta}} \tag{4.46.3}$$

This states that the size of the limit cycle $A$ is a function of the ratio of the rotor speed to the whirl threshold speed and is also inversely proportional to the square root of the nonlinear component $\delta$.

## 4.8 NONSYNCHRONOUS ROTOR PRECESSION—ASYMMETRIC BEARING SUPPORT

The analysis of Sec. 4.6.2 shows that with a symmetric bearing support, damping must be introduced into the foundation to increase stability. To verify Newkirk's findings that stability can be improved by foundation flexibility, we will examine the stability criteria of Eq. (4.33) in detail over a wide range of the flexibility parameters $R$ and $\alpha$, and damping parameter $D$.

Equation (4.33) was programed on the digital computer to calculate the rotor threshold of stability. These calculations are given in Tables 2 through 9. In each table, the ratio $R$ of rotor stiffness to vertical foundation flexibility is held constant and the horizontal stiffness $K_x$ and damping parameter $D$ are varied. The dimensionless parameter $A$ is arbitrarily chosen and is a measure of the ratio of the rotor elastic forces to the internal friction damping. In the absence of external damping, $A$ represents the rotor critical amplification factor. That is, at the critical speed, the maximum rotor orbit is $Ae_\mu$. For a lightly damped system, $A$ should be of the order 5 or larger.

The first column in the tables is $\alpha$, the foundation flexibility ratio $K_x/K_y$, where $K_y$ is constant. The second column represents the ratio of the horizontal system critical speed to the rotor critical speed on rigid supports. The values in the third column represent the rotor threshold speed in the absence of external damping. The values in the remaining columns represent the rotor threshold speed for various values of external damping. The rotor threshold speed is given in the dimensionless form $\omega_s/\omega_{CR_0}$.

### 4.8.1 Zero Foundation Damping

When no external damping is introduced into the system $D=\infty$. Taking the limit of Eq. (4.33) as $D\to\infty$ yields the stability condition

$$\left(\frac{\omega}{\omega_{CR_0}}\right)^2 < \left[\left(\frac{\omega_{CR_0}}{D^2}\right)\frac{(1+R)(\alpha+R)(1-\alpha)R}{[\alpha^2(1+R)^2+(\alpha+R)^2]}\right]^2 + \frac{\alpha[(R+\alpha)+\alpha(R+1)]}{\alpha^2(R+1)^2+(R+\alpha)^2} \tag{4.47}$$

Check: when $\alpha=1$

$$\left(\frac{\omega}{\omega_{CR_0}}\right)^2 < \frac{1}{1+R}$$

or

$$\omega < \omega_{CR_0}\sqrt{\frac{1}{1+R}} = \omega_{CR}$$

TABLE 2.—*Rotor stability threshold with internal friction damping for* R = *0.01*

| R = K21KY = 0.01 | | | A = WCRO/D2 = 5.00 | | | | WCY/WCRO = 0.995 | | | |
|---|---|---|---|---|---|---|---|---|---|---|
| ALPHA | WCX/WCRO | D1=00.0 | D = 0.0 | D = 0.2 | D = 0.5 | D = 1.0 | D = 5.0 | D= 10.0 | D= 100.0 | D= 1000.0 |
| 0.04 | 0.8944 | 1.10 | 0.06 | 1.23 | 1.16 | 1.13 | 1.11 | 1.11 | 1.10 | 1.10 |
| 0.10 | 0.9535 | 1.00 | 0.05 | 1.02 | 1.01 | 1.00 | 1.00 | 1.00 | 1.00 | 1.00 |
| 0.20 | 0.9759 | 0.99 | 0.04 | 1.00 | 0.99 | 0.99 | 0.99 | 0.99 | 0.99 | 0.99 |
| 0.40 | 0.9877 | 0.99 | 0.03 | 0.99 | 0.99 | 0.99 | 0.99 | 0.99 | 0.99 | 0.99 |
| 0.50 | 0.9901 | 0.99 | 0.02 | 0.99 | 0.99 | 0.99 | 0.99 | 0.99 | 0.99 | 0.99 |
| 0.60 | 0.9918 | 0.99 | 0.01 | 0.99 | 0.99 | 0.99 | 0.99 | 0.99 | 0.99 | 0.99 |
| 0.70 | 0.9929 | 0.99 | 0.01 | 0.99 | 0.99 | 0.99 | 0.99 | 0.99 | 0.99 | 0.99 |
| 0.80 | 0.9938 | 0.99 | 0.01 | 1.00 | 0.99 | 0.99 | 0.99 | 0.99 | 0.99 | 0.99 |
| 0.90 | 0.9945 | 0.99 | 0.00 | 1.00 | 0.99 | 0.99 | 0.99 | 0.99 | 0.99 | 0.99 |
| 1.00 | 0.9950 | 1.00 | 0.00 | 1.00 | 1.00 | 1.00 | 1.00 | 1.00 | 1.00 | 1.00 |
| 1.10 | 0.9955 | 1.00 | 0.00 | 1.00 | 1.00 | 1.00 | 1.00 | 1.00 | 1.00 | 1.00 |
| 1.20 | 0.9959 | 1.00 | 0.00 | 1.00 | 1.00 | 1.00 | 1.00 | 1.00 | 1.00 | 1.00 |
| 1.30 | 0.9962 | 1.00 | 0.01 | 1.00 | 1.00 | 1.00 | 1.00 | 1.00 | 1.00 | 1.00 |
| 1.50 | 0.9967 | 1.00 | 0.01 | 1.00 | 1.00 | 1.00 | 1.00 | 1.00 | 1.00 | 1.00 |
| 1.70 | 0.9971 | 1.00 | 0.01 | 1.00 | 1.00 | 1.00 | 1.00 | 1.00 | 1.00 | 1.00 |
| 2.00 | 0.9975 | 1.00 | 0.01 | 1.00 | 1.00 | 1.00 | 1.00 | 1.00 | 1.00 | 1.00 |
| 2.50 | 0.9980 | 1.00 | 0.01 | 1.00 | 1.00 | 1.00 | 1.00 | 1.00 | 1.00 | 1.00 |
| 3.00 | 0.9983 | 1.00 | 0.01 | 1.00 | 1.00 | 1.00 | 1.00 | 1.00 | 1.00 | 1.00 |
| 4.00 | 0.9988 | 1.00 | 0.01 | 1.00 | 1.00 | 1.00 | 1.00 | 1.00 | 1.00 | 1.00 |
| 6.00 | 0.9992 | 1.00 | 0.01 | 1.00 | 1.00 | 1.00 | 1.00 | 1.00 | 1.00 | 1.00 |
| 8.00 | 0.9994 | 1.00 | 0.01 | 1.00 | 1.00 | 1.00 | 1.00 | 1.00 | 1.00 | 1.00 |
| 10.00 | 0.9995 | 1.00 | 0.00 | 1.00 | 1.00 | 1.00 | 1.00 | 1.00 | 1.00 | 1.00 |
| 25.00 | 0.9998 | 1.00 | 0.00 | 1.00 | 1.00 | 1.00 | 1.00 | 1.00 | 1.00 | 1.00 |

219-720 O-66—6

TABLE 3.—*Rotor stability threshold with internal friction damping for* R = 0.10

| R = K21KY = 0.10 | | | | A = WCRO/D2 = 5.00 | | | WCY/WCRO = 0.953 | | | |
|---|---|---|---|---|---|---|---|---|---|---|
| ALPHA | WCX/WCRO | D1=00.0 | D = 0.0 | D = 0.2 | D = 0.5 | D = 1.0 | D = 5.0 | D= 10.0 | D= 100.0 | D= 1000.0 |
| 0.04 | 0.5345 | 3.48 | 1.80 | 7.24 | 6.65 | 6.24 | 4.72 | 4.21 | 3.57 | 3.49 |
| 0.10 | 0.7071 | 2.05 | 1.27 | 3.08 | 2.68 | 2.46 | 2.16 | 2.11 | 2.06 | 2.05 |
| 0.20 | 0.8165 | 1.29 | 1.12 | 1.70 | 1.47 | 1.39 | 1.31 | 1.30 | 1.29 | 1.29 |
| 0.40 | 0.8944 | 0.99 | 1.04 | 1.15 | 1.06 | 1.02 | 1.00 | 1.00 | 0.99 | 0.99 |
| 0.50 | 0.9129 | 0.96 | 1.02 | 1.08 | 1.01 | 0.99 | 0.97 | 0.97 | 0.96 | 0.96 |
| 0.60 | 0.9258 | 0.95 | 1.01 | 1.04 | 0.99 | 0.97 | 0.96 | 0.96 | 0.95 | 0.95 |
| 0.70 | 0.9354 | 0.95 | 1.00 | 1.02 | 0.98 | 0.96 | 0.95 | 0.95 | 0.95 | 0.95 |
| 0.80 | 0.9428 | 0.95 | 1.00 | 1.01 | 0.97 | 0.96 | 0.95 | 0.95 | 0.95 | 0.95 |
| 0.90 | 0.9487 | 0.95 | 1.00 | 1.00 | 0.97 | 0.96 | 0.95 | 0.95 | 0.95 | 0.95 |
| 1.00 | 0.9535 | 0.95 | 1.00 | 1.00 | 0.97 | 0.96 | 0.96 | 0.95 | 0.95 | 0.95 |
| 1.10 | 0.9574 | 0.96 | 1.00 | 1.00 | 0.97 | 0.96 | 0.96 | 0.96 | 0.96 | 0.96 |
| 1.20 | 0.9608 | 0.96 | 1.00 | 1.00 | 0.97 | 0.97 | 0.96 | 0.96 | 0.96 | 0.96 |
| 1.30 | 0.9636 | 0.96 | 1.00 | 1.00 | 0.98 | 0.97 | 0.96 | 0.96 | 0.96 | 0.96 |
| 1.50 | 0.9682 | 0.96 | 1.00 | 1.00 | 0.98 | 0.97 | 0.97 | 0.96 | 0.96 | 0.96 |
| 1.70 | 0.9718 | 0.97 | 1.00 | 1.00 | 0.98 | 0.97 | 0.97 | 0.97 | 0.97 | 0.97 |
| 2.00 | 0.9759 | 0.97 | 1.00 | 1.00 | 0.98 | 0.98 | 0.97 | 0.97 | 0.97 | 0.97 |
| 2.50 | 0.9806 | 0.98 | 1.00 | 1.01 | 0.99 | 0.98 | 0.98 | 0.98 | 0.98 | 0.98 |
| 3.00 | 0.9837 | 0.98 | 1.00 | 1.01 | 0.99 | 0.99 | 0.98 | 0.98 | 0.98 | 0.98 |
| 4.00 | 0.9877 | 0.99 | 1.00 | 1.01 | 1.00 | 0.99 | 0.99 | 0.99 | 0.99 | 0.99 |
| 6.00 | 0.9918 | 0.99 | 1.00 | 1.02 | 1.00 | 1.00 | 0.99 | 0.99 | 0.99 | 0.99 |
| 8.00 | 0.9938 | 1.00 | 1.00 | 1.02 | 1.01 | 1.00 | 1.00 | 1.00 | 1.00 | 1.00 |
| 10.00 | 0.9950 | 1.00 | 1.00 | 1.02 | 1.01 | 1.00 | 1.00 | 1.00 | 1.00 | 1.00 |
| 25.00 | 0.9980 | 1.00 | 1.00 | 1.03 | 1.01 | 1.01 | 1.00 | 1.00 | 1.00 | 1.00 |

TABLE 4.—*Rotor stability threshold with internal friction damping for* R = *0.20*

| R = K21KY = 0.20 | | | A = WCRO/D2 = 5.00 | | | | WCY/WCRO = 0.913 | | | |
|---|---|---|---|---|---|---|---|---|---|---|
| ALPHA | WCX/WCRO | D1=00.0 | D = 0.0 | D = 0.2 | D = 0.5 | D = 1.0 | D = 5.0 | D= 10.0 | D= 100.0 | D= 1000.0 |
| 0.04 | 0.4082 | 4.64 | 4.72 | 14.00 | 12.79 | 12.55 | 9.55 | 7.92 | 5.13 | 4.69 |
| 0.10 | 0.5774 | 3.17 | 2.33 | 5.78 | 5.08 | 4.77 | 3.85 | 3.56 | 3.21 | 3.17 |
| 0.20 | 0.7071 | 1.92 | 1.55 | 2.97 | 2.48 | 2.28 | 2.02 | 1.98 | 1.93 | 1.92 |
| 0.40 | 0.8165 | 1.13 | 1.14 | 1.61 | 1.33 | 1.23 | 1.15 | 1.14 | 1.13 | 1.13 |
| 0.50 | 0.8452 | 1.00 | 1.07 | 1.39 | 1.16 | 1.08 | 1.02 | 1.01 | 1.01 | 1.00 |
| 0.60 | 0.8660 | 0.95 | 1.02 | 1.26 | 1.07 | 1.01 | 0.96 | 0.95 | 0.95 | 0.95 |
| 0.70 | 0.8819 | 0.92 | 1.00 | 1.19 | 1.03 | 0.97 | 0.93 | 0.93 | 0.92 | 0.92 |
| 0.80 | 0.8944 | 0.91 | 0.98 | 1.14 | 1.00 | 0.96 | 0.92 | 0.92 | 0.91 | 0.91 |
| 0.90 | 0.9045 | 0.91 | 0.98 | 1.11 | 0.99 | 0.95 | 0.92 | 0.91 | 0.91 | 0.91 |
| 1.00 | 0.9129 | 0.91 | 0.97 | 1.10 | 0.99 | 0.95 | 0.92 | 0.92 | 0.91 | 0.91 |
| 1.10 | 0.9199 | 0.92 | 0.98 | 1.08 | 0.98 | 0.95 | 0.92 | 0.92 | 0.92 | 0.92 |
| 1.20 | 0.9258 | 0.92 | 0.98 | 1.08 | 0.99 | 0.95 | 0.93 | 0.93 | 0.92 | 0.92 |
| 1.30 | 0.9309 | 0.93 | 0.98 | 1.07 | 0.99 | 0.96 | 0.93 | 0.93 | 0.93 | 0.93 |
| 1.50 | 0.9393 | 0.94 | 0.99 | 1.07 | 0.99 | 0.97 | 0.95 | 0.94 | 0.94 | 0.94 |
| 1.70 | 0.9459 | 0.95 | 0.99 | 1.07 | 1.00 | 0.98 | 0.96 | 0.95 | 0.95 | 0.95 |
| 2.00 | 0.9535 | 0.96 | 1.00 | 1.08 | 1.01 | 0.99 | 0.97 | 0.97 | 0.96 | 0.96 |
| 2.50 | 0.9623 | 0.98 | 1.00 | 1.09 | 1.02 | 1.00 | 0.99 | 0.98 | 0.98 | 0.98 |
| 3.00 | 0.9682 | 0.99 | 1.00 | 1.09 | 1.03 | 1.01 | 1.00 | 1.00 | 0.99 | 0.99 |
| 4.00 | 0.9759 | 1.01 | 0.99 | 1.11 | 1.05 | 1.03 | 1.02 | 1.01 | 1.01 | 1.01 |
| 6.00 | 0.9837 | 1.03 | 0.99 | 1.12 | 1.07 | 1.05 | 1.03 | 1.03 | 1.03 | 1.03 |
| 8.00 | 0.9877 | 1.04 | 0.98 | 1.13 | 1.08 | 1.06 | 1.04 | 1.04 | 1.04 | 1.04 |
| 10.00 | 0.9901 | 1.05 | 0.98 | 1.13 | 1.08 | 1.06 | 1.05 | 1.05 | 1.05 | 1.05 |
| 25.00 | 0.9960 | 1.06 | 0.98 | 1.15 | 1.10 | 1.08 | 1.06 | 1.06 | 1.06 | 1.06 |

TABLE 5.—*Rotor stability threshold with internal friction damping for* R = *0.50*

| R = K2/KY = 0.50 | | | | A = WCRC/D2 = 5.00 | | | WCY/WCRO = 0.816 | | | |
|---|---|---|---|---|---|---|---|---|---|---|
| ALPHA | WCX/WCRO | D1=00.0 | D = 0.0 | D = 0.2 | D = 0.5 | D = 1.0 | D = 5.0 | D= 10.0 | D= 100.0 | D= 1000.0 |
| 0.04 | 0.2722 | 6.59 | 19.15 | 39.09 | 30.99 | 30.71 | 26.94 | 22.44 | 10.34 | 7.07 |
| 0.10 | 0.4082 | 5.31 | 7.82 | 15.65 | 12.20 | 11.79 | 10.00 | 8.62 | 5.85 | 5.37 |
| 0.20 | 0.5345 | 3.67 | 3.95 | 7.79 | 5.84 | 5.42 | 4.60 | 4.25 | 3.74 | 3.68 |
| 0.40 | 0.6667 | 1.87 | 1.91 | 3.86 | 2.64 | 2.30 | 1.99 | 1.93 | 1.88 | 1.87 |
| 0.50 | 0.7071 | 1.41 | 1.49 | 3.10 | 2.05 | 1.73 | 1.48 | 1.45 | 1.42 | 1.41 |
| 0.60 | 0.7385 | 1.12 | 1.24 | 2.62 | 1.69 | 1.40 | 1.18 | 1.15 | 1.13 | 1.12 |
| 0.70 | 0.7638 | 0.95 | 1.08 | 2.30 | 1.48 | 1.21 | 1.00 | 0.98 | 0.95 | 0.95 |
| 0.80 | 0.7845 | 0.86 | 1.00 | 2.09 | 1.35 | 1.10 | 0.91 | 0.88 | 0.86 | 0.86 |
| 0.90 | 0.8018 | 0.82 | 0.96 | 1.94 | 1.27 | 1.04 | 0.87 | 0.84 | 0.82 | 0.82 |
| 1.00 | 0.8165 | 0.82 | 0.95 | 1.84 | 1.22 | 1.02 | 0.86 | 0.84 | 0.82 | 0.82 |
| 1.10 | 0.8292 | 0.83 | 0.95 | 1.76 | 1.20 | 1.02 | 0.87 | 0.85 | 0.83 | 0.83 |
| 1.20 | 0.8402 | 0.85 | 0.97 | 1.71 | 1.20 | 1.02 | 0.89 | 0.87 | 0.86 | 0.85 |
| 1.30 | 0.8498 | 0.88 | 0.99 | 1.68 | 1.20 | 1.04 | 0.91 | 0.90 | 0.88 | 0.88 |
| 1.50 | 0.8660 | 0.94 | 1.03 | 1.63 | 1.21 | 1.07 | 0.96 | 0.95 | 0.94 | 0.94 |
| 1.70 | 0.8790 | 0.99 | 1.06 | 1.61 | 1.24 | 1.11 | 1.01 | 1.00 | 0.99 | 0.99 |
| 2.00 | 0.8944 | 1.05 | 1.10 | 1.60 | 1.27 | 1.16 | 1.07 | 1.06 | 1.05 | 1.05 |
| 2.50 | 0.9129 | 1.13 | 1.12 | 1.61 | 1.33 | 1.23 | 1.15 | 1.14 | 1.13 | 1.13 |
| 3.00 | 0.9258 | 1.18 | 1.12 | 1.63 | 1.37 | 1.28 | 1.20 | 1.19 | 1.18 | 1.18 |
| 4.00 | 0.9428 | 1.25 | 1.10 | 1.67 | 1.43 | 1.35 | 1.27 | 1.26 | 1.25 | 1.25 |
| 6.00 | 0.9608 | 1.32 | 1.05 | 1.72 | 1.50 | 1.41 | 1.34 | 1.33 | 1.32 | 1.32 |
| 8.00 | 0.9701 | 1.35 | 1.02 | 1.75 | 1.54 | 1.45 | 1.37 | 1.36 | 1.35 | 1.35 |
| 10.00 | 0.9759 | 1.37 | 1.00 | 1.77 | 1.56 | 1.47 | 1.39 | 1.38 | 1.37 | 1.37 |
| 25.00 | 0.9901 | 1.42 | 0.96 | 1.82 | 1.61 | 1.52 | 1.44 | 1.43 | 1.42 | 1.42 |

TABLE 6.—*Rotor stability threshold with internal friction damping for* R = *1.00*

| R = K21KY = 1.00 | | | A = WCRO/D2 = 5.00 | | | | WCY/WCRO = 0.707 | | | |
|---|---|---|---|---|---|---|---|---|---|---|
| ALPHA | WCX/WCRO | D1=00.0 | D = 0.0 | D = 0.2 | D = 0.5 | D = 1.0 | D = 5.0 | D= 10.0 | D= 100.0 | D= 1000.0 |
| 0.04 | 0.1961 | 9.18 | 49.13 | 99.60 | 65.82 | 60.84 | 58.62 | 52.38 | 23.73 | 11.65 |
| 0.10 | 0.3015 | 7.93 | 19.02 | 39.64 | 25.67 | 23.33 | 21.82 | 19.50 | 10.82 | 8.28 |
| 0.20 | 0.4082 | 6.02 | 8.87 | 19.66 | 12.22 | 10.75 | 9.69 | 8.84 | 6.54 | 6.07 |
| 0.40 | 0.5345 | 3.28 | 3.63 | 9.73 | 5.50 | 4.45 | 3.77 | 3.60 | 3.33 | 3.29 |
| 0.50 | 0.5774 | 2.39 | 2.55 | 7.79 | 4.21 | 3.23 | 2.62 | 2.52 | 2.41 | 2.39 |
| 0.60 | 0.6124 | 1.73 | 1.85 | 6.54 | 3.39 | 2.47 | 1.87 | 1.80 | 1.73 | 1.73 |
| 0.70 | 0.6417 | 1.25 | 1.37 | 5.67 | 2.85 | 1.98 | 1.38 | 1.31 | 1.25 | 1.25 |
| 0.80 | 0.6667 | 0.92 | 1.07 | 5.05 | 2.50 | 1.68 | 1.06 | 0.99 | 0.93 | 0.92 |
| 0.90 | 0.6882 | 0.75 | 0.92 | 4.59 | 2.27 | 1.50 | 0.90 | 0.82 | 0.76 | 0.75 |
| 1.00 | 0.7071 | 0.71 | 0.88 | 4.24 | 2.12 | 1.41 | 0.85 | 0.78 | 0.71 | 0.71 |
| 1.10 | 0.7237 | 0.75 | 0.90 | 3.98 | 2.03 | 1.39 | 0.88 | 0.81 | 0.76 | 0.75 |
| 1.20 | 0.7385 | 0.83 | 0.97 | 3.77 | 1.98 | 1.39 | 0.94 | 0.89 | 0.84 | 0.83 |
| 1.30 | 0.7518 | 0.93 | 1.05 | 3.61 | 1.96 | 1.42 | 1.02 | 0.97 | 0.93 | 0.93 |
| 1.50 | 0.7746 | 1.10 | 1.19 | 3.38 | 1.96 | 1.51 | 1.18 | 1.14 | 1.11 | 1.10 |
| 1.70 | 0.7935 | 1.25 | 1.32 | 3.23 | 1.99 | 1.60 | 1.32 | 1.28 | 1.25 | 1.25 |
| 2.00 | 0.8165 | 1.41 | 1.45 | 3.10 | 2.05 | 1.73 | 1.48 | 1.45 | 1.42 | 1.41 |
| 2.50 | 0.8452 | 1.60 | 1.56 | 2.99 | 2.16 | 1.90 | 1.67 | 1.64 | 1.60 | 1.60 |
| 3.00 | 0.8660 | 1.72 | 1.59 | 2.95 | 2.25 | 2.03 | 1.79 | 1.76 | 1.72 | 1.72 |
| 4.00 | 0.8944 | 1.85 | 1.56 | 2.95 | 2.39 | 2.18 | 1.94 | 1.90 | 1.86 | 1.85 |
| 6.00 | 0.9258 | 1.97 | 1.41 | 3.00 | 2.55 | 2.34 | 2.07 | 2.02 | 1.98 | 1.97 |
| 8.00 | 0.9428 | 2.02 | 1.27 | 3.04 | 2.63 | 2.42 | 2.13 | 2.08 | 2.03 | 2.02 |
| 10.00 | 0.9535 | 2.05 | 1.18 | 3.08 | 2.68 | 2.46 | 2.16 | 2.11 | 2.06 | 2.05 |
| 25.00 | 0.9806 | 2.11 | 0.95 | 3.19 | 2.80 | 2.56 | 2.24 | 2.18 | 2.12 | 2.11 |

TABLE 7.—*Rotor stability threshold with internal friction damping for* R = *2.00*

| R = K2/KY = 2.00 | | | A = WCRO/D2 = 5.00 | | | | WCY/WCRO = 0.577 | | | |
|---|---|---|---|---|---|---|---|---|---|---|
| ALPHA | WCX/WCRO | D1=00.0 | D = 0.0 | D = 0.2 | D = 0.5 | D = 1.0 | D = 5.0 | D= 10.0 | D= 100.0 | D= 1000.0 |
| 0.04 | 0.1400 | 14.07 | 111.60 | 270.67 | 152.11 | 126.89 | 120.63 | 116.87 | 64.98 | 26.05 |
| 0.10 | 0.2182 | 12.60 | 42.29 | 108.38 | 59.38 | 48.56 | 45.26 | 43.65 | 25.68 | 14.76 |
| 0.20 | 0.3015 | 10.14 | 19.09 | 54.37 | 28.52 | 22.43 | 20.14 | 19.37 | 13.24 | 10.56 |
| 0.40 | 0.4082 | 6.02 | 7.36 | 27.56 | 13.26 | 9.44 | 7.64 | 7.37 | 6.34 | 6.05 |
| 0.50 | 0.4472 | 4.44 | 4.98 | 22.28 | 10.32 | 6.93 | 5.18 | 4.99 | 4.55 | 4.45 |
| 0.60 | 0.4804 | 3.16 | 3.39 | 18.81 | 8.43 | 5.33 | 3.56 | 3.41 | 3.20 | 3.17 |
| 0.70 | 0.5092 | 2.14 | 2.27 | 16.36 | 7.16 | 4.27 | 2.44 | 2.30 | 2.16 | 2.15 |
| 0.80 | 0.5345 | 1.35 | 1.47 | 14.57 | 6.27 | 3.58 | 1.68 | 1.50 | 1.37 | 1.35 |
| 0.90 | 0.5571 | 0.79 | 0.95 | 13.20 | 5.64 | 3.14 | 1.21 | 0.99 | 0.81 | 0.79 |
| 1.00 | 0.5774 | 0.58 | 0.77 | 12.12 | 5.20 | 2.89 | 1.04 | 0.81 | 0.60 | 0.58 |
| 1.10 | 0.5957 | 0.74 | 0.90 | 11.27 | 4.88 | 2.76 | 1.11 | 0.92 | 0.76 | 0.74 |
| 1.20 | 0.6124 | 1.02 | 1.14 | 10.57 | 4.65 | 2.72 | 1.30 | 1.15 | 1.03 | 1.02 |
| 1.30 | 0.6276 | 1.29 | 1.39 | 10.00 | 4.49 | 2.73 | 1.51 | 1.39 | 1.30 | 1.29 |
| 1.50 | 0.6547 | 1.73 | 1.82 | 9.11 | 4.31 | 2.84 | 1.91 | 1.82 | 1.74 | 1.73 |
| 1.70 | 0.6778 | 2.05 | 2.16 | 8.47 | 4.23 | 3.00 | 2.24 | 2.16 | 2.06 | 2.05 |
| 2.00 | 0.7071 | 2.39 | 2.52 | 7.79 | 4.21 | 3.23 | 2.62 | 2.52 | 2.41 | 2.39 |
| 2.50 | 0.7454 | 2.72 | 2.88 | 7.09 | 4.27 | 3.56 | 3.03 | 2.91 | 2.74 | 2.72 |
| 3.00 | 0.7746 | 2.90 | 3.04 | 6.67 | 4.37 | 3.81 | 3.28 | 3.13 | 2.93 | 2.90 |
| 4.00 | 0.8165 | 3.07 | 3.10 | 6.21 | 4.55 | 4.15 | 3.55 | 3.36 | 3.10 | 3.07 |
| 6.00 | 0.8660 | 3.16 | 2.85 | 5.88 | 4.81 | 4.50 | 3.76 | 3.51 | 3.20 | 3.16 |
| 8.00 | 0.8944 | 3.17 | 2.53 | 5.79 | 4.98 | 4.67 | 3.82 | 3.55 | 3.21 | 3.18 |
| 10.00 | 0.9129 | 3.17 | 2.25 | 5.78 | 5.08 | 4.77 | 3.85 | 3.56 | 3.21 | 3.17 |
| 25.00 | 0.9623 | 3.12 | 1.31 | 5.91 | 5.37 | 4.98 | 3.86 | 3.55 | 3.17 | 3.13 |

TABLE 8.—*Rotor stability threshold with internal friction damping for* R = *5.00*

| R = K21KY = 5.00 | | | | A = WCRO/D2 = 5.00 | | | WCY/WCRO = 0.408 | | | |
|---|---|---|---|---|---|---|---|---|---|---|
| ALPHA | WCX/WCRO | D1=00.0 | D = 0.0 | D = 0.2 | D = 0.5 | D = 1.0 | D = 5.0 | D= 10.0 | D= 100.0 | D= 1000.0 |
| 0.04 | 0.0891 | 28.51 | 295.50 | 1038.58 | 497.36 | 358.19 | 301.89 | 300.79 | 249.35 | 110.99 |
| 0.10 | 0.1400 | 26.11 | 111.03 | 421.02 | 197.39 | 138.33 | 113.52 | 112.86 | 93.75 | 46.71 |
| 0.20 | 0.1961 | 21.91 | 49.50 | 215.28 | 97.69 | 65.27 | 50.72 | 50.22 | 42.47 | 26.80 |
| 0.40 | 0.2722 | 13.92 | 18.66 | 112.59 | 48.42 | 29.29 | 19.36 | 18.92 | 16.99 | 14.48 |
| 0.50 | 0.3015 | 10.51 | 12.47 | 92.12 | 38.81 | 22.38 | 13.13 | 12.69 | 11.70 | 10.71 |
| 0.60 | 0.3273 | 7.59 | 8.34 | 78.50 | 32.55 | 17.97 | 9.04 | 8.55 | 8.01 | 7.66 |
| 0.70 | 0.3504 | 5.13 | 5.39 | 68.80 | 28.19 | 15.02 | 6.20 | 5.64 | 5.27 | 5.15 |
| 0.80 | 0.3714 | 3.09 | 3.19 | 61.55 | 25.02 | 12.99 | 4.22 | 3.52 | 3.14 | 3.10 |
| 0.90 | 0.3906 | 1.44 | 1.53 | 55.93 | 22.65 | 11.59 | 2.97 | 2.05 | 1.48 | 1.44 |
| 1.00 | 0.4082 | 0.41 | 0.63 | 51.44 | 20.82 | 10.61 | 2.45 | 1.43 | 0.51 | 0.42 |
| 1.10 | 0.4247 | 1.21 | 1.30 | 47.78 | 19.39 | 9.95 | 2.58 | 1.78 | 1.24 | 1.21 |
| 1.20 | 0.4399 | 2.10 | 2.18 | 44.74 | 18.25 | 9.51 | 3.03 | 2.46 | 2.13 | 2.11 |
| 1.30 | 0.4543 | 2.85 | 2.95 | 42.17 | 17.34 | 9.23 | 3.57 | 3.15 | 2.89 | 2.86 |
| 1.50 | 0.4804 | 3.98 | 4.20 | 38.08 | 15.98 | 8.97 | 4.60 | 4.33 | 4.06 | 3.99 |
| 1.70 | 0.5037 | 4.74 | 5.16 | 34.97 | 15.04 | 8.94 | 5.47 | 5.25 | 4.87 | 4.76 |
| 2.00 | 0.5345 | 5.46 | 6.21 | 31.49 | 14.12 | 9.08 | 6.48 | 6.27 | 5.67 | 5.48 |
| 2.50 | 0.5774 | 6.02 | 7.34 | 27.56 | 13.26 | 9.44 | 7.64 | 7.37 | 6.34 | 6.05 |
| 3.00 | 0.6124 | 6.20 | 8.03 | 24.95 | 12.82 | 9.80 | 8.40 | 8.02 | 6.61 | 6.25 |
| 4.00 | 0.6667 | 6.18 | 8.68 | 21.66 | 12.40 | 10.35 | 9.27 | 8.64 | 6.67 | 6.23 |
| 6.00 | 0.7395 | 5.84 | 8.78 | 18.31 | 12.15 | 11.06 | 9.90 | 8.87 | 6.38 | 5.90 |
| 8.00 | 0.7845 | 5.54 | 8.35 | 16.62 | 12.14 | 11.49 | 10.02 | 8.77 | 6.08 | 5.60 |
| 10.00 | 0.8165 | 5.31 | 7.78 | 15.65 | 12.20 | 11.79 | 10.00 | 8.62 | 5.85 | 5.37 |
| 25.00 | 0.9129 | 4.64 | 4.66 | 14.00 | 12.79 | 12.55 | 9.55 | 7.92 | 5.13 | 4.69 |

TABLE 9.—*Rotor stability threshold with internal friction damping for* R = *10.00*

| R = K21KY = 10.00 | | | | A = WCRC/D2 = 5.00 | | | WCY/WCRO = 0.302 | | | |
|---|---|---|---|---|---|---|---|---|---|---|
| ALPHA | WCX/WCRO | D1=00.0 | D = 0.0 | D = 0.2 | D = 0.5 | D = 1.0 | D = 5.0 | D= 10.0 | D= 100.0 | D= 1000.0 |
| 0.04 | 0.0631 | 52.49 | 597.51 | 2898.00 | 1282.98 | 824.91 | 609.60 | 602.25 | 581.13 | 359.69 |
| 0.10 | 0.0995 | 48.44 | 224.18 | 1182.52 | 514.12 | 323.26 | 229.47 | 226.10 | 217.83 | 138.55 |
| 0.20 | 0.1400 | 41.22 | 99.72 | 610.44 | 260.98 | 156.67 | 102.83 | 100.73 | 96.93 | 67.03 |
| 0.40 | 0.1961 | 26.91 | 37.44 | 324.00 | 134.25 | 74.69 | 39.73 | 38.10 | 36.65 | 30.50 |
| 0.50 | 0.2182 | 20.55 | 24.98 | 266.56 | 109.23 | 58.88 | 27.26 | 25.62 | 24.58 | 21.90 |
| 0.60 | 0.2379 | 14.96 | 16.66 | 228.19 | 92.72 | 48.69 | 19.12 | 17.35 | 16.48 | 15.43 |
| 0.70 | 0.2558 | 10.16 | 10.72 | 200.73 | 81.06 | 41.72 | 13.55 | 11.54 | 10.66 | 10.30 |
| 0.80 | 0.2722 | 6.13 | 6.26 | 180.08 | 72.43 | 36.76 | 9.75 | 7.36 | 6.26 | 6.16 |
| 0.90 | 0.2873 | 2.78 | 2.81 | 163.97 | 65.82 | 33.14 | 7.38 | 4.52 | 2.84 | 2.79 |
| 1.00 | 0.3015 | 0.30 | 0.44 | 151.06 | 60.60 | 30.45 | 6.33 | 3.32 | 0.60 | 0.33 |
| 1.10 | 0.3148 | 2.29 | 2.32 | 140.46 | 56.41 | 28.43 | 6.34 | 3.85 | 2.35 | 2.29 |
| 1.20 | 0.3273 | 4.12 | 4.19 | 131.60 | 52.97 | 26.89 | 6.95 | 5.10 | 4.19 | 4.13 |
| 1.30 | 0.3392 | 5.62 | 5.78 | 124.08 | 50.11 | 25.71 | 7.81 | 6.41 | 5.76 | 5.65 |
| 1.50 | 0.3612 | 7.82 | 8.34 | 111.99 | 45.65 | 24.10 | 9.62 | 8.72 | 8.19 | 7.89 |
| 1.70 | 0.3812 | 9.26 | 10.28 | 102.68 | 42.36 | 23.14 | 11.21 | 10.57 | 9.94 | 9.39 |
| 2.00 | 0.4082 | 10.51 | 12.46 | 92.12 | 38.81 | 22.38 | 13.13 | 12.69 | 11.70 | 10.71 |
| 2.50 | 0.4472 | 11.31 | 14.88 | 79.97 | 35.05 | 21.95 | 15.42 | 15.10 | 13.21 | 11.60 |
| 3.00 | 0.4804 | 11.37 | 16.44 | 71.70 | 32.72 | 21.93 | 16.99 | 16.68 | 13.78 | 11.72 |
| 4.00 | 0.5345 | 10.84 | 18.22 | 61.05 | 30.03 | 22.17 | 18.97 | 18.50 | 13.76 | 11.24 |
| 6.00 | 0.6124 | 9.55 | 19.46 | 49.73 | 27.55 | 22.66 | 20.86 | 19.75 | 12.65 | 9.94 |
| 8.00 | 0.6667 | 8.60 | 19.47 | 43.58 | 26.36 | 23.03 | 21.59 | 19.80 | 11.61 | 8.97 |
| 10.00 | 0.7071 | 7.93 | 19.01 | 39.64 | 25.67 | 23.33 | 21.82 | 19.50 | 10.82 | 8.28 |
| 25.00 | 0.8452 | 6.02 | 13.74 | 29.74 | 24.79 | 24.75 | 20.85 | 17.16 | 8.38 | 6.30 |

The values of the rotor threshold for zero foundation damping are presented in Column 3 of Tables 2 through 9. These results are shown in Fig. 20 which depicts the rotor threshold speed vs. the bearing foundation stiffness ratio $\alpha$ for various values of the rotor flexibility ratio $R$.

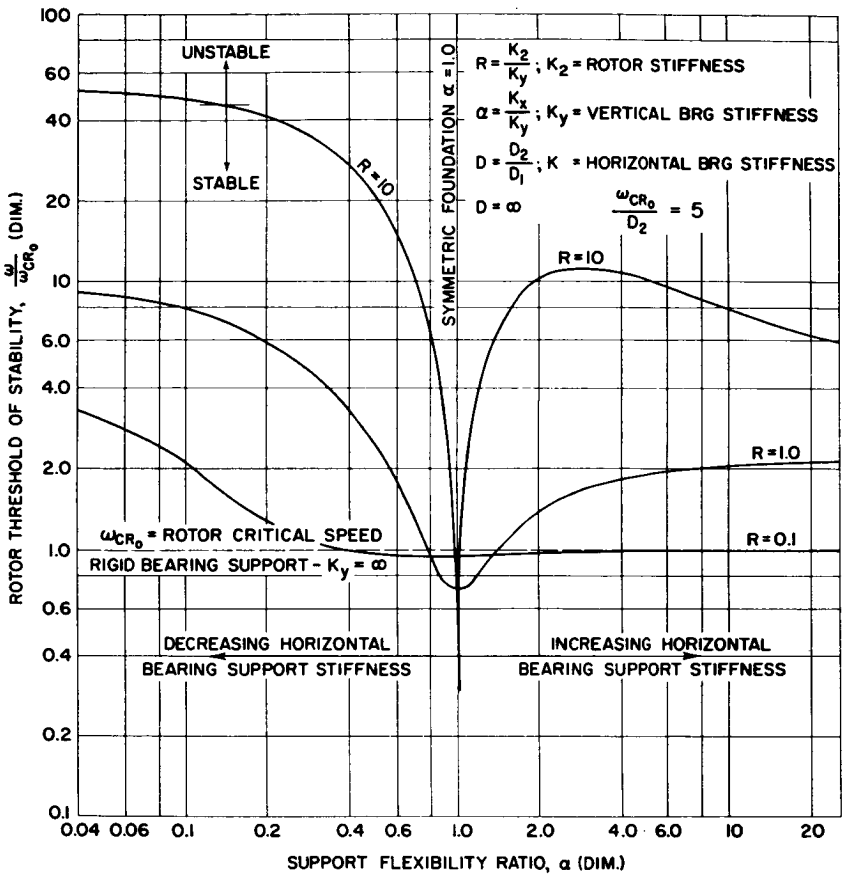


FIGURE 20.—Effect of unsymmetric bearing support flexibility on the rotor whirl threshold speed, zero foundation damping.

Figure 21 shows as a comparison the stability for stiffness values of $R=0.1$, 1.0, and 10.0. Examination of the stability curve for $R=10$ shows clearly the influence of even small changes in $\alpha$ on stability. For example, for $R=10$ and $\alpha=1$, the threshold is 0.3 of the rotor critical speed. Increasing $\alpha$ to 2 improves the threshold ratio to 10, while a reduction in $\alpha$ to 0.5 causes the stability threshold ratio to increase to 20.

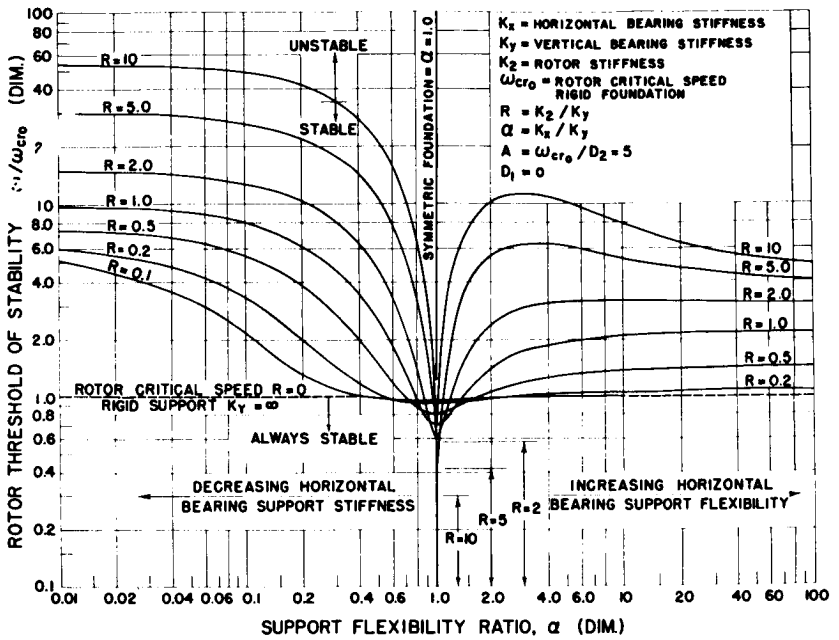


FIGURE 21.—The effect of unsymmetric bearing support flexibility on the rotor whirl threshold speed for various values of $R$, zero foundation damping.

At low values of $R$, that is, when the vertical foundation is considerably stiffer than the rotor, very little change in performance is obtained by varying the horizontal stiffness. As the values of $R$ increase, a change of $\alpha$ from unity causes an increase in stability. Notice that stability is improved both by increasing as well as decreasing the horizontal bearing stiffness. There are asymptotes to the stability limit (Fig. 20) that will be obtained as $\alpha$ approaches zero or infinity. Note that for rotor stiffness ratios of $R = 1$ or higher and $\alpha > 1$, there are optimum values of $\alpha$ for each $R$ value to obtain maximum stability. Increasing the horizontal stiffness above this value causes a reduction in stability. Thus little improvement in stability is gained by having $\alpha$ greater than 3.

To more vividly illustrate the rotor stability characteristics in the absence of foundation damping, Figs. 10 and 20 were combined to form a three-dimensional stability model which is shown in Figs. 22, 23, and 24. Figure 22 shows the stability model viewed in the direction of increasing $R$. The model profile is fairly level for low values of $R$. As the vertical foundation flexibility increases, the rotor critical speed diminishes, as represented by the centerline $\alpha = 1.0$. The model is constructed into two segments which may be detached to permit exami-

nation of the rotor threshold for large $R$. Figure 24 represents the segment of the stability model for the region $\alpha \leq 1$.

### 4.8.2 Foundation Damping

The stability model of Sec. 4.8.1 represents the lower limit to the threshold of stability. When foundation damping is introduced into the system, the stability will be improved. The data of Tables 2–9 were drawn up into field maps to illustrate the influence of damping on stability. For example, Fig. 25, obtained from Table 2, represents the rotor threshold for $R = 0.1$ and various values of the dimensionless damp-

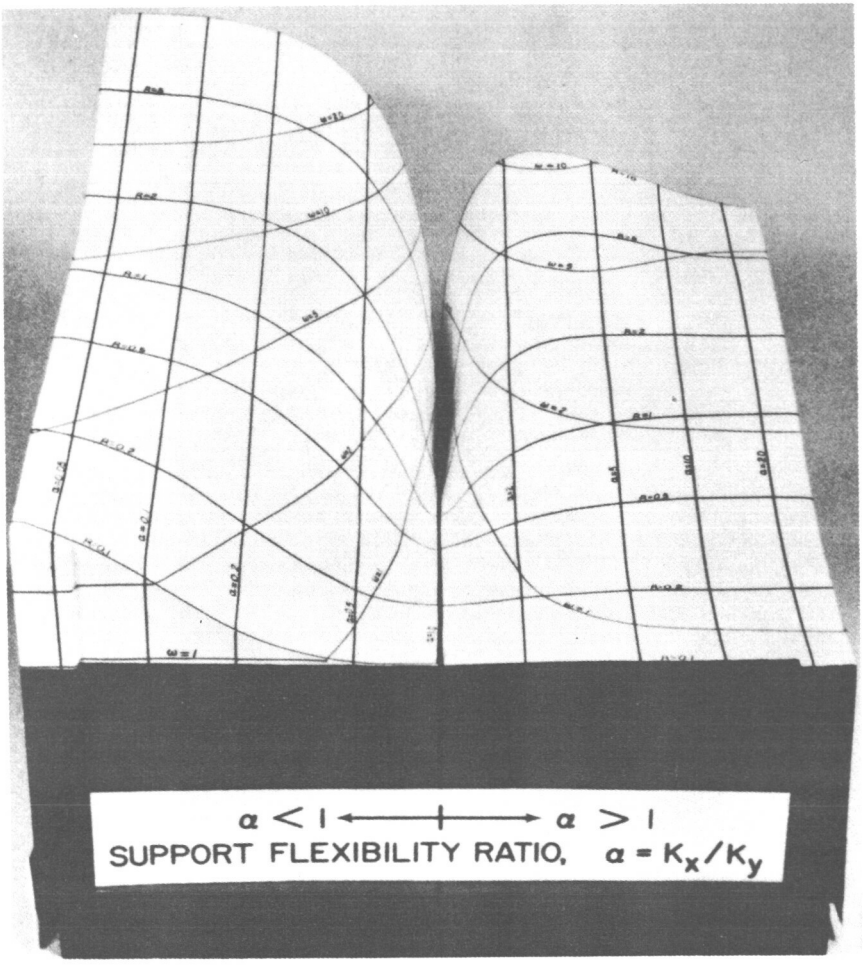


FIGURE 22.—Topological model of rotor stability characteristics with zero foundation damping, front view.

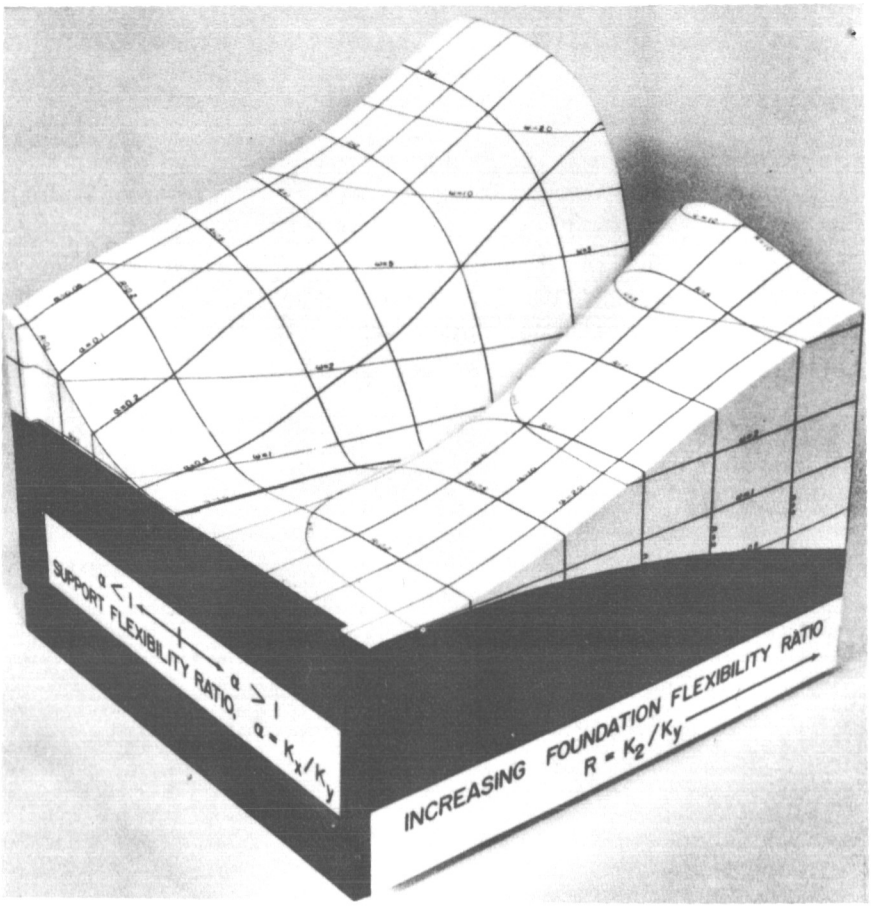


FIGURE 23.—Topological model of rotor stability characteristics with zero foundation damping, three-quarter view.

ing parameter $D$. At this low value of $R$, very little increase in stability is realized by increasing the horizontal bearing stiffness. In this particular case only when the horizontal stiffness becomes less than one-fifth of the vertical stiffness ($\alpha < 0.2$) is any appreciable gain in stability obtained. At the low values of $R$, the horizontal bearing stiffness must be of the same order of magnitude as the rotor stiffness to achieve an increase.

Figure 26 represents the section for $R = 0.5$ (the vertical bearing stiffness is twice the value of the rotor stiffness). At this value of $R$, substantial increases are obtained by introducing external damping and bearing asymmetry. For values of $D < 0.5$, little change is obtained by increasing $\alpha$ over 1. In fact, for low $D$ values (high external damping),

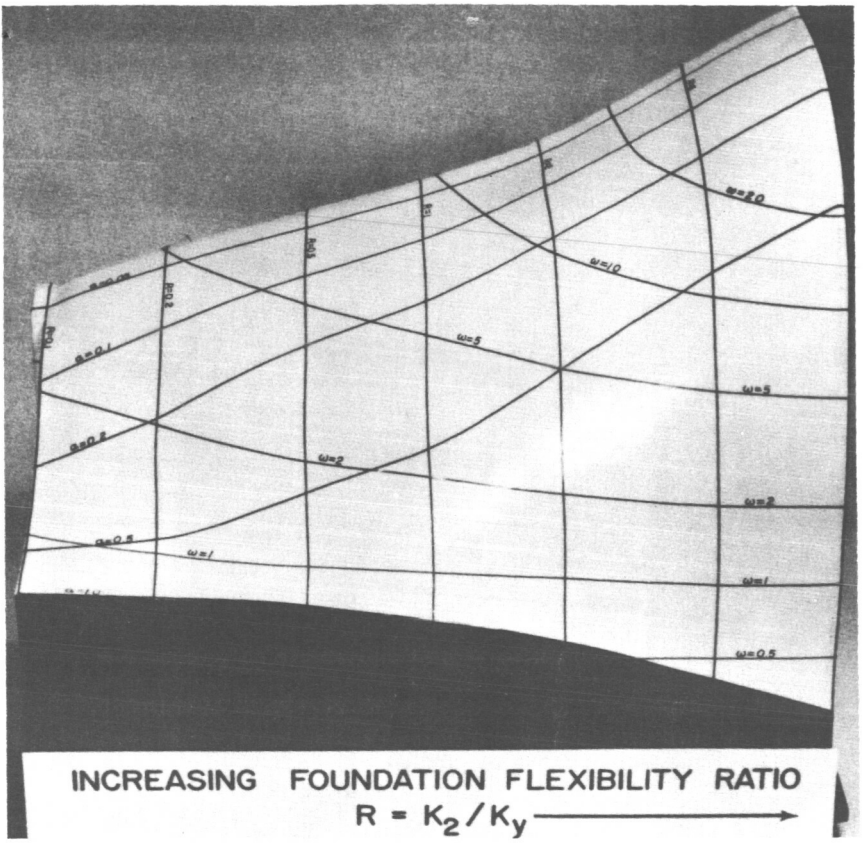


FIGURE 24.—Topological model of rotor stability characteristics with zero foundation damping, side view.

increasing the horizontal stiffness will result in a reduction of stability. Note that in all cases, a reduction in $\alpha$ causes a rise in stability, this rise being more pronounced the higher the value of external damping present. Figure 27 represents the rotor characteristics for $R = 1.0$ and shows how these effects become more pronounced as $R$ increases.

### 4.8.3 Whirl Orbits of a Balanced Horizontal Rotor

To illustrate the influence of foundation asymmetry on the rotor whirl threshold, consider the following example.

*Example 3*

Assume a rotor system with the following characteristics

$$K_2 = K_y = 250\,000 \text{ lb/in.}; \qquad R = 1$$
$$K_x = 125\,000 \text{ lb/in.}; \qquad \alpha = 0.5$$

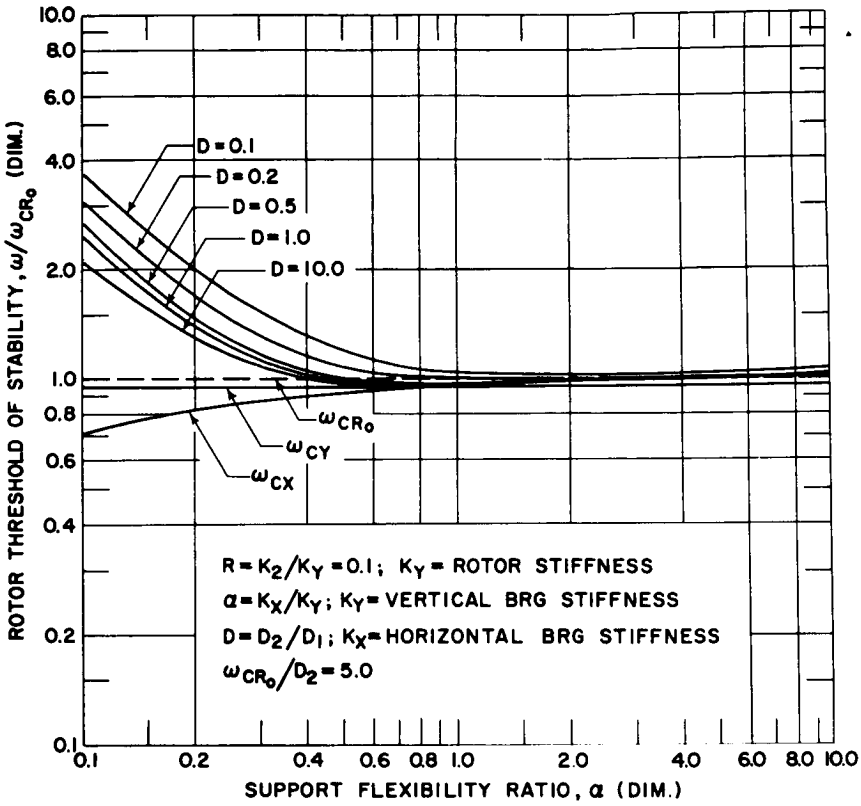


FIGURE 25.—Effect of unsymmetric bearing support flexibility on the rotor whirl threshold speed for $R = 0.1$ and $A = 5.0$.

$$D_1 = D_2 = 200 \text{ rad/sec}; \qquad D = 1.0$$
$$M = 0.25 \text{ lb-sec}^2/\text{in}.$$

The above conditions correspond to Examples 1 and 2 with the modification that the horizontal stiffness $K_x$ has been reduced to 1/2 $K_y$.

The system natural resonance frequencies in the $X$ and $Y$ directions, respectively, are

$$\omega_{cy} = \omega_{CR_o} \sqrt{\frac{1}{1+R}} = 0.707 \ \omega_{CR_o}$$

$$\omega_{cx} = \omega_{CR_o} \sqrt{\frac{\alpha}{\alpha+R}} = 0.577 \ \omega_{CR_o}$$

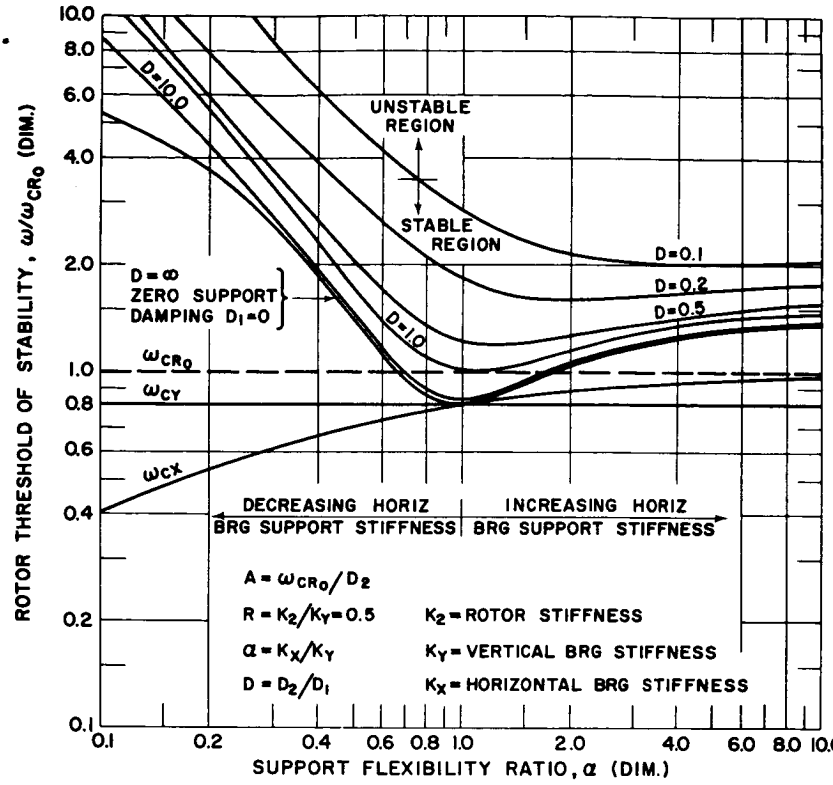


FIGURE 26.—Effect of unsymmetric bearing support flexibility on the rotor whirl threshold speed for $R=0.5$ and $A=5.0$.

where $\omega_{CR_0}=1000$ rad/sec.

The rotor whirl threshold speed is given by Eq. (4.33) and is

$$\omega_s=\omega_{CR_0}\sqrt{F_1+F_2}=3230 \text{ rad/sec.}$$

A comparison of this value to the results of Example 1 reveals that the threshold has been increased almost 130 percent by reducing $\alpha$ from 1 to 0.5. This effect is clearly seen in the stability map (Fig. 27) for $R=1.0$. The results of the first example are represented by the intersection of the lines $D=1.0$ and $\alpha=1.0$. Keeping $D$ constant and decreasing $\alpha$ to 0.5, we see that a rapid rise in stability occurs. Notice that if $K_x$ were increased instead of reduced, there would be a slight drop in stability for $\alpha$ slightly larger than one and then a gradual increase in the threshold occurs for larger values of $\alpha$.

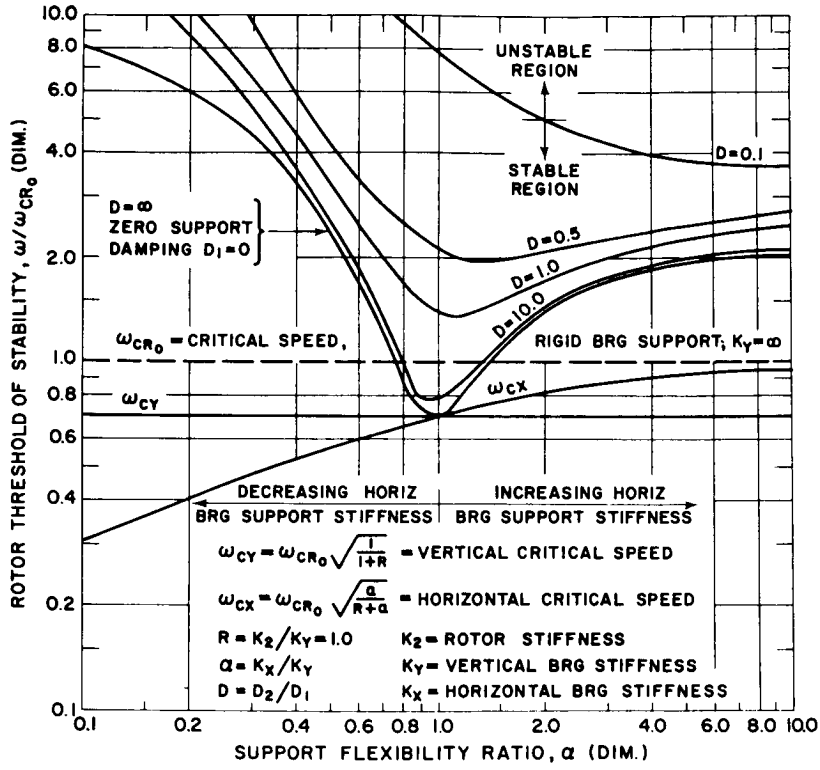


FIGURE 27.—Effect of unsymmetric bearing support flexibility on the rotor whirl threshold speed for $R = 1.0$ and $A = 5.0$.

To visualize the motion of a balanced rotor under these conditions, analog computer traces were made of the rotor motion up to the threshold speed as shown in Figs. 28–31. In Fig. 28, the rotor motion is given for the speed range of 500 to 1450 rad/sec. Notice that at 1450 rad/sec, the rotor motion is extremely stable, whereas for the case of the symmetric foundation (Fig. 11), the rotor is at the threshold of stability.

Figure 29 is of interest as it illustrates that the rotor transient motion exhibits both net forward and backward precession. For example, the rotor motion from time 0 to $T$ is net forward precession and then the motion reverses from $T_1$ to $T_2$ and backward precession predominates. The motion continues in this fashion until it is completely damped out. Figure 30 represents the rotor motion from 1700 to 2500 rad/sec. After a particular speed is obtained, the backward precession component is suppressed and only net forward precession is observed in the transient motion. Figure 31 illustrates the rotor motion below and above the rotor threshold. As the rotor speed approaches the threshold speed, the time

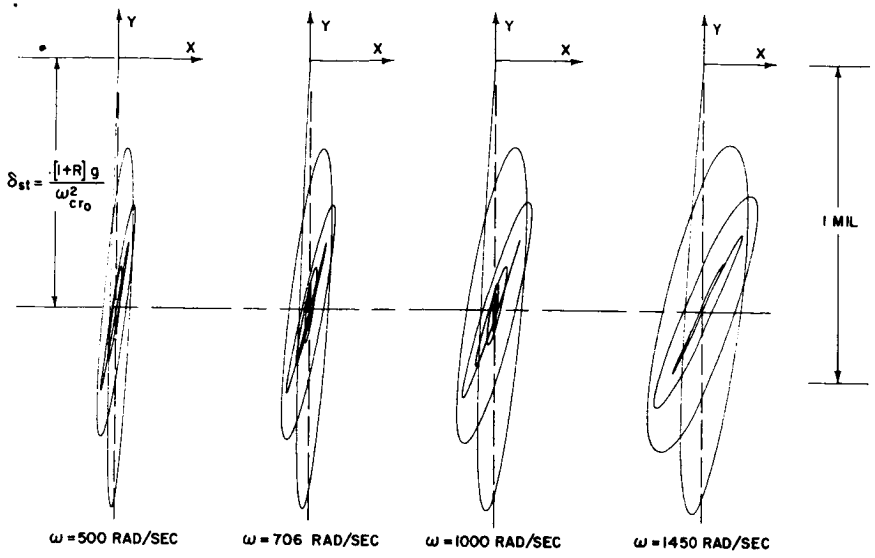


FIGURE 28.—Stable transient precessive motion of a balanced horizontal rotor with foundation asymmetry, $\omega = 500$–$1450$ rad/sec. Stable transient precession (forward and backward). Conditions: $M = 0.25$ lb-sec$^2$/in., $K_y = K_z = 250\,000$ lb/in., $K_x = 125\,000$ lb/in., $D_1 = D_2 = 200$ rad/sec, $\omega_s = 3230$ rad/sec.

required for the transient motion to die out increases. Once the threshold is exceeded, the transient grows rapidly in the case of the linear system, as shown by the second figure of Fig. 31.

### 4.8.4 Whirling of an Unbalanced Rotor

The addition of rotor unbalance does not effect the whirl threshold speed in the linear system, but it does introduce a particular solution composed of synchronous forward motion as described by Eq. (4.26). Figure 32 represents the steady-state synchronous orbits of a rotor with identical conditions to Example 3. If the rotor speed is below the threshold speed, the transient motion as shown in Figs. 28–30 will die out, and only the rotor synchronous precession caused by unbalance will remain. In Fig. 32, the computer program was run for a sufficient time to eliminate the transient. As the rotor speed approaches the threshold speed, the time required for the transient to disappear increases. Note that the rotor trace for $\omega = 3000$ rad/sec still shows a slight nonsynchronous whirl component even after 300 cycles. Since the time scale of the analog program is 1/1000, this represents 10 min of running time on the computer.

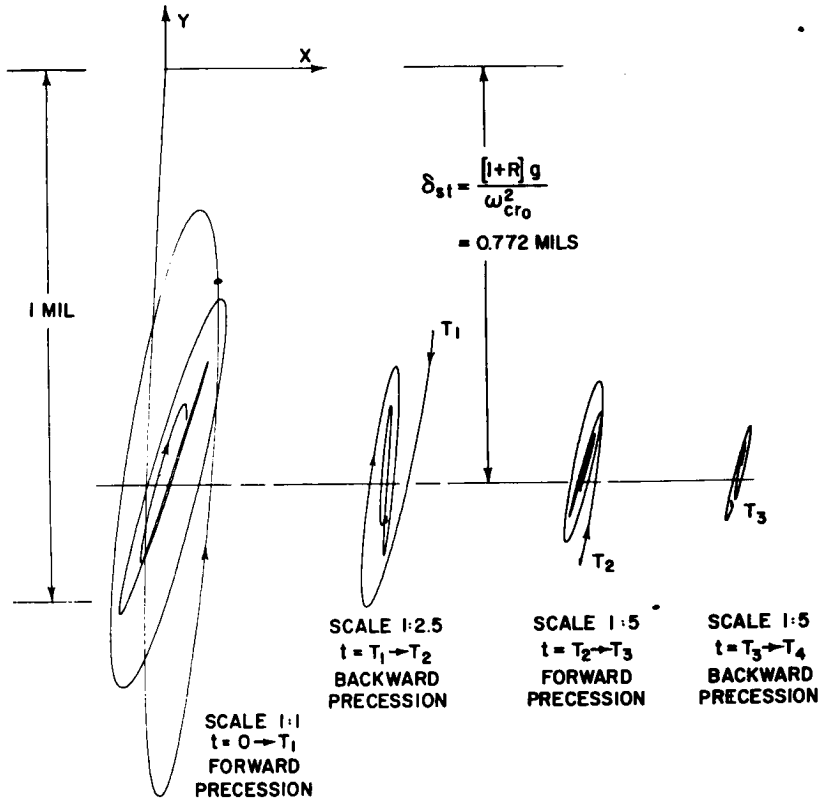


FIGURE 29.—Forward and backward precessive motion of a balanced horizontal rotor with foundation asymmetry, $\omega = 1000$ rad/sec. Conditions: $M = 0.25$ lb-sec$^2$/in., $K_y = K_z = 250\,000$ lb/in., $K_x = 125\,000$ lb/in., $D_1 = D_2 = 200$ rad/sec, $\omega = 1000$ rad/sec.

Dr. Newkirk noted that if his experimental rotor was running smoothly near the threshold speed, a disturbance to the system would cause the rotor to whirl. He observed that the time required for the whirl to damp out increased as the rotor speed approached the threshold.

At the threshold of stability, a strong nonsynchronous component develops. The whirl orbit formed is almost a stationary pattern composed of four internal loops (two of which are degenerate), indicating the presence of a one-fifth harmonic.[8]

The calculation of the rotor precession rate by a method similar to Sec. 4.6.3 shows that in general

$$\omega_P = \frac{\omega_{cx} + \omega_{cy}}{2} \tag{4.48}$$

[8] When a stationary whirl pattern is developed, the subsynchronous frequency is equal to $\omega/(1 +$ number of internal loops).

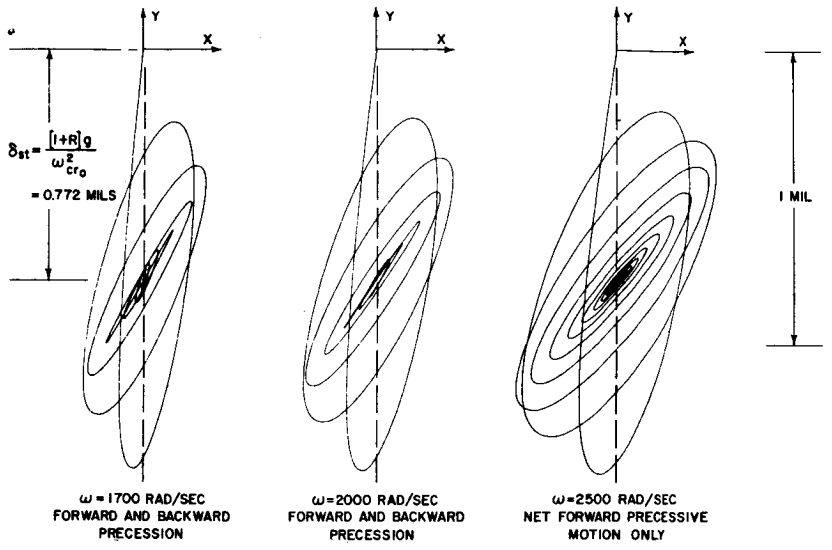


FIGURE 30.—Stable transient precessive motion of a balanced horizontal rotor with foundation asymmetry, $\omega = 1700$–$2500$ rad/sec. Stable transient precession (forward and backward). Conditions: $M = 0.25$ lb-sec$^2$/in., $K_y = K_2 = 250\,000$ lb/in., $K_x = 125\,000$ lb/in., $D_1 = D_2 = 200$ rad/sec, $\omega_s = 3230$ rad/sec.

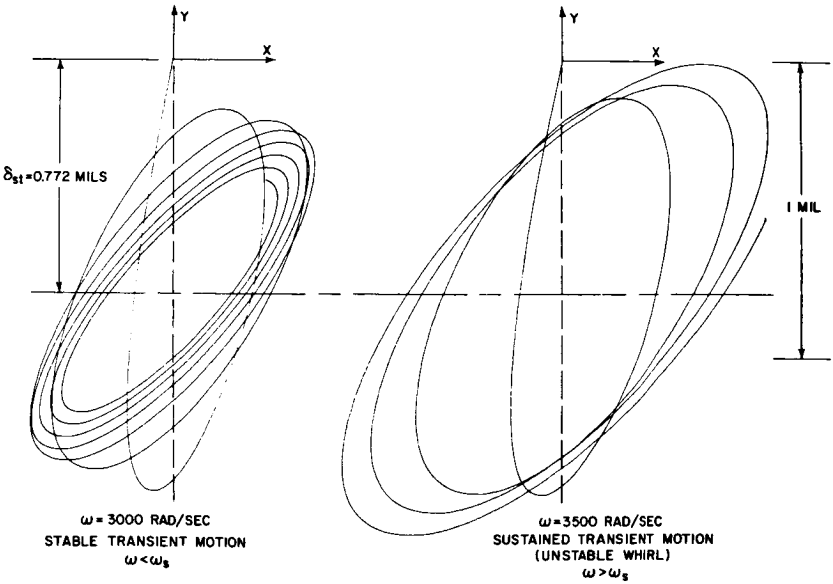


FIGURE 31.—Stable and unstable transient motion of a balanced horizontal rotor with foundation asymmetry, $\omega = 3000$ and 3500 rad/sec. Stable and unstable transient precession. Conditions: $M = 0.25$ lb-sec$^2$/in., $K_y = K_2 = 250\,000$ lb/in., $K_x = 125\,000$ lb/in., $D_1 = D_2 = 200$ rad/sec, $\omega_s = 3230$ rad/sec.

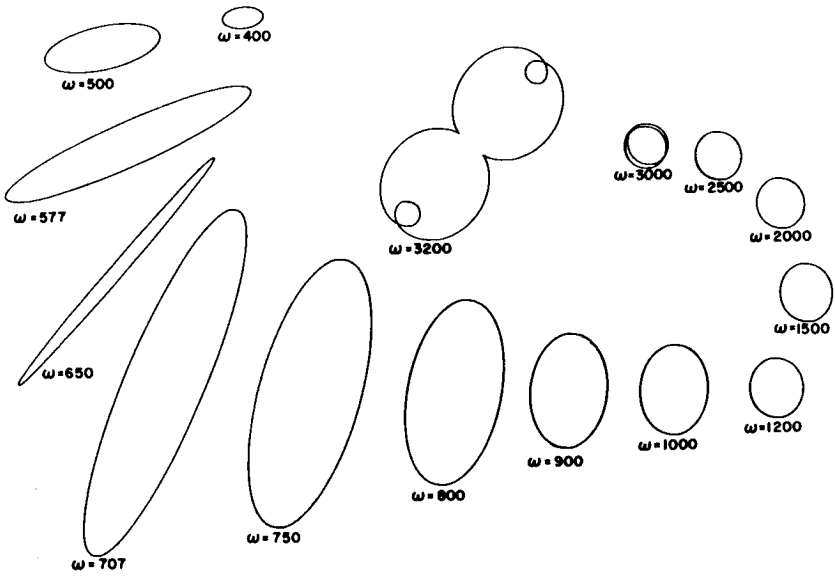


FIGURE 32.—Steady-state whirl orbits of an unbalanced rotor with foundation asymmetry, $\omega = 400$–$3200$ rad/sec. Conditions: $M = 0.25$ lb-sec²/in., $K_y = K_2 = 250\,000$ lb/in., $K_x = 125\,000$ lb/in., $D_1 = D_2 = 200$ rad/sec, $\omega_{cx} = 577$ rad/sec, $\omega_{cy} = 707$ rad/sec, $\omega_s = 3230$ rad/sec.

The rotor precession rate for Figs. 32–34 is $(577 + 707)/2 = 641$ rad/sec. Notice $5\omega_P = 3205$ is approximately the whirl threshold.

Figure 33 shows the rotor motion at the threshold for a large number of cycles. This whirl pattern is very reminiscent of whirl orbits of certain gas-bearing rotors at the threshold. (We shall see later that the analog computer programs developed in Ch. 4 may be used to approximate fluid film whirl.) Only if the nonsynchronous component is an exact portion of running speed will a stationary pattern develop. In Fig. 34, the operating speed is above the threshold. In this case the nonsynchronous component grows rapidly and predominates over the synchronous motion.

For the case of the system under consideration, the rotor motion may be roughly classified into four regions as follows:

1. Subcritical speed region
2. Critical speed region
3. Postcritical speed region
4. Supercritical speed region

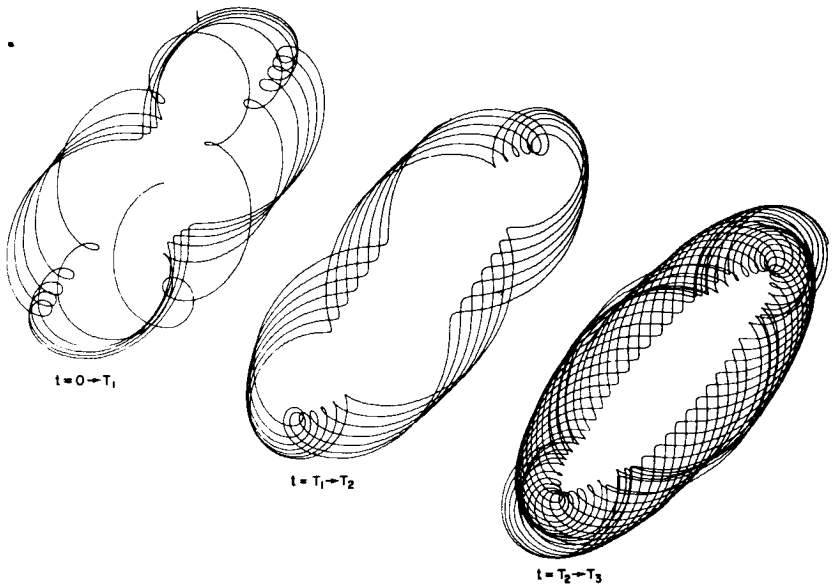


FIGURE 33.—Whirl orbit of an unbalanced rotor at the threshold of stability, $\omega = \omega_s$. Conditions: $M = 0.25$ lb-sec$^2$/in., $K_y = K_2 = 250\,000$ lb/in., $K_x = 125\,000$ lb/in., $D_1 = D_2 = 200$ rad/sec, $\omega = 3200$ rad/sec, $\omega_s = 3230$ rad/sec.

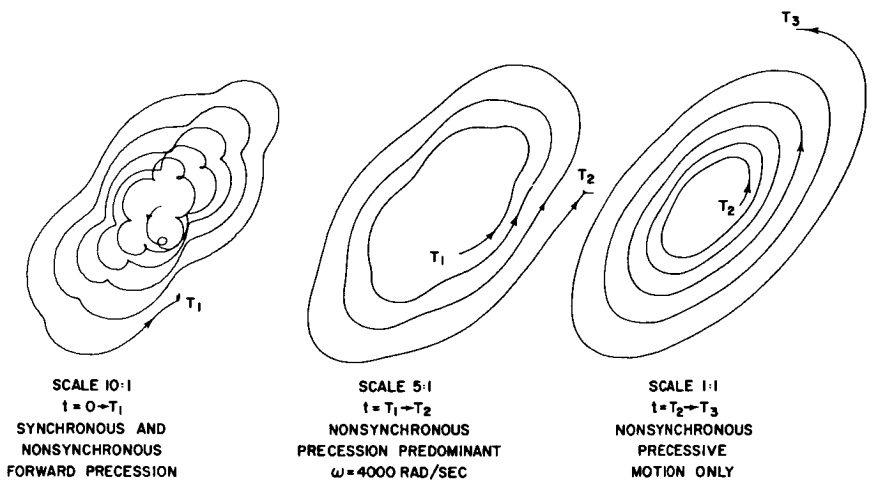


FIGURE 34.—Whirl orbit of an unbalanced rotor above the threshold of stability, $\omega = 4000$ rad/sec. Conditions: $M = 0.25$ lb-sec$^2$/in., $K_y = K_2 = 250\,000$ lb/in., $K_x = 125\,000$ lb/in., $D_1 = D_2 = 200$ rad/sec, $\omega_s = 3200$ rad/sec, $\omega = 4000$ rad/sec.

The divisions between the different regions is somewhat arbitrary,[9] but in general the following convention can be made: the subcritical speed region is defined as the speed range in which the rotor phase angles $\beta_x$ and $\beta_y$ are less than 90°. The critical speed range is the region bounded by $\beta_x = 90°$ and $\beta_y = 90°$ and represents the region where the largest rotor orbits due to unbalance occur. In the postcritical region, both $\beta_x$ and $\beta_y$ are greater than 90° but less than 180°. In the supercritical region, the rotor-phase angles are approximately 180° representing complete inversion of the rotor mass and elastic axes. For example in Fig. 32, the rotor-phase angles are approximately 180° at $\omega = 2500$ rad/sec. The rotor orbit becomes a circle of radius $e_\mu$ and would remain at this value, regardless of speed if self-excited whirl instability did not take place. It is important to note that self-excited whirl instability cannot occur in the subcritical speed region, but only in the postcritical speed region or higher.

## 4.9 GENERAL EQUATIONS OF MOTION

### 4.9.1 Discussion of System

The derivation of the equations of motion presented in Sec. 4.4 lack in generality and cannot be easily extended to a more complex system, which includes bearing mass, large damping forces, and rotor acceleration. The general equations of motion may be readily obtained from Lagrange's equations of motion, provided the system kinetic, potential, and dissipation functions are known. The only quantity which presents some difficulty is the proper representation of the internal friction forces. The internal friction force cannot be derived from a potential function (system would be inherently stable), but must be obtained from a dissipation function of the proper form. This seems logical, since the internal friction assumes the characteristics of a damping force in the subcritical speed range.

Thus to properly investigate stability, it is necessary to examine the performance of nonconservative systems in which the dissipation function has particular properties. For example, Chapter 3 shows that the conservative Jeffcott system derived from only the potential and kinetic energy does not produce self-excited whirl, contrary to the recent papers by Green [22] and Kane [45].

[9] The arbitrariness of the division of the different speed regions increases with the external damping present. For example, Fig. 5 shows that if the system is critically damped, the rotor amplitude increases uniformly from 0 to $e_\mu$ without the indication of a critical speed vibration. The division of the speed range may still be made in this case by the examination of the rotor phase angle.

### 4.9.2 Derivation of General Equations of Motion

The position vectors to the mass stations are given by

$m_1$: bearing mass

$$^{O}\vec{P}^{M_1} = X_1\vec{n}_x + Y_1\vec{n}_y \tag{4.49}$$

$m_2$: rotor mass

$$^{O}\vec{P}^{M_2} = (X_1 + X_2 + e_\mu \cos \omega t)\vec{n}_x + (Y_1 + Y_2 + e_\mu \sin \omega t)\vec{n}_y \tag{4.50}$$

if $\omega t$ is replaced by $\theta$, the system possesses five degrees of freedom and hence five equations of motion will be required to completely describe the system.

The velocities of the mass stations are given by

$m_1$:

$$^{R}\vec{V}^{M_1/O} = \dot{X}_1\vec{n}_x + \dot{Y}_1\vec{n}_y \tag{4.51}$$

$m_2$:

$$^{R}\vec{V}^{M_2/O} = (\dot{X}_1 + \dot{X}_2 - e_\mu\dot{\theta} \sin \theta)\vec{n}_x + (\dot{Y}_1 + \dot{Y}_2 + e_\mu\dot{\theta} \cos \theta)\vec{n}_y \tag{4.52}$$

The kinetic energy of the system is given by

$$T = \tfrac{1}{2}\{M_2[(\dot{X}_1 + \dot{X}_2 - e_\mu\dot{\theta} \sin \theta)^2 + (\dot{Y}_1 + \dot{Y}_2 + e_\mu\dot{\theta} \cos \theta)^2] + m_1[\dot{X}_1^2 + \dot{Y}_1^2] + \Phi\dot{\theta}^2\} \tag{4.53}$$

The potential energy of the system is given by

$$V = \tfrac{1}{2}[K_x X_1^2 + K_y Y_1^2] + \tfrac{1}{2} K_2[X_2^2 + Y_2^2] \tag{4.54}$$

The dissipation function caused by the external damping is given by

$$D_1 = \tfrac{1}{2} C_1[\dot{X}_1^2 + \dot{Y}_1^2] \tag{4.55}$$

and the dissipation function caused by the internal rotor friction can be obtained from the force relationship Eq. (4.14) and is given by

$$D_2 = C_2\left[\frac{\dot{X}_2^2 + \dot{Y}_2^2}{2} + \omega(Y_2\dot{X}_2 - X_2\dot{Y}_2)\right] \tag{4.56}$$

Close investigation of the dissipation function $D_2$ shows that it may be expressed in the following form

$$D_2 = C_2\left[\frac{1}{2}\left({}^R\vec{V}^{C/O_b}\right)^2 + \omega\rho_2^2\frac{d\phi}{dt}\right] \tag{4.57}$$

where

$\phi$ = rotor attitude angle $= \tan^{-1}\dfrac{X_2}{Y_2}$

$\dot{\phi}$ = rotor precession rate

$\rho_2 = \sqrt{X_2^2 + Y_2^2}$

Thus when the rotor precession rate $\dot{\phi}$ is zero, the internal friction dissipation function assumes the characteristics of conventional viscous damping. It is very important to note that only in the case when the dissipation function has this special characteristic of being dependent upon the rotor or bearing precession rate can self-excited whirl instability be developed. When the system damping terms are represented entirely by functions of the form in Eq. (4.55), the system is inherently stable.

The governing equations of motion of the system are obtained from Lagrange's equation, which states

$$\frac{d}{dt}\left(\frac{L}{\partial\dot{q}_r}\right) - \frac{\partial L}{\partial q_r} + \frac{\partial D}{\partial\dot{q}_r} = F_{qr} \tag{4.58}$$

where $L = T - V$

Application of the above for the five generalized coordinates yields the following equations

$$X_1:\ m_1\ddot{X}_1 + m_2[\ddot{X}_1 + \ddot{X}_2 - e_\mu\ddot{\theta}\sin\theta + e_\mu(\dot{\theta})^2\cos\theta] + C_1\dot{X}_1 + K_xX_1 = 0 \tag{4.59}$$

$$Y_1:\ m_1\ddot{Y}_1 + m_2[\ddot{Y}_1 + \ddot{Y}_2 + e_\mu\ddot{\theta}\cos\theta - e_\mu(\dot{\theta})^2\sin\theta] + C_1\dot{Y}_1 + K_yY_1 = 0 \tag{4.60}$$

$$X_2:\ m_2[\ddot{X}_1 + \ddot{X}_2 - e_\mu\ddot{\theta}\sin\theta - e_\mu(\dot{\theta})^2\cos\theta] + C_2[\dot{X}_2 + \omega Y_2] + K_2X_2 = 0 \tag{4.61}$$

$$Y_2:\ m_2[\ddot{Y}_1 + \ddot{Y}_2 + e_\mu\ddot{\theta}\cos\theta - e_\mu(\dot{\theta})^2\sin\theta] + C_2(\dot{Y}_2 - \omega X_2) + K_2Y_2 = 0 \tag{4.62}$$

$$\begin{aligned}\theta:\ \Phi\ddot{\theta} + m_2[&-(\ddot{X}_1 + \ddot{X}_2)e_\mu\sin\theta + (\ddot{Y}_1 + \ddot{Y}_2)e_\mu\cos\theta \\ &- (\dot{X}_1 + \dot{X}_2)\dot{\theta}e_\mu\cos\theta - (\dot{Y}_1 + \dot{Y}_2)\dot{\theta}e_\mu\sin\theta \\ &+ e_\mu^2\ddot{\theta}] - m_2[-(\dot{X}_1 + \dot{X}_2 - e_\mu\dot{\theta}\sin\theta)e_\mu\dot{\theta}\cos\theta \\ &- (\dot{Y}_1 + \dot{Y}_2 + e_\mu\theta\cos\theta)e_\mu\dot{\theta}\sin\theta] = T\end{aligned}$$

upon simplification

$$\Phi\ddot{\theta}+m_2[-(\ddot{X}_1+\ddot{X}_2)e_\mu \sin\theta+(\ddot{Y}_1+\ddot{Y}_2)e_\mu\cos\theta+e_\mu^2\ddot{\theta}]=T \quad (4.63)$$

Neglecting rotor acceleration, the five governing equations reduce to the four following equations

$$(1+\delta m)\ddot{X}_1+\ddot{X}_2+D_1\dot{X}_1+\omega_x^2X_1=e_\mu\omega^2\cos\omega t \quad (4.64)$$

$$(1+\delta m)\ddot{Y}_1+\ddot{Y}_2+D_1\dot{Y}_1+\omega_y^2Y_1=e_\mu\omega^2\sin\omega t \quad (4.65)$$

$$\ddot{X}_1+\ddot{X}_2+D_2\dot{X}_2+D_2\omega Y_2+\omega_2^2X_2=e_\mu\omega^2\cos\omega t \quad (4.66)$$

$$\ddot{Y}_1+\ddot{Y}_2+D_2\dot{Y}_2-D_2\omega X_2+\omega_2^2Y_2=e_\mu\omega^2\sin\omega t \quad (4.67)$$

where

$$\delta m=\frac{m_1}{m_2}$$

$$\omega_x^2=\frac{K_x}{m_2}$$

$$\omega_y^2=\frac{K_y}{m_2}$$

$$\omega_2^2=\frac{K_2}{m_2}=\omega_{\mathrm{CR}_0}^2$$

The above four equations can be represented by two complex equations in $Z_1$ and $Z_2$. The introduction of foundation asymmetry will give rise to a complex conjugate term in $Z_1$.

$$(1+\delta m)\ddot{Z}_1+\ddot{Z}_2+D_1\dot{Z}_1+\frac{\omega_x^2+\omega_y^2}{2}Z_1+\frac{\omega_x^2-\omega_y^2}{2}\overline{Z}_1=e_\mu\omega^2e^{i\omega t} \quad (4.68)$$

$$\ddot{Z}_1+\ddot{Z}_2+D_2\dot{Z}_2+(\omega_2^2-iD_2\omega)Z_2=e_\mu\omega^2e^{i\omega t} \quad (4.69)$$

### 4.9.3 Uniform Foundation Flexibility and Zero Bearing Mass

If bearing mass is neglected and the rotor is considered as balanced, that is $m_1=0$ and $e_\mu=0$, the system reduces to

$$m_2\ddot{Z}+C_1\dot{Z}_1+K_1Z_1=0 \quad (4.70)$$

(4.68)

$$m_2\ddot{Z} + C_2\dot{Z}_2 + [K_2 - iC_2\omega]Z_2 \underset{(4.69)}{=} 0 \tag{4.71}$$

where

$$Z = Z_1 + Z_2$$

and hence

$$C_1\dot{Z}_1 + K_1Z_1 \underset{(4.70,\ 4.71)}{=} C_2\dot{Z}_2 + (K_2 - iC_2\omega)Z_2 \underset{(4.10)}{=} -\vec{F}_c \tag{4.72}$$

For the case of light damping where $\omega C_1/K_1$ and $\omega C_2/K_2 < 1$, then

$$Z_1 = \left(\frac{K_2 - iC_2\omega}{K_1}\right) Z_2 = Z - Z_2 \tag{4.73}$$

Solving for $Z_2$ in terms of $Z$

$$Z_2 = \frac{K_1(K_1 + K_2 + iC_2\omega)}{(K_1 + K_2)^2 + (C_2\omega)^2} Z \tag{4.74}$$

Equation (4.72) may be expressed in the following form

$$\left.\begin{aligned} &\text{(a)}\ \vec{F}_c = -(C_1\dot{Z}_1 + K_1Z_1) \\ &\text{(b)}\ \vec{F}_c = -[C_2\dot{Z}_2 + (K_2 - iC_2\omega)Z_2] \end{aligned}\right\} \tag{4.75}$$

Divide Eq. (4.75a) by $K_1$ and Eq. (4.75b) by $K_2$ and add, and solve for $\vec{F}_c$

$$\vec{F}_c = -\frac{K_1K_2}{K_1 + K_2}\left[\frac{C_1}{K_1}\dot{Z} + \left(\frac{C_2}{K_2} - \frac{C_1}{K_1}\right)\dot{Z}_2 - \frac{iC_2\omega}{K_2}Z_2 + Z\right] \tag{4.76}$$

$$\therefore \vec{F}_c \underset{(4.76,\ 4.74)}{=} -\left\{\left[C_1K_2 + (C_2K_1 - CK_2)\left(\frac{K_1(K_1 + K_2 + iC_2\omega)}{(K_1 + K_2)^2 + (C_2\omega)^2}\right)\right]\frac{\dot{Z}}{K_1 + K_2}\right.$$

$$\left. + \left[\left(K_1K_2 + \frac{(C_2\omega)^2}{(K_1 + K_2)^2 + (C_2\omega)^2}\right) - i\,\frac{C_2\omega K_1^2(K_1 + K_2)}{(K_1 + K_2)^2 + (C_2\omega)^2}\right]\frac{Z}{K_1 + K_2}\right\} \tag{4.77}$$

The complete equations of motion of the whirling rotor (neglecting bearing mass) is given by

$$\ddot{Z}+\left[\frac{D_1K_2}{K_1+K_2}+\frac{D_2K_1-D_1K_2}{K_1-K_2}\left[\frac{\omega_1^2(\omega_1^2+\omega_2^2+iD_2\omega)}{(\omega_1^2+\omega_2^2)^2+(D_2\omega)^2}\right]\right]\dot{Z}$$

$$+\frac{1}{K_1+K_2}\left[\omega_1^2\omega_2^2+\frac{(D_2\omega)^2}{(\omega_1^2+\omega_2^2)^2+(D_2\omega)^2}-i\frac{D_2\omega\omega_1^4(\omega_1^2+\omega_2^2)}{(\omega_1^2+\omega_2^2)^2+(D_2\omega)^2}\right]Z$$

$$\underset{(4.71,\,4.77)}{=}e_\mu\omega^2e^{i\omega t} \quad (4.78)$$

For the range of speeds to be considered and with light damping the parameter

$$\left(\frac{D_2\omega}{\mathscr{K}_1+\mathscr{K}_2}\right)^2\ll 1 \quad (4.79)$$

Hence upon reduction:

$$\ddot{Z}+\left[D_2\left(\frac{K_1}{K_1+K_2}\right)^2+D_1\left(\frac{K_2}{K_1+K_2}\right)^2\right]\dot{Z}+\left[\omega_{CR}^2-iD_2\left(\frac{K_1}{K_1+K_2}\right)^2\omega\right]Z$$

$$\underset{(4.78,\,4.79)}{=}e_\mu\omega^2e^{i\omega t} \quad (4.80)$$

Note that Eq. (4.80) is identical to Eq. (4.36) of the original derivation.

### 4.9.4 Approximate Effect of Bearing Mass on Stability

Assume that the system is being driven with constant angular velocity $\omega$ and that the foundation support is uniform in all directions. Equations (4.68) and (4.69) reduce to

$$\ddot{Z}+\delta m\ddot{Z}_1+D_1\dot{Z}_1+\omega_1^2Z_1=e_\mu\omega^2e^{i\omega t} \quad (4.81)$$

$$\ddot{Z}+D_2\dot{Z}_2+(\omega_2^2-iD_2\omega)Z_2=e_\mu\omega^2e^{i\omega t} \quad (4.82)$$

Combining the above two equations in terms only of the complex rotor deflection $Z_2$, we obtain, after considerable manipulation, the following third-order complex equation

$$[D_1+D_2(1+\delta m)]\dddot{Z}_2+[\omega_1^2+\omega_2^2+D_1D_2-iD_2\omega]\ddot{Z}_2+[\omega_2^2D_1+\omega_1^2D_2$$

$$-iD_1D_2\omega]\dot{Z}_2+\omega_1^2[\omega_2^2-iD_2\omega]Z_2=e_\mu\omega^2[\omega_1^2-\delta m\omega^2+iD_1\omega]e^{i\omega t} \quad (4.83)$$

In general, the above equation may be written as

$$R_3\dddot{Z}_2+(R_2-iI_2)\ddot{Z}_2+(R_1-iI_1)\dot{Z}_2+[R_0-iI_0]Z_2=F_r+iF_i \quad (4.84)$$

where

$$R_3 = D_1 + D_2(1+\delta m) \qquad I_3 = 0$$
$$R_2 = \omega_1^2 + \omega_2^2 + D_1 D_2 \qquad I_2 = D_2\omega$$
$$R_1 = \omega_2^2 D_1 + \omega_1^2 D_2 \qquad I_1 = D_1 D_2 \omega$$
$$R_0 = \omega_2^2 \omega_1^2 \qquad I_0 = D_2 \omega \omega_1^2$$

Considering only the homogeneous equation, let

$$Z_2 = Z_0 e^{(P+iS)t}$$

Separating real and imaginary quantities

$$Re:\ R_3P^3 + R_2P^2 + R_1P + R_0 - [3R_3P + R_2]S^2 + [2I_2P + I_1]S = 0 \qquad (4.85)$$

$$Im:\ -R_3S^3 + I_2S^2 + (3R_3P^2 + 2R_2P + R_1]S - [I_0 + I_1P + I_2P^2] = 0$$

At the threshold of stability, $P = 0$ and the real part reduces to

$$Re:\ R_2S^2 - I_1S - R_0 = 0 \qquad (4.86)$$

Solving for the positive root of $S$ to obtain the rotor precession rate

$$S_+ = \omega_P = \frac{\omega_1\omega_2}{\sqrt{\omega_1^2 + (1+\delta m)\omega_2^2 + D_1D_2}} \times \left[\frac{D_1D_2\omega}{2\omega_1\omega_2\sqrt{[\omega_1^2 + (1+\delta m)\omega_2^2] + D_1D_2}}\right.$$
$$\left. + \sqrt{1 + \frac{D_1D_2}{2\omega_1\omega_2\sqrt{\omega_1^2 + (1+\delta m)\omega_2^2 + D_1D_2}}}\right] \qquad (4.87)$$

*Order of Magnitude Analysis*

To determine the relative magnitude of the various parameters, a sample calculation will be made corresponding to a lightly damped rotor. Let

$$M = 0.25\ \frac{\text{lb-sec}^2}{\text{in.}}\ \text{(96.6-lb rotor)}$$

$$K_1 = K_2 = 250\,000\ \text{lb/in.}$$

$$\omega_1^2 = \omega_2^2 = \frac{K}{M} = 1 \times 10^6\ \text{rad}^2/\text{sec}^2$$

$$D_1 = D_2 = \frac{C}{M} = 200\ \text{rad/sec}$$

$$\omega_{CR_0} = \sqrt{\frac{K_2}{M}} = 1000 \text{ rad/sec}$$

$$= \text{rotor natural frequency (on rigid supports)}$$

$$\omega_{CR} = \sqrt{\frac{K_1 K_2}{M(K_1 + K_2)}} = \sqrt{\frac{K}{2M}} = 706 \text{ rad/sec}$$

the rotor precession speed is given by

$$S = \sqrt{\frac{K_1 K_2}{M\{K_1 + (1+\delta m)K_2\} + D_1 D_2}} \left\{ \frac{D_1 D_2 \omega}{2\sqrt{R_0 R_2}} \pm \sqrt{1 + \frac{D_1 D_2 \omega}{2\sqrt{R_0 R_2}}} \right\}$$

$$R_0 = \omega_1^2 \omega_2^2 = 10^{12}$$

$$R_2 = \frac{1}{M}\{K_1 + (1+\delta m)K_2\} + D_1 D_2 \approx 2 \times 10^6$$

$$2\sqrt{R_0 R_2} = 2.828 \times 10^9$$

$$D_1 D_2 = 4 \times 10^4$$

$$\omega \approx 1 \times 10^3$$

$$D_1 D_2 \omega \approx 4 \times 10^7$$

and

$$\frac{D_1 D_2 \omega}{2\sqrt{R_0 R_2}} = 1.414 \times 10^{-2} = 0.014$$

Thus in the normal turborotor the parameter

$$\frac{D_1 D_2 \omega}{2\sqrt{R_0 R_2}} \ll 1$$

and hence the precession rate is approximated by

$$S = \sqrt{\frac{K_1 D_2}{(K_1 + (1+\delta m)K_2)M}} = \sqrt{\frac{R_0}{R_2}} \tag{4.88}$$

Note that if bearing mass $\delta m = m_1/M_2 = 0$, then the precession rate is

$$S = \sqrt{\frac{K_1 K_2}{M(K_1 + K_2)}} = \text{system critical speed of Sec. 4.5}$$

The assumption that $S=\omega_P$ is known at the threshold greatly simplifies the stability criterion. Combining the *Re* and *Im* equations of Eq. (4.85) and taking the limit as $P\rightarrow 0$ results in the following equation

$$\left[I_2-\frac{R_3R_0}{R_2}\right]S^2+\left[R_1-\frac{R_3R_0}{R_2}\right]S-I_0=0 \tag{4.89}$$

Solving for the threshold of stability

$$\omega \underset{(4.88,\,4.89)}{=} \frac{\left[R_3\frac{R_2}{R_2}-R_1\right]\omega_P}{D_2\left[\left(1-\frac{R_3}{R_2}D_1\right)\omega_P^2-\omega_1^2\right]} \tag{4.90}$$

Evaluation of the threshold of stability by Eq. (4.90) shows that the addition of bearing mass lowers the threshold of stability when $\omega_s > \omega_{CR}$. For example, very high values of $\delta_m$ cause the foundation to act as a rigid base and $\omega_s$ approaches Eq. (4.40) as a limiting case.

## 4.10 GENERAL STABILITY ANALYSIS

A very general stability analysis of the rotor system as shown in Fig. 7 may now be made. This analysis includes the effects of bearing mass and is not restricted to small values of damping as is the analysis of Sec. 4.6.1.

Assume a complementary solution to Eqs. (4.64–4.67) of the form

$$X_1=Ae^{\lambda t}; \qquad Y_1=Be^{\lambda t}$$

$$X_2=Ce^{\lambda t}; \qquad Y_2=De^{\lambda t}$$

results in

$$\begin{bmatrix} [\lambda^2 & (1+\delta m)+D_1\lambda+K_x] & 0 & \lambda^2 & 0 \\ 0 & [\lambda^2(1+\delta m)+D_1\lambda+K_y] & 0 & \lambda^2 & \\ \lambda^2 & 0 & [\lambda^2+\lambda D_2+K_2] & & D_2\omega \\ 0 & \lambda^2 & -D_2\omega & [\lambda^2+D_2\lambda+K_2] & \end{bmatrix} \begin{bmatrix} A \\ B \\ C \\ D \end{bmatrix} = 0 \tag{4.91}$$

Since the coefficients $A$, $B$, $C$, $D$ are arbitrary, the determinant of the coefficients must vanish. Expanding the determinant we obtain the following eighth-order frequency equation in $\lambda$.

$$
\begin{aligned}
&\{\delta m\}^2\lambda^8+\{2\delta m[(1+\delta m)D_2+D_1]\}\lambda^7\\
&+\{(1+\delta m)^2(2K_2+D_2^2)+(3+4\delta m)D_1D_2\\
&+\delta_m(K_y+K_x)-2(1+\delta m)K_2+D_1^2\}\lambda^6\\
&\times\{2(1+\delta m)[D_1(2K_2+D_2^2)+D_2K_2(1+\delta m)]\\
&+D_1(K_x+K_y+2K_2)+D_2[(1+2\delta m)(K_x+K_y)\\
&+2D_1^2]\}\lambda^5+\{(1+\delta m)[(K_x+K_y)(2K_2+D_2^2)\\
&+4D_1D_2K_2+(1+\delta m)(D_2^2\omega^2+K_2^2)]+2D_1D_2(K_x\\
&+K_y)+2D_1^2K_2+D_1^2D_2^2+K_xK_y-K_2(K_x+K_y)\}\lambda^4\\
&+\{(1+\delta m)[K_2(K_x+K_y)2D_2+2D_2+2D_1(D_2^2\omega^2+K_2^2)]\\
&+D_1(K_x+K_y)(2K_2+D_2^2)+2D_2(D_1^2K_2\\
&+K_xK_y)\}\lambda^3+\{(1+\delta m)(K_x+K_y)(D_2^2\omega^2+K_2^2)\\
&+2D_1D_2K_2(K_x+K_y)+D_2^2\omega^2+K_xK_y)\\
&+K_2(D_1^2K_2+2K_xK_y)\}\lambda^2\\
&+\{D_1(D_2^2\omega^2+K_2^2)(K_x+K_y)+2D_2K_2K_xK_y\}\lambda\\
&+K_xK_y[D_2^2\omega^2+K_2^2]=0
\end{aligned}
\tag{4.92}
$$

Equation (4.92) is of the form

$$\sum_{K=0}^{N=8}A_{n-k}\lambda^k=0$$

Thus instead of a fourth-order equation as was obtained in Sec. 4.6.1, the introduction of bearing mass and large damping forces requires an eighth-order system. If bearing mass is neglected, Eq. (4.92) reduces to a sixth-order equation which is equivalent to a three-degree-of-freedom system.

For systems larger than fourth order, the Routh-Hurwitz determinant method becomes cumbersome and unwieldy to use. In such cases, the original Routh method is preferable. This method is outlined as follows:

Consider the following array of coefficients:

| | | | | |
|---|---|---|---|---|
| $A_0$ | $A_2$ | $A_4$ | $A_6$ | $A_8$ |
| $A_1$ | $A_3$ | $A_5$ | $A_7$ | |
| $C_1$ | $C_2$ | $C_3$ | $C_4$ | |

$$
\begin{array}{lll}
D_1 & D_2 & D_3 \\
E_1 & E_2 & E_3 \\
F_1 & F_2 & \\
G_1 & G_2 & \\
H_1 & &
\end{array}
$$

where

$$
\begin{aligned}
&C_1 = A_2 - A_0A_3/A_1;\ C_3 = A_6 - A_0A_7/A_1 \\
&C_2 = A_4 - A_0A_5/A_1;\ C_4 = A_8 \\
&D_1 = A_3 - A_1C_2/C_1;\ D_3 = A_7 - A_1C_4/C_1 \\
&D_2 = A_5 - A_1C_3/C_1 \\
&E_1 = C_2 - C_1D_2/D_1;\ E_3 = D_3 \\
&E_2 = C_3 - C_1D_3/D_1 \\
&F_1 = D_2 - D_1E_2/E_1;\ F_2 = D_3 - D_1E_3/E_1 \\
&G_1 = E_2 - E_1F_2/F_1;\ G_2 = E_3 \\
&H_1 = F_2 - F_1G_2/G_1
\end{aligned}
$$

The necessary and sufficient condition of stability is that all of the coefficients of the first column of the array must be positive.

### 4.10.1 Digital Computer Program

A digital computer program for the Honeywell 1400 computer was developed to calculate the threshold of stability of Eq. (4.92) by the general Routh procedure as outlined. Since the coefficients of the characteristic equation are speed dependent, an iterative approach was employed to obtain the threshold speed. The method consists of assuming an initial value of $\omega$ and calculating the coefficients $A_0$ to $A_8$. If these are all positive, the program continues, calculates the Routh coefficients and tests to see if any coefficient in the first column is negative. If no negative coefficient appears, the initial value of $\omega$ is incremented to a new value and the process is repeated. If a negative coefficient appears, the next value of $\omega$ is obtained by averaging the unstable speed with the last previous stable value. This procedure is continued until a convergence criterion is satisfied.

The computer program is presented in detail in Appendix C. Following the program listing are two typical cases illustrating the iterative procedure. To obtain these two examples, print statements were inserted into the computer program to obtain the values of the coefficients for each $\omega$ value. For example, in the first case, $D = 0.0$, $R = 1$ and $\alpha = 0.5$, the Routh coefficient $F_1$ becomes negative after seven iterations and $\omega$ converges to within 1 percent of the threshold value in seven more steps.

Table 10 represents a comparison between some typical values of the approximate system of Sec. 4.8 and the general solution of Sec. 4.10. The table shows that for zero foundation damping ($D_1=0$), the approximate solution indicates a slightly higher threshold of stability. When external damping is introduced into the system, the stability threshold for the exact solution increases rapidly. At $D=1$ ($D_1=200$ rad/sec), the general computer solution indicates that the threshold value is over 40 percent larger than the approximate analysis. When the external damping was doubled to $D_1=400$ rad/sec, the computer program did not find any negative values in the leading Routh coefficients. (When the rotor speed $\omega$ reaches 100 times the critical speed, the system is assumed stable and the iterative procedure is discontinued.)

TABLE 10.—*Comparison of the stability threshold of approximate and general system for* R = *1.0 and various damping values*

$\delta M=0.00$ $R=1.0$ $A=5.0$ $\alpha=0.5$ $D_2=200$

| | $D_1=0$ | $D_1=40$ | $D_1=200$ | $D_1=400$ |
|---|---|---|---|---|
| Approximate (table 6)..... | 2.39 | 2.62 | 3.23 | 4.21 |
| Exact..... | 2.143 | 3.683 | 5.50 | [1] |
| Percent deviation..... | +11.5 | −29 | −41 | ..... |

[1] Stable.

In the majority of cases examined, the Routh coefficient $F_1$ was found to be the term which indicates the system stability. In the computer program, $F_1$ is determined by the difference between $D22$ and $E2$; Fig. 35 represents a plot of these two functions—for various values of external damping and over a range of rotor speeds. The threshold of stability is determined by the intersection of $D22$ and $E2$. In a number of cases, the values of $D22$ and $E2$ are only slightly different. As an example, for $D_1=200$ rad/sec, the values of $D22$ and $E2$ are very close and it is difficult to determine the intersection point from the inspection of the plot of the two functions. As the value of the external damping increases, a point is reached in which the two functions will no longer intersect. Note, in Fig. 35, for $D_1=400$ rad/sec, $D22$ and $E2$ rapidly diverge. In this case, since the coefficients $G_1$ and $H_1$ are also positive, it seems to indicate that the system is stable.

Since the numerical operations involve the sum and differences of some large numbers, it was considered possible that numerical insta-

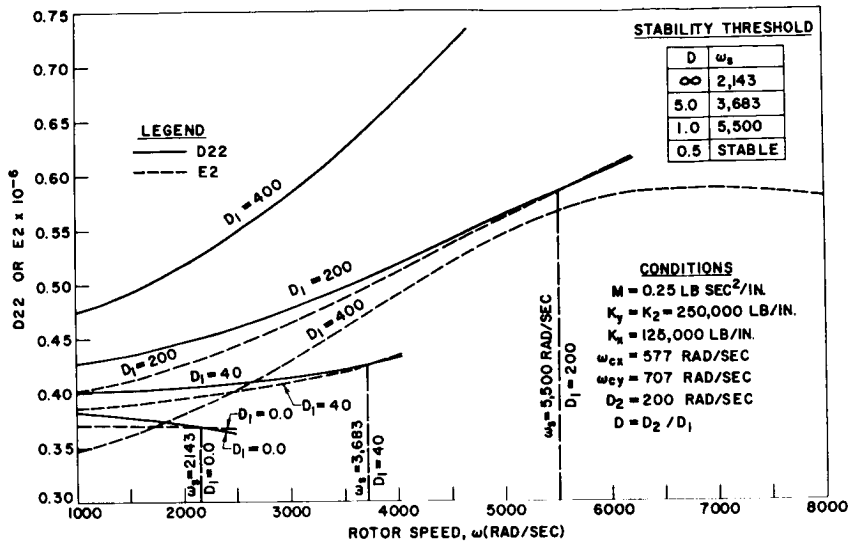


FIGURE 35.—Routh stability coefficients at various rotor speeds. Stability condition no. 12: $F_1 = D22 - E2 > 0$ for stability.

bility could be occurring, particularly for such cases as $D_1 = 400$ of Fig. 35, which shows the two functions $D22$ and $E2$ diverging.

To insure greater accuracy in the calculations, the computer program was rewritten in Fortran IV language for the IBM 7094 computer to make use of a double-precision routine. In this routine, all calculations were carried out to 16-place accuracy. Results calculated with double precision indicate that Fig. 35 is correct.

Approximately 10 000 data points were calculated using the double-precision routine. These points represent the rotor stability characteristics over a wide range of rotor, foundation flexibilities, and internal and external damping values. Since a single point requires several days to compute on a desk calculator, it is conservatively estimated that these points would require 50 years to calculate by hand. The high-speed digital computer does it in 15 min.

A selected group of performance charts, covering a range of internal damping values, are given in Appendix C.

### 4.10.2 Rotor Stability With Symmetric Bearing Support

Figure 36 represents the stability characteristics of a rotor on a symmetric foundation with conditions that correspond exactly to Fig. 10. Comparison of the two charts shows that for zero foundation damping,

the approximate and the exact solutions coincide. Both predict the rotor will be unstable above the critical speed. As external damping is introduced into the system, the rotor stability increases in much the same manner as given by the approximate solution. In fact, considering the number of terms deleted in the approximate analysis, it provides a surprisingly accurate representation of the rotor stability characteristics.

The important point which the general analysis brings out, which is not obtained from the approximate solution, is that for each given value of external damping, there is a value of foundation flexibility which will make the system entirely stable for all speeds. For example, in Fig. 36, for $D=0.2$ the rotor is completely stable for any flexibility ratio $R > 1.0$. As the foundation damping is decreased, greater foundation flexibility is required to completely stabilize the rotor.

To verify that this is indeed the case, the governing equations of motion were programed on the analog computer. This analog computer program is discussed in detail in Appendix B.3.

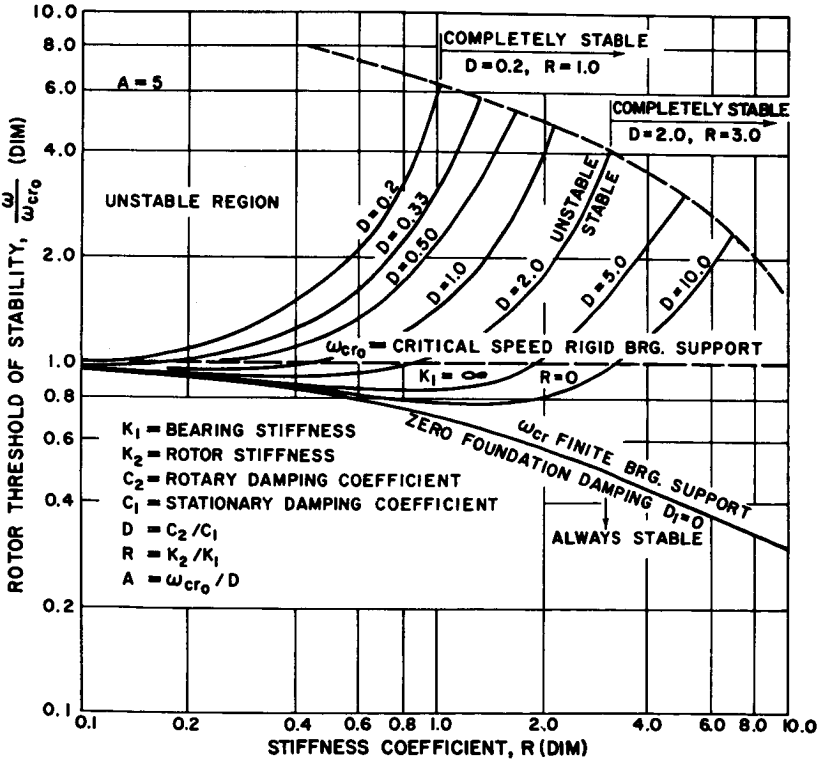


FIGURE 36.—Effect of external damping and bearing flexibility on the rotor whirl threshold speed, symmetric support.

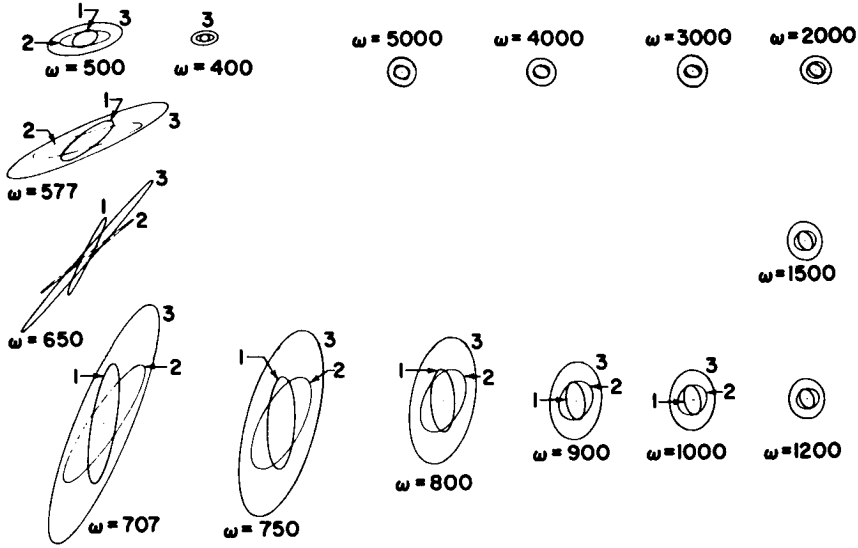


FIGURE 37.—Steady-state whirl orbits of an unbalanced rotor from $\omega = 400$ to $\omega = 5000$ rad/sec, general system. Conditions: $M_2 = 0.25$ lb-sec²/in., $K_y = K_2 = 250\,000$ lb/in., $K_x = 125\,000$ lb/in., $D_1 = D_2 = 200$ rad/sec, $\omega_{cx} = 577$ rad/sec, $\omega_{cy} = 707$ rad/sec, $\omega_s = 5500$ rad/sec.

1 = relative rotor motion, 2 = foundation motion, 3 = total rotor motion.

The analog program was run for conditions corresponding to $D = 0.2$, $R = 1.0$. It was found that when the $R$ value was increased above 1.0, no rotor instability was observed. (Also see Fig. 37.)

### 4.10.3 Rotor Stability With Unsymmetric Bearing Support

Figure 38 represents the rotor stability characteristics for $R = 1$ and $A = 5$, which is identical to the conditions of Fig. 27. With no foundation damping present, the exact and approximate solutions are almost identical for $\alpha > 1$. When $\alpha < 1$, the approximate solution indicates a higher threshold of stability. In both cases, reduction of horizontal bearing flexibility and increase in foundation damping produce a rapid rise in the stability threshold.

In all cases, the approximate solution predicts that increasing foundation damping will always raise the rotor threshold speed for a given value of $\alpha$ and $R$. The exact solution shows a very interesting phenomenon that for large values of $\alpha$, increasing the foundation damping may actually reduce the stability threshold. In Fig. 38, the value of $\alpha = 3$ represents a crossover point with respect to the influence of damping. For example, at $R = 3$, and $D = 1.0$, the dimensionless threshold speed is 2.319. Increasing the external damping by a factor of 5 ($D = 0.20$) only causes the threshold speed to increase to 2.381.

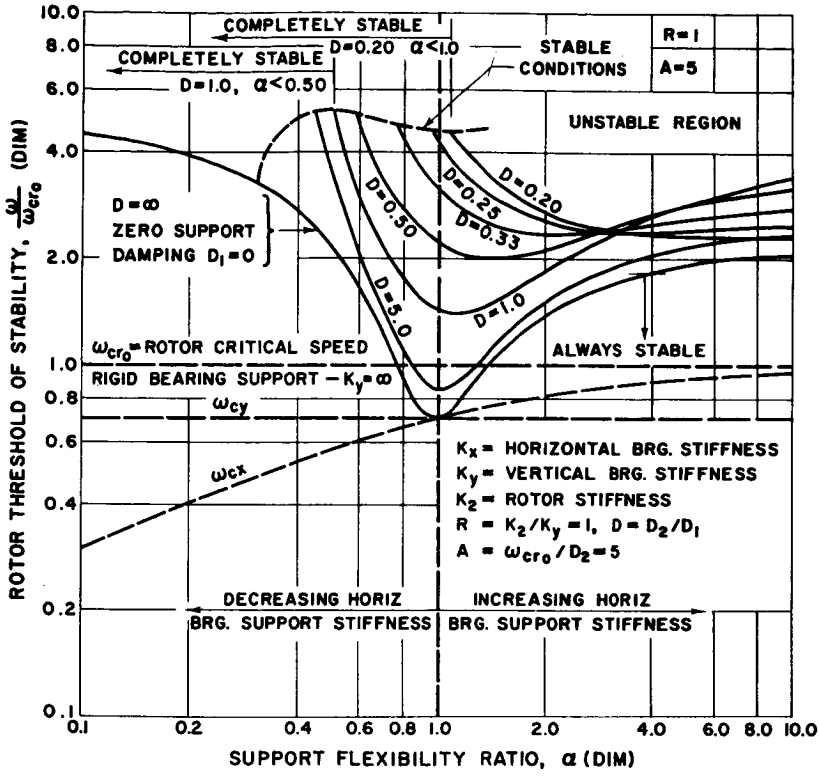


FIGURE 38.—Effect of unsymmetric bearing support flexibility on the rotor whirl threshold speed for $R=1.0$ and $A=5.0$, general system.

For values of $\alpha > 3$, the higher value of external damping actually produces a lower threshold speed. If the foundation is constrained in the horizontal direction, and only vertical motion permitted, the value of $\alpha \rightarrow \infty$. In this case we find that light values of external damping will improve stability, but there exists a limiting damping value which will result in a reduction of the threshold. For the case of extremely high external damping, the threshold speed is depressed down to the rotor critical speed (the foundation is acting as if it were rigid).

From Fig. 38, the rotor threshold for the conditions of $\alpha=0.5$, $R=1$, $D=1$, and $A=5$ is approximately 5500 rad/sec. This condition is also shown in Fig. 35 for the value of $D_1=200$ rad/sec. The approximate stability analysis (see Table 10) predicts a lower threshold speed of 3230 rad/sec, and Figs. 32–34 represent the total rotor motion as predicted by the approximate system. Figure 38 shows the interesting aspect that for $\alpha=0.5$ and $D=1.0$, the rotor is on the verge of complete stability. That is, if the external damping should be slightly increased or the hori-

zontal foundation stiffness slightly reduced, no rotor instability will be encountered throughout the entire operating range.

To demonstrate this, the rotor motion was simulated by the analog computer for the above conditions. Figure 37 represents the steady-state orbits of the rotor for conditions identical to Fig. 32. Contrary to Fig. 32, Fig. 37 shows that the rotor is stable to 5000 rad/sec. At the predicted threshold speed of 5500 rad/sec, the unstable orbit could be easily suppressed by increasing the damping, or reducing the flexibility ratio $\alpha$. In the general analog computer program, the relative rotor motion and foundation motion can be examined for various speeds as shown in Fig. 37.

Figure 39 represents an extension of Fig. 38 to cover the range of $\alpha$ from 1 to 100. At a value of $\alpha = 100$, the foundation can be considered as fixed in the horizontal direction, with only vertical motion allowable. As the horizontal stiffness increases, the rotor threshold increases from

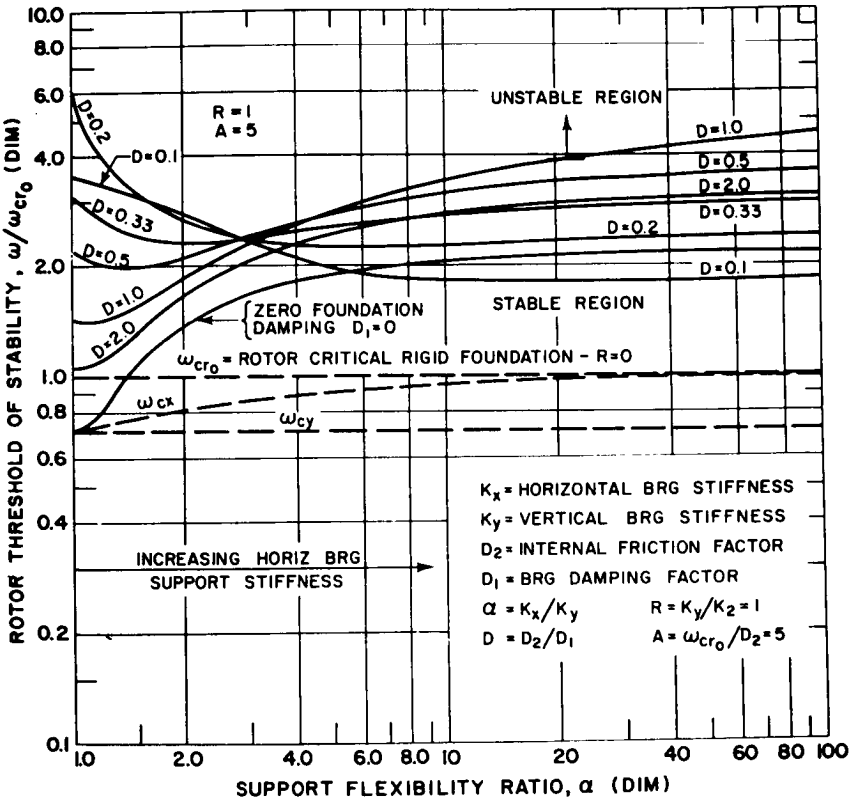


FIGURE 39.—Effect of unsymmetric bearing support flexibility on the rotor whirl threshold speed for $R = 1.0$, $A = 5.0$, and $\alpha = 1.0$ to 100, general system.

0.7 to slightly over 2 for the case of zero foundation damping. Little gain in stability is attained for a stiffness ratio of $\alpha > 10$ for this case. As light damping is added to the system, the threshold increases for all values of $\alpha$. When the foundation is constrained in the horizontal direction ($\alpha \to \infty$), Fig. 39 shows that the addition of light damping will improve stability. It is important to note that when the external damping $D_1$ exceeds the internal damping value, the stability is reduced for large values of $\alpha$. The physical reason for this is that the external damping restricts the motion of the foundation. If the value of $D_1$ becomes excessively high, the foundation will behave as a rigid foundation and the rotor threshold will be at the critical speed. The maximum stability is obtained by a symmetric foundation with a damping value of $D = 0.2$.

Note that when the external damping $D_1$ is doubled to $D = 0.1$, the threshold is reduced from 6.0 to approximately 3.5.

In Fig. 40, the foundation vertical stiffness has been reduced to a tenth of the value in Fig. 39. Here we see that the addition of light external

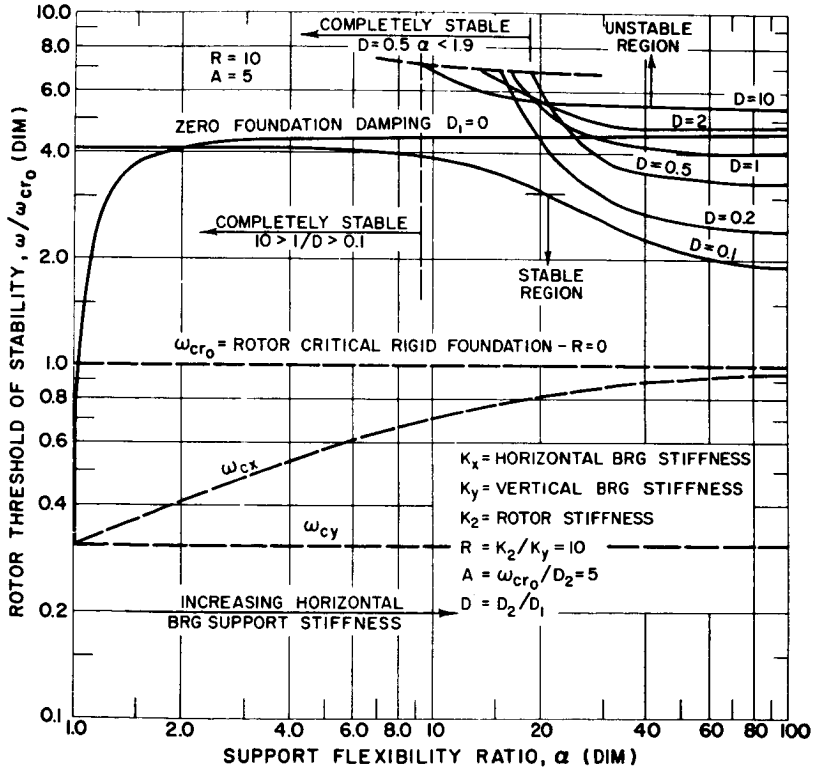


FIGURE 40.—Effect of unsymmetric bearing support flexibility on the rotor whirl threshold speed for $R = 10$ and $A = 5$, general system.

damping produces startling changes in the stability characteristics. For example, as $\alpha$ increases from unity for the case of zero foundation damping, the threshold value rapidly rises to four times the rotor critical speed. When damping is introduced, the system becomes completely stable for all speeds for $\alpha < 10$. When the horizontal stiffness increases to $\alpha > 10$, the threshold reappears, depending upon the $D$ value. If extremely heavy damping is employed ($D = 0.1$), a definite threshold exists for all values of $\alpha$. Thus Fig. 40 shows the important result that if the foundation is 10 times softer than the rotor stiffness, the rotor may be completely stabilized by the addition of small external foundation damping, or it may be raised to over 4 times the rotor critical by bearing asymmetry alone.

Figure 41 represents the rotor stability characteristics for a range of values of internal damping and no external damping. The smaller the value of $A$, the larger the amount of internal friction damping. For example, if we assume the rotor critical speed to be 1000 rad/sec, the value of $A = 10$ would correspond to a damping value of $D_2 = 100$ rad/sec and $A = 1$ is equivalent to $D_2 = 1000$ rad/sec. As mentioned in Sec. 4.2, actual measurements of the internal damping factor by Kimball indicate that $A$ should be of the order of 5 to 10, or larger. In this case, Fig. 41 shows that large increases in rotor stability are possible by the introduction of bearing asymmetry for $A > 5$. Figure 41 shows the important conclusion that the larger the internal friction becomes, the less the effectiveness of bearing asymmetry on improving the stability. In fact, for the value of $A = 1$, the rotor stability threshold is below the rotor critical speed. In this case rotor stability may be improved only by the addition of external damping.

Figure 41 is important in another respect, as it indirectly answers the question (see Sec. 4.3) posed by Dr. Newkirk in 1925. That is why foundation flexibility will improve rotor stability in the case of internal friction, but will produce violent whipping in the case of fluid-film bearings. The fluid-film bearing produces a force relationship similar to Eq. (4.10). (See App. D for derivation, and discussion of the general fluid-film equations.) In the case of a fluid-film bearing, the force component which is responsible for the rotor instability is not necessarily small, as is the case with the rotor internal friction, but can be of the same order as the rotor elastic forces. Thus the ratio $A$ may be of the order unity for a fluid-film bearing. In this case the introduction of foundation flexibility will result in a reduction of the rotor threshold speed and only if external foundation damping is added can the threshold be raised.

## 4.11 EXPERIMENTAL OBSERVATIONS OF KUSHUL' ON ROTOR INSTABILITY CAUSED BY INTERNAL FRICTION

The number of instances in which rotor instability caused by internal friction have been observed and reported in the literature are few. In

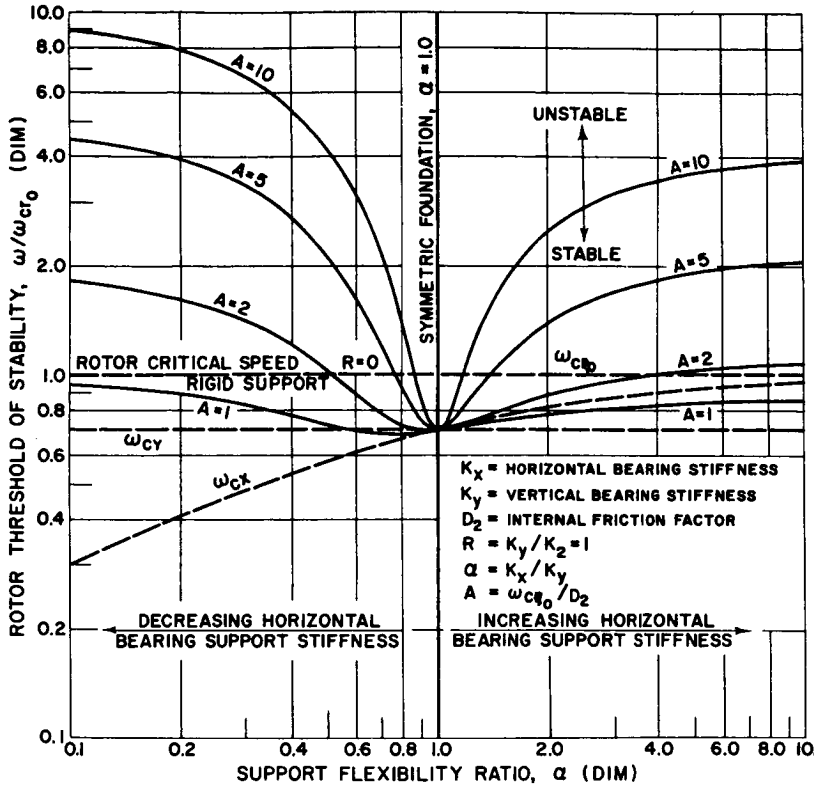


FIGURE 41.—Effect of unsymmetric bearing support on the rotor whirl threshold speed for various values of internal friction, zero foundation damping.

particular, there is very little information available on the rotor behavior in the unstable region. Recently, a translation of the Russian work of Kushul'[54] on self-induced oscillations of rotors became available in this country. In this investigation, Kushul' discusses some experimental observations of the motion of some high-speed textile spindles which exhibited self-excited whirl motion. Examination of the construction of the spindles as shown in Figs. 25 and 26 of Ref. 54 reveals why instability occurred. The spindles are composed of a built-up structure of a long wooden spindle inserted over a thin steel shaft. It is easy to visualize how such a long shrink fit could lead to stability problems. (See Sec. 4.2.)

Some of the major conclusions that Kushul' states on the rotor stability characteristics are:

1. The self-excited rotor motion occurs only above the first critical speed (see Eq. 4.33).

2. The whirl frequency remains almost constant at all speeds and is close to the characteristic first-order frequency of the spindle. In certain cases well above the threshold, the whirl frequency can abruptly change from the first- to the second-order spindle natural frequency (see Sec. 4.6.3).
3. The use of an elastic support by itself, without any increase in damping force, does not reduce the self-excitation (see Fig. 36).
4. External damping improves the rotor stability.
5. The most effective means to control the instability consisted of a spring-loaded bushing and damping sleeves. No dangerous self-induced vibrations were observed with any spindle with this type of bushing (see Figs. 36 and 40).

Figure 42 represents typical rotor orbits that Kushul' obtained on his textile spindle above the stability threshold. Unfortunately Kushul' did not have available precision electronic linear capacitance probes to monitor rotor motion (as depicted later in Fig. 44) and so had to resort to an optical system. He attached a fine needle to the spindle end and obtained the following pictures by photographing the resulting motion under a microscope. Figure 42 represents the rotor motion for a con-

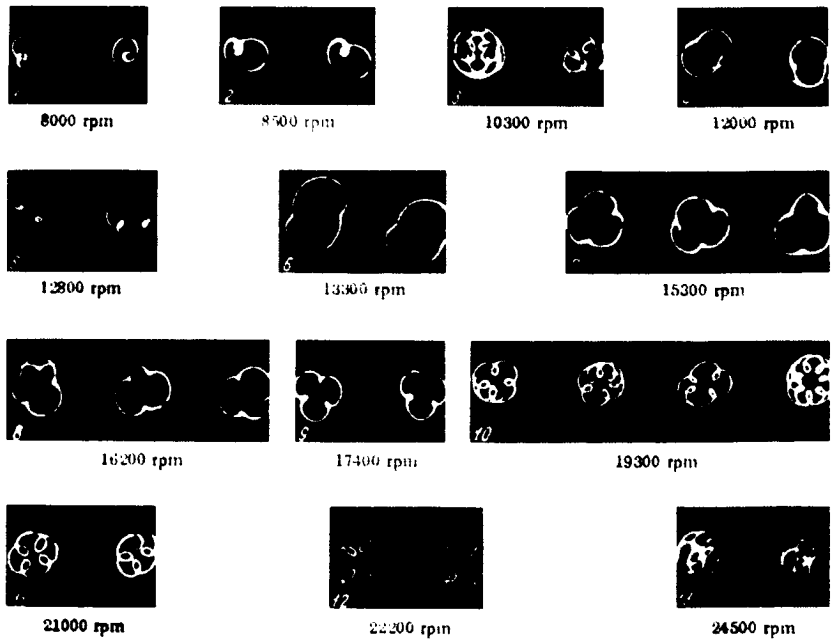


FIGURE 42.—Photographs of rotor motion with internal friction over a wide range of speed (ref. Kushul').

siderable range above the rotor threshold speed. This figure is of importance as it illustrates the conclusions of Sec. 4.6.3 that the rotor precession rate is approximately equal to the rotor critical speed and also that the precession rate is constant over a large speed interval.

The critical speed of the spindle was determined to be about 4300 rpm. The fact that the rotor nonsynchronous precession rate remains constant can be easily verified by inspection of the various whirl patterns of Fig. 42. For example, at the speed range of 8000 to 8500 rpm, the rotor orbit forms one stationary internal loop. This indicates that the whirl ratio $\omega_P/\omega = 1/(1+n) = 1/2$ or $\omega_P$ is approximately 4200 rpm. At 12 800 rpm, a stationary orbit with two internal loops is formed, which indicates a whirl ratio of one-third or $\omega_P = 4300$ rpm. Also at 21 000 to 22 000 rpm, a stationary pattern is formed with four internal loops to indicate a 1/5-whirl ratio. Likewise, the rotor nonsynchronous precession rate at 22 000 rpm is still approximately 4300 rpm.

Based on the analysis of Sec. 4.6.3 and the experimental observations of Kushul', we see that the assumption of $\omega_P = \omega_{CR} =$ constant has considerable justification and will be used in Chapter 6 in the development of some of the characteristics of rotor instability due to fluid-film bearings.

The top portion of Fig. 43 (from Kushul') represents the spindle motion at a speed slightly above four times the critical. The upper left-hand picture represents the motion for only two cycles. Since the total rotor speed is not an exact multiple of the precession rate $\omega_P$, the pattern is not stationary. The upper right-hand figure represents a time exposure of the motion. Notice the similarity between this figure and the analog computer orbit of 19b which includes a nonlinear radial stiffness term.

The lower portion of Fig. 43 represents the rotor motion above the stability threshold. In the lower left-hand figure, the rotor precession rate was equal to the first critical speed. When the rotor speed was increased, the precession rate abruptly changed from the first to the second critical speed as shown in the lower right-hand figure. Such an effect cannot be obtained with the present model because (neglecting bearing mass) there is only one system critical speed.

In summary, Kushul's experimental findings verify many of the theoretical statements and conclusions of Chapter 4 on the characteristics of the whirl orbits and on the influence of foundation flexibility and damping on stability.

## 4.12 DISCUSSION AND CONCLUSIONS

In Chapter 4 the equations of motion of the extended Jeffcott rotor have been developed to include internal rotor friction. Chapter 4 shows that the introduction of internal rotor friction will cause unstable, nonsynchronous rotor precession above the critical speed. The analysis

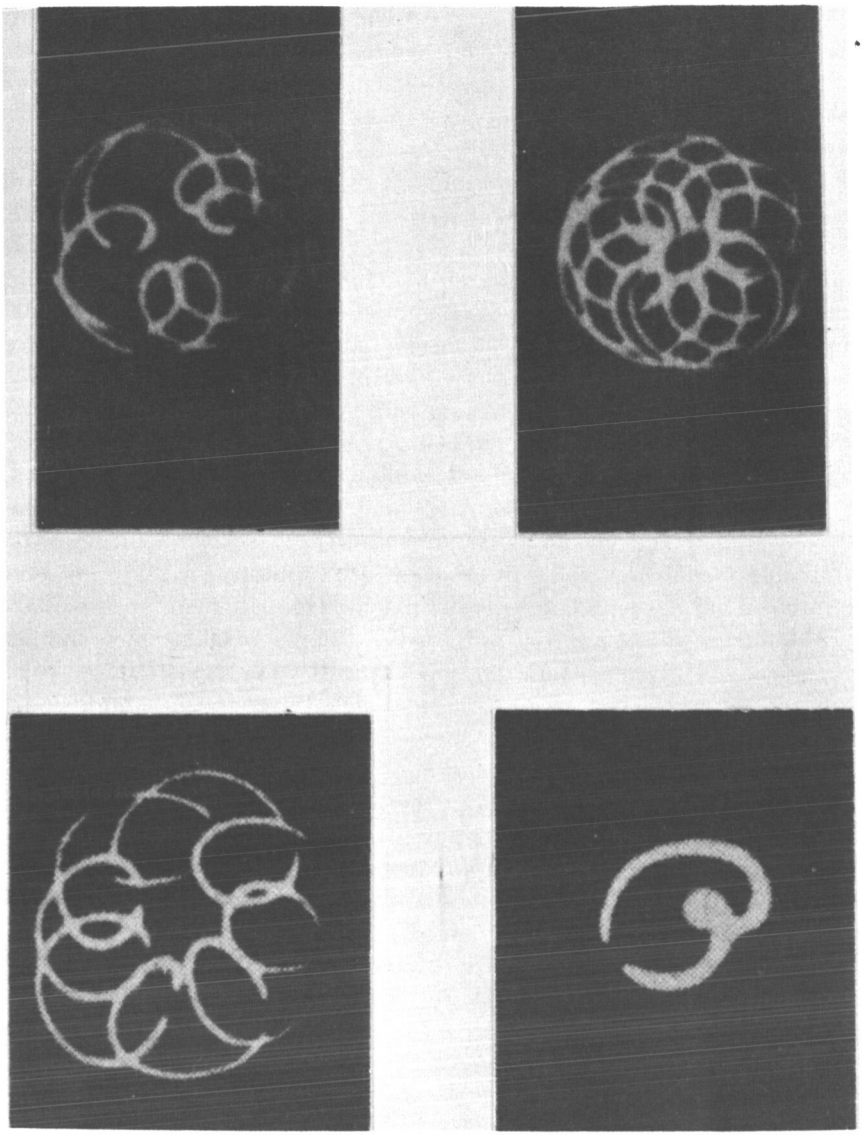

FIGURE 43.—Photographs of rotor motion with internal friction (ref. Kushul').

of the precession rate shows that the nonsynchronous motion is approximately equal to the rotor critical speed and remains constant over a considerable speed range. This is in accordance with the observations of Newkirk and Kushul' (see Sec. 4.11) on the rotor whirl.

One of the most important aspects of Chapter 4 is the influence of foundation flexibility and damping on the rotor stability. A symmetric

flexible foundation will reduce the rotor critical speed and also the whirl threshold in the absence of external damping. If external damping is added, the stability threshold can be greatly improved. The interesting aspect of the problem is that foundation asymmetry alone, without foundation damping, can create a large increase in the whirl threshold speed. This effect can be readily seen from the three-dimensional model shown in Figs. 22–24.

It is relatively easy to visualize how foundation damping improves stability, but it is rather difficult to see why bearing asymmetry alone should improve stability. A mathematical reason for this is given by Eq. (5.20) in Chapter 5 for the two-dimensional system. A heuristic argument for this is given by the following. Section 4.6.1 states that the system will be unstable if it possesses repeated conjugate imaginary roots. These roots are closely related to the rotor critical speed. For the symmetric system, the resonant frequencies in the $X$ and $Y$ directions are equal. The introduction of foundation asymmetry shifts the resonance in the two directions creating two critical speeds which shift the conjugate roots, causing an improvement in stability. There is a slight penalty for this in that larger amplitudes are encountered at the rotor critical speed (see Sec. 4.5). Also, Sec. 4.5 shows that a component of synchronous backward precession can only be developed in an asymmetric system.

In general, once the whirl threshold speed has been exceeded, the linear system predicts that the nonsynchronous component becomes unbounded. The analysis of Sec. 4.7 shows that only for the case of a nonlinear, nonconservative system can a finite limit cycle be obtained above the threshold speed. A similar result is obtained for the case of fluid-film bearings. Thus, the orbital pictures of rotor motion above the threshold obtained by Kushul', discussed in Sec. 4.11, and Hinkle and Gunter, discussed in Chapter 5, can be caused only nonlinear, nonconservative systems.

In Sec. 4.9, general equations of motion are derived to include bearing mass, and are not restricted to lightly damped systems as Eqs. (4.17) are. The derivation of these extended equations is made possible by the development of a general dissipation function to represent the internal rotor friction. The important characteristic of this function is that the energy level is a function of the rotor precession rate as well as the rotor absolute velocity. In fact, if the dissipation function is a function of only the rotor absolute motion, it can be shown that the system is always stable. A similar conclusion can be drawn for the linearized fluid-film bearing. Its characteristics can be derived from a potential function and a dissipation function similar in nature to the rotary damping function.

Section 4.9.4, on the approximate effect of bearing mass on stability, shows that bearing mass will lower the threshold for the symmetric case.

One interesting aspect of bearing mass is that the mass of the bearing and flexibility of the support may be designed to attenuate the displacement amplitude at the rotor critical speed; that is, to act as a dynamic vibration absorber. This seems to have a deleterious effect on the rotor stability.

The stability analysis of the general equations of motion in Sec. 4.10 reveals a number of important stability characteristics which are not obtained from the analysis in Sec. 4.6.1. The general analysis shows that, under certain conditions, the rotor can be completely stabilized by foundation flexibility and damping. The approximate analysis indicates that the greater the external foundation damping, the higher the threshold of stability will be. The general analysis shows that there is a limiting value of external damping that should be used, and that values higher than this will result in a reduction of stability.

In conclusion we find that the work presented in Chapter 4 furnishes an explanation of the rotor whirl motion observed by Dr. Newkirk in 1924.

In particular, we see that this unstable motion occurs only above the critical speed and never below it. Obviously, it appears that this problem can be simply avoided by designing the rotor to operate only in the subcritical speed region. This is not entirely a satisfactory design procedure, since it will result in a more rigid, heavier rotor. Such a design would not be acceptable in certain applications, such as spacepower where weight is at a premium. Successful operation of a high-speed subcritical rotor also requires extremely accurate rotor balancing in order to limit the dynamic bearing loads to acceptable limits.

A second approach to insure stable rotor performance is to minimize all sources of internal rotor friction. The designer should see that all shrink fits, impeller spacers, etc., are properly designed so as to minimize this effect. Robertson[85] discusses a number of hub designs which were found effective in reducing internal friction. It is important to note that even in a well-designed rotor, instability can result due to a poorly alined gear-type flexible coupling.

Internal rotor friction is only one of many sources which can cause rotor instability. Recently Alford[10] demonstrated that aerodynamic exciting forces developed by labyrinth seals and local variations in blade efficiency can cause severe rotor whirl of axial compressors and turbines.

---

[10] J. S. Alford, "Protecting Turbomachinery From Self-Excited Rotor Whirl," *Journal of Engineering for Power*, ASME, Oct. 1965, pp. 333–344.

# Chapter 5

# Stability of Motion for Small Oscillations

Consider the single-mass Jeffcott rotor of Sec. 2.3 as shown in Fig. 3, or the journal bearing of Fig. D.2 in Appendix D. In either case both may be treated as a point mass rotor. The equations of motion will be examined for small oscillations in a Cartesian reference frame. By assuming only small perturbations or displacements from an equilibrium configuration, we obtain linearized equations by which stability characteristics can be examined by the standard Routh procedure.

The usual procedure in the case of fluid-film bearings has been to express the motion of the system in polar coordinates, since the film forces express themselves conviently in this form. Since the resulting equations of motion are nonlinear, most investigators, such as Reddi and Trumpler,[79] have linearized these equations by the small perturbation approach and have then applied the Routh criterion.

There are several basic difficulties with the latter method. First, it is difficult to extend the system to additional degrees of freedom in which foundation and rotor deflection, and bearing mass are taken into consideration. The resulting equations of motion become highly nonlinear and intractable to handle. For example, the governing equations of motion of Chapter 3 were extended to include foundation and bearing characteristics in polar coordinates. After several months effort, the only meaningful solution obtained was for the case of synchronous precession. As it turns out, the synchronous precessive solution, which is presented in Chapter 6, is much better handled by a fixed Cartesian coordinate approach in which the bearing forces are transformed to an $X-Y$ system.

The second difficulty with the polar coordinate approach is that it is difficult to generalize as to what influence the various bearing terms have on the rotor stability. The third problem is that it is extremely difficult to simulate the rotor orbital behavior by means of an analog computer because of the nonlinear terms. Jennings[1] in 1960 investigated the oil

[1] Jennings, U. D., "An Investigation of Oil Bearing Whirl by Electronic-Analog Computer Techniques," Cornell University, Ph. D. thesis, 1960.

film whirl problem on the analog computer. The motion of his system had to be limited to cases in which the orbit does not encircle the origin. This limitation can be circumvented by transforming the rotor precession rate $\dot{\phi}$ to $X,Y$ coordinates, but that is adding an unwarranted complication to the problem.

The only hope in extending the rotor stability analysis beyond the current state of art in which the rotor is considered as a point mass in a rigid bearing lies in the ability to express the equations of motion in Cartesian coordinates. Dr. V. Castelli[5] used the Cartesian coordinate approach with excellent results in his analysis of the 360° infinite-width gas bearings. He derived the governing isothermal Reynolds equation in Cartesian coordinates and linearized it by assuming small perturbations in the $X,Y$ coordinates. The resulting coupled linear differential equations were then solved to yield the threshold of stability with the aid of a high-speed digital computer. Such an approach could easily be extended to a more complex system.

## 5.1 EQUATIONS OF MOTION FOR SMALL DISPLACEMENTS

The force system exerted on a journal by hydrodynamic fluid film forces is a complex function of the bearing eccentricity, precession rate, aspect ratio, rotor speed, etc. In the case of an oil-lubricated finite-width journal bearing or a gas-lubricated bearing, closed-form analytical expressions for the bearing forces are difficult to obtain, except in certain limiting cases. It will be assumed that the hydrodynamic fluid film forces developed by a journal bearing may be considered as functions of displacement and velocity as follows:

$$\vec{F} = F_x(X, Y, \dot{X}, \dot{Y})\,\vec{n}_x + F_y(X, Y, \dot{X}, \dot{Y})\,\vec{n}_y \tag{5.1}$$

The above relationship is valid in the case of incompressible fluids, or for compressible lubricants at high or low value of the compressibility parameter $\Lambda$, in which the force Eq. (5.1) is not an explicit function of time.

If we take a Taylor's series expansion about the equilibrium configuration, we obtain

$$F_x - F_{x_0} = \left.\frac{\partial F_x}{\partial X}\right|_{x=x_0} \delta X + \left.\frac{\partial F_x}{\partial Y}\right|_{y=y_0} \delta Y + \left.\frac{\partial F_x}{\partial \dot{X}}\right|_{\dot{x}=\dot{x}_0} \delta \dot{X} + \left.\frac{\partial F_x}{\partial \dot{Y}}\right|_{\dot{y}=\dot{y}_0} \delta \dot{Y}$$

$$+ \text{higher order terms} \tag{5.2}$$

$$F_y - F_{y_0} = \left.\frac{\partial F_y}{\partial X}\right|_{x=x_0} \delta X + \left.\frac{\partial F_y}{\partial Y}\right|_{y=y_0} \delta Y + \left.\frac{\partial F_y}{\partial \dot{Y}}\right|_{\dot{y}=\dot{y}_0} \delta \dot{Y} + \left.\frac{\partial F_y}{\partial \dot{X}}\right|_{\dot{x}=\dot{x}_0} \delta \dot{X}$$

$$+ \text{higher order terms} \tag{5.3}$$

If only small perturbations from the equilibrium position are considered then the higher order terms may be neglected. The force relationships reduce to

$$\Delta F_i = K_{ij} X_j + C_{ij} \dot{X}_j; \qquad i = 1, 2; \qquad j = 1, 2 \tag{5.4}$$

where

$1 = X$ direction, $2 = Y$ direction

$$K_{ij} = \left.\frac{\partial F_i}{\partial X_j}\right|_{x_j = x_{j_0}}; \qquad C_{ij} = \left.\frac{\partial F_i}{\partial \dot{X}_j}\right|_{\dot{x}_j = \dot{x}_{j_0}}$$

The quantities $K_{ij}$ and $C_{ij}$ may be loosely labeled as the bearing "stiffness" and "damping" coefficients. Thus, for small displacements from an equilibrium configuration, the bearing characteristics may be approximated by eight coefficients: four stiffness and four damping quantities.[71, 96] Note that these bearing coefficients are not in general constants, but are complex functions of the equilibrium position $X_0$, $Y_0$, total rotor angular velocity, and bearing geometry.

The equations of motion of the single mass unbalanced rotor are given by

$$M\ddot{X} + C_{xx}\dot{X} + C_{xy}\dot{Y} + K_{xx}X + K_{xy}Y = Me_\mu\omega^2 \cos \omega t + F_x \tag{5.5}$$

$$M\ddot{Y} + C_{yy}\dot{Y} + C_{yx}\dot{X} + K_{yy}Y + K_{yx}X = Me_\mu\omega^2 \sin \omega t + F_y \tag{5.6}$$

The terms $K_{xx}$ and $K_{yy}$ are termed the principal stiffness coefficients, and $K_{yx}$ and $K_{xy}$ the cross-coupling coefficients. The significance of the cross-coupling terms is that they couple the equations of motion. That is, the $K_{xy}$ term produces a force in the $X$-direction due to a displacement in the $Y$-direction. It is the bearing cross-coupling coefficients which are responsible for self-excited rotor instability. If these coefficients can be entirely eliminated, then the governing system equations in the $X$ and $Y$ direction become uncoupled and the system is stable for small disturbances from an equilibrium position.

219-720 O-66—9

## 5.2 ROTOR STABILITY ANALYSIS

The stability of the governing equations of motion of the system is obtained by examination of the homogeneous differential equations which are

$$\ddot{X}_i + D_{ij}\dot{X}_j + \mathscr{K}_{ij}X_j = 0 \tag{5.7}$$

where

$$D_{ij} = \frac{C_{ij}}{M}; \qquad \mathscr{K}_{ij} = \frac{K_{ij}}{M}$$

Assume a solution for the form

$$X_1 = Ae^{\alpha t}; \qquad X_2 = Be^{\alpha t}$$

results in

$$\left.\begin{aligned}(\alpha^2 + D_{11}\alpha + \mathscr{K}_{11})A + (D_{12}\alpha + \mathscr{K}_{12})B = 0\\ (D_{21}\alpha + \mathscr{K}_{21})A + (\alpha^2 + D_{22}\alpha + \mathscr{K}_{22})B = 0\end{aligned}\right\} \tag{5.8}$$

Expanding the determinant of the coefficients results in

$$\alpha^4 + (D_{11} + D_{22})\alpha^3 + (\mathscr{K}_{11} + \mathscr{K}_{22} + D_{11}D_{22} - D_{12}D_{21})\alpha^2$$
$$+ [\mathscr{K}_{11}D_{22} + \mathscr{K}_{22}D_{11} - (\mathscr{K}_{12}D_{21} + \mathscr{K}_{21}D_{12})]\alpha$$
$$+ \mathscr{K}_{22}\mathscr{K}_{11} - \mathscr{K}_{12}\mathscr{K}_{21} = 0 \tag{5.9}$$

The general stability of the system can be determined by the Routh-Hurwitz as outlined in Sec. 4.61. Let Eq. (5.9) be represented by

$$\sum_{K=0}^{N} A^{N-K}\alpha^K = 0$$

The stability condition is given by

$$D_0 = A_1 > 0$$

$$D_1 = A_1A_2 - A_0A_3 > 0$$

$$D_2 = A_3D_1 - A_4A_1^2 > 0$$

expanding $D_2$ yields

$$A_1A_2A_3 > A_4A_1^2 + A_0A_3^2 \tag{5.10}$$

Thus we obtain

$$(D_{11}+D_{22})(\mathscr{K}_{11}+\mathscr{K}_{22}+D_{11}D_{22}-D_{12}D_{21})\times(\mathscr{K}_{11}D_{22}+\mathscr{K}_{22}D_{11}$$
$$-\mathscr{K}_{12}D_{21}-\mathscr{K}_{21}D_{12})>(\mathscr{K}_{11}D_{22}+\mathscr{K}_{22}D_{11}-\mathscr{K}_{12}D_{21}-\mathscr{K}_{21}D_{12})^2$$
$$+(D_{11}+D_{22})^2(\mathscr{K}_{22}\mathscr{K}_{11}-\mathscr{K}_{12}\mathscr{K}_{21}) \qquad (5.11)$$

## 5.3 EFFECT OF STIFFNESS CROSS-COUPLING ON STABILITY

It is difficult to evaluate the influence of the cross coupling coefficients $\mathscr{K}_{ij}$ and $C_{ij}$, $i\neq j$, on stability by examination of Eq. (5.11). If these coefficients are zero, then the system is stable (provided all other coefficients are positive). It is of particular importance to determine the influence of the $\mathscr{K}_{ij}$ terms on stability. To do this we will first simplify the system by assuming the damping coefficients to be of the form

$$C_{ij}=\begin{pmatrix} C & O \\ O & C \end{pmatrix}$$

Equation (5.7) reduces to

$$\left.\begin{aligned} &\text{(a)}\ \ddot{X}+D\dot{X}+\mathscr{K}_{11}X+\mathscr{K}_{12}Y=0 \\ &\text{(b)}\ \ddot{Y}+D\dot{Y}+\mathscr{K}_{21}X+\mathscr{K}_{22}Y=0 \end{aligned}\right\} \qquad (5.12)$$

Replace the simple $X$, $Y$ coordinates by the general transformation

$$\xi=X+aY \qquad (5.13)$$

Combining Eqs. (5.12) and (5.13) results in

$$\ddot{\xi}+D\xi+(\mathscr{K}_{11}+a\mathscr{K}_{21})\left(X+\frac{\mathscr{K}_{12}+a\mathscr{K}_{22}}{\mathscr{K}_{11}+a\mathscr{K}_{22}}Y\right)=0 \qquad (5.14)$$

Let

$$\xi=X+\frac{\mathscr{K}_{12}+a\mathscr{K}_{22}}{\mathscr{K}_{11}+a\mathscr{K}_{21}}Y$$

Hence

$$\ddot{\xi}+D\dot{\xi}+(\mathscr{K}_{11}+a\mathscr{K}_{21})\xi=0 \qquad (5.15)$$

and

$$a=\frac{\mathscr{K}_{12}+a\mathscr{K}_{22}}{\mathscr{K}_{11}+a\mathscr{K}_{21}}$$

Solving for $a$:

$$a=\frac{\mathscr{K}_{22}-\mathscr{K}_{11}\pm\sqrt{(\mathscr{K}_{22}-\mathscr{K}_{11})^2+4\mathscr{K}_{21}\mathscr{K}_{12}}}{2\mathscr{K}_{21}} \tag{5.16}$$

To determine the stability of Eq. (5.14), let $\xi=Ae^{(P+iS)t}$. This results in the following equations for $P$ and $S$

Case I: $a$ is real

$$\left.\begin{aligned}&\text{(a) } P^2-S^2+DP+\mathscr{K}_{11}+a\mathscr{K}_{21}=0\\&\text{(b) } S(C+2MP)=0\end{aligned}\right\} \tag{5.17}$$

Case II: $a$ is complex $=a_r+ia_i$

$$\left.\begin{aligned}&\text{(a) } P^2-S^2+DP+\mathscr{K}_{11}+a_r\mathscr{K}_{21}=0\\&\text{(b) } S(D+2P)+a_i\mathscr{K}_{21}=0\end{aligned}\right\} \tag{5.18}$$

Consider the stability of motion for Case I when $a$ is real. Assuming the precession rate $S$ is nonzero

$$P=-\frac{C}{2M}=-\frac{D}{2}$$

when both damping $C$ and mass $M$ are real quantities. Thus the real root is negative which indicates that the motion is damped out and hence is stable. The roots of $S$ corresponding to the above system are given by

$$S_{1,2}^2=\frac{1}{2M}\left\{K_{11}+K_{22}\pm\sqrt{(K_{22}-K_{11})^2+4K_{21}K_{12}}+\frac{C^2}{2}\right\}$$

The roots $S_{1,2}$ represent the natural resonance frequency of the system. These values can be best visualized by a Mohr circle type of construction. (See sketch on page 127.)

The roots $S_1$ and $S_2$ refer to the first and second critical speeds of the system. Thus if $a$ is real, the motion of the system is stable and may possess two resonance frequencies.

The stiffness coefficients $K_{11}$ and $K_{22}$ are assumed to be always positive. In order to assure that $a$ is a real quantity, it is necessary to have either

1. $K_{12}$ and $K_{21}$ of the same sign
2. $K_{12}$ and $K_{21}$ identically zero (no cross-coupling terms)
3. If $K_{12}$ is of opposite sign to $K_{21}$, then it is necessary that $|K_{22}-K_{11}|>2\sqrt{|K_{21}K_{12}|}$

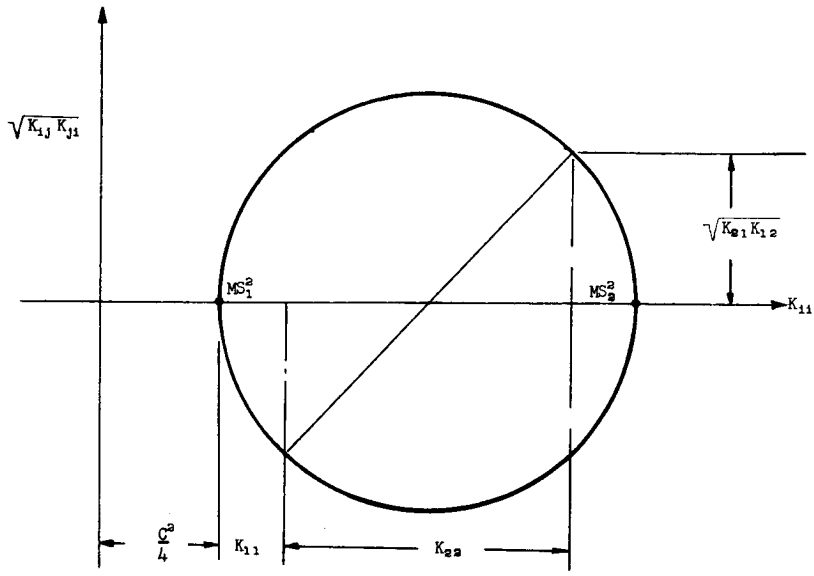


The above represent the necessary conditions to obtain system stability. Examination of Case II reveals an additional requirement is necessary to obtain instability. Eliminating $S$ from Eq. (5.18), we obtain the following equation in terms of $P$ only

$$4P^4+8DP^3+[5D^2+4(\mathscr{K}_{11}+a_r\mathscr{K}_{21})]P^2$$

$$+[D^3+4D(\mathscr{K}_{11}+a_r\mathscr{K}_{21})]P+(\mathscr{K}_{21}a_r+\mathscr{K}_{11})D^2-(a_i\mathscr{K}_{21})^2=0 \qquad (5.19)$$

Investigation of Eq. (5.19) reveals the additional condition that $K_{21}<0$ in an unstable system. The previous calculations have shown that the bearing cross-coupling coefficients must be of opposite sign in order to obtain a self-excited oscillation. The general stability criterion of Eq. (5.11) may be somewhat simplified by the assumption that

$$\mathscr{K}_{21}=-\mathscr{K}_{12} \qquad \text{and} \qquad D_{21}=-D_{12}$$

Expanding and collecting terms results in

$$(\mathscr{K}_{11}-\mathscr{K}_{22})^2+(D_{11}+D_{22})(D_{22}\mathscr{K}_{11}+D_{11}\mathscr{K}_{22})\left(1+\frac{D_{12}^2}{D_{11}D_{22}}\right)$$

$$+\frac{2D_{12}^2(D_{11}+D_{22})}{D_{11}D_{22}}\mathscr{K}_{12}>\frac{\mathscr{K}_{12}}{D_{11}D_{22}}[2D_{12}(D_{22}-D_{11})(\mathscr{K}_{11}-\mathscr{K}_{22})$$

$$+4D_{12}\mathscr{K}_{12}+(D_{11}+D_{22})^2\mathscr{K}_{12}] \qquad (5.20)$$

The stability criterion expressed in the above form shows very clearly that if $\mathscr{K}_{12}$ is zero, the system is completely stable since the right-hand side vanishes. Equation (5.20) also demonstrates the important conclusion of Chapter IV that bearing asymmetry ($K_{11} \neq K_{22}$) will increase the threshold of stability.

## 5.4 COMPARISON OF APPROXIMATE ROTOR EQUATIONS OF MOTION WITH INTERNAL FRICTION TO GENERALIZED EQUATIONS

Reexamination of the approximate equations of rotor motion with internal friction damping, Eq. (4.17), shows that they are of identical form to Eqs. (5.5) and (5.6).

The generalized coefficients in this case are given by

$$D_{11} = D_{22} = \frac{C_2}{M}\left(\frac{K_y}{K_x + K_y}\right)^2 + \frac{C_1}{M}\left(\frac{K_2}{K_x + K_2}\right)^2$$

$$D_{12} = D_{21} = 0$$

$$\mathscr{K}_{11} = \omega_{cx}^2$$
$$\mathscr{K}_{22} = \omega_{cy}^2$$
$$\mathscr{K}_{12} = -\mathscr{K}_{21} = \frac{\omega C_2}{M}\left(\frac{K_y^2}{(K_x + K_2)(K_y + K_2)}\right)$$

In the above case, we see that the cross-coupling coefficients $\mathscr{K}_{12}$ and $\mathscr{K}_{21}$ are of opposite sign and also that $\mathscr{K}_{21}$ is negative. If the internal friction damping coefficient $C_2$ vanishes, then $\mathscr{K}_{12}$ and $\mathscr{K}_{21}$ are zero and the system is stable.

## 5.5 INFLUENCE OF HYDRODYNAMIC BEARING CHARACTERISTICS ON STABILITY

The forces developed by a hydrodynamic fluid film bearing can be represented by the general relationship (see App. D)

$$\vec{F} = -[f_r(e)|(\omega - 2\dot{\phi})| + \dot{e}D_r(e)]\vec{n}_\phi + [f_\phi(e)(\omega - 2\dot{\phi}) - \dot{e}D_\phi(e) - \omega D_f(e)]\vec{n}_\phi \qquad (5.21)$$

The force components in the $X$ and $Y$ directions, respectively, are given by

$$F_x = \vec{F} \cdot \vec{n}_x; \qquad F_y = \vec{F} \cdot \vec{n}_y \qquad (5.22)$$

where the transformation between the fixed unit vectors $\vec{n}_{x,y}$ and $\vec{n}_{e,\phi}$ is given by (see Fig. D.2)

$$\begin{pmatrix} \cos\phi & \sin\phi \\ -\sin\phi & \cos\phi \end{pmatrix} \begin{pmatrix} \vec{n}_x \\ \vec{n}_y \end{pmatrix} = \begin{pmatrix} \vec{n}_e \\ \vec{n}_\phi \end{pmatrix} \tag{5.23}$$

Thus the component torces are given by

$$F_x = -[f_r|(\omega - 2\dot{\phi})| + \dot{e}D_r]\cos\phi + [\dot{e}D_\phi + \omega D_f - f_\phi(\omega - 2\dot{\phi}]\sin\phi \tag{5.24}$$

$$F_y = -[f_r|(\omega - 2\dot{\phi})| + \dot{e}D_r]\sin\phi - [\dot{e}D_\phi + \omega D_f - f_\phi(\omega - 2\dot{\phi})]\cos\phi \tag{5.25}$$

For small displacements from the origin, the force components are approximated by

$$F_x = -\left[\frac{\partial f_r}{\partial e}|(\omega - 2\dot{\phi})| + \dot{e}\frac{\partial D_r}{\partial e}\right] e\cos\phi + \left[\dot{e}\frac{\partial D_\phi}{\partial e} + \omega\frac{\partial D_f}{\partial e} - \frac{\partial f_\phi}{\partial e}(\omega - 2\dot{\phi})\right] e\sin\phi \tag{5.26}$$

$$F_y = -\left[\frac{\partial f_r}{\partial e}|(\omega - 2\dot{\phi})| + \dot{e}\frac{\partial D_r}{\partial e}\right] e\sin\phi - \left[\dot{e}\frac{\partial D_\phi}{\partial e} + \omega\frac{\partial D_f}{\partial e} - \frac{\partial f_\phi}{\partial e}(\omega - 2\dot{\phi})\right] e\cos\phi \tag{5.27}$$

The eccentricity vector $\vec{e}$ is given by

$$\vec{e} = e\vec{n}_e = +X\vec{n}_x + Y\vec{n}_y \tag{5.28}$$

Taking the dot product of Eq. (5.28) with respect to $\vec{n}_x$ and $\vec{n}_y$ yields

$$X \underset{(5.23)}{=} e\cos\phi$$

$$Y \underset{(5.23)}{=} e\sin\phi \tag{5.29}$$

Differentiating Eq. (5.29) gives

$$\dot{X} = \dot{e}\cos\phi - \dot{\phi}e\sin\phi$$

$$\dot{Y} = \dot{e}\sin\phi + \dot{\phi}e\cos\phi$$

When the rotor is near the threshold of stability, it is operating in the post-critical-speed region. Hence the rotor phase angle $\beta > 90°$ and the rotor orbit is approximately equal to the rotor unbalance displacement $e_\mu$. For example, consider Fig. 44 which represents the motion of a high-speed gas bearing rotor above and below the threshold of stability. Below the threshold of stability, the rotor motion is forward synchronous precession in which $e \approx e_\mu$. Above the rotor threshold, Fig. 8 shows that the rotor develops a large nonsynchronous component. In this region the squeeze film terms ($\dot{e}$) have considerable influence.

Near the threshold, the velocity components may be approximated by

$$\begin{aligned} \dot{X} &\approx -\dot{\phi}e \sin \phi = -\dot{\phi}Y \\ \dot{Y} &\approx \dot{\phi}e \cos \phi = \dot{\phi}X \end{aligned} \tag{5.30}$$

$$\therefore F_{x_{(5.27,\,29,\,30)}} = -\left\{\omega C_s \left| \left(1 - \frac{2\omega_p}{\omega}\right) \right| + 2C_d\dot{X} + \omega(C_d - C_f)Y\right\} \tag{5.31}$$

$$F_{y_{(5.28\text{–}5.30)}} = -\left\{\omega C_s \left| \left(1 - \frac{2\omega_p}{\omega}\right) \right| + 2C_d\dot{Y} - \omega(C_d - C_f)X\right\} \tag{5.32}$$

where

$$C_s = \frac{\partial f_r}{\partial e}\bigg|_{e=e_0} \qquad C_d = \frac{\partial f_\phi}{\partial e}\bigg|_{e=e_0}$$

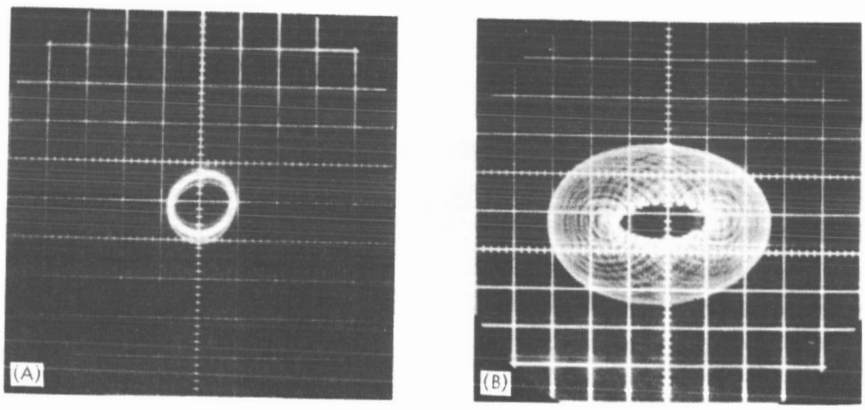


A. Stable synchronous precession, $\omega < \omega_s$.

B. Unstable nonsynchronous precession, $\omega > \omega_s$.

FIGURE 44.—Oscilloscope pictures of the motion of a 360° gas bearing rotor at the threshold of stability (ref. Hinkle, Franklin Institute). Conditions: $\omega_s = 5500$ rad/sec, $\Lambda = 3.5$, scale: 1 major division = 100 $\mu$in.

$$C_f = \frac{\partial D_f}{\partial e}\bigg|_{e=e_0} \quad \omega_P = \text{rotor precession rate}$$

The functions $\omega K_r$ and $\omega K_\phi$ may be termed the bearing radial and tangential stiffness coefficients respectively. The function $\omega D_f$ represents the force component developed normal to the bearing line of centers due to friction effects (see App. D.5 for derivation). This component is usually neglected in most bearing analyses as it is normally small in comparison to the pressure forces. When the rotor precession rate approaches half the total rotor angular velocity, the pressure forces vanish. In this case the friction force can be of the same order of magnitude or larger than the hydrodynamic forces, since $D_f$ becomes infinite as the bearing eccentricity ratio approaches 1. By applying D'Alembert's principle, we obtain the following equations of motion

$$M\ddot{X} + 2C_d\dot{X} + \omega C_s \left|\left(1 - \frac{2\omega_P}{\omega}\right)\right| X + \omega(C_d - C_f)Y = Me_\mu\omega^2 \cos \omega t \tag{5.33}$$

$$M\ddot{Y} + 2C_d\dot{Y} + \omega C_s \left|\left(1 - \frac{2\omega_P}{\omega}\right)\right| Y - \omega(C_d - C_f)X = Me_\mu\omega^2 \sin \omega t \tag{5.34}$$

The absolute value signs have been carried through in the analysis because the function $\omega C_s$ never reverses direction, regardless of the rotor precession rate. As previously mentioned when the rotor precession rate approaches half speed, the hydrodynamic pressure field collapses and the bearing is unable to support a load. Experimental measurements of half-frequency whirl [73] indicate that the whirl ratio, $\omega_P/\omega$, is always equal to or less than one-half. At the inception of instability, the precession rate $\omega$ is synchronous, and the term $\omega C_s|(1 - 2\omega_P/\omega)|$ reduces to $\omega C_s$.

Comparison of the coefficients of Eqs. (5.33) and (5.34) to the generalized coefficients of Eq. 5.7 yields

$$\mathscr{K}_{11} = \mathscr{K}_{22} = \mathscr{K}_r = \frac{\omega C_s}{M}$$

$$\mathscr{K}_{12} = -\mathscr{K}_{21} = \frac{\omega(C_d - C_f)}{M}$$

$$D_{11} = D_{22} = \frac{2\mathscr{K}_\phi}{\omega} = \frac{2C_d}{M}$$

$$D_{12} = D_{21} = 0$$

The general stability criterion of Eq. (5.20) reduces to

$$2D(2D\mathscr{K}_r) > \frac{\mathscr{K}_{12}}{D^2}\,[4D^2\mathscr{K}_{12}]$$

or

$$D\sqrt{\mathscr{K}_r} > \mathscr{K}_{12} \tag{5.35}$$

for stability.

The problem of oil film instability was first reported by Newkirk and Taylor[65] in 1925. They found that the whip motion, as they termed it, started at a speed of twice the critical and persisted to higher speeds. The rotor precession rate was observed to be approximately equal to the rotor critical speed and remained constant over a large speed range. Poritsky,[75] in his treatment of oil film instability, shows that the rotor threshold speed is given by the relationship

$$\omega_s = 2\omega_{CR} \tag{5.36}$$

The Poritsky relationship can be readily demonstrated by Eq. (5.35). Neglecting the bearing friction force coefficient $C_f$, Eq. (5.35) reduces to

$$2\sqrt{\frac{\omega C_s}{M}} > \omega$$

Chapter 6 shows that for the single-mass rotor in a fixed fluid film bearing, the rotor critical speed is a function of only the bearing radial stiffness coefficient and is given by

$$\omega_{CR} = \sqrt{\frac{\omega C_s}{M}} = \sqrt{\mathscr{K}_r}$$

The analysis of the rotor precession rate at the threshold of stability was performed similar to that of Sec. 4.6.3. The precession rate $\omega_p$ was found to be approximately equal to $\sqrt{\mathscr{K}_r} = \omega_{CR}$. Notice that when the bearing friction force is excluded from the analysis, the rotor threshold speed is a function of only the bearing radial stiffness. The cross-coupling term caused by the bearing attitude angle does not enter into the stability criterion. It is clearly obvious that if the cross-coupling term is entirely absent, the rotor must be stable. This is easily seen by letting $C_d \to 0$ in Eq. (5.35).

$$\frac{2C_d}{M}\sqrt{\mathscr{K}_r} > \frac{\omega(C_d - C_f)}{M}$$

$C_d \to 0$

$$0 > -\frac{C_f \omega}{M} \tag{5.37}$$

The above relationship indicates that the rotor is stable for all speeds when the bearing attitude angle goes to zero. Another important relationship that the general stability criterion of Eq. (5.20) reveals is that if the principal stiffness terms $\mathscr{K}_{11}$ and $\mathscr{K}_{22}$ are zero, the system will be inherently unstable. For the case of a symmetric fluid film bearing, the principal stiffness terms transform into the radial stiffness coefficients.

## 5.6 DISCUSSION OF DR. REDDI'S RESULTS ON OIL FILM STABILITY

We can easily deduce Reddi's results from the above analysis that the ideal 360° incompressible fluid film bearing is always unstable. The hydrodynamic fluid film forces for the ideal 360° bearing with no film rupture can be expressed as

$$F_r = -C_b\dot{\epsilon}$$

$$F_t = C_b\omega\left[1-2\frac{\dot{\phi}}{\omega}\right]\frac{\epsilon}{(2+\epsilon^2)\sqrt{1-\epsilon^2}}$$

where

$$C_b = 12\pi\mu LR\left(\frac{R}{C}\right)^2$$

Examination of the bearing radial force term $F_r$ reveals that there is only a squeeze film term present. In this case the bearing has no radial stiffness and hence is unstable for all speeds. In practice, the ideal 360° bearing conditions cannot be maintained because the incompressible lubricant cannot support a negative pressure. The film will thus rupture and cavitate, causing a reduction in the bearing steady-state attitude angle to a value of $\phi < \pi/2$. Reddi represents the cavitated 360° bearing as a 180° partial film bearing which introduces a radial film stiffness term into the system. By taking the 180° bearing characteristics employed by Reddi, differentiating them with respect to the eccentricity $\epsilon$, and applying the stability criterion of Eq. (5.34), one is able to derive the stability chart, Fig. 10 of Ref. 79.

## 5.7 ANALOG COMPUTER SIMULATION OF ROTOR WHIRL MOTION

The linearized fluid film bearing equations of motion, Eqs. (5.33) and (5.34), were programed on the analog computer to illustrate the whirl motion encountered with fluid film bearings. This whirl motion has often been referred to in the literature as "half frequency whirl" because the rotor precession rate is approximately one-half of the rotor speed $\omega$.

Figure 45 represents the rotor motion at the threshold of stability. Figure 45A illustrates the rotor motion for one cycle. The formation of the single internal loop indicates that the nonsynchronous component

is approximately half of the total rotor speed, Fig. 45B represents the rotor motion for a number of cycles. Since the system is linear, the nonsynchronous component becomes unbounded above the threshold. The whirl ratio in this system is slightly less than one-half, causing the internal node to revolve in a counterclockwise manner. (Note the similarity between Fig. 45B and Fig. 19A.)

When the rotor threshold of stability is reached for a fluid film bearing, the development of a small nonsynchronous component causes the rotor orbit to form a double trace as shown in Fig. 46. Figure 46 represents the vectorial addition of varying combinations of synchronous and half-frequency precession. When the half-frequency component is very small ($B \ll 1$), the synchronous orbit forms a double trace. When this type of rotor motion is observed on the oscilloscope, it is an indication that the rotor stability threshold has been reached (Fig. 47).

As the half-frequency component increases, the size of the internal loop diminishes until it degenerates into a cusp when $A/B < 0.5$. Thus, by comparison of Fig. 46 to an actual rotor orbit such as shown in Fig. 47, an estimate of the ratio of the synchronous to the nonsynchronous component of rotor motion can be quickly made.

A nonlinear radial bearing stiffness term was added to Eqs. (5.33), (5.34) to produce a set of equations similar to Eq. (4.46) in Chapter 4.

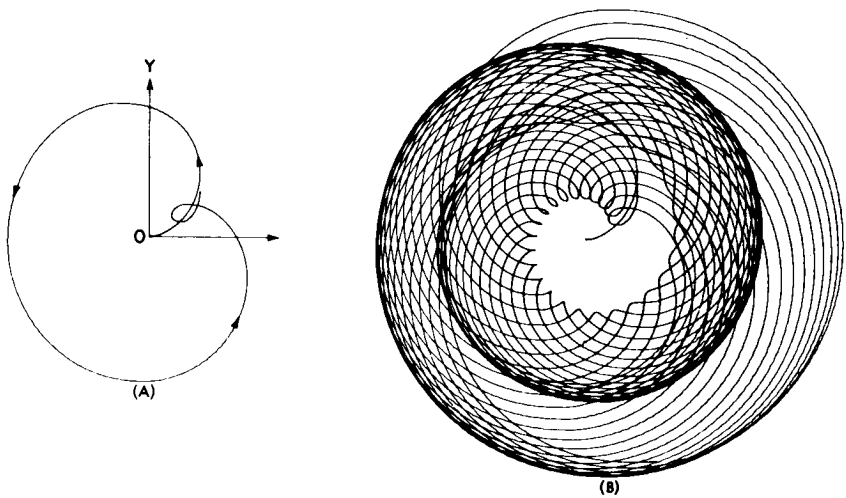


FIGURE 45.—Rotor half-frequency whirl motion of a fluid film bearing at the threshold of stability. (A) Rotor motion for one orbit; $\omega = \omega_s$ synchronous and nonsynchronous precession. (B) Rotor motion for 40 cycles; nonsynchronous component is unbounded in linear system.

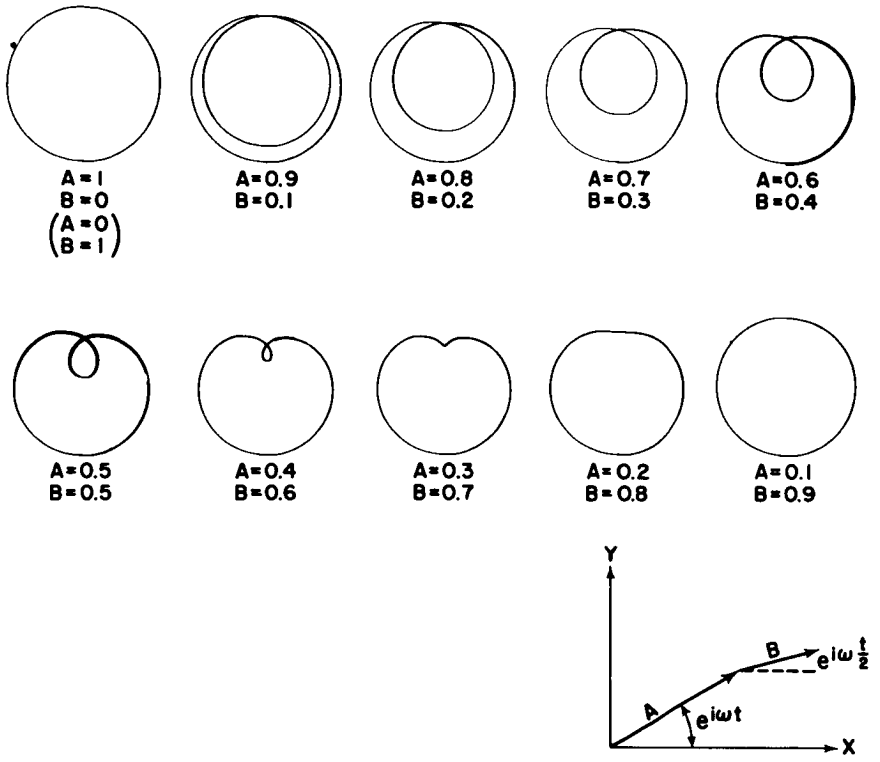


FIGURE 46.—Analog computer traces of various combinations of synchronous and half-frequency whirl. $A$= Magnitude of synchronous whirl component, $B$= magnitude of half-frequency whirl component.

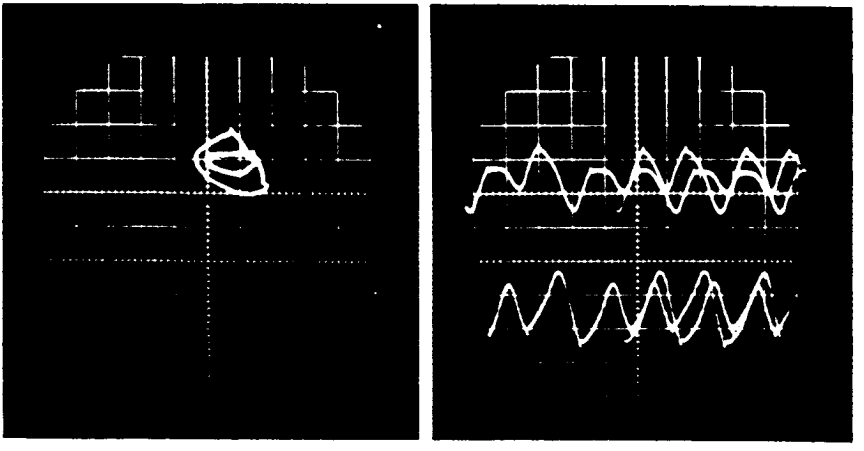

FIGURE 47.—Oscilloscope picture of half-frequency whirl motion in a tilting pad gas bearing rotor (ref. Gunter, Franklin Institute).

The analog computer program B–2 was run over a wide range of speeds for various values of the nonlinear component $\alpha$, where $\alpha = 0$ represents the linear system. Figure 48 represents a comparison between the orbital motion obtained with the linear system (A) and when a small nonlinear component is added as shown in Fig. 45B. In this case, $\alpha = 0.05$ represents only approximately a 5-percent increase in the bearing radial stiffness in comparison to the linear system at the threshold of stability. It was observed that a limit cycle could be obtained on the analog computer even when the potentiometer setting for $\alpha$ was zero. To simulate the true linear system, the switch $F_2$ (see analog computer diagram II in App. B) was installed to eliminate the nonlinear circuit. To measure the deviation between the nonlinear system with $\alpha$ set equal to zero and the linear circuit, a digital voltmeter was used to monitor voltages in the two circuits. The digital voltmeter readings indicate that there exists no more than a fraction of a percent deviation between the two circuits.

The implication of this is quite important. Since in all fluid-film bearings the film forces are nonlinear, the rotor motion does not become unbounded above the stability threshold but forms a limit cycle, as shown in Figs. 44 and 47. Previous stability investigations, such as given by Refs. 4, 5, 7, and 8, have been primarily concerned with the determination of the stability threshold by examination of the linearized equations of motion. It is well known in reality that the rotor motion does not become unbounded above the threshold but forms a finite limit cycle. Thus the limiting safe operating speed for an actual rotor system may be considerably above the threshold value.

This is illustrated by Fig. 49 which represents the rotor steady-state motion over a widespread range of various values of $\alpha$. The analog computer orbits in this case were obtained by allowing the rotor transient motion to die out. Notice that for the case of the linear system ($\alpha = 0$), the rotor motion becomes unstable at approximately twice the rotor critical speed, as was first predicted by Poritsky.[75] Once the threshold is exceeded, the motion is unbounded. As the nonlinear coefficient $\alpha$ is increased, the amplitude and frequency of the critical speed increases. Above the threshold the motion is bounded and forms orbits similar to that represented by Fig. 48(B). Examination of the curves for $\alpha = 0.05$ and 0.10 indicate that the rotor limit cycles increase in approximately a linear relationship with speed for this particular system.

Figure 50 represents the rotor transient motion at the stability threshold for various values of the parameter $\alpha$. In Fig. 50(A) we see that the nonsynchronous component grows rapidly and becomes unbounded in the case of the linear system. In Fig. 50(B) for $\alpha = 0.01$, a large but finite rotor orbit develops. As the value of $\alpha$ increases, the size of the limit cycle diminishes until, for values of $\alpha$ exceeding 0.10, the non-

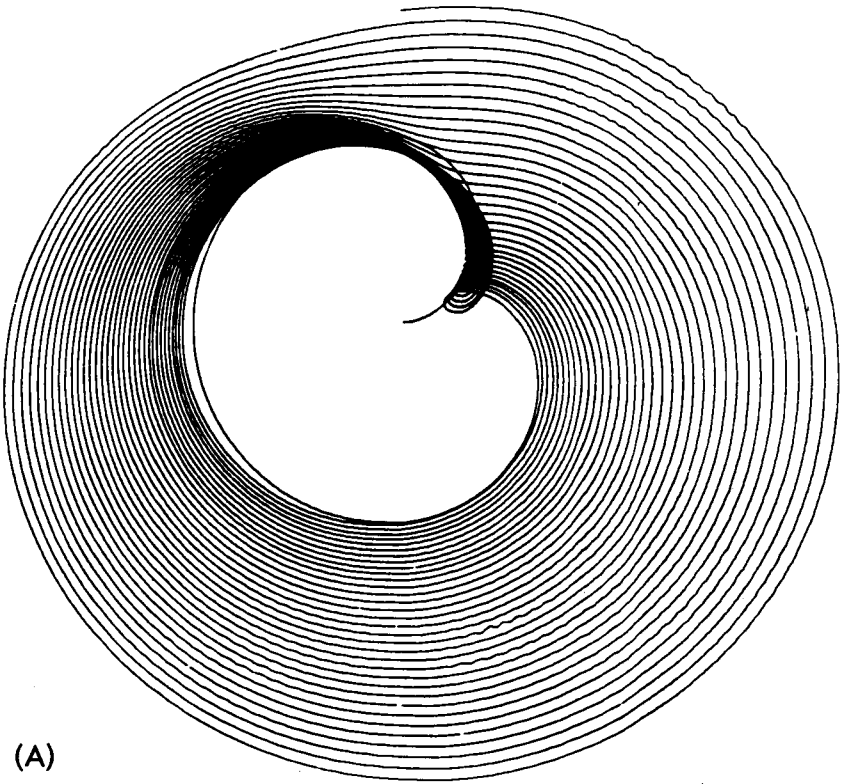


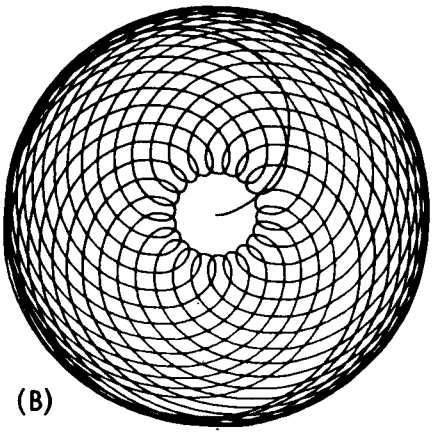


FIGURE 48.—Comparison of rotor half-frequency whirl motion at the threshold of stability for linear and nonlinear system, fluid film bearing. (A) Linear system—unstable motion. Nonsynchronous precession predominates for $N > 20$ cycles. (B) Nonlinear system—finite limit cycle. Nonsynchronous component remains bounded.

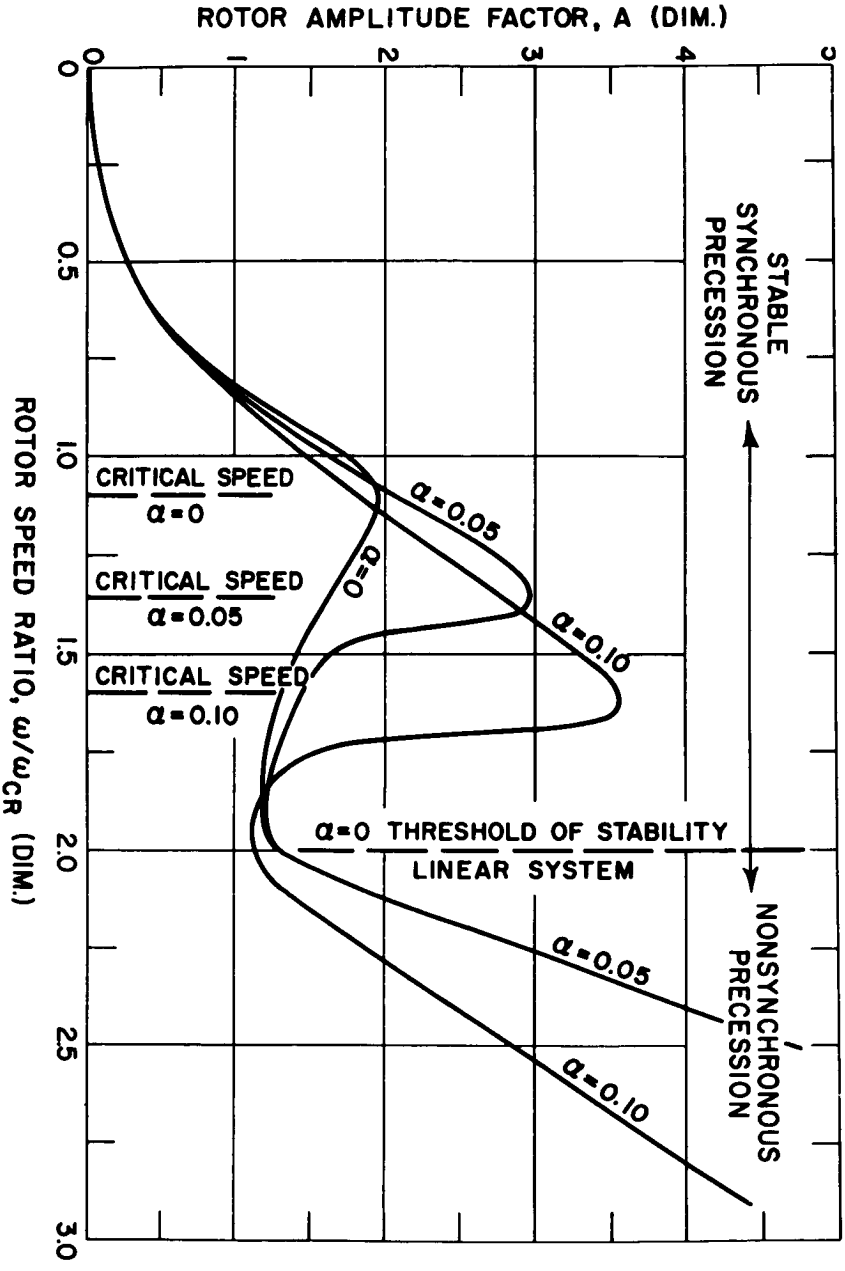


FIGURE 49.—Rotor steady-state motion over a speed range for various values of $\alpha$.

synchronous component is eventually suppressed, leaving only the synchronous precessive motion caused by rotor unbalance. For example, Fig. 50(E) shows that for $\alpha = 0.25$, the rotor motion becomes stable synchronous precession after approximately 50 cycles. The occurrence of half-frequency whirl in a fluid film bearing is not restricted to the conventional 360° journal bearing, but can occur in complicated bearing arrangements such as the tilting pad configuration shown in Fig. 51. Considerable interest and investigation has been directed toward this bearing arrangement because of its superior stability characteristics. (Refer to Refs. 26, 27, and 28 for further details.)

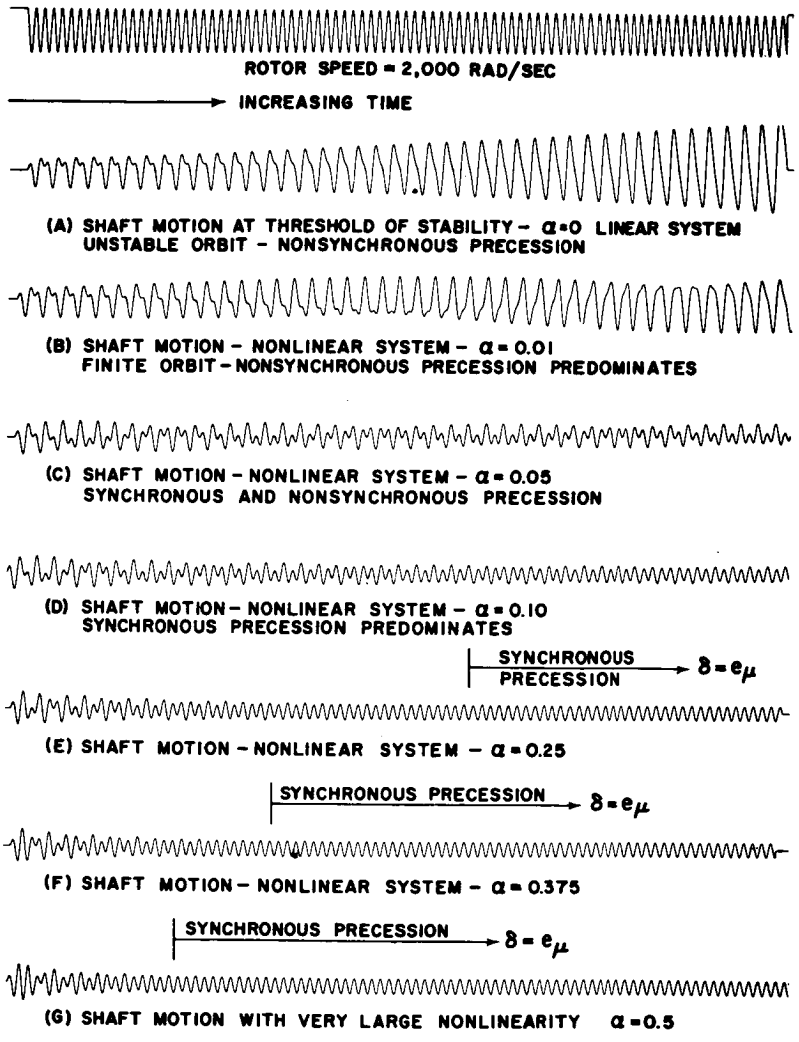


FIGURE 50.—Effect of nonlinearity on rotor transient motion at the threshold of stability.

219-720 O-66—10

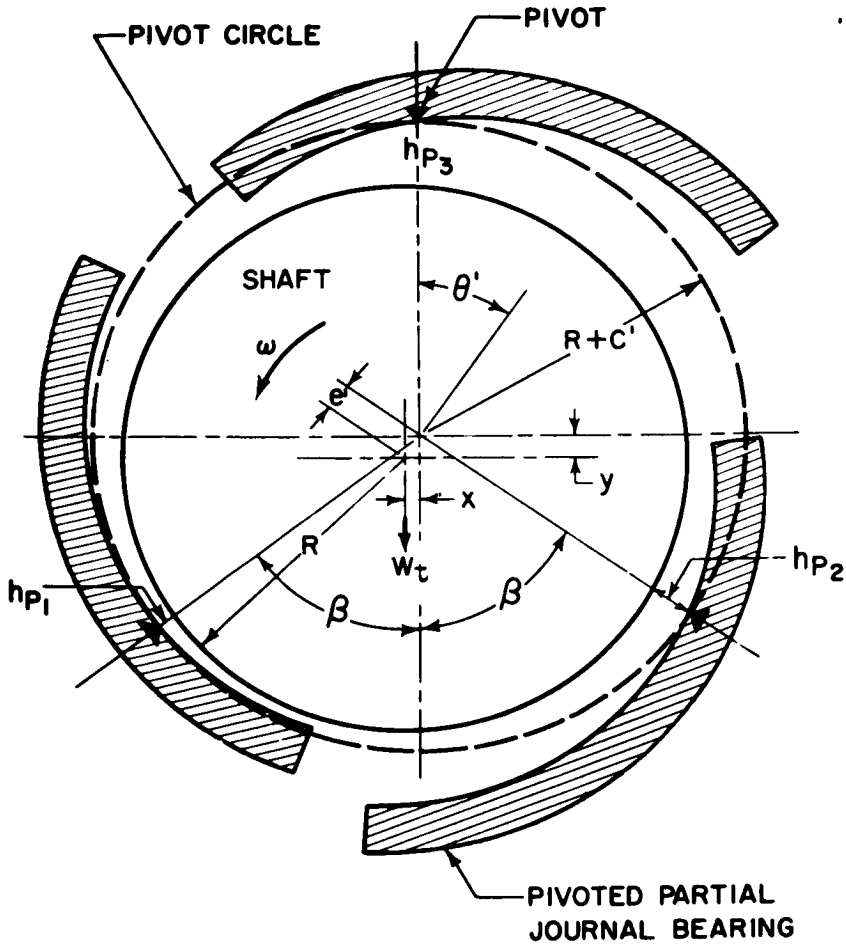


FIGURE 51.—Pivoted-pad journal configuration with three shoes.

Figure 47 represents the actual motion of a tilting-pad gas bearing rotor at the threshold of stability. This picture is of interest because it not only illustrates the half-frequency whirl phenomena, but because it also represents the first published picture of nonsynchronous precession in a tilting pad bearing.[25] This is of particular interest because in 1946, Hagg,[29] in his article on bearing stability, stated that the tilting pad bearing is inherently stable and was not capable of supporting self-excited whirl instability. The fallacy in Hagg's argument lies in his assumption that the forces acting on the shoes are single-valued

functions of eccentricity.[1] The ability of the pads to pivot causes the bearing to operate with an almost-zero-attitude angle. If the bearing attitude angle remains identically zero, the bearing cross-coupling terms will vanish and hence the bearing will be stable. The stability criterion of Eq. (5.20) shows that if the cross-coupling terms $K_{12}$ is zero, the system is inherently stable.[2]

## 5.8 INFLUENCE OF LUBRICANT COMPRESSIBILITY OF ROTOR STABILITY

The compressibility of the lubricant in a fluid film bearing[3] can have a considerable influence on the bearing stability characteristics. For example, Fig. 52 represents the steady-state pressure profile for conditions of incompressible lubrication, moderate compressibility, and the limiting pressure profile when the compressibility parameter $\Lambda$ approaches infinity. (See Eq. (2.11).)

The bearing pressure profile for the case of an incompressible lubricant or for a compressible fluid at very low values of $\Lambda$ is given by the solid line as shown in Fig. 52. Note that the pressure profile in this case is asymmetric with respect to the bearing line of centers. Integration of this pressure distribution around the circumference of the bearing indicates that the steady-state bearing attitude angle is 90°. This implies that an applied force to the journal will result in a deflection normal to the applied load. Since the system has no radial stiffness under these circumstances, the rotor is unstable as shown by Eq. (5.35).

Harrison,[31] who analyzed the infinite width 360° incompressible fluid film bearing in 1913, and later Robertson[82] in 1933 both concluded that the 360° bearing is unstable at all speeds. As previously mentioned, Reddi shows that the oil film bearing has finite ranges of stability by assuming a ruptured film. In actuality, the oil film bearing is unable to sustain a large negative pressure so it cavitates, creating a partial arc condition. Reddi simulates this condition by ignoring the negative part of the pressure profile, which then allows a finite stable range of operation to occur.

---

[1] The stability analysis of a pivoted pad bearing arrangement is complicated by the fact that individual shoe motion as well as shaft motion must be taken into account. For additional details, see E. J. Gunter and V. Castelli, "Stability Investigation of Tilting-Pad Bearings I—Theoretical Foundations," Interim Report I-B2131-1, Franklin Institute Research Laboratories, Feb. 1965, Contract DA-31-124-ARO(D)147.

[2] A detailed discussion and sample calculations of the design and stability characteristics of tilting pad bearings is given in the report by E. J. Gunter, Jr., J. G. Hinkle, and D. D. Fuller, "Manual for the Design of Gas-Lubricated, Tilting-Pad, Journal and Thrust Bearings With Special Reference to High Speed Rotors," Report I-A2392-3-1, Franklin Institute Research Laboratories, Contract AT(30-1)-2512, Task 3.

[3] The derivation of the general Reynolds equation including lubricant compressibility is given in App. D.

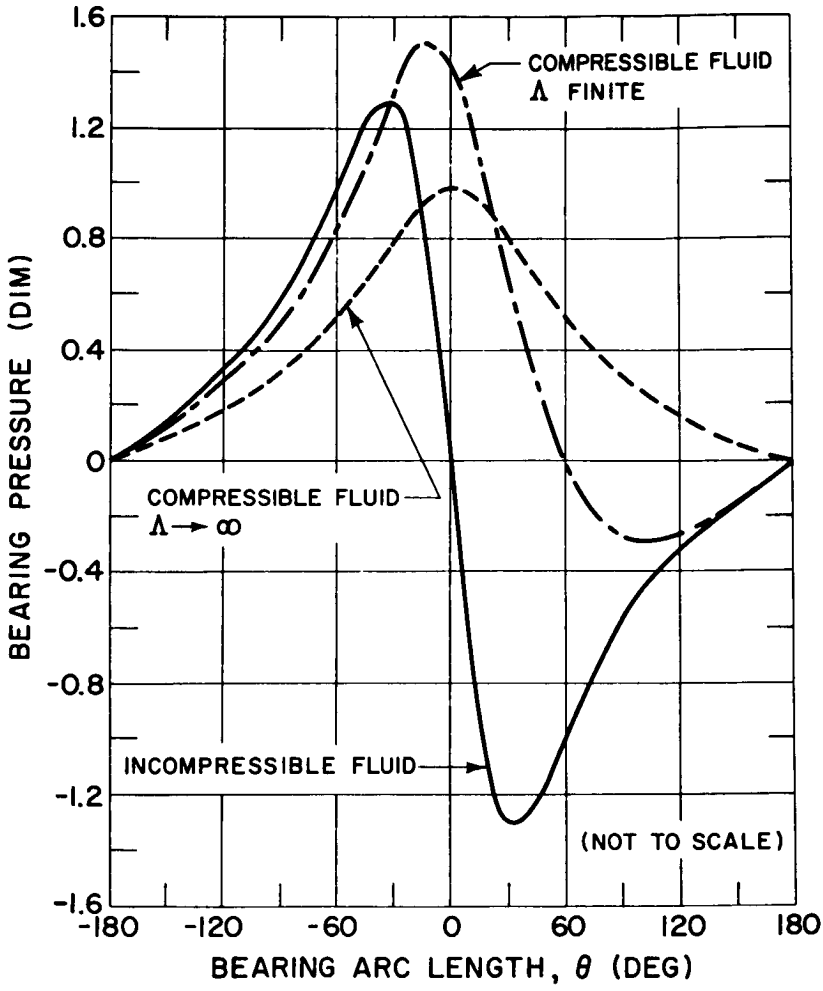


FIGURE 52.—Effect of lubricant compressibility on the pressure distribution in a 360° journal bearing.

In the case of a compressible media, the lubricant is able to sustain a subambient pressure as shown in Fig. 52. Thus lubricant compressibility has the net effect of reducing the bearing steady-state load capacity and also the bearing attitude angle. The stability analysis as performed by Cheng[6] and Castelli[5] is considerably more difficult than the incompressible situation due to the nonlinearity of the governing Reynolds equation and the introduction of the time-dependent squeeze film term. The fact that the gas bearing has an attitude angle less than 90° accounts in part for its ability to develop a finite threshold speed.

The stability characteristics of the 360° infinite-width gas bearing as determined by Cheng and Castelli are shown in Fig. 53. Although each used considerably different techniques, the results show considerable agreement. Note that in both analyses, as the compressibility parameter $\Lambda$ approaches zero, the bearing is unstable for all eccentricity ratios as predicted by incompressible theory. As the compressibility parameter increases, the bearing attitude angle approaches zero and the bearing can develop only a finite load capacity. Notice that Fig. 52 shows that the influence of lubricant compressibility changes the bearing pressure profile from asymmetric to symmetric at high values of $\Lambda$.[4]

Under these circumstances the gas film behaves as a nonlinear undamped spring system.[5] Although Fig. 53 shows a threshold of stability at high $\Lambda$, in reality we find that it does not exist. Since the bearing attitude angle goes to zero as $\Lambda \rightarrow \infty$, the mechanism which is responsible for self-excited whirling vanishes.

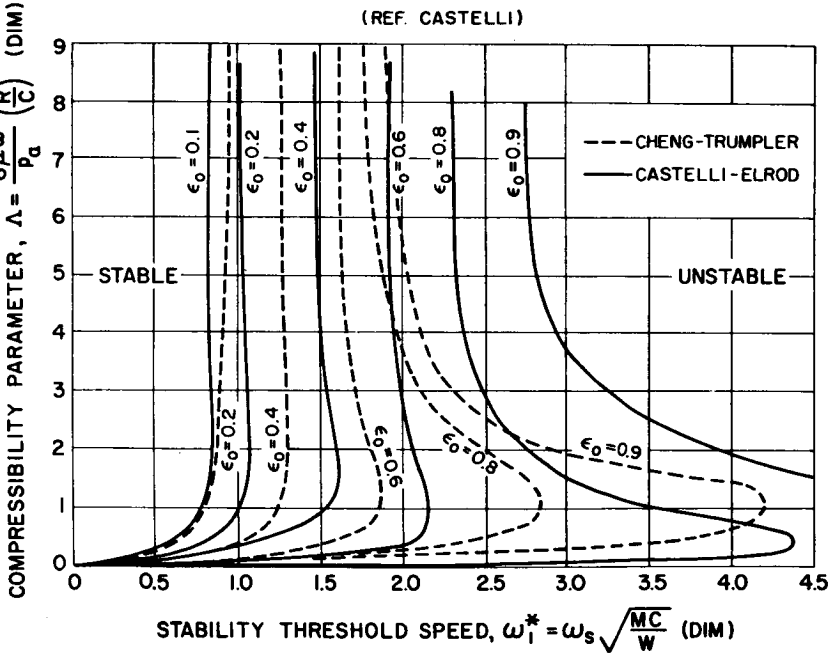


FIGURE 53.—Threshold of stability for the 360° infinite-width gas bearing.

[4] For additional discussion of the influence of lubricant compressibility on the bearing pressure profile, refer to the paper by G. Ford, D. Harris, and D. Pantall, "Principles and Applications of Hydrodynamic-Type Gas Bearings," *Instit. of Mech. Eng.*, Oct. 1956.

[5] See W. A. Gross, *Gas Film Lubrication*, J. Wiley, 1962, p. 128, for the asymptotic solution of the gas bearing at high compressibility numbers.

Examination of the real positive root which governs stability reveals that it is zero at the threshold and remains zero as the rotor speed exceeds the threshold.[6] Routh referred to this special condition as neutral or critical stability. If we should add a small amount of external damping or bearing friction force to the system, we would find that the gas bearing is completely stable at high values of $\Lambda$.

## 5.9 DISCUSSION AND CONCLUSIONS

In Chapter 5 we have evaluated the stability characteristics of the general linearized equations of motion for a system of two degrees of freedom by considering the first-order terms of the Taylor's expansion of the forces. The general stability criterion developed (Eq. (5.20)) is useful because it provides considerable insight into the mechanism of rotor whirl instability caused by both internal friction and fluid film bearings. Equation (5.20) shows why bearing asymmetry will increase stability and also indicates that the system will be stable if the generalized cross-coupling coefficient $k_{12}$ is zero.

The linearized equations of motion for a fluid film bearing were programed on the analog computer. Comparison of these orbits to the motion obtained with internal friction damping clearly shows the similarity between the two mechanisms.

---

[6] This is similar to the situation encountered in Ch. 4 in the limiting case when the internal damping coefficient goes to zero. The Routh criterion still predicts a stability threshold, but examination of the real positive root $P$ reveals that it is zero. See Eq. (4.41).

# Chapter 6

# Analysis of the Extended Jeffcott Model — Synchronous Precession

In the analysis of the single-mass rotor (Jeffcott model), the rotor end conditions were assumed as rigid or simply supported.

The assumption of simple-support boundary conditions as a basis for rotor critical speeds is obviously inadequate, since the bearings and foundation flexibility will considerably alter the behavior. Numerous investigators such as Smith,[93] Linn and Prohl,[57] Koenig, [102] and Lund and Sternlicht [58] have considered the effects of the bearings on the rotor critical speeds and the bearing attenuation. In each of these approaches, the bearings are treated as linear springs and dashpots. The problem of determining the system critical speeds is reduced to the problem of finding the natural lateral frequencies of an equivalent beam on damped elastic supports.

A fluid film bearing cannot be adequately represented by a single spring and damping coefficient. For small perturbations from an equilibrium position, the bearing characteristics may be approximated by eight film coefficients, four damping factors, and four film stiffness terms. For a symmetric bearing, this further reduces to four: two damping and two spring coefficients.

As an example, Reddi and Trumpler [79] show that the bearing forces generated by a cavitated 360° oil bearing are of the form

$$F_t = 3\mu\epsilon_n' LD\left(\frac{D}{C}\right)^2\left[\frac{\epsilon}{(2+\epsilon^2)(1-\epsilon^2)}\right][\pi(\omega-2\dot{\phi})(1-\epsilon^2)^{1/2}+4\dot{\epsilon}]-W\sin\phi \tag{6.1}$$

$$F_r = -3\mu\epsilon_r' LD\left(\frac{D}{C}\right)^2\left[\frac{2\epsilon^2(\omega-2\dot{\phi})}{(1-\epsilon^2)(2+\epsilon^2)} + \frac{\dot{\epsilon}}{(1-\epsilon^2)^{3/2}}\left\{\pi-\frac{16}{\pi(2+\epsilon^2)}\right\}\right]+W\cos\phi \tag{6.2}$$

This can be expressed in the general form

$$F_t - F_{t_0} = \omega \left[ C_s \left( 1 - \frac{2\dot{\phi}}{\omega} \right) + \mathscr{D} D_s \right] \epsilon$$

$$F_r - F_{r_0} = -\omega \left[ C_d \left| \left( 1 - \frac{2\dot{\phi}}{\omega} \right) \right| + \mathscr{D} D_d \right] \epsilon \tag{6.3}$$

where

$\mathscr{D}$ = differential operator = $d/dt$
$D_s$; $D_d$ = damping coefficients
$C_s$; $C_d$ = film stiffness coefficients

Note that depending upon whether the rotor motion is synchronous or nonsynchronous, precession will determine the sign of the tangential bearing force $F_t$. The radial bearing force is invariant in direction regardless of precession rate. If the motion is assumed to be synchronous precession, then the vector fluid force acting on the journal is given by

$$\vec{F}_{br} = [K_{br} + D_{br}\mathscr{D}]\, \vec{\delta}_j \tag{6.4}$$

where

$K_{br}$ = Complex bearing stiffness coefficient
$= \omega[C_s + iC_d]$
$D_{br}$ = Complex damping coefficient
$= \omega[D_s + iD_d]$

The most common practice is to neglect the normal or cross-coupling coefficient $C_d$ in order to reduce the bearing to a one-dimensional representation. Lund and Sternlicht have attempted to improve upon this assumption by lumping the cross-coupling coefficients with the principal spring rates, but the manner in which this is done is nebulous and the results are not general.

The normal film coefficient has a considerable influence not only on the system critical speeds but also on the forces transmitted through the bearings. As an illustration, by expressing the bearing characteristics in complex vector form, it is possible to write the equations of motion of the single-mass symmetric rotor including the bearings and foundation flexibility. This represents a system of seven degrees of freedom as compared to the original three.

If the bearing housing is considered as flexible, then the forces exerted on it by the journal will cause it to deflect. The total displacement of the journal center $O_j$ will be given by the sum of the bearing housing (or foundation) flexibility, plus the relative displacement of the journal in the bearing

$$\vec{\delta}_c = \vec{\delta}_j + \vec{\delta}_b \tag{6.5}$$

If a linear relationship between $\vec{F}_{br}$ and $\vec{\delta}_b$ is postulated then:

$$\vec{F}_{br} = -K_b \vec{\delta}_b \tag{6.6}$$

Combining Eqs. (6.4), (6.5), and (6.6) and neglecting bearing damping

$$\vec{F}_{br} = \frac{-K_b \omega [C_s + iC_d]}{K_b + \omega [C_s + iC_d]} \vec{\delta}_c$$

$$= -K^*_{br} \vec{\delta}_c = -[K^*_s + iK^*_d] \vec{\delta}_c \tag{6.7}$$

where

$$K^*_s = \frac{K_b^2 K_s + (K_s^2 + K_d^2) K_b}{(K_b + K_s)^2 + K_d^2}$$

$$K^*_d = \frac{K_b^2 K_d}{(K_b + K_s)^2 + K_d^2}$$

If the elastic forces acting on the rotor center are similar in form to Eq. (6.7), then

$$\vec{F}_s = -\alpha \vec{\delta}_r \tag{6.8}$$

Let

$$\vec{\delta} = \text{total rotor deflection} = \vec{\delta}_r + \vec{\delta}_j + \vec{\delta}_b \tag{6.9}$$

Combining Eqs. (6.7–6.9)

$$\vec{F}_s = -K_s \vec{\delta} \tag{6.10}$$

where

$K_s$ = total system complex stiffness coefficient

$$K_s = \frac{\alpha K_{br}}{\alpha + K_{br}} = K_{sr} + iK_{si} \tag{6.11}$$

and

$$K_{sr} = \frac{\alpha [(\omega C^*_s)^2 + (\omega C^*_d)^2 + \alpha \omega C^*_s]}{(\alpha + \omega C^*_s)^2 + (\omega C^*_d)^2}$$

$$K_{si} = \frac{\alpha^2 \omega C^*_d}{(\alpha + \omega C^*_s)^2 + (\omega C^*_d)^2} \tag{6.12}$$

If rotor damping and unbalance is considered, then the vectorial equation of motion of the rotor is given by

$$M\ddot{\vec{\delta}} + M\mu_f\omega\,\dot{\vec{\delta}} + K_s\,\vec{\delta} = -M\ddot{\vec{e}} \tag{6.13}$$

(Note that total time derivatives are used in Eq. (6.13).)

If the disk is revolving with constant angular velocity

$$\vec{e} = e_\mu[e^{i\omega t}]$$

and

$$\ddot{\vec{e}} = -e_\mu\omega^2[e^{i\omega t}] \tag{6.14}$$

where $e_\mu$ = rotor unbalance eccentricity. Equation (6.7) becomes

$$\ddot{\vec{\delta}} + \mu_f\omega\,\dot{\vec{\delta}} + \frac{K_s}{M}\,\vec{\delta} = (e_\mu\omega^2)e^{i\omega t} \tag{6.15}$$

If the motion of the system is assumed to be forward synchronous precession (rotor motion may be nonsynchronous precessive which is associated with self-excited whirling), then a particular steady-state solution of the following form may be assumed.

$$\vec{\delta} = \vec{\delta}_0 e^{i\omega t} \tag{6.16}$$

Solving for $\delta_0$, the complex rotor amplitude

$$\delta_0 = \frac{e_\mu}{1 - \dfrac{K_s}{M\omega^2} + i\mu_f} \tag{6.17}$$

$$\delta_0 \underset{(6.11)}{=} \frac{e_\mu}{1 - \dfrac{K_{sr}}{M\omega^2} + i\left(\mu_f + \dfrac{K_{si}}{M\omega^2}\right)} \tag{6.18}$$

The complex rotor amplitude

$$\delta_0 = A - iB \tag{6.19}$$

where

$$A = \frac{e_\mu\left(1 - \dfrac{K_{sr}}{M\omega^2}\right)}{\left(1 - \dfrac{K_{sr}}{M\omega^2}\right)^2 + \left(\mu_f + \dfrac{K_{si}}{M\omega^2}\right)}$$

$$B=\frac{e_\mu\left(\mu_f+\frac{K_{si}}{M\omega^2}\right)}{\left(1-\frac{K_{sr}}{M\omega^2}\right)^2+\left(\mu+\frac{K_{si}}{M\omega^2}\right)} \tag{6.20}$$

The vectorial rotor deflection $\delta$ may be expressed in terms of real quantities by the introduction of the rotor phase angle $\beta$.

$$\delta=R_e\, e^{i(\omega t-\beta)} \tag{6.21}$$

$R_e$ = total rotor deflection

$$R_e=\sqrt{A^2+B^2}=\sqrt{\left(1-\frac{K_{sr}}{M\omega^2}\right)^2+\left(\mu_f+\frac{K_{si}}{M\omega^2}\right)^2} \tag{6.22}$$

$$\beta=\tan^{-1}\left[\frac{\mu_f+\frac{K_{si}}{M\omega^2}}{\frac{K_{sr}}{M\omega^2}-1}\right] \tag{6.23}$$

When $\omega=\omega_{cs}$, the system critical speed, the displacement vector is lagging the eccentricity vector $\vec{e}$ by 90°. This is given by the conditions that

$$A=0$$

and

$$\beta=90° \tag{6.24}$$

This is only possible if

$$1-\frac{K_{sr}}{M\omega^2}=0 \tag{6.25}$$

Hence the system critical speed is given by

$$\omega_{CS}=\sqrt{\frac{K_{sr}}{M}}=\sqrt{\frac{\alpha[K_s^{*2}+K_d^{*2}+\alpha K_s^*]}{M[(\alpha+K_s^*)^2+K_d^{*2}]}} \tag{6.26}$$

Let

$$R=\frac{\alpha}{K_s^*}$$

and

$$\tan\phi=\frac{K_d^*}{K_s}$$

$$\frac{\omega_{CS}}{\omega_{CR}}=\sqrt{\frac{1+R+\tan^2\phi}{(1+R)^2+\tan^2\phi}}=N \tag{6.27}$$

Equation (6.27) represents the ratio of the system critical speed to the critical speed of the rotor on simple or fixed supports. The ratio $N$ is always less than 1.

Figure 54 represents a plot of Eq. (6.27) for various values of $N$. From the graph it is seen that the bearing attitude angle has a pronounced effect on the system critical speed, particularly at high values of $\phi$. Previous rotor dynamic programs have neglected the normal bearing coefficients $K^*$ in the calculation of critical speeds. This approximation is justified only if the effective bearing attitude angle is low or less than 20°.

For the case of a rigid rotor ($\alpha \rightarrow \infty$), Eq. (6.26) reduces to

$$\omega_{CS} = \sqrt{\frac{K_s^*}{M}} \tag{6.28}$$

where

$$K_s^* = \frac{K_s + \frac{1}{K_b}(K_s^2 + K_d^2)}{\left(1 + \frac{K_s}{K_b}\right)^2 + \left(\frac{K_d}{K_b}\right)^2}$$

For the case of a rigid foundation ($K_b \rightarrow \infty$), the rotor resonance frequency reduces to a function of only the radial oil film stiffness coefficient $K_s$.

The rotor displacement at the critical speed is given by

$$\left.\frac{\delta}{e_\mu}\right|_{\omega=\omega_{cs}} = \frac{B}{e_\mu} = \frac{K_{sr}}{K_{si} + \mu_f K_{sr}} \tag{6.29}$$

If the external damping coefficient $\mu_f = 0$, then the rotor amplitude at the critical speed is unbounded for the case of the simple support rotor. When oil film bearings are introduced, the deflection is limited due to the influence of the out-of-phase bearing coefficient. Eq. (6.29) reduces to

$$\left.\frac{\delta}{e_\mu}\right|_{\omega=\omega_{cs}} = \frac{1 + R + \tan^2\phi}{R \tan\phi} \tag{6.30}$$

Thus Eq. (6.30) shows that the rotor amplification at the critical speed is a function of the bearing attitude angle. In Chapter 5 it was demonstrated that the bearing attitude angle is primarily responsible for rotor instability. That is, the ideal 360° bearing with a 90° attitude angle is always unstable, and the tilting pad bearing or the 360° compressible fluid film bearing at high $\Lambda$ number with a zero attitude angle is stable.

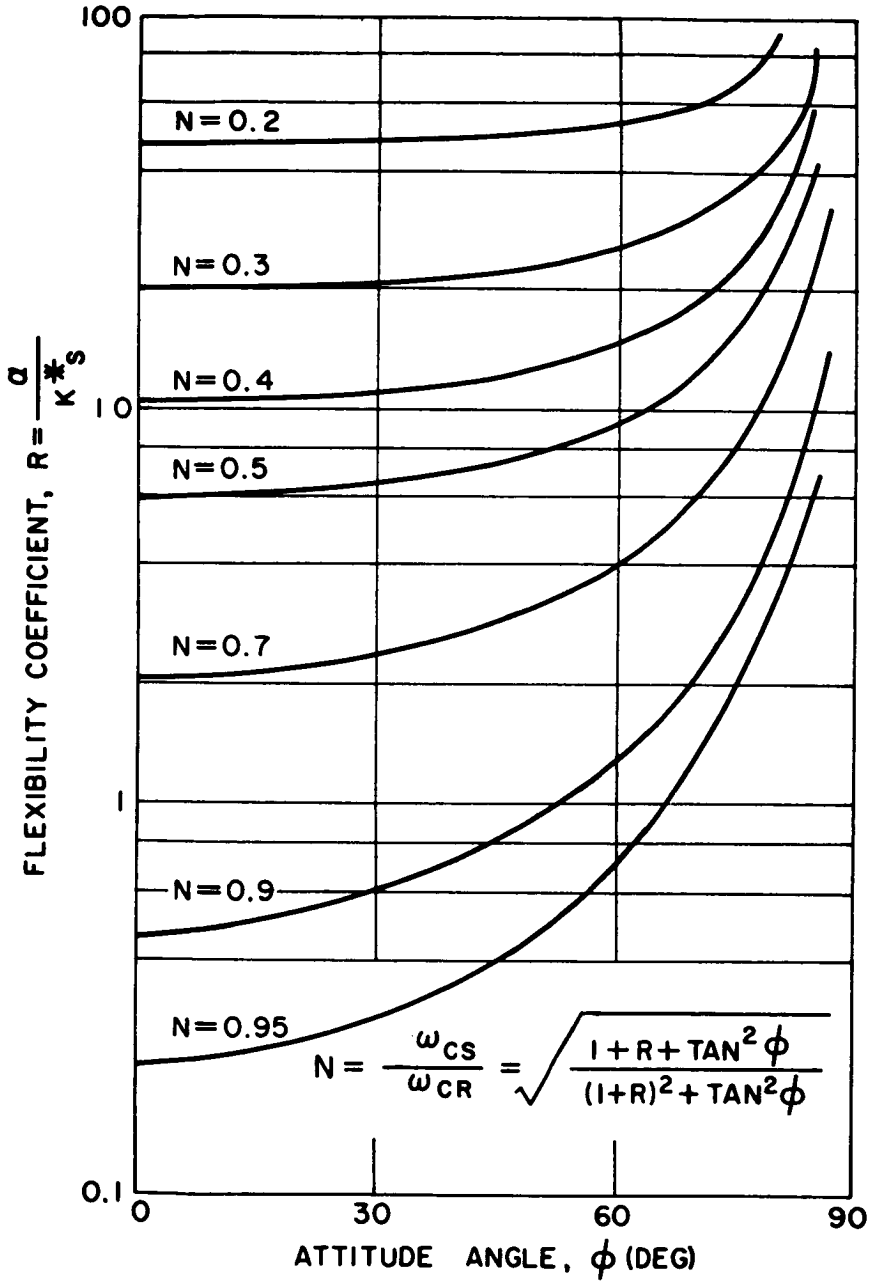


FIGURE 54. – The effects of bearing attitude angle and foundation flexibility on rotor critical speed.

Therefore if the bearing attitude angle is decreased to improve the rotor stability characteristics, the rotor will develop higher amplitudes when passing through the critical speed.

# Chapter 7

# Discussion of the Assumptions, Results, and General Conclusions

## 7.1 DISCUSSION OF ASSUMPTIONS

The major assumptions that are made in the analysis are—

1. The rotor mass is concentrated in a single plane which is equidistant from the points of shaft support.
2. No gyroscopic forces act on the disk.
3. The mass of the shaft is negligible in comparison to the mass of the disk.
4. The total rotor angular speed is constant.
5. The shaft is axially symmetric.

The first three assumptions define the single-mass Jeffcott model. In this model no gyroscopic terms are taken into consideration. It is well known that the gyroscopic terms can have a considerable influence on the rotor critical speeds and the rotor precession rate. Stodola[100] considered in detail the influence of gyroscopic forces on the critical speeds. Less well understood is its influence on rotor nonsynchronous precession. Green,[22] in his article on the gyroscopic effects on critical speeds, assumes a conservative system and arrives at both forward and backward nonsynchronous precessive solutions. It appears that his backward precessive solutions will vanish when damping is added to the system, as was the case with the work of Kane.[45] The author has observed a case of backward nonsynchronous precession in a high-speed gas bearing rotor as shown in Fig. 55. This occurred when a thrust bearing was overloaded creating a moment on the shaft. It is believed that the interaction between the external friction moment and rotor gyroscopic moments created the nonsynchronous backward precessive motion shown in Fig. 55.[1]

[1] Analog computer simulation of the rotor motion indicates that the five-star pattern is a combination of forward synchronous and $1\frac{1}{2}$ times synchronous backward precession.

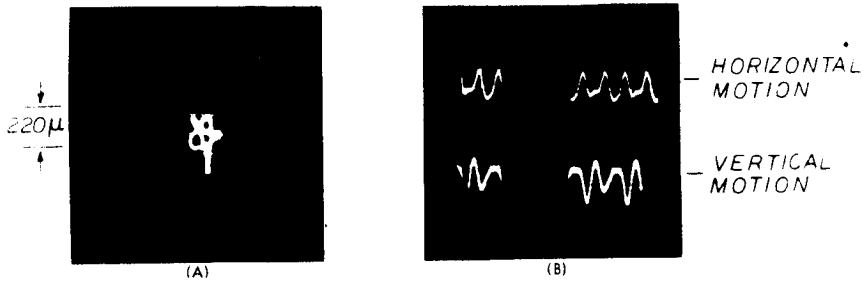


FIGURE 55.—Nonsynchronous backward precession in a gas bearing rotor (ref. Gunter, Franklin Institute). Journal Orbit, 9–5–63. $N = 3000$ rpm, Pivot No. 4, $P_T = 50$ psig, $P_B = 70$ psig, $L/B = 1.0$, $C'/C = 0.731$, Load cell = 3½ in. $H_2O$. (A) Rotor orbit. (B) Sweep traces.

In the analysis, asymmetric foundation support is considered, but the shaft is assumed to be axially symmetric. D. M. Smith[93] analyzed an unsymmetric shaft in 1933 and concluded that shaft asymmetry will result in large vibrations between the dual critical speed range, and that the addition of sufficient external damping to the system will suppress the motion. Smith's analysis was extended in 1943, by Foote, Poritsky, and Slade.[2] Recently Yamamoto[3] also demonstrated that shaft asymmetry can lead to large amplitude vibrations.

Thus we see that while foundation asymmetry can have a beneficial influence with respect to stability, shaft asymmetry should always be avoided.

## 7.2 DISCUSSION OF RESULTS AND CONCLUSIONS

The major results and conclusions of this investigation are summarized as follows:

1. Rotor nonsynchronous precession cannot be adequately investigated from the standpoint of a conservative system.
2. Nonsynchronous rotor precession is a self-excited phenomenon which occurs only in certain dissipative systems (neglecting gyroscopic forces) in which the dissipation function is dependent upon the rotor precession rate.
3. Rotor instability never occurs below the first critical speed, but only in the post- or super-critical-speed region.

---

[2] Foote, W. R., Poritsky, H., and J. J. Slade, Jr., "Critical Speeds of a Rotor With Unequal Shaft Flexibilities," *ASME Trans. J. Appl. Mech.*, A–77, June 1943.

[3] Yamamoto, T., and O. Hiroshi, "On the Unstable Vibrations of a Shaft Carrying an Unsymmetric Rotor," *ASME Trans. J. Appl. Mech.*, Paper No. 64, APM–32.

4. The rotor precession rate is closely related to the system natural frequency (single-mass rotor) and remains approximately constant over a wide range of speeds.
5. Two common causes of rotor instability are rotor internal friction caused by shrink fits, couplings, and fluid film bearings.
6. The mechanism which causes instability has a beneficial influence in the critical-speed range by acting as a damping force to reduce the rotor amplitude of motion.
7. The rotor may pass through the critical-speed region if proper damping and balancing are obtained, but rotor speed cannot exceed the stability threshold for the linear system. (The author has observed instances in which the rotor passed through the threshold and then returned to stable operation. No explanation for this is available. This behavior cannot be explained by linear theory).
8. In the linear system the rotor whirl orbit grows exponentially above the threshold speed of stability. In order to develop a finite whirl orbit above the threshold speed, the system must be nonlinear.
9. The subcritical resonance at half the rotor critical speed that sometimes occurs in heavy horizontal rotors is caused by gravitational effects. Contrary to the analysis by Soderberg, this motion remains bounded and can be easily damped out.
10. The introduction of a symmetrical flexible support into the system will lower the rotor critical speed and also the rotor stability threshold.
11. If external damping is incorporated into a flexible foundation, the stability threshold may be greatly increased above its original value.
12. There are certain combinations of foundation flexibility and damping which will make the rotor completely stable for all speeds.
13. There is an optimum value of foundation damping to promote stability. Excessive damping causes a reduction in stability.
14. If the bearing or rotor cross-coupling terms are small, a large increase in the stability threshold may be obtained by foundation asymmetry alone without addition of external damping.
15. In the case of fluid film bearings with low-attitude angles, such as the hydrostatic, tilting pad, or gas bearing at high compressibility numbers, the stability characteristics may be greatly improved by bearing asymmetry. For example, this would indicate that the three-tilting pad bearing is preferable to the four-pad bearing for stability.

219-720 O-66—11

16. When the self-excitation force component (normal to line of centers) is large, such as in a fluid film bearing with a large attitude angle, the introduction of asymmetric foundation flexibility will not improve the stability threshold, but may reduce it. In this case external damping must be incorporated into the foundation to raise the threshold.
17. The mass of the bearing has a considerable influence on the rotor stability. If the bearing mass is large in comparison to the rotor mass, there will be a reduction in the stability.
18. The stability of a fluid film bearing may be improved by raising the bearing radial stiffness or reducing the bearing attitude angle.
19. The tilting pad bearing arrangement has excellent stability characteristics because of its small attitude angle, but the price one pays is poor attenuation in the critical-speed range.
20. Contrary to the analysis by Hagg, the tilting pad bearing will support whirl instability under special circumstances.
21. The analysis of the stability threshold by the Routh method is based on the perturbated equation of motion about an equilibrium configuration. The Routh method predicts the threshold of stability, but furnishes no information on the degree of instability (growth rate of the positive real root).
22. The threshold of stability obtained by the Routh method does not necessarily represent the limit of safe operation. In some cases the motion may grow rapidly once the threshold is exceeded (Fig. 44), but in other cases the rotor orbit may remain small and grow only slightly with speed (Fig. 47). The upper limit of safe operation may be considerably in excess of the threshold value. This limit can be obtained only through a nonlinear analysis.
23. The rigid or flexible rotor with ideal 360° incompressible fluid film bearings (90° attitude angle) mounted on a rigid foundation is unstable at all speeds because the system has zero radial stiffness. This corresponds to the conclusions reached by Reddi and others.
24. If the bearings in the above system have a partial (cavitated) film, the rotor has a definite threshold speed because the bearing attitude angle is below 90° and the journal has a finite radial stiffness.
25. Lubricant compressibility increases the stability of a 360° gas bearing by causing a reduction in the attitude angle.
26. At high compressibility numbers, the attitude angle goes to zero; thus the rotor behaves as an undamped nonlinear spring-mass system as $\Lambda$ approaches infinity. Under these conditions the regions of instability change to neutral stability.

27. Other investigations have usually excluded the influence of friction in bearing stability analyses because the friction term is very small in comparison to the pressure terms. This has led to the erroneous conclusion of instability at high $\Lambda$. If friction is included in the analysis, the motion at high $\Lambda$ becomes completely stable.

# Appendix A

# Shaft Internal Friction Characteristics

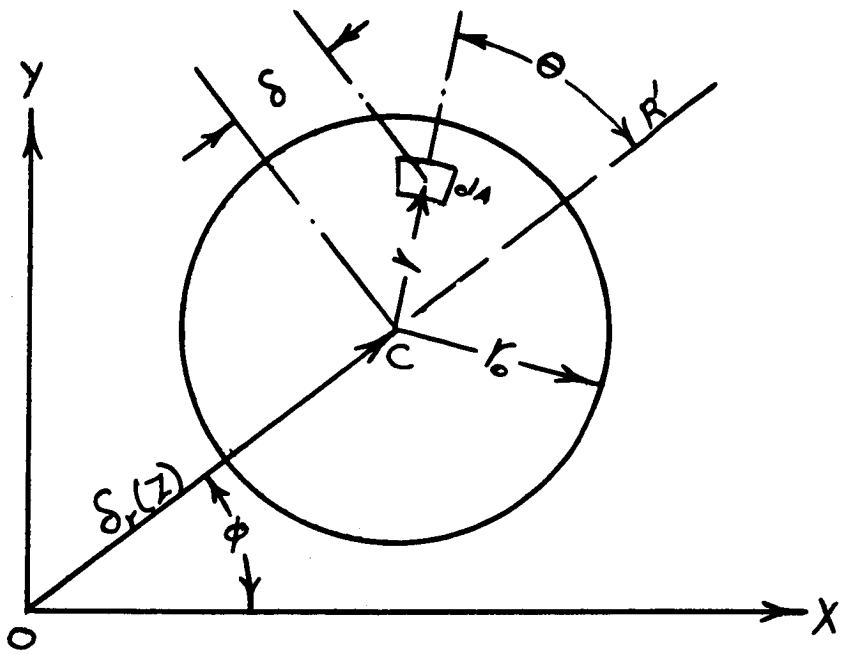


*Nomenclature*

$\delta_r(z)$ = shaft deflection at location $z$

$\omega^s$ = angular velocity of rotor = $\omega$

${}^R\omega^{R'}$ = angular velocity of rotating reference frame $R'$ = rotor precession speed $\dot{\phi}$

${}^{R'}\omega^s$ = angular velocity of shaft in relative reference frame $R' = \dot{\theta}$

$r_0$ = shaft radius

$z$ = axial shaft coordinate

$\rho$ = radius of curvature

To include the internal damping phenomena for a rotating shaft, a stress-strain relationship will be assumed in which the shaft fiber stress is proportional to the rate of change of fiber strain in addition to the con-

ventional term. In a manner similar to that assumed by Ehrich,[14] the stress is given by

$$\sigma_z = E\epsilon_z + \mu_i \frac{d\epsilon_z}{dt} \tag{A.1}$$

where

$$\epsilon_z = \frac{\delta}{\rho} = \delta \frac{d^2\delta_r}{dz^2}$$

for simple beam theory. The strain at any point for a circular shaft is given by

$$\epsilon_z = \epsilon_0 \left(\frac{r}{r_0}\right) cos\ \theta \tag{A.2}$$

where

$$\epsilon_0 = r_0 \frac{d^2\delta_r}{dz^2} = \frac{r_0}{\rho}$$

The stress $\sigma_z$ for a rotating shaft is given by

$$\sigma_z = \epsilon_0 \left(\frac{r}{r_0}\right) \left[E \cos\theta - \mu_i \sin\theta\dot{\theta}\right] + \mu_i \frac{d\epsilon_0}{dt} \left(\frac{r}{r_0}\right) \cos\theta \tag{A.3}$$

The bending moments acting at any cross section are given by

$$M_R = \int\int_A \sigma_z r \cos\theta dA = \int_0^{2\pi} \int_0^r \left(\frac{r}{r_0}\right) \left[\left(\epsilon_0 E + \mu_i \frac{d\epsilon_0}{dt}\right) \cos\theta - \epsilon_0 \mu_i \sin\theta\dot{\theta}\right] \cos\theta r^2 dr d\theta = \frac{I}{r_0} \left[\epsilon_0 E + \mu_i \frac{d\epsilon_0}{dt}\right] \tag{A.4}$$

$$M_\phi = \int\int_A \sigma_z r \sin\theta dA = -\left(\frac{\epsilon_0}{r_0}\right) \mu_i I\dot{\theta} \tag{A.5}$$

The radial force development per unit length is given by

$$f_r = -\left[EI \frac{d^4\delta_r}{dz^4} + \mu_i I \frac{d^4\dot{\delta}_r}{dz^4}\right] \tag{A.6}$$

and the tangential force per unit length is given by

$$f_\phi = -\mu_i I \frac{d^4\delta_r}{dz^4} \dot{\theta} \tag{A.7}$$

where

$$\dot{\theta} = \omega - \dot{\phi}$$

Note that the unit tangential force has the characteristics of a damping or a driving force depending upon whether the rotor precession speed is greater or less than shaft speed $\omega$.

Assume the rotor deflection may be represented by

$$\delta_r(z) = \sum_{n=1}^{\infty} \delta_n \sin \frac{n\pi z}{L} \tag{A.8}$$

For the case of the single-mass rotor placed symmetrically along the shaft axis, then the rotor deflection may be approximated by the first mode.

The total radial and tangential force acting on the rotor mass is found by integrating the characteristics along the shaft to obtain

$$\left.\begin{aligned} F_r &= \int_0^L f_r dz = -\left(\frac{\pi}{L}\right)^3 [EI\delta_1 + \mu_i I\dot{\delta}_1] \\ F_\phi &= \left(\frac{\pi}{L}\right)^3 \mu_i I\delta_1(\dot{\phi} - \omega) \end{aligned}\right\} \tag{A.9}$$

where $\delta_1 = \delta_r =$ deflection of the rotor mass center.

Thus we can postulate a force system of the form

$$\vec{F} = K_r \vec{\delta} + C_i \frac{d^{R'}}{dt}(\vec{\delta}) \tag{A.10}$$

where:

$K_r =$ rotor stiffness characteristics $= \left(\frac{\pi}{L}\right)^3 EI$

$C_i =$ internal friction coefficient $= \left(\frac{\pi}{L}\right)^3 \mu_i I$

It is of interest to mention the work by Dr. Howland on rotor whirl in 1931.[35] Most of his article is devoted to an attempted explanation of the whirl instability observed by Newkirk and the theory postulated by Kimball on internal rotor friction as the cause of whirl. Howland concludes that –

> The results do not give support to Kimball's theory, and alternate explanations are suggested. No final conclusion is reached. A much more elaborate analysis appears to be needed before the conditions at speeds above $\Omega_1$ can be dealt with adequately.

Dr. Howland, in his analysis, assumes a stress-strain relationship of Filon and Jessop, and by assuming the usual Euler-Bernoulli assumptions arrives at the following simplified stress-strain relationship:

$$\sigma = E\frac{y}{\rho} + \mu y \frac{\partial}{\partial t}\left(\frac{1}{\rho}\right) \tag{A.11}$$

Since $y$ is much smaller than the radius of curvature $\rho$, the above relationship is equivalent to Eq. (A.1).

Howland, in his derivation, does not consider general precessive motion and hence does not arrive at the general form of the internal friction force as stated in Eq. (A.10). At this point he stops and concludes that although a normal shaft force is produced, as Kimball first suggested, "the force can act continuously—only if there is a steady force, such as the weight, to keep the shaft deflected—and the result is only a slight permanent change of deflection."

Howland is correct in one aspect; that is, an initial rotor deflection such as that caused by gravity or rotor unbalance is required to produce the internal friction force required to initiate the whirl motion.

Dr. Robertson presented a rebuttal to Howland's paper in the following year[35] in which he strongly refuted Howland's statements that internal rotor friction could not possibly cause shaft instability. Robertson states from experimental observation that—

> Any accidental disturbance of the shaft from its position of equilibrium under the action of the main whirling forces will produce a transient whirl which rotates at the critical speed. When the shaft speed is higher than this the elastic hysteresis gives a driving force maintaining this whirl, and if this force exceeds the friction opposing the transient whirl that transient will grow until the shaft strikes the stops.

These observations of Robertson are in substantial agreement with the statements by Newkirk in his paper on "Shaft Whipping."

Robertson, in his paper, draws strong objections to Howland's use of the Filon and Jessop relationship, since experimental measurements have shown that the internal friction force developed is independent of the velocity of strain. He concludes that such an approach would produce misleading results. Although Robertson is correct on this point, the use of the Filon and Jessop relationship does not incur serious limitations.

# Appendix B

# Analog Computer Circuits of Rotor Motion

## B.1 INTERNAL ROTOR FRICTION—LIGHT DAMPING

The approximate equations of motion for internal rotor friction are given by Eq. (4.17)

$$\frac{d^2X}{dt^2}=-(\mu_x+\nu_x)\frac{dX}{dt}-\omega\sqrt{\mu_x\mu_y}Y-\omega_{cx}^2X+\omega^2\cos\omega t$$

$$\frac{d^2Y}{dt^2}=-(\mu_y+\nu_y)\frac{dY}{dt}+\omega\sqrt{\mu_y\mu_x}X-\omega_{cx}^2Y+\omega^2\sin\omega t+g \qquad \text{(B.1)}$$

where $X$ and $Y$ are dimensionless with respect to $e_\mu$.

Let $t=\beta_t\tau$ and take the following scaling relationships:

$$\frac{d^2X}{d\tau^2}=\alpha_{32}e_{32} \qquad \frac{d^2Y}{d\tau^2}=\alpha_{34}e_{34}$$

$$\frac{dX}{d\tau}=-\alpha_{11}e_{12}=+\alpha_{11}e_{33} \qquad \frac{dY}{d\tau}=-\alpha_{13}e_{13}$$

$$X=\alpha_{12}e_{12}=-\alpha_{12}e_{31} \qquad Y=\alpha_{14}e_{14}$$

The analog equations of motion become

$$e_{32}=-P_{66}e_{33}-P_{24}e_{12}-P_{28}e_{14}+P_5e_3$$

$$e_{34}=-P_{62}e_{31}-P_{27}e_{14}-P_{70}e_{35}+P_3e_2$$

where

$$P_{66}=\beta_t(\mu_x+\nu_x)\frac{\alpha_{11}}{\alpha_{32}}; \qquad P_{27}=\beta_t^2\omega_{cy}^2\frac{\alpha_{14}}{\alpha_{34}}$$

$$P_{24}=\beta_t^2\omega_{cx}^2\frac{\alpha_{12}}{\alpha_{32}}; \qquad P_{70}=\beta_t(\mu_y+\nu_y)\frac{\alpha_{13}}{\alpha_{34}}$$

$$P_{28}=\beta_t^2\omega\sqrt{\mu_x\mu_y}\,\frac{\alpha_{14}}{\alpha_{32}};\qquad P_{62}=\beta_t^2\omega\sqrt{\mu_x\mu_y}\,\frac{\alpha_{12}}{\alpha_{34}}$$

$$P_5=0.1000;\qquad P_3=0.100$$

$$e_3=100\,p_6\cos\omega\beta_t\tau;\qquad e_2=100\,P_3\sin\omega\beta_t\tau$$

$$P_6=\frac{8\times10^{-8}}{\alpha_{32}}\omega^2\qquad P_2=P_4=0.2\omega\beta_t$$

For most of the cases run, the values of $\beta_t=1\times10^{-3}$ and $\alpha_{ij}=1.0$ were used.

Since a number of the potentiometers are frequency dependent, this requires changes in the pot setting with each speed change. Table B.1 represents the pot settings for a typical case study.

TABLE B.1.—*Rotor conditions*

| $M$-lb-sec$^2$/in. 0.25 | $K_2$-lb/in. 250 000 | $K$-lb/in. 250 000 | $K$-lb/in. 125 000 | $D_1$-rad/sec 200 | $D_2$-rad/sec 200 |
|---|---|---|---|---|---|
| Run | $\omega$ | $P_2$, $P_4$ | $P_6$ | $P_{28}$, $P_{62}$ | $P_3$, $P_5$ |
| 1 | 500 | 0.1000 | 0.0200 | 0.0167 | 0.1000 |
| 2 | 577 | .1154 | .0266 | .0192 | .1000 |
| 3 | 650 | .1300 | .0338 | .0217 | .1000 |
| 4 | 706 | .1412 | .0399 | .0236 | .1000 |
| 5 | 750 | .1500 | .0449 | .0250 | .1000 |
| 6 | 800 | .1600 | .0512 | .0267 | .1000 |
| 7 | 900 | .1800 | .0648 | .0300 | .1000 |
| 8 | 1000 | .2000 | .0800 | .0333 | .1000 |
| 9 | 1450 | .2900 | .1682 | .0483 | .1000 |
| 10 | 1500 | .3000 | .1800 | .0500 | .1000 |
| 11 | 2000 | .4000 | .3200 | .0666 | .1000 |
| 12 | 2500 | .5000 | .5000 | .0833 | .1000 |
| 13 | 3000 | .6000 | .7200 | .1000 | .1000 |
| 14 | 3200 | .6400 | .8190 | .1067 | .1000 |
| 15 | 3500 | .7000 | .9810 | .1167 | .1000 |

The analog computer circuit for this system is represented by Fig. B.1.

## B.2 EQUATIONS OF MOTION INCLUDING ROTOR NONLINEARITY

The equations of motion of this system are similar to the system of B.1, with the addition that nonlinear radial stiffness has been added and

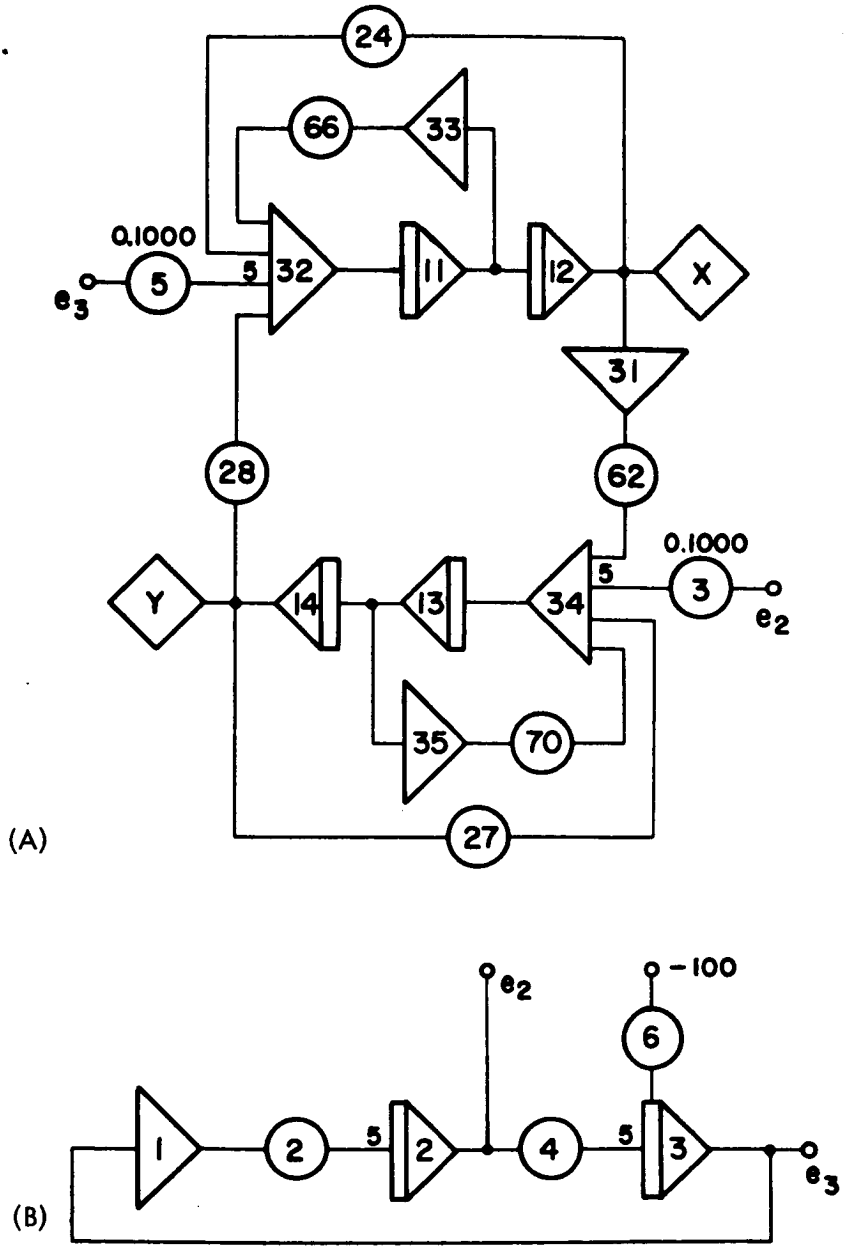


FIGURE B.1.—Analog computer program I. Equations of motion for light damping with internal rotor friction.

(A) Circuit for balanced rotor.

(B) Circuit for unbalanced rotor.

$e_3 = +100\, P_6 \cos \omega\beta\tau$

$e_2 = +100\, P_6 \sin \omega\beta\tau$

the rotor stiffness and damping coefficients may be speed dependent. These equations in general form are given by

$$\left.\begin{aligned}\frac{d^2X}{dt^2}&=-\left[C_x+\frac{D_x}{\omega}\right]\frac{dX}{dt}-\omega_x^2[1+\delta(X^2+Y^2)]X-\omega_{xy}^2Y+e_\mu\omega^2\cos\omega t\\ \frac{d^2Y}{dt^2}&=-\left[C_y+\frac{D_y}{\omega}\right]\frac{dY}{dt}-\omega_y^2[1+\delta(X^2+Y^2)]Y+\omega_y^2X+e_\mu\omega^2\sin\omega t\end{aligned}\right\}\quad(B.2)$$

**Scaling Relationships**

$$t=\beta_t\tau \qquad \therefore dt=\beta_t d\tau$$

$$\frac{d^2X}{dt^2}=\alpha_{24}e_{24}; \qquad \frac{d^2Y}{dt^2}=\alpha_{26}e_{26}$$

$$\frac{dX}{dt}=-\alpha_4e_4; \qquad \frac{dy}{dt}=-\alpha_6e_6$$

$$X=\alpha_5e_5; \qquad Y=\alpha_7e_7$$

Substituting the above into Eq. (B.2) results in

$$\left.\begin{aligned}e_{24}&=\frac{\alpha_4}{\alpha_{24}}\beta_t\left[C_x+\frac{D_x}{\omega}\right]e_4-\frac{\alpha_5}{\alpha_{24}}\beta_t^2\omega_x^2[1+\delta(\alpha_5^2e_5^2+\alpha_7^2e_7^2)]e_5\\ &\quad-\frac{\alpha_7}{\alpha_{24}}\beta_t^2\omega_{xy}^2e_7+\frac{e_\mu\omega^2\beta_t^2}{\alpha_{24}}\cos\omega\beta_t\tau\\ e_{26}&=\frac{\alpha_6}{\alpha_{26}}\beta_t\left[C_y+\frac{D_y}{\omega}\right]e_6-\frac{\alpha_7}{\alpha_{26}}\beta_t^2\omega_y^2[1+\delta(\alpha_5^2e_5^2+\alpha_7^2e_7^2)]e_7\\ &\quad+\frac{\alpha_5}{\alpha_{26}}\beta_t^2\omega_{yx}^2e_5+\frac{e_\mu\omega^2\beta_t}{\alpha_{26}}\cos\omega\beta_t\tau\end{aligned}\right\}\quad(B.3)$$

The circuit voltage equations are given by

$$\left.\begin{aligned}e_{24}&=P_8e_4-[25\ P_{21}P_{57}P_{59}+0.0125P_{21}P_{56}\ (e_5^2+e_7^2)]\ e_5-P_{22}e_7\\ &\quad+100\ P_{43}P_5\cos\omega\beta_t\tau\\ e_{26}&=P_{12}e_6-[25\ P_{23}P_{77}P_{78}+0.0125\ P_{23}P_{76}\ (e_5^2+e_7^2)]\ e_7+P_{20}e_5\\ &\quad+100\ P_{41}P_6\sin\omega\beta_t\tau\end{aligned}\right\}\quad(B.4)$$

**General Pot Formulas**

$$P_5=\frac{0.01\ e_\mu\omega^2\beta_t^2}{P_{41}\alpha_{26}} \qquad P_6=\frac{0.01\ e_\mu\omega^2\beta_t^2}{P_{43}\alpha_{24}}$$

$$P_8 = \frac{\alpha_4}{\alpha_{24}}\beta_t\left[C_x + \frac{\dot{D}_x}{\omega}\right]; \qquad P_{12} = \frac{\alpha_6}{\alpha_{26}}\beta_t\left[C_y + \frac{D_y}{\omega}\right]$$

$$P_{20} = \frac{\alpha_5}{\alpha_{26}}\beta_t^2\omega_{xy}^2; \qquad P_{22} = \frac{\alpha_7}{\alpha_{24}}\beta_t^2\omega_{yx}^2$$

$$P_{56} = \frac{\delta\alpha_5^3\beta_t^2\omega_x^2}{1.25\ \alpha_{24}P_{21}}; \qquad P_{76} = \frac{\delta\alpha_7^3\beta_t^2\omega_y^2}{1.25\ \alpha_{26}P_{23}}$$

$$P_{57} = \frac{\alpha_5\beta_t^2\omega_x^2}{25\ P_{21}P_{58}\alpha_{24}}; \qquad P_{77} = \frac{\alpha_7\beta_t^2\omega_y^2}{25\ P_{23}P_{78}\alpha_{26}}$$

$$P_{21} = P_{23} = 0.4000$$

$$P_{41} = P_{43} = 0.1000$$

$$P_{58} = P_{78} = 0.1000$$

The analog computer circuit which represents Eq. (B.2) is shown in Fig. B.2.

Example 1—*Internal Rotor Friction and Nonlinear Shaft Stiffness*

Consider the system represented by Eq. (4.46)

$$\left.\begin{aligned} \ddot{X} + D_f\dot{X} + k_f[1+\delta(X^2+Y^2)]X - SY &= e_\mu\omega^2\cos\omega t \\ \ddot{Y} + D_f\dot{Y} + k_f[1+\delta(X^2+Y^2)]Y - SX &= e_\mu\omega^2\sin\omega t \end{aligned}\right\} \tag{B.5}$$

where

$$D_f = \frac{D_2}{\left(1+\frac{K_2}{K_1}\right)^2}\left[1+\frac{K_2^2D_1}{K_1^2D_2}\right]$$

$$k_f = \omega_{CR}^2 = \frac{K_2K_1}{M(K_2+K_1)}; \qquad S = \omega D_2\left(\frac{K_1}{K_1+K_2}\right)^2$$

Consider the following operating conditions

$$M = 0.25 \text{ lb-sec}^2/\text{in.}$$

$$K_1 = K_2 = 250\,000 \text{ lb/in.}$$

$$D_1 = D_2 = 200 \text{ rad/sec}$$

$$e_\mu = 100 \times 10^{-6} \text{ in./in rotor unbalance}$$

$$\delta = 0.01 - 0.1$$

Let

$$\alpha_4 = 5.0 \qquad \alpha_7 = 1.0 \qquad \beta_t = 1 \times 10^{-3}$$

$$\alpha_5 = 1.0 \qquad \alpha_{24} = 5.0$$

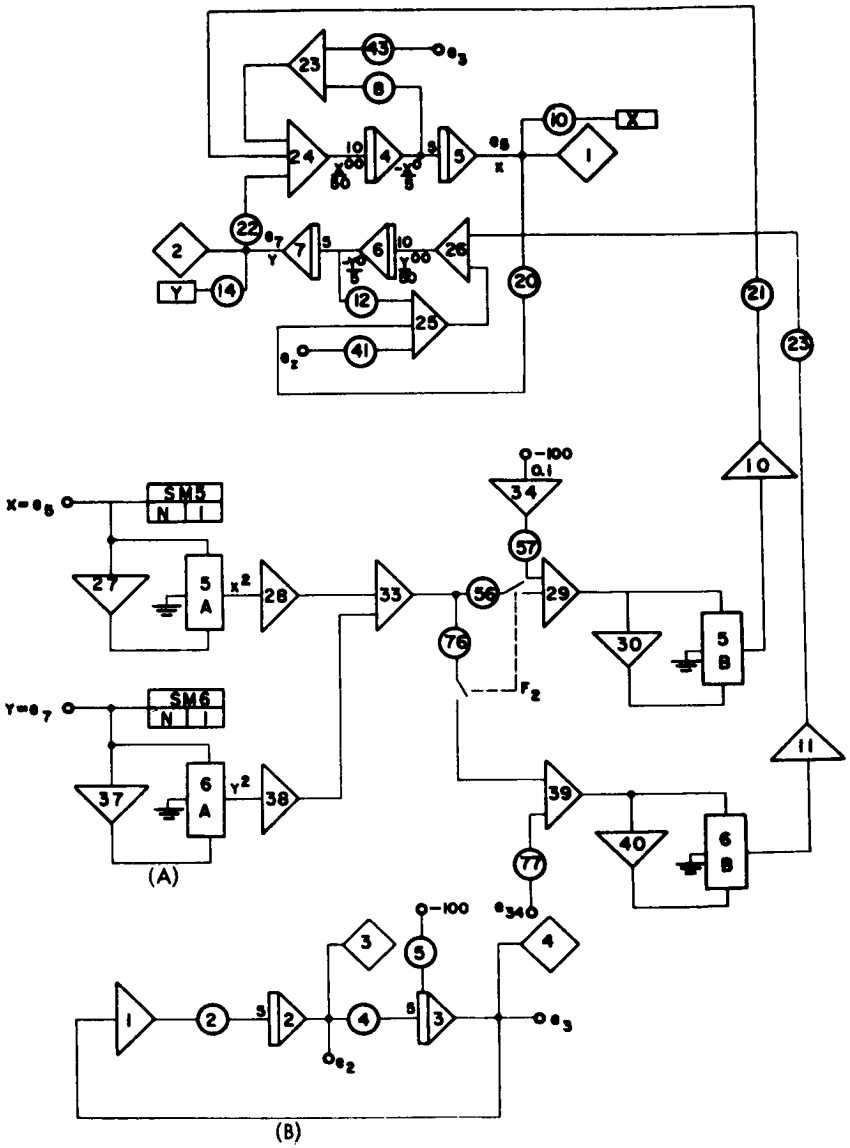


FIGURE B.2.—Analog computer program II. (A) Nonlinear circuit for balanced rotor. (B) Rotor unbalanced circuit.

$$\alpha_6 = 5.0 \qquad \alpha_{26} = 5.0$$

$$P_8 = P_{12} = \frac{\beta_t \alpha_6}{\alpha_{26}} D_f = 0.100$$

$$P_{20} = P_{22} = \frac{\alpha_5}{\alpha_{26}} \beta_f^2 S = 0.050(\omega \times 10^{-3})$$

$$P_{56} = P_{76} = \frac{\delta \alpha_5^3 \beta_f^2 k_f}{0.0125 \alpha_{24} P_{21}} = 3.65\delta$$

$$P_{57} = P_{77} = \frac{\alpha_5 \beta_f^2 k_f}{25 P_{21} P_{58} \alpha_{24}} = 0.707$$

Figure 19 of Sec. 4.7 is an example of the above circuit and shows the influence of small nonlinearity on the rotor motion at the threshold of stability.

## B.3 GENERAL EQUATIONS OF MOTION WITH INTERNAL ROTOR DAMPING

The general equations of motion of Sec. 4.9.2 are given by

$$\frac{d^2X_1}{dt^2} = -\frac{1}{1+\delta m} \frac{d^2X_2}{dt^2} - D_1 \frac{dX_1}{dt} - K_x X_1 + e_\mu \omega^2 \cos \omega t$$

$$\frac{d^2X_2}{dt^2} = -\frac{d^2X_1}{dt^2} - D_2 \frac{dX_2}{dt} - D_2 \omega Y_2 - K_2 X_2 + e_\mu \omega^2 \cos \omega t$$

$$\frac{d^2Y_1}{dt^2} = -\frac{1}{1+\delta m} \frac{d^2Y_2}{dt^2} - D_1 \frac{dY_1}{dt} - K_y Y_1 + e_\mu \omega^2 \sin \omega t$$

$$\frac{d^2Y_2}{dt^2} = -\frac{d^2Y_1}{dt^2} - D_2 \frac{dY_2}{dt} + D_2 \omega X_2 - K_2 Y_2 + e_\mu \omega^2 \sin \omega t \qquad \text{(B.6)}$$

Let

$$\frac{d^2X_1}{dt} = \alpha_{21} e_{21} \qquad \frac{d^2X_2}{dt^2} = \alpha_{24} e_{24}$$

$$\frac{dX_1}{dt} = -\alpha_4 e_4 \qquad \frac{dX_2}{dt} = -\alpha_6 e_6$$

$$X_1 = \alpha_5 e_5 \qquad X_2 = \alpha_7 e_7$$

$$\frac{d^2Y_1}{dt^2} = \alpha_{27} e_{27} \qquad \frac{d^2Y_2}{dt^2} = \alpha_{29} e_{29}$$

$$\frac{dY_1}{dt^2}=-\alpha_8 e_8 \qquad \frac{dY_2}{dt}=-\alpha_{10} e_{10}$$

$$Y_1=\alpha_9 e_9 \qquad Y_2=\alpha_{11} e_{11}$$

and $t=\beta_t \tau$.

Substitution of the above into the Eqs. (B.6) results in

$$e_{21}=-\frac{\alpha_{24}}{\alpha_{21}}\cdot\frac{1}{1+\delta m}\,e_{24}-\beta_t^2\frac{\alpha_5}{\alpha_{21}}\,\frac{K}{1+\delta m}\,e_5+\beta_t\frac{\alpha_4}{\alpha_{21}}\frac{D_1}{1+\delta m}\,e_4$$
$$+\frac{\beta^2}{\alpha_{21}}\frac{e_\mu\omega^2}{1+\delta m}\cos\omega\beta_t\tau$$

$$e_{24}=-\frac{\alpha_{21}}{\alpha_{24}}\,e_{21}-\beta_t^2\frac{\alpha_{11}}{\alpha_{24}}\,D_2\omega e_{11}-\beta_t^2\frac{\alpha_7}{\alpha_{24}}\,K_2 e_7+\beta_t\frac{\alpha_6}{\alpha_{24}}\,D_2 e_6$$
$$+\frac{\beta_t^2}{\alpha_{24}}\,e_\mu\omega^2\cos\omega\beta_t\tau$$

$$e_{27}=-\frac{\alpha_{29}}{\alpha_{27}}\cdot\frac{1}{1+\delta m}\,e_{29}-\beta_t^2\frac{\alpha_9}{\alpha_{27}}\,\frac{K}{1+\delta m}\,e_9+\beta_t\frac{\alpha_8}{\alpha_{27}}\,\frac{D_1}{1+\delta m}\,e_8$$
$$+\frac{\beta_t^2}{\alpha_{27}}\cdot\frac{e_\mu\omega^2}{1+\delta m}\sin\omega\beta_t\tau$$

$$e_{29}=-\frac{\alpha_{27}}{\alpha_{29}}\,e_{27}-\beta_t^2\frac{\alpha_{11}}{\alpha_{29}}\,K_2 e_{11}+\beta_t\frac{\alpha_{10}}{\alpha_{29}}\,D_2 e_{10}+\beta_t^2\frac{\alpha_7}{\alpha_{29}}\,D_2\omega e_7$$
$$+\frac{\beta_t^2}{\alpha_{29}}\,e_\mu\omega^2\sin\omega\beta_t\tau \qquad \text{(B.7)}$$

Let all $\alpha$'s be equal to 1 and $\beta_t=0.001$; then

$$e_{21}=-\frac{1}{1+\delta m}\,e_{24}-\frac{1\times10^{-6}K_x}{1+\delta m}\,e_5+\frac{1\times10^{-3}D_1}{1+\delta m}\,e_4$$
$$+\frac{1\times10^{-6}e_\mu\omega^2}{1+\delta m}\cos\omega\beta_t\tau$$

$$e_{24}=-e_{21}-1\times10^{-6}D_2\omega e_{11}-1\times10^{-6}K_2 e_7+1\times10^{-3}D_2 e_6$$
$$+1\times10^{-6}e_\mu\omega^2\cos\beta_t\tau$$

$$e_{27}=-\frac{1}{1+\delta m}\,e_{29}-\frac{1\times10^{-6}K_y}{1+\delta m}\,e_9+\frac{1\times10^{-3}D_1}{1+\delta m}\,e_8$$

$$+\frac{1\times10^{-6}e_\mu\omega^2}{1+\delta m}\sin\omega\beta_t\tau$$

$$e_{29}=-e_{27}-1\times10^{-6}K_2e_{11}+1\times10^{-3}D_2e_{10}+1\times10^{-6}D_2\omega e_7$$

$$+1\times10^{-6}e_\mu\omega^2\sin\omega\beta_t\tau \qquad \text{(B.8)}$$

$$e_{21}=-P_{48}e_{24}-P_{10}e_5+P_8e_4+100P_6P_{41}\cos\omega\beta_t\tau$$

$$e_{24}=-5P_{42}e_{21}-P_{21}e_{11}-P_{14}e_7+P_{12}e_6+100P_6P_{43}\cos\omega\beta_t\tau$$

$$e_{27}=-P_{58}e_{29}-P_{18}e_9+P_{16}e_8+100P_6P_{45}\sin\omega\beta_t\tau$$

$$e_{29}=-e_{27}-P_{22}e_{11}+P_{20}e_{10}+P_{13}e_7+100P_6P_{47}\sin\omega\beta_t\tau \qquad \text{(B.9)}$$

The analog computer circuit which represents the system of Eqs. (B.9) is shown in Fig. B.3.

**General Pot Formulas**

$$P_2=P_4=0.0002\omega$$

$$P_8=P_{16}=\frac{1\times10^{-3}D_1}{1\times\delta m}$$

$$P_{10}=\frac{1\times10^{-6}K_x}{(1+\delta m)};\qquad P_{18}=\frac{1\times10^{-6}K_y}{(1\times\delta m)}$$

$$P_{12}=P_{20}=1\times10^{-3}D_2$$

$$P_{13}=P_{21}=1\times10^{-6}D_2\omega$$

$$P_{14}=P_{22}=1\times10^{-6}K_2$$

$$P_{41}=P_{45}=\frac{0.1250}{1+\delta m}$$

$$P_{43}=P_{47}=0.1250$$

$$P_{48}=P_{58}=\frac{1}{(1+\delta m)}$$

$$P_{42}=P_{52}=0.2000$$

219-720 O-66—12

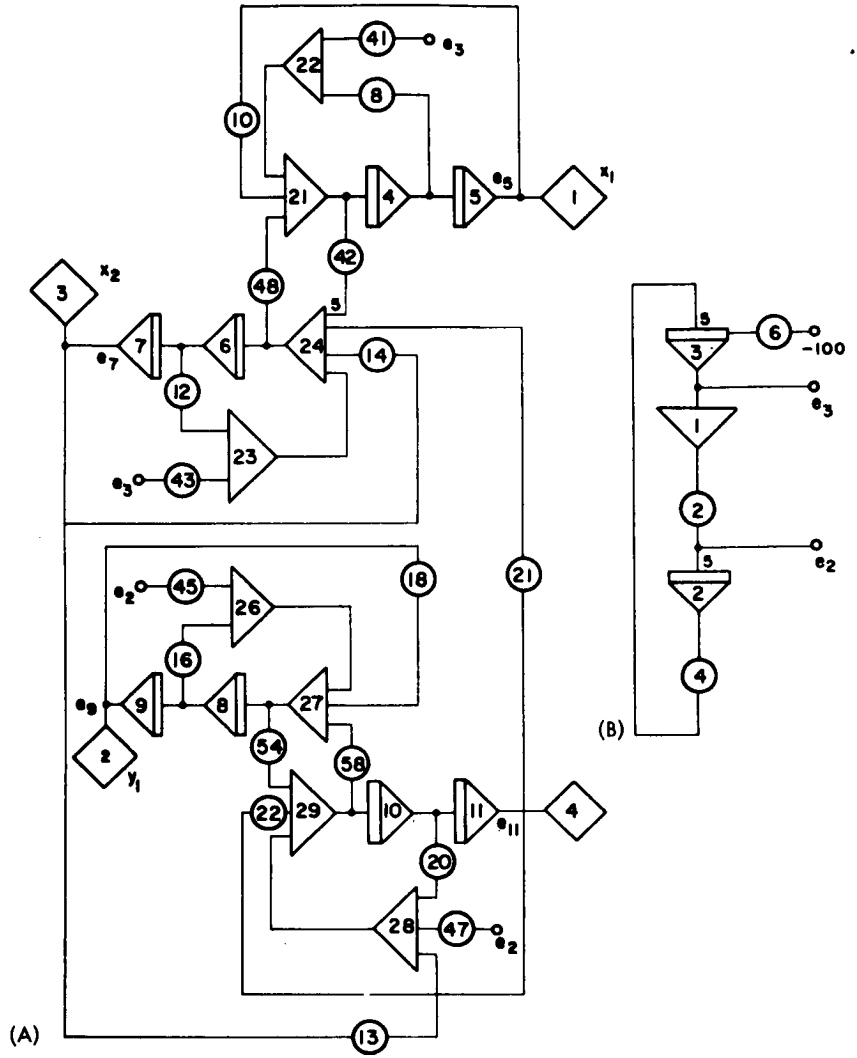


FIGURE B.3.—Analog computer program III. General equations of motion with internal rotor damping.

(A) Circuit for balanced rotor.

(B) Circuit for unbalanced rotor.

$e_3 = +100\ P_6 \cos \omega\beta_i\tau$

$e_2 = +100\ P_6 \sin \omega\beta_i\tau$

# Appendix C

# Digital Computer Program of Stability Analysis Using the Routh Method

AUTOMATH SYSTEM 02/10/65

* * * SOURCE PROGRAM LISTING * * *

```
TITLE  STABLE                                                          100
      DIMENSION  RR(20),DD2(10),ALPHA(30),D1(10),OMEGA(25,10),WCX(25),
     1 D(10)
C         STABILITY ANALYSIS OF GENERAL EIGHT ORDER SYSTEM USING THE     2
C        ROUTH  METHOD -  FOUR DEGREE OF FREEDOM SYSTEM                 3
C        PROGRAMED   BY E.J.GUNTER       RUN NO.9
   10 READ 11,KLUE                                                      5      1
   11 FORMAT (I1)                                                       6      2
      GO TO (20,500),KLUE                                               7      3
   20 READ 21,NR,(RR(II),II=1,NR)                                       8      4
   21 FORMAT(I2/(8F10.3))                                               9      5
C     NUMBER OF R VALUES NR FOLLOWS THE KLUE CARD AND THE R VALUES ARE  10
C     GIVEN ON THE NEXT CARD WITH  8 FIELDS OF 10.3                     11
      READ 21,ND2,(DD2(JJ),JJ=1,ND2)                                    12     6
C
      READ 21,NA,(ALPHA(I),I=1,NA)                                      13     7
C
      READ 21,ND1,(D1(J),J=1,ND1)                                       14     8
C
      DO 70 JJ =1,ND2                                                   15     9
      D2 =DD2(JJ)                                                       16     10
      DO 60 II =1,NR                                                    17     11
       R =RR(II)                                                        18     12
      WCY =SQRTF(1.0/(1.0+6))                                           19     13
       WCRO=1000.0                                                             14
       AK2  =WCRO**2                                                           15
      PRINT 190                                                         191    16
  190 FORMAT(1H1// 30B,32H DATA OUTPUT  STABILITY ANALYSIS//)                    17
      PRINT 191 ,D2,R,WCY                                               191    18
  191 FORMAT(1HO,25H ENTER DO LOOP 60    D2 =F10.3, 5H R = F10.3, 7H WCY  192    19
     1 = F10.3)
      DO 40 I=1,NA                                                      20     20
      DO 40 J=1,ND1                                                     21     21
      PRINT 211, D2,D1(J),R,WCY,I,J  ,ALPHA(I)                          2100   22
  211 FORMAT(1HO,23H ENTER DO LOOP 40  D2 =F8.2,4B, 5H D1 =F8.2,3B, 4H R 2110   23
     1 =F8.3,4B, 6H WCY = F7.3,4H  I=I2,4H  J=I2,4B,8HALPHA =  F7.3/)
      KOUNT =1                                                          22     24
      KEY   =1                                                          23     25
      WP =0.0                                                           24     26
      W = 1000.0                                                               27
```

```
      EPS =0.01                                                          26    28
  100 KOUNT =KOUNT+1                                                     27    29
      IF(KOUNT- 20) 101,101,102                                          28    30
  102 PRINT 103,W,R,D2,D1(J),ALPHA(I)                                    29    31
  103 FORMAT(1H0//4B,15HKOUNT =20   W =E10.3,4B,3HR =F6.2,4B,5H D2 =F6.1 30    32
     1 ,6B, 6H D1 = F7.2, 6B,8H ALPHA = F6.2 //)                         31
      GO TO 200                                                          32    33
  101 CONTINUE                                                           33    34
      WCX(I) =SQRTF(ALPHA(I)/(R+ALPHA(I)))                               34    35
C         ZERO BEARING MASS IS NOW SPECIFIED                             35
      DM =0.0                                                            36    36
C                                                                        37
C     FOR 8 DEGREE EQUATION ADD IF BRANCH HERE                           38
      AKY =  AK2/R                                                       41    37
      AKX =  ALPHA(I)*AKY                                                42    38
      A   =  WCRO/D2                                                     43    39
      IF(D1(J)) 90,90,95                                                431    40
   95 D(J) =D2/D1(J)                                                    432    41
   90 CONTINUE                                                          44    42
      T1 = D1(J) +D2                                                   4500    43
      T2 = AKX + AKY                                                   4600    44
      T3 = 2.0 *D1(J)*D2                                               4700    45
      T4 = D1(J)*D1(J)                                                 4800    46
      T5 = D2 * D2                                                     4900    47
      T6 =  T4*T5                                                      5000    48
      T7 =   T5*W*W                                                    5100    49
      T8 =   AK2*AK2                                                   5200    50
      T9 = AKX*AKY                                                     5500    51
      A6 = T1*T1                                                       5300    52
C
      A5 = ( D1(J)-D2)*( T2-2.0*AK2) +4.0*D1(J)*AK2+2.0*D2*T2+ T3*T1   5400    53
C
      A4 = T8 +AK2*T2 +T9 +T5*(W*W +T2)+T3*(2.0*AK2+T2)+2.*T4*AK2+T4*T5 5600    54
C
      A3 = 2.0*D1(J)*T7 +2.0*(D1(J)*T8+D2*T9)+T2*(2.0*AK2*T1+D1(J)*T5)+ 5700    55
     1 2.0*T4*D2*AK2                                                    5800
C
      A2 = T7*(T2+T4)+2.0*AK2*T9+ T8*T2 +T4*T8+T5*T9 +T3*T2*AK2        5900    56
C
      A1 = T7*D1(J)*T2 + D1(J)*T2*T8 +2.0*D2*AK2*T9                    6000    57
C                                                                        50
      A0 = T7*T9 + T9*T8                                               6100    58
      AA5 =A5/A6                                                       6200    59
```

```
      AA4 =A4/A6                                                        6300   60
      AA3 =A3/A6                                                        6400   61
      AA2 =A2/A6                                                        6500   62
      AA1 =A1/A6                                                        6600   63
      AA0 =A0/A6                                                        6700   64
      PRINT 651 ,A6,A5,A4,A3,A2,A1,A0,W,KOUNT                                  65
  651 FORMAT(1HO,5H A6 =E10.3,4H A5=E10.3,4H A4=E10.3,4H A3=E10.3,4H A2=       66
     1 E10.3,5H  A1=E10.3,5H  A0=E10.3 /4H  W=E11.4,20B, 7HKOUNT = I2/)     6701
      IF(A6) 120,104,104                                                66   67
  104 CONTINUE                                                          67   68
      IF(A5) 120,105,105                                                68   69
  105 C1 = AA4 -AA3/AA5                                                 6900   70
      C2 = (AA2 -AA1/AA5)/C1                                            6910   71
      C3 = (AA0 )/ C1                                                   6920   72
      PRINT 691 ,C1,C2,C3                                               6930   73
  691 FORMAT(1H ,6H C1 = E15.8,15B,4HC2 = E15.8,15B,4HC3 = E15.8)       6940   74
      IF(C1)120,106,106                                                 70   75
  106 CONTINUE                                                          7100   76
      D11= AA3 -C2*AA5                                                  7200   77
      D22 = (AA1-AA5*C3)/D11                                            7210   78
      PRINT 721,D11,D22                                                 7220   79
  721 FORMAT(1H ,6H D11 = E15.8,15B,5HD22 = E15.8)                      7230   80
  771 FORMAT(1H , 5H F1 =E15.8)                                              81
      IF(D11) 120,107,107                                               73   82
  107 CONTINUE                                                          7400   83
      E1 =  C2 -D22                                                     7500   84
      E2 = C3 /F1                                                       7520   85
      PRINT 751, E1,E2                                                  7530   86
  751 FORMAT(1H ,5H E1 = E15.8,15B,5HE2 = E15.8 )                       7540   87
      IF(E1) 120,108,108                                                76   88
  108 CONTINUE                                                          7700   89
      F1 = D22-E2                                                       7720   90
       PRINT 771   ,F1                                                       91
      G1 =  E2                                                          7800   92
      PRINT 775,G1                                                      7810   93
      IF(F1) 120,110,110                                                78   94
  110 IF(G1) 120,112,112                                                7900   95
  775 FORMAT(1H ,5H G1 =E15.8//)                                        7820   96
  112  GO TO (132,134),KEY                                              80   97
  132 WP =W                                                             81   98
      W = 1.2*W                                                         82   99
      WCROA =1000.0                                                     83  100
      IF(W/WCROA -100.0)130,202,202                                     84  101
```

```
  130 GO TO 100                                                          85      102
  134 WP = W                                                             86      103
      W = (WP+WN)/2.0                                                    87      104
       TEST = SQRTF((W-WP)**2)/W                                    88           105
      PRINT 881,W,WP,WN,KOUNT,TEST                                           106
      GO TO 140                                                          89      107
  140 IF(TEST-EPS) 200,200,100                                           90      108
C                                                                        91
  120 KEY = 2                                                            92      109
      WN  = W                                                            93      110
      W =(WN+WP)/2.0                                                     94      111
       TEST = SQRTF((W-WN)**2)/W                                    95           112
      PRINT 881,W,WP,WN,KOUNT,TEST                                           113
  881 FORMAT(1HO,4H W =E12.4,4B,5H WP =E12.4,5B,5H WN =E12.4,20B,7HKOUNT    9520  114
     1 = I2,5B,7H TEST =E12.4/)                                            9530
      GO TO 140                                                          96      115
C                                                                        97
  202 PRINT 203 ,W,DM,R,D2,D1(J),ALPHA(I)                                98      116
  203 FORMAT(/55H  THE SYSTEM IS STABLE FOR THE ROTOR CONDITIONS OF W =   100     117
     1E10.3, 5HDM = F6.2,13H  R = K2/KY =F6.2, 6H D2 = F6.1 /4H D1=F6.1,  101
     2 7H ALPHA=F6.2///)                                                 102
       OMEGA(I,J) = 99.99                                          1021        118
      GO TO 40                                                           103     119
C                                                                        104
  200 OMEGA(I,J)=W /WCRO                                                 105     120
   40 CONTINUE                                                           106     121
      PRINT 300                                                          107     122
  300 FORMAT(1H1)                                                        108     123
  310 PRINT 311                                                          109     124
  311 FORMAT(1H ,18B,84HGENERAL STABILITY OF A ROTOR ON AN ELASTIC FOUND  110     125
     1ATION WITH INTERNAL FRICTION DAMPING //)                           111
  312 PRINT 313 ,DM,R,A,WCY                                              112     126
  313 FORMAT(1HO,12HDM = M1/M2 =F6.2,10B,11HR = K2/KY =F6.2,10B,13HA = W  113     127
     1CRO/D2 =F7.2,10B,10HWCY/WCRO =F6.3,6B, 9HD = D2/D1)                114
  314 PRINT 315                                                          115     128
  315 FORMAT(1HO ,115HALPHA   WCX/WCRO      D1=0.00     D =100.0   D = 10.0  116     129
     1   D = 5.0     D = 2.0     D = 1.0     D = 0.5     D = 0.20   D =0.10)  117
      DO 350   I=1,NA                                                    118     130
      PRINT 320,ALPHA(I),WCX(I),( OMEGA(I,J),J=1,ND1)                119     131
  320 FORMAT(1HO,F6.2,1B,F6.3,4B,9(F10.4,1B))                             120     132
  350 CONTINUE                                                           121     133
      PRINT  300                                                         12101   134
      PRINT  311                                                         12102   135
      PRINT  313 ,DM,R,A,WCY                                             12103   136
      PRINT  360 , (D(J),J=2,ND1)                                        12104   137
  360 FORMAT (1HO ,31HALPHA   WCX/WCRO      D1=0.00     , 3( 2HD=  F6.1,2B)  12105   138
```

```
     1 , 6( 3HD =F6.3,2B))                                          12106
       DO 370    I =1,NA                                           12107   139
370 PRINT 365 ,ALPHA(I),WCX(I), (OMEGA(I,J),J=1,ND1)               12108   140
365 FORMAT (1HO,F6.2,1X,F6.3,6X,9(E11.4     ))                             141
 60 CONTINUE                                                       122     142
 70 CONTINUE                                                       123     143
500 PRINT 600                                                      1251    144
600 FORMAT(1H1///20B,11H END OF RUN/1H1//)                                 145
      STOP                                                         1253    146
      END                                                          126     147
```

DATA OUTPUT STABILITY ANALYSIS

ENTER DO LOOP 60 D2 = 200.000 R = 1.000 WCY = 0.707 $W_S = 21840\Omega$, $W_S = 2{,}390$ approx.

ENTER DO LOOP 40 D2 = 200.00 D1 = 0.00 R = 1.000 WCY = 0.707 I= 1 J= 1 ALPHA = 0.500

A6 = 0.400E 05 A5= 0.700E 09 A4= 0.310E 13 A3= 0.800E 15 A2= 0.258E 19 A1= 0.200E 21 A0= 0.520E 24

W= 0.1000E 04 KOUNT = 2

C1 = 0.76357143E 08 C2 = 0.84097287E 06 C3 = 0.17025257E 12
D11 = 0.52829748E 10 D22 = 0.38247012E 06
E1 = 0.45850276E 06 E2 = 0.37132290E 06
F1 = 0.11147219E 05
G1 = 0.37132290E 06

A6 = 0.400E 05 A5= 0.700E 09 A4= 0.312E 13 A3= 0.800E 15 A2= 0.261E 19 A1= 0.200E 21 A0= 0.529E 24

W= 0.1200E 04 KOUNT = 3

C1 = 0.76797143E 08 C2 = 0.84474869E 06 C3 = 0.17214182E 12
D11 = 0.52168980E 10 D22 = 0.38097700E 06
E1 = 0.46377169E 06 E2 = 0.37117794E 06
F1 = 0.97990610E 04
G1 = 0.37117794E 06

A6 = 0.400E 05 A5= 0.700E 09 A4= 0.314E 13 A3= 0.800E 15 A2= 0.264E 19 A1= 0.200E 21 A0= 0.541E 24

W= 0.1440E 04 KOUNT = 4

C1 = 0.77430743E 08 C2 = 0.85011048E 06 C3 = 0.17482462E 12
D11 = 0.51230667E 10 D22 = 0.37879054E 06
E1 = 0.47131994E 06 E2 = 0.37092557E 06
F1 = 0.78649690E 04
G1 = 0.37092557E 06

A6 = 0.400E 05 A5= 0.700E 09 A4= 0.318E 13 A3= 0.800E 15 A2= 0.270E 19 A1= 0.200E 21 A0= 0.560E 24

```
W= 0.1728E 04                    KOUNT = 5

C1 =  0.78343127E 08               C2 = 0.85767909E 06              C3 = 0.17861161E 12
D11 = 0.49906160E 10               D22 = 0.37556423E 06
E1 = 0.48211486E 06                E2 =  0.37047522E 06
F1 = 0.50890100E 04
G1 = 0.37047522E 06

A6 = 0.400E 05 A5= 0.700E 09 A4= 0.323E 13 A3= 0.800E 15 A2= 0.278E 19  A1= 0.200E 21  A0= 0.586E 24

W= 0.2074E 04                    KOUNT = 6

C1 =  0.79656960E 08               C2 = 0.86827330E 06              C3 = 0.18391247E 12
D11 = 0.48052174E 10               D22 = 0.37074946E 06
E1 = 0.49752384E 06                F2 =  0.36965560E 06
F1 = 0.10938600E 04
G1 = 0.36965560E 06

A6 = 0.400E 05 A5= 0.700E 09 A4= 0.331E 13 A3= 0.800E 15 A2= 0.289E 19  A1= 0.200E 21  A0= 0.624E 24

W= 0.2488E 04                    KOUNT = 7

C1 =  0.81548879E 08               C2 = 0.88292925E 06              C3 = 0.19124565E 12
D11 = 0.45487383E 10               D22 = 0.36344170E 06
E1 = 0.51948755E 06                E2 =  0.36814289E 06
F1 =-0.47011910E 04
G1 = 0.36814289E 06

W =  0.2281E 04     WP =  0.2074E 04     WN =  0.2488E 04                KOUNT = 7     TEST =  0.9091E-01

A6 = 0.400E 05 A5= 0.700E 09 A4= 0.327E 13 A3= 0.800E 15 A2= 0.283E 19  A1= 0.200E 21  A0= 0.604E 24

W= 0.2281E 04                    KOUNT = 8

C1 =  0.80559921E 08               C2 = 0.87535405E 06              C3 = 0.18745536E 12
D11 = 0.46813042E 10               D22 = 0.36731883E 06
E1 = 0.50803522E 06                E2 =  0.36898104E 06
F1 =-0.16622040E 04
G1 = 0.36898104E 06
```

```
W =  0.2177E 04      WP =  0.2074E 04      WN =  0.2281E 04                    KOUNT = 8       TEST =  0.4762E-01

A6 = 0.400E 05 A5= 0.700E 09 A4= 0.325E 13 A3= 0.800E 15 A2= 0.280E 19  A1= 0.200E 21  A0= 0.595E 24

W= 0.2177E 04                      KOUNT = 9

C1 =  0.80097691E 08                 C2 = 0.87174933E 06              C3 = 0.18565172E 12
D11 = 0.47443869E 10                 D22 = 0.36908772E 06
E1 = 0.50266161E 06                  E2 =  0.36933737E 06
F1 =-0.24965500E 03
G1 = 0.36933737E 06

W =  0.2125E 04      WP =  0.2074E 04      WN =  0.2177E 04                    KOUNT = 9       TEST =  0.2439E-01

A6 = 0.400E 05 A5= 0.700E 09 A4= 0.324E 13 A3= 0.800E 15 A2= 0.279E 19  A1= 0.200E 21  A0= 0.590E 24

W= 0.2125E 04                      KOUNT =10

C1 =  0.79874638E 08                 C2 = 0.86999491E 06              C3 = 0.18477389E 12
D11 = 0.47750891E 10                 D22 = 0.36993173E 06
E1 = 0.50006319E 06                  E2 =  0.36950108E 06
F1 = 0.43064200E 03
G1 = 0.36950108E 06

W =  0.2151E 04      WP =  0.2125E 04      WN =  0.2177E 04                    KOUNT =10       TEST =  0.1205E-01

D11 = 0.47471993E 10                 D22 = 0.53247216E 06
E1 = 0.42022541E 06                  E2 =  0.52748505E 06
F1 = 0.49871040E 04
G1 = 0.52748505E 06

A6 = 0.160E 06 A5= 0.143E 10 A4= 0.449E 13 A3= 0.225E 16 A2= 0.432E 19  A1= 0.819E 21  A0= 0.103E 25

W= 0.5160E 04                      KOUNT =11

C1 =  0.26466830E 08                 C2 = 0.99852235E 06              C3 = 0.24381147E 12
```

```
D11 = 0.51505584E 10              D22 = 0.57074148E 06
E1 = 0.42778086E 06               E2 =  0.56994478E 06
F1 = 0.79670300E 03
G1 = 0.56994478E 06

A6 = 0.160E 06 A5= 0.143E 10 A4= 0.496E 13 A3= 0.244E 16 A2= 0.504E 19  A1= 0.960E 21  A0= 0.127E 25

W= 0.6192E 04                     KOUNT =12

C1 =  0.29264511E 08              C2 = 0.10538208E 07              C3 = 0.27053929E 12
D11 = 0.58270641E 10              D22 = 0.61420181E 06
E1 = 0.43961895E 06               E2 =  0.61539497E 06
F1 =-0.11931550E 04
G1 = 0.61539497E 06

W =  0.5676E 04     WP =  0.5160E 04     WN =  0.6192E 04                  KOUNT =12      TEST =  0.9091E-01

A6 = 0.160E 06 A5= 0.143E 10 A4= 0.471E 13 A3= 0.234E 16 A2= 0.466E 19  A1= 0.887E 21  A0= 0.114E 25

W= 0.5676E 04                     KOUNT =13

C1 =  0.27802086E 08              C2 = 0.10263030E 07              C3 = 0.25723893E 12
D11 = 0.54610110E 10              D22 = 0.59307315E 06
E1 = 0.43322989E 06               E2 =  0.59377005E 06
F1 =-0.69690100E 03
G1 = 0.59377005E 06

W =  0.5418E 04     WP =  0.5160E 04     WN =  0.5676E 04                  KOUNT =13      TEST =  0.4762E-01

A6 = 0.160E 06 A5= 0.143E 10 A4= 0.460E 13 A3= 0.230E 16 A2= 0.449E 19  A1= 0.852E 21  A0= 0.109E 25

W= 0.5418E 04                     KOUNT =14

C1 =  0.27118562E 08              C2 = 0.10124237E 07              C3 = 0.25053054E 12
D11 = 0.52990300E 10              D22 = 0.58202510E 06
E1 = 0.43039864E 06               E2 =  0.58208953E 06
F1 =-0.64427000E 02
```

```
G1 = 0.58208953E 06

W =  0.5289E 04     WP =  0.5160E 04     WN =  0.5418E 04                    KOUNT =14     TEST =  0.2439E-01

A6 = 0.160E 06 A5= 0.143E 10 A4= 0.454E 13 A3= 0.228E 16 A2= 0.440E 19  A1= 0.836E 21  A0= 0.106E 25

ENTER DO LOOP 40  D2 =  200.00     D1 =  200.00     R =   1.000     WCY =  0.707  I= 1  J= 6     ALPHA :   0.500

A6 = 0.160E 06 A5= 0.143E 10 A4= 0.346E 13 A3= 0.184E 16 A2= 0.274E 19  A1= 0.512E 21  A0= 0.520E 24

W= 0.1000E 04                    KOUNT = 2

C1 =  0.20347291E 08              C2 = 0.82455490E 06              C3 = 0.15972643E 12
D11 = 0.41452337E 10              D22 = 0.42710463E 06
E1 = 0.39745027E 06               E2 =  0.40187776E 06
F1 = 0.25226870E 05
G1 = 0.40187776E 06

A6 = 0.160E 06 A5= 0.143E 10 A4= 0.348E 13 A3= 0.185E 16 A2= 0.277E 19  A1= 0.517E 21  A0= 0.529E 24

W= 0.1200E 04                    KOUNT = 3

C1 =  0.20452374E 08              C2 = 0.82842073E 06              C3 = 0.16159493E 12
D11 = 0.41546345E 10              D22 = 0.43005597E 06
E1 = 0.39836476E 06               E2 =  0.40564564E 06
F1 = 0.24410331E 05
G1 = 0.40564564E 06

A6 = 0.160E 06 A5= 0.143E 10 A4= 0.350E 13 A3= 0.186E 16 A2= 0.281E 19  A1= 0.525E 21  A0= 0.541E 24

W= 0.1440E 04                    KOUNT = 4

C1 =  0.20603695E 08              C2 = 0.83391826E 06              C3 = 0.16425209E 12
D11 = 0.41687916E 10              D22 = 0.43428983E 06
E1 = 0.39962843E 06               E2 =  0.41101202E 06
F1 = 0.23277804E 05
G1 = 0.41101202E 06
```

```
A6 = 0.160E 06 A5= 0.143E 10 A4= 0.354E 13 A3= 0.188E 16 A2= 0.286E 19  A1= 0.536E 21  A0= 0.560E 24

W= 0.1728E 04                    KOUNT = 5

C1 =  0.20821597E 08               C2 = 0.84169431E 06              C3 = 0.16801055E 12
D11 = 0.41904343E 10               D22 = 0.44034919E 06
E1 = 0.40134512E 06                E2 =  0.41861865E 06
F1 = 0.21730541E 05
G1 = 0.41861865E 06


A6 = 0.160E 06 A5= 0.143E 10 A4= 0.359E 13 A3= 0.190E 16 A2= 0.294E 19  A1= 0.552E 21  A0= 0.586E 24

W= 0.2074E 04                    KOUNT = 6

C1 =  0.21135375E 08               C2 = 0.85261016E 06              C3 = 0.17328659E 12
D11 = 0.42241207E 10               D22 = 0.44898605E 06
E1 = 0.40362411E 06                E2 =  0.42932666E 06
F1 = 0.19659391E 05
G1 = 0.42932666E 06


A6 = 0.160E 06 A5= 0.143E 10 A4= 0.367E 13 A3= 0.193E 16 A2= 0.306E 19  A1= 0.574E 21  A0= 0.624E 24

W= 0.2488E 04                    KOUNT = 7

C1 =  0.21587216E 08               C2 = 0.86777147E 06              C3 = 0.18061463E 12
D11 = 0.42776190E 10               D22 = 0.46120968E 06
E1 = 0.40656179E 06                E2 =  0.44424890E 06
F1 = 0.16960784E 05
G1 = 0.44424890E 06


A6 = 0.160E 06 A5= 0.143E 10 A4= 0.378E 13 A3= 0.197E 16 A2= 0.323E 19  A1= 0.607E 21  A0= 0.678E 24

W= 0.2986E 04                    KOUNT = 8

C1 =  0.22237868E 08               C2 = 0.88852138E 06              C3 = 0.19064384E 12
D11 = 0.43643437E 10               D22 = 0.47829531E 06
E1 = 0.41022607E 06                E2 =  0.46472874E 06
F1 = 0.13566571E 05
G1 = 0.46472874E 06
```

```
A6 = 0.160E 06 A5= 0.143E 10 A4= 0.394E 13 A3= 0.203E 16 A2= 0.347E 19  A1= 0.654E 21  A0= 0.757E 24

W= 0.3583E 04                    KOUNT = 9

C1 =  0.23174805E 08               C2 = 0.91635433E 06              C3 = 0.20409656E 12
D11 = 0.45075472E 10               D22 = 0.50166410E 06
E1 = 0.41469022E 06                E2 =  0.49216632E 06
F1 = 0.94977840E 04
G1 = 0.49216632E 06


A6 = 0.160E 06 A5= 0.143E 10 A4= 0.416E 13 A3= 0.212E 16 A2= 0.382E 19  A1= 0.722E 21  A0= 0.870E 24

W= 0.4300E 04                    KOUNT =10

C1 =  0.24523996E 08               C2 = 0.95269757E 06              C3 = 0.22166262E 12
```

GENERAL STABILITY OF A ROTOR ON AN ELASTIC FOUNDATION WITH INTERNAL FRICTION DAMPING

| DM = M1/M2 = 0. | | R = K2/KY = 0.10 | | | A = WCRO/D2 = 1.00 | | | WCY/WCRO = 0.953 | | D = D2/D1 |
|---|---|---|---|---|---|---|---|---|---|---|
| ALPHA | WCX/WCRO | D1=0.00 | D1=20.0 | D1=40.00 | D1=100 | D1=200 | D1=400 | D1=600 | D1=800 | D1=1000 |
| 0.04 | 0.53 | 0.879 | 1.070 | 2.040 | 2.021 | 1.970 | 1.839 | 1.685 | 1.542 | 1.453 |
| 0.10 | 0.71 | 0.855 | 0.871 | 0.887 | 0.941 | 1.033 | 1.263 | 1.403 | 1.378 | 1.329 |
| 0.20 | 0.82 | 0.887 | 0.887 | 0.895 | 0.902 | 0.918 | 0.949 | 0.980 | 1.014 | 1.033 |
| 0.40 | 0.89 | 0.926 | 0.926 | 0.926 | 0.926 | 0.934 | 0.941 | 0.949 | 0.957 | 0.965 |
| 0.50 | 0.91 | 0.934 | 0.934 | 0.934 | 0.934 | 0.941 | 0.941 | 0.949 | 0.957 | 0.957 |
| 0.60 | 0.93 | 0.941 | 0.941 | 0.941 | 0.941 | 0.941 | 0.949 | 0.949 | 0.957 | 0.957 |
| 0.70 | 0.94 | 0.941 | 0.941 | 0.941 | 0.949 | 0.949 | 0.949 | 0.957 | 0.957 | 0.957 |
| 0.80 | 0.94 | 0.949 | 0.949 | 0.949 | 0.949 | 0.949 | 0.949 | 0.957 | 0.957 | 0.957 |
| 0.90 | 0.95 | 0.949 | 0.949 | 0.949 | 0.949 | 0.957 | 0.957 | 0.957 | 0.957 | 0.965 |
| 1.00 | 0.95 | 0.957 | 0.957 | 0.957 | 0.957 | 0.957 | 0.957 | 0.957 | 0.965 | 0.965 |
| 1.10 | 0.96 | 0.957 | 0.957 | 0.957 | 0.957 | 0.957 | 0.957 | 0.957 | 0.965 | 0.965 |
| 1.20 | 0.96 | 0.957 | 0.957 | 0.957 | 0.957 | 0.957 | 0.957 | 0.965 | 0.965 | 0.965 |
| 1.30 | 0.96 | 0.957 | 0.957 | 0.957 | 0.957 | 0.957 | 0.965 | 0.965 | 0.965 | 0.965 |
| 1.50 | 0.97 | 0.957 | 0.957 | 0.965 | 0.965 | 0.965 | 0.965 | 0.965 | 0.965 | 0.965 |
| 1.70 | 0.97 | 0.965 | 0.965 | 0.965 | 0.965 | 0.965 | 0.965 | 0.965 | 0.965 | 0.973 |
| 2.00 | 0.98 | 0.965 | 0.965 | 0.965 | 0.965 | 0.965 | 0.965 | 0.965 | 0.973 | 0.973 |
| 2.50 | 0.98 | 0.965 | 0.965 | 0.965 | 0.965 | 0.965 | 0.973 | 0.973 | 0.973 | 0.973 |
| 3.00 | 0.98 | 0.965 | 0.965 | 0.965 | 0.973 | 0.973 | 0.973 | 0.973 | 0.973 | 0.973 |
| 4.00 | 0.99 | 0.973 | 0.973 | 0.973 | 0.973 | 0.973 | 0.973 | 0.973 | 0.973 | 0.973 |
| 6.00 | 0.99 | 0.973 | 0.973 | 0.973 | 0.973 | 0.973 | 0.973 | 0.973 | 0.980 | 0.980 |
| 8.00 | 0.99 | 0.973 | 0.973 | 0.973 | 0.973 | 0.973 | 0.973 | 0.973 | 0.980 | 0.980 |
| 10.00 | 1.00 | 0.973 | 0.973 | 0.973 | 0.973 | 0.973 | 0.973 | 0.980 | 0.980 | 0.980 |
| 25.00 | 1.00 | 0.973 | 0.973 | 0.973 | 0.973 | 0.973 | 0.980 | 0.980 | 0.980 | 0.980 |

GENERAL STABILITY OF A ROTOR ON AN ELASTIC FOUNDATION WITH INTERNAL FRICTION DAMPING

| DM = M1/M2 = 0. | | R = K2/KY = 1.00 | | | A = WCRO/D2 = 1.00 | | | WCY/WCRO = 0.707 | | D = D2/D1 |
|---|---|---|---|---|---|---|---|---|---|---|
| ALPHA | WCX/WCRO | D1=0.00 | D1=20.0 | D1=40.00 | D1=100 | D1=200 | D1=400 | D1=600 | D1=800 | D1=1000 |
| 0.04 | 0.20 | 0.980 | 1.378 | 1.440 | 1.728 | 28.625 | 28.625 | 28.625 | 28.625 | 28.625 |
| 0.10 | 0.30 | 0.949 | 1.453 | 1.515 | 1.856 | 28.625 | 28.625 | 28.625 | 28.625 | 28.625 |
| 0.20 | 0.41 | 0.887 | 1.599 | 1.685 | 28.625 | 28.625 | 28.625 | 28.625 | 28.625 | 28.625 |
| 0.40 | 0.53 | 0.775 | 0.902 | 1.108 | 28.625 | 28.625 | 28.625 | 28.625 | 28.625 | 28.625 |
| 0.50 | 0.58 | 0.736 | 0.793 | 0.855 | 1.145 | 28.625 | 28.625 | 28.625 | 28.625 | 28.625 |
| 0.60 | 0.61 | 0.709 | 0.744 | 0.779 | 0.895 | 1.117 | 28.625 | 28.625 | 28.625 | 28.625 |
| 0.70 | 0.64 | 0.697 | 0.721 | 0.744 | 0.816 | 0.957 | 1.285 | 28.625 | 28.625 | 28.625 |
| 0.80 | 0.67 | 0.693 | 0.713 | 0.732 | 0.793 | 0.895 | 1.136 | 1.557 | 28.625 | 28.625 |
| 0.90 | 0.69 | 0.697 | 0.717 | 0.732 | 0.779 | 0.863 | 1.070 | 1.341 | 28.625 | 28.625 |
| 1.00 | 0.71 | 0.709 | 0.721 | 0.736 | 0.779 | 0.855 | 1.033 | 1.252 | 1.542 | 28.625 |
| 1.10 | 0.72 | 0.717 | 0.729 | 0.744 | 0.785 | 0.855 | 1.014 | 1.199 | 1.415 | 1.614 |
| 1.20 | 0.74 | 0.725 | 0.740 | 0.752 | 0.793 | 0.855 | 1.005 | 1.166 | 1.341 | 1.502 |
| 1.30 | 0.75 | 0.736 | 0.748 | 0.760 | 0.801 | 0.863 | 1.005 | 1.155 | 1.296 | 1.428 |
| 1.50 | 0.77 | 0.752 | 0.764 | 0.775 | 0.816 | 0.879 | 1.005 | 1.136 | 1.252 | 1.341 |
| 1.70 | 0.79 | 0.764 | 0.775 | 0.793 | 0.824 | 0.895 | 1.014 | 1.136 | 1.220 | 1.296 |
| 2.00 | 0.82 | 0.779 | 0.793 | 0.809 | 0.848 | 0.910 | 1.042 | 1.145 | 1.209 | 1.263 |
| 2.50 | 0.85 | 0.801 | 0.809 | 0.824 | 0.871 | 0.941 | 1.070 | 1.166 | 1.220 | 1.242 |
| 3.00 | 0.87 | 0.809 | 0.824 | 0.840 | 0.887 | 0.957 | 1.098 | 1.199 | 1.231 | 1.242 |
| 4.00 | 0.89 | 0.824 | 0.840 | 0.855 | 0.902 | 0.988 | 1.145 | 1.242 | 1.263 | 1.252 |
| 6.00 | 0.93 | 0.840 | 0.855 | 0.871 | 0.926 | 1.014 | 1.199 | 1.317 | 1.317 | 1.285 |
| 8.00 | 0.94 | 0.848 | 0.863 | 0.879 | 0.934 | 1.023 | 1.242 | 1.366 | 1.353 | 1.306 |
| 10.00 | 0.95 | 0.855 | 0.871 | 0.887 | 0.941 | 1.033 | 1.263 | 1.403 | 1.378 | 1.329 |
| 25.00 | 0.98 | 0.863 | 0.879 | 0.902 | 0.957 | 1.061 | 1.329 | 1.515 | 1.440 | 1.378 |

GENERAL STABILITY OF A ROTOR ON AN ELASTIC FOUNDATION WITH INTERNAL FRICTION DAMPING

| DM = M1/M2 = 0. | | R = K2/KY = 10.00 | | | A = WCRO/D2 = 1.00 | | | WCY/WCRO = 0.302 | | D = D2/D1 |
|---|---|---|---|---|---|---|---|---|---|---|
| ALPHA | WCX/WCRO | D1=0.00 | D1=20.0 | D1=40.00 | D1=100 | D1=200 | D1=400 | D1=600 | D1=800 | D1=1000 |
| 0.04 | 0.06 | 0.996 | 28.625 | 28.625 | 28.625 | 28.625 | 28.625 | 28.625 | 28.625 | 28.625 |
| 0.10 | 0.10 | 0.996 | 28.625 | 28.625 | 28.625 | 28.625 | 28.625 | 28.625 | 28.625 | 28.625 |
| 0.20 | 0.14 | 0.988 | 28.625 | 28.625 | 28.625 | 28.625 | 28.625 | 28.625 | 28.625 | 28.625 |
| 0.40 | 0.20 | 0.957 | 28.625 | 28.625 | 28.625 | 28.625 | 28.625 | 28.625 | 28.625 | 28.625 |
| 0.50 | 0.22 | 0.934 | 28.625 | 28.625 | 28.625 | 28.625 | 28.625 | 28.625 | 28.625 | 28.625 |
| 0.60 | 0.24 | 0.895 | 28.625 | 28.625 | 28.625 | 28.625 | 28.625 | 28.625 | 28.625 | 28.625 |
| 0.70 | 0.26 | 0.832 | 28.625 | 28.625 | 28.625 | 28.625 | 28.625 | 28.625 | 28.625 | 28.625 |
| 0.80 | 0.27 | 0.732 | 28.625 | 28.625 | 28.625 | 28.625 | 28.625 | 28.625 | 28.625 | 28.625 |
| 0.90 | 0.29 | 0.533 | 28.625 | 28.625 | 28.625 | 28.625 | 28.625 | 28.625 | 28.625 | 28.625 |
| 1.00 | 0.30 | 0.302 | 28.625 | 28.625 | 28.625 | 28.625 | 28.625 | 28.625 | 28.625 | 28.625 |
| 1.10 | 0.31 | 0.494 | 28.625 | 28.625 | 28.625 | 28.625 | 28.625 | 28.625 | 28.625 | 28.625 |
| 1.20 | 0.33 | 0.643 | 28.625 | 28.625 | 28.625 | 28.625 | 28.625 | 28.625 | 28.625 | 28.625 |
| 1.30 | 0.34 | 0.725 | 28.625 | 28.625 | 28.625 | 28.625 | 28.625 | 28.625 | 28.625 | 28.625 |
| 1.50 | 0.36 | 0.809 | 28.625 | 28.625 | 28.625 | 28.625 | 28.625 | 28.625 | 28.625 | 28.625 |
| 1.70 | 0.38 | 0.848 | 28.625 | 28.625 | 28.625 | 28.625 | 28.625 | 28.625 | 28.625 | 28.625 |
| 2.00 | 0.41 | 0.879 | 28.625 | 28.625 | 28.625 | 28.625 | 28.625 | 28.625 | 28.625 | 28.625 |
| 2.50 | 0.45 | 0.902 | 28.625 | 28.625 | 28.625 | 28.625 | 28.625 | 28.625 | 28.625 | 28.625 |
| 3.00 | 0.48 | 0.918 | 28.625 | 28.625 | 28.625 | 28.625 | 28.625 | 28.625 | 28.625 | 28.625 |
| 4.00 | 0.53 | 0.926 | 28.625 | 28.625 | 28.625 | 28.625 | 28.625 | 28.625 | 28.625 | 28.625 |
| 6.00 | 0.61 | 0.941 | 1.515 | 28.625 | 28.625 | 28.625 | 28.625 | 28.625 | 28.625 | 28.625 |
| 8.00 | 0.67 | 0.941 | 1.453 | 1.585 | 28.625 | 28.625 | 28.625 | 28.625 | 28.625 | 28.625 |
| 10.00 | 0.71 | 0.949 | 1.453 | 1.515 | 1.856 | 28.625 | 28.625 | 28.625 | 28.625 | 28.625 |
| 25.00 | 0.85 | 0.949 | 1.557 | 1.557 | 1.585 | 1.599 | 1.599 | 1.557 | 1.515 | 1.465 |

GENERAL STABILITY OF A ROTOR ON AN ELASTIC FOUNDATION WITH INTERNAL FRICTION DAMPING

| DM = M1/M2 = 0. | | R = K2/KY = 0.10 | | | A = WCRO/D2 = 2.00 | | | WCY/WCRO = 0.953 | | D = D2/D1 |
|---|---|---|---|---|---|---|---|---|---|---|
| ALPHA | WCX/WCRO | D1=0.00 | D1=20.0 | D1=40.00 | D1=100 | D1=200 | D1=400 | D1=600 | D1=800 | D1=1000 |
| 0.04 | 0.53 | 1.453 | 3.245 | 3.188 | 3.022 | 2.772 | 2.367 | 2.077 | 1.888 | 1.742 |
| 0.10 | 0.71 | 1.080 | 1.117 | 1.155 | 1.274 | 1.477 | 1.856 | 1.823 | 1.713 | 1.614 |
| 0.20 | 0.82 | 0.949 | 0.949 | 0.957 | 0.980 | 1.014 | 1.070 | 1.117 | 1.155 | 1.188 |
| 0.40 | 0.89 | 0.934 | 0.934 | 0.934 | 0.941 | 0.949 | 0.965 | 0.980 | 0.988 | 1.005 |
| 0.50 | 0.91 | 0.934 | 0.941 | 0.941 | 0.941 | 0.949 | 0.957 | 0.965 | 0.973 | 0.988 |
| 0.60 | 0.93 | 0.941 | 0.941 | 0.941 | 0.941 | 0.949 | 0.957 | 0.965 | 0.973 | 0.980 |
| 0.70 | 0.94 | 0.941 | 0.949 | 0.949 | 0.949 | 0.949 | 0.957 | 0.965 | 0.965 | 0.973 |
| 0.80 | 0.94 | 0.949 | 0.949 | 0.949 | 0.949 | 0.957 | 0.957 | 0.965 | 0.965 | 0.973 |
| 0.90 | 0.95 | 0.949 | 0.949 | 0.949 | 0.957 | 0.957 | 0.957 | 0.965 | 0.965 | 0.973 |
| 1.00 | 0.95 | 0.957 | 0.957 | 0.957 | 0.957 | 0.957 | 0.965 | 0.965 | 0.973 | 0.973 |
| 1.10 | 0.96 | 0.957 | 0.957 | 0.957 | 0.957 | 0.957 | 0.965 | 0.965 | 0.973 | 0.973 |
| 1.20 | 0.96 | 0.957 | 0.957 | 0.957 | 0.957 | 0.957 | 0.965 | 0.965 | 0.973 | 0.973 |
| 1.30 | 0.96 | 0.957 | 0.957 | 0.957 | 0.957 | 0.965 | 0.965 | 0.965 | 0.973 | 0.973 |
| 1.50 | 0.97 | 0.965 | 0.965 | 0.965 | 0.965 | 0.965 | 0.965 | 0.973 | 0.973 | 0.973 |
| 1.70 | 0.97 | 0.965 | 0.965 | 0.965 | 0.965 | 0.965 | 0.965 | 0.973 | 0.973 | 0.980 |
| 2.00 | 0.98 | 0.965 | 0.965 | 0.965 | 0.965 | 0.965 | 0.973 | 0.973 | 0.973 | 0.980 |
| 2.50 | 0.98 | 0.965 | 0.965 | 0.965 | 0.973 | 0.973 | 0.973 | 0.973 | 0.980 | 0.980 |
| 3.00 | 0.98 | 0.973 | 0.973 | 0.973 | 0.973 | 0.973 | 0.973 | 0.980 | 0.980 | 0.980 |
| 4.00 | 0.99 | 0.973 | 0.973 | 0.973 | 0.973 | 0.973 | 0.980 | 0.980 | 0.980 | 0.980 |
| 6.00 | 0.99 | 0.973 | 0.973 | 0.973 | 0.973 | 0.980 | 0.980 | 0.980 | 0.980 | 0.988 |
| 8.00 | 0.99 | 0.973 | 0.973 | 0.973 | 0.980 | 0.980 | 0.980 | 0.980 | 0.988 | 0.988 |
| 10.00 | 1.00 | 0.980 | 0.980 | 0.980 | 0.980 | 0.980 | 0.980 | 0.980 | 0.988 | 0.988 |
| 25.00 | 1.00 | 0.980 | 0.980 | 0.980 | 0.980 | 0.980 | 0.980 | 0.988 | 0.988 | 0.988 |

GENERAL STABILITY OF A ROTOR ON AN ELASTIC FOUNDATION WITH INTERNAL FRICTION DAMPING

| OM = M1/M2 = 0. | | R = K2/KY = 1.00 | | | A = WCRO/D2 = 2.00 | | | WCY/WCRO = 0.707 | | D = C2/D1 |
|---|---|---|---|---|---|---|---|---|---|---|
| ALPHA | WCK/WCRO | D1=0.00 | D1=20.0 | D1=40.00 | D1=100 | D1=200 | D1=400 | D1=600 | D1=800 | D1=1000 |
| 0.04 | 0.20 | 1.921 | 2.411 | 2.627 | 28.625 | 28.625 | 28.625 | 28.625 | 28.625 | 28.625 |
| 0.10 | 0.30 | 1.823 | 2.562 | 2.822 | 28.625 | 28.625 | 28.625 | 28.625 | 28.625 | 28.625 |
| 0.20 | 0.41 | 1.614 | 2.922 | 3.245 | 28.625 | 28.625 | 28.625 | 28.625 | 28.625 | 28.625 |
| 0.40 | 0.53 | 1.209 | 1.628 | 28.625 | 28.625 | 28.625 | 28.625 | 28.625 | 28.625 | 28.625 |
| 0.50 | 0.58 | 1.023 | 1.166 | 1.329 | 28.625 | 28.625 | 28.625 | 28.625 | 28.625 | 28.625 |
| 0.60 | 0.61 | 0.879 | 0.949 | 1.023 | 1.231 | 1.585 | 28.625 | 28.625 | 28.625 | 28.625 |
| 0.70 | 0.64 | 0.785 | 0.824 | 0.871 | 1.005 | 1.242 | 1.806 | 28.625 | 28.625 | 28.625 |
| 0.80 | 0.67 | 0.725 | 0.764 | 0.801 | 0.910 | 1.098 | 1.542 | 2.266 | 28.625 | 28.625 |
| 0.90 | 0.69 | 0.705 | 0.736 | 0.768 | 0.863 | 1.033 | 1.403 | 1.888 | 28.625 | 28.625 |
| 1.00 | 0.71 | 0.709 | 0.736 | 0.764 | 0.848 | 0.996 | 1.329 | 1.713 | 2.228 | 28.625 |
| 1.10 | 0.72 | 0.721 | 0.748 | 0.771 | 0.855 | 0.988 | 1.285 | 1.614 | 1.987 | 2.324 |
| 1.20 | 0.74 | 0.740 | 0.764 | 0.793 | 0.863 | 0.996 | 1.263 | 1.557 | 1.856 | 2.115 |
| 1.30 | 0.75 | 0.760 | 0.785 | 0.809 | 0.879 | 1.005 | 1.252 | 1.515 | 1.774 | 1.970 |
| 1.50 | 0.77 | 0.801 | 0.824 | 0.848 | 0.918 | 1.033 | 1.252 | 1.465 | 1.656 | 1.806 |
| 1.70 | 0.79 | 0.840 | 0.863 | 0.887 | 0.957 | 1.070 | 1.274 | 1.453 | 1.599 | 1.713 |
| 2.00 | 0.82 | 0.879 | 0.902 | 0.934 | 1.005 | 1.117 | 1.317 | 1.453 | 1.557 | 1.628 |
| 2.50 | 0.85 | 0.934 | 0.957 | 0.988 | 1.061 | 1.188 | 1.378 | 1.490 | 1.542 | 1.571 |
| 3.00 | 0.87 | 0.965 | 0.996 | 1.023 | 1.108 | 1.242 | 1.453 | 1.528 | 1.542 | 1.542 |
| 4.00 | 0.89 | 1.005 | 1.042 | 1.070 | 1.166 | 1.317 | 1.557 | 1.599 | 1.585 | 1.542 |
| 6.00 | 0.93 | 1.052 | 1.080 | 1.117 | 1.220 | 1.403 | 1.699 | 1.713 | 1.642 | 1.571 |
| 8.00 | 0.94 | 1.070 | 1.108 | 1.145 | 1.252 | 1.453 | 1.790 | 1.790 | 1.685 | 1.599 |
| 10.00 | 0.95 | 1.080 | 1.117 | 1.155 | 1.274 | 1.477 | 1.856 | 1.823 | 1.713 | 1.614 |
| 25.00 | 0.98 | 1.108 | 1.145 | 1.188 | 1.317 | 1.557 | 2.077 | 1.970 | 1.806 | 1.685 |

GENERAL STABILITY OF A ROTOR ON AN ELASTIC FOUNDATION WITH INTERNAL FRICTION DAMPING

| DM = M1/M2 = 0. | | R = K2/KY = 10.00 | | | A = WCRO/D2 = 2.00 | | | WCY/WCRO = 0.302 | | D = D2/D1 |
|---|---|---|---|---|---|---|---|---|---|---|
| ALPHA | WCX/WCRO | D1=0.00 | D1=20.0 | D1=40.00 | D1=100 | D1=200 | D1=400 | D1=600 | D1=800 | D1=1000 |
| 0.04 | 0.06 | 1.987 | 28.625 | 28.625 | 28.625 | 28.625 | 28.625 | 28.625 | 28.625 | 28.625 |
| 0.10 | 0.10 | 1.987 | 28.625 | 28.625 | 28.625 | 28.625 | 28.625 | 28.625 | 28.625 | 28.625 |
| 0.20 | 0.14 | 1.954 | 28.625 | 28.625 | 28.625 | 28.625 | 28.625 | 28.625 | 28.625 | 28.625 |
| 0.40 | 0.20 | 1.888 | 28.625 | 28.625 | 28.625 | 28.625 | 28.625 | 28.625 | 28.625 | 28.625 |
| 0.50 | 0.22 | 1.823 | 28.625 | 28.625 | 28.625 | 28.625 | 28.625 | 28.625 | 28.625 | 28.625 |
| 0.60 | 0.24 | 1.742 | 28.625 | 28.625 | 28.625 | 28.625 | 28.625 | 28.625 | 28.625 | 28.625 |
| 0.70 | 0.26 | 1.614 | 28.625 | 28.625 | 28.625 | 28.625 | 28.625 | 28.625 | 28.625 | 28.625 |
| 0.80 | 0.27 | 1.378 | 28.625 | 28.625 | 28.625 | 28.625 | 28.625 | 28.625 | 28.625 | 28.625 |
| 0.90 | 0.29 | 0.934 | 28.625 | 28.625 | 28.625 | 28.625 | 28.625 | 28.625 | 28.625 | 28.625 |
| 1.00 | 0.30 | 0.302 | 28.625 | 28.625 | 28.625 | 28.625 | 28.625 | 28.625 | 28.625 | 28.625 |
| 1.10 | 0.31 | 0.832 | 28.625 | 28.625 | 28.625 | 28.625 | 28.625 | 28.625 | 28.625 | 28.625 |
| 1.20 | 0.33 | 1.177 | 28.625 | 28.625 | 28.625 | 28.625 | 28.625 | 28.625 | 28.625 | 28.625 |
| 1.30 | 0.34 | 1.353 | 28.625 | 28.625 | 28.625 | 28.625 | 28.625 | 28.625 | 28.625 | 28.625 |
| 1.50 | 0.36 | 1.515 | 28.625 | 28.625 | 28.625 | 28.625 | 28.625 | 28.625 | 28.625 | 28.625 |
| 1.70 | 0.38 | 1.599 | 28.625 | 28.625 | 28.625 | 28.625 | 28.625 | 28.625 | 28.625 | 28.625 |
| 2.00 | 0.41 | 1.671 | 28.625 | 28.625 | 28.625 | 28.625 | 28.625 | 28.625 | 28.625 | 28.625 |
| 2.50 | 0.45 | 1.728 | 28.625 | 28.625 | 28.625 | 28.625 | 28.625 | 28.625 | 28.625 | 28.625 |
| 3.00 | 0.48 | 1.757 | 28.625 | 28.625 | 28.625 | 28.625 | 28.625 | 28.625 | 28.625 | 28.625 |
| 4.00 | 0.53 | 1.774 | 28.625 | 28.625 | 28.625 | 28.625 | 28.625 | 28.625 | 28.625 | 28.625 |
| 6.00 | 0.61 | 1.806 | 3.699 | 28.625 | 28.625 | 28.625 | 28.625 | 28.625 | 28.625 | 28.625 |
| 8.00 | 0.67 | 1.806 | 2.722 | 28.625 | 28.625 | 28.625 | 28.625 | 28.625 | 28.625 | 28.625 |
| 10.00 | 0.71 | 1.823 | 2.562 | 2.822 | 28.625 | 28.625 | 28.625 | 28.625 | 28.625 | 28.625 |
| 25.00 | 0.85 | 1.823 | 2.454 | 2.454 | 2.432 | 2.389 | 2.266 | 2.134 | 2.040 | 1.954 |

GENERAL STABILITY OF A RCTOR ON AN ELASTIC FOUNDATION WITH INTERNAL FRICTION DAMPING

| OM = M1/M2 = 0. | | R = K2/KY = 0.10 | | | A = WCRO/D2 = 5.00 | | | WCY/WCRO = 0.953 | | D = D2/D1 |
|---|---|---|---|---|---|---|---|---|---|---|
| ALPHA | WCX/WCRO | D1=0.00 | D1=20.0 | D1=40.00 | D1=100 | D1=200 | D1=400 | D1=600 | D1=800 | D1=1000 |
| 0.04 | 0.53 | 3.389 | 7.175 | 6.758 | 5.777 | 4.761 | 3.600 | 3.047 | 2.697 | 2.454 |
| 0.10 | 0.71 | 2.058 | 2.209 | 2.346 | 2.797 | 3.418 | 3.159 | 2.747 | 2.476 | 2.304 |
| 0.20 | 0.82 | 1.296 | 1.306 | 1.329 | 1.366 | 1.428 | 1.528 | 1.599 | 1.642 | 1.656 |
| 0.40 | 0.89 | 0.996 | 0.996 | 1.005 | 1.014 | 1.033 | 1.061 | 1.089 | 1.127 | 1.155 |
| 0.50 | 0.91 | 0.965 | 0.965 | 0.973 | 0.973 | 0.988 | 1.014 | 1.033 | 1.061 | 1.080 |
| 0.60 | 0.93 | 0.957 | 0.957 | 0.957 | 0.965 | 0.973 | 0.988 | 1.005 | 1.023 | 1.042 |
| 0.70 | 0.94 | 0.949 | 0.949 | 0.949 | 0.957 | 0.965 | 0.980 | 0.996 | 1.005 | 1.023 |
| 0.80 | 0.94 | 0.949 | 0.949 | 0.949 | 0.957 | 0.965 | 0.973 | 0.988 | 0.996 | 1.014 |
| 0.90 | 0.95 | 0.949 | 0.949 | 0.957 | 0.957 | 0.965 | 0.973 | 0.980 | 0.996 | 1.005 |
| 1.00 | 0.95 | 0.957 | 0.957 | 0.957 | 0.957 | 0.965 | 0.973 | 0.980 | 0.988 | 1.005 |
| 1.10 | 0.96 | 0.957 | 0.957 | 0.957 | 0.957 | 0.965 | 0.973 | 0.980 | 0.988 | 0.996 |
| 1.20 | 0.96 | 0.957 | 0.957 | 0.957 | 0.965 | 0.965 | 0.973 | 0.980 | 0.988 | 0.996 |
| 1.30 | 0.96 | 0.957 | 0.965 | 0.965 | 0.965 | 0.965 | 0.973 | 0.980 | 0.988 | 0.996 |
| 1.50 | 0.97 | 0.965 | 0.965 | 0.965 | 0.965 | 0.973 | 0.980 | 0.988 | 0.996 | 0.996 |
| 1.70 | 0.97 | 0.965 | 0.965 | 0.973 | 0.973 | 0.973 | 0.980 | 0.988 | 0.996 | 1.005 |
| 2.00 | 0.98 | 0.973 | 0.973 | 0.973 | 0.973 | 0.980 | 0.988 | 0.988 | 0.996 | 1.005 |
| 2.50 | 0.98 | 0.980 | 0.980 | 0.980 | 0.980 | 0.980 | 0.988 | 0.996 | 1.005 | 1.005 |
| 3.00 | 0.98 | 0.980 | 0.980 | 0.980 | 0.988 | 0.988 | 0.996 | 0.996 | 1.005 | 1.014 |
| 4.00 | 0.99 | 0.988 | 0.988 | 0.988 | 0.988 | 0.996 | 0.996 | 1.005 | 1.005 | 1.014 |
| 6.00 | 0.99 | 0.996 | 0.996 | 0.996 | 0.996 | 0.996 | 1.005 | 1.005 | 1.014 | 1.023 |
| 8.00 | 0.99 | 0.996 | 0.996 | 0.996 | 0.996 | 1.005 | 1.005 | 1.014 | 1.014 | 1.023 |
| 10.00 | 1.00 | 0.996 | 0.996 | 0.996 | 1.005 | 1.005 | 1.005 | 1.014 | 1.023 | 1.023 |
| 25.00 | 1.00 | 1.005 | 1.005 | 1.005 | 1.005 | 1.005 | 1.014 | 1.014 | 1.023 | 1.033 |

GENERAL STABILITY OF A ROTOR ON AN ELASTIC FOUNDATION WITH INTERNAL FRICTION DAMPING

| DM = M1/M2 = 0. | | R = K2/KY = 1.00 | | | A = WCRO/D2 = 5.00 | | | WCY/WCRO = 0.707 | | D = D2/D1 |
|---|---|---|---|---|---|---|---|---|---|---|
| ALPHA | WCX/WCRO | D1=0.00 | D1=20.0 | D1=40.00 | D1=100 | D1=200 | D1=400 | D1=600 | D1=800 | D1=1000 |
| 0.04 | 0.20 | 4.805 | 6.470 | 28.625 | 28.625 | 28.625 | 28.625 | 28.625 | 28.625 | 28.625 |
| 0.10 | 0.30 | 4.482 | 6.989 | 28.625 | 28.625 | 28.625 | 28.625 | 28.625 | 28.625 | 28.625 |
| 0.20 | 0.41 | 3.930 | 8.328 | 28.625 | 28.625 | 28.625 | 28.625 | 28.625 | 28.625 | 28.625 |
| 0.40 | 0.53 | 2.722 | 28.625 | 28.625 | 28.625 | 28.625 | 28.625 | 28.625 | 28.625 | 28.625 |
| 0.50 | 0.58 | 2.153 | 2.822 | 3.699 | 5.476 | 5.375 | 28.625 | 28.625 | 28.625 | 28.625 |
| 0.60 | 0.61 | 1.642 | 1.856 | 2.040 | 2.411 | 2.897 | 4.936 | 28.625 | 28.625 | 28.625 |
| 0.70 | 0.64 | 1.220 | 1.329 | 1.415 | 1.671 | 2.134 | 3.303 | 28.625 | 28.625 | 28.625 |
| 0.80 | 0.67 | 0.918 | 0.996 | 1.070 | 1.306 | 1.728 | 2.722 | 4.368 | 28.625 | 28.625 |
| 0.90 | 0.69 | 0.748 | 0.824 | 0.902 | 1.127 | 1.528 | 2.411 | 3.534 | 28.625 | 28.625 |
| 1.00 | 0.71 | 0.709 | 0.779 | 0.848 | 1.061 | 1.428 | 2.209 | 3.131 | 4.292 | 28.625 |
| 1.10 | 0.72 | 0.752 | 0.816 | 0.879 | 1.070 | 1.403 | 2.096 | 2.872 | 3.732 | 4.444 |
| 1.20 | 0.74 | 0.832 | 0.887 | 0.941 | 1.117 | 1.415 | 2.040 | 2.697 | 3.389 | 3.930 |
| 1.30 | 0.75 | 0.926 | 0.973 | 1.023 | 1.188 | 1.453 | 2.003 | 2.584 | 3.159 | 3.600 |
| 1.50 | 0.77 | 1.089 | 1.145 | 1.199 | 1.341 | 1.557 | 2.003 | 2.454 | 2.872 | 3.188 |
| 1.70 | 0.79 | 1.231 | 1.285 | 1.341 | 1.477 | 1.685 | 2.040 | 2.389 | 2.697 | 2.922 |
| 2.00 | 0.82 | 1.391 | 1.453 | 1.515 | 1.671 | 1.856 | 2.134 | 2.346 | 2.541 | 2.697 |
| 2.50 | 0.85 | 1.571 | 1.656 | 1.728 | 1.905 | 2.115 | 2.285 | 2.367 | 2.432 | 2.476 |
| 3.00 | 0.87 | 1.685 | 1.774 | 1.872 | 2.077 | 2.324 | 2.411 | 2.411 | 2.389 | 2.367 |
| 4.00 | 0.89 | 1.823 | 1.938 | 2.040 | 2.324 | 2.627 | 2.627 | 2.476 | 2.367 | 2.285 |
| 6.00 | 0.93 | 1.970 | 2.096 | 2.209 | 2.584 | 2.997 | 2.897 | 2.606 | 2.411 | 2.266 |
| 8.00 | 0.94 | 2.021 | 2.172 | 2.304 | 2.722 | 3.245 | 3.073 | 2.697 | 2.454 | 2.285 |
| 10.00 | 0.95 | 2.058 | 2.209 | 2.346 | 2.797 | 3.418 | 3.159 | 2.747 | 2.476 | 2.304 |
| 25.00 | 0.98 | 2.153 | 2.304 | 2.476 | 3.022 | 3.996 | 3.446 | 2.922 | 2.584 | 2.367 |

GENERAL STABILITY OF A ROTOR ON AN ELASTIC FOUNDATION WITH INTERNAL FRICTION DAMPING

| DM = M1/M2 = 0. | | R = K2/KY = 10.00 | | | A = WCRO/D2 = 5.00 | | | WCY/WCRO = 0.302 | | D = D2/D1 |
|---|---|---|---|---|---|---|---|---|---|---|
| ALPHA | WCK/WCRO | D1=0.00 | D1=20.0 | D1=40.00 | D1=100 | D1=200 | D1=400 | D1=600 | D1=800 | D1=1000 |
| 0.04 | 0.06 | 4.980 | 28.625 | 28.625 | 28.625 | 28.625 | 28.625 | 28.625 | 28.625 | 28.625 |
| 0.10 | 0.10 | 4.936 | 28.625 | 28.625 | 28.625 | 28.625 | 28.625 | 28.625 | 28.625 | 28.625 |
| 0.20 | 0.14 | 4.892 | 28.625 | 28.625 | 28.625 | 28.625 | 28.625 | 28.625 | 28.625 | 28.625 |
| 0.40 | 0.20 | 4.674 | 28.625 | 28.625 | 28.625 | 28.625 | 28.625 | 28.625 | 28.625 | 28.625 |
| 0.50 | 0.22 | 4.520 | 28.625 | 28.625 | 28.625 | 28.625 | 28.625 | 28.625 | 28.625 | 28.625 |
| 0.60 | 0.24 | 4.330 | 28.625 | 28.625 | 28.625 | 28.625 | 28.625 | 28.625 | 28.625 | 28.625 |
| 0.70 | 0.26 | 3.963 | 28.625 | 28.625 | 28.625 | 28.625 | 28.625 | 28.625 | 28.625 | 28.625 |
| 0.80 | 0.27 | 3.389 | 28.625 | 28.625 | 28.625 | 28.625 | 28.625 | 28.625 | 28.625 | 28.625 |
| 0.90 | 0.29 | 2.247 | 28.625 | 28.625 | 28.625 | 28.625 | 28.625 | 28.625 | 28.625 | 28.625 |
| 1.00 | 0.30 | 0.302 | 28.625 | 28.625 | 28.625 | 28.625 | 28.625 | 28.625 | 28.625 | 28.625 |
| 1.10 | 0.31 | 1.954 | 28.625 | 28.625 | 28.625 | 28.625 | 28.625 | 28.625 | 28.625 | 28.625 |
| 1.20 | 0.33 | 2.847 | 28.625 | 28.625 | 28.625 | 28.625 | 28.625 | 28.625 | 28.625 | 28.625 |
| 1.30 | 0.34 | 3.303 | 28.625 | 28.625 | 28.625 | 28.625 | 28.625 | 28.625 | 28.625 | 28.625 |
| 1.50 | 0.36 | 3.732 | 28.625 | 28.625 | 28.625 | 28.625 | 28.625 | 28.625 | 28.625 | 28.625 |
| 1.70 | 0.38 | 3.930 | 28.625 | 28.625 | 28.625 | 28.625 | 28.625 | 28.625 | 28.625 | 28.625 |
| 2.00 | 0.41 | 4.102 | 28.625 | 28.625 | 28.625 | 28.625 | 28.625 | 28.625 | 28.625 | 28.625 |
| 2.50 | 0.45 | 4.254 | 28.625 | 28.625 | 28.625 | 28.625 | 28.625 | 28.625 | 28.625 | 28.625 |
| 3.00 | 0.48 | 4.330 | 28.625 | 28.625 | 28.625 | 28.625 | 28.625 | 28.625 | 28.625 | 28.625 |
| 4.00 | 0.53 | 4.406 | 28.625 | 28.625 | 28.625 | 28.625 | 28.625 | 28.625 | 28.625 | 28.625 |
| 6.00 | 0.61 | 4.444 | 28.625 | 28.625 | 28.625 | 28.625 | 28.625 | 28.625 | 28.625 | 28.625 |
| 8.00 | 0.67 | 4.482 | 28.625 | 28.625 | 28.625 | 28.625 | 28.625 | 28.625 | 28.625 | 28.625 |
| 10.00 | 0.71 | 4.482 | 6.989 | 28.625 | 28.625 | 28.625 | 28.625 | 28.625 | 28.625 | 28.625 |
| 25.00 | 0.85 | 4.520 | 5.526 | 5.425 | 5.110 | 4.718 | 4.140 | 3.798 | 3.600 | 3.418 |

GENERAL STABILITY OF A ROTOR ON AN ELASTIC FOUNDATION WITH INTERNAL FRICTION DAMPING

| DM = M1/M2 = 0. | | R = K2/KY = 0.10 | | | A = WCRO/D2 = 10.00 | | | WCY/WCRO = 0.953 | | D = D2/D1 |
|---|---|---|---|---|---|---|---|---|---|---|
| ALPHA | WCX/WCRO | D1=0.00 | D1=20.0 | D1=40.00 | D1=100 | D1=200 | D1=400 | D1=600 | D1=800 | D1=1000 |
| 0.04 | 0.53 | 6.701 | 13.246 | 11.921 | 9.243 | 6.931 | 5.067 | 4.216 | 3.732 | 3.389 |
| 0.10 | 0.71 | 3.897 | 4.406 | 4.936 | 6.297 | 5.977 | 4.558 | 3.864 | 3.446 | 3.159 |
| 0.20 | 0.82 | 2.115 | 2.153 | 2.172 | 2.266 | 2.367 | 2.454 | 2.454 | 2.411 | 2.367 |
| 0.40 | 0.89 | 1.188 | 1.188 | 1.199 | 1.220 | 1.242 | 1.296 | 1.353 | 1.391 | 1.428 |
| 0.50 | 0.91 | 1.061 | 1.061 | 1.061 | 1.080 | 1.098 | 1.145 | 1.188 | 1.220 | 1.263 |
| 0.60 | 0.93 | 0.996 | 0.996 | 1.005 | 1.014 | 1.033 | 1.061 | 1.098 | 1.127 | 1.166 |
| 0.70 | 0.94 | 0.965 | 0.973 | 0.973 | 0.980 | 0.996 | 1.023 | 1.052 | 1.080 | 1.108 |
| 0.80 | 0.94 | 0.957 | 0.957 | 0.965 | 0.965 | 0.980 | 1.005 | 1.033 | 1.052 | 1.080 |
| 0.90 | 0.95 | 0.949 | 0.957 | 0.957 | 0.965 | 0.973 | 0.996 | 1.014 | 1.033 | 1.061 |
| 1.00 | 0.95 | 0.957 | 0.957 | 0.957 | 0.965 | 0.973 | 0.988 | 1.014 | 1.033 | 1.052 |
| 1.10 | 0.96 | 0.957 | 0.957 | 0.957 | 0.965 | 0.973 | 0.988 | 1.005 | 1.023 | 1.042 |
| 1.20 | 0.96 | 0.957 | 0.965 | 0.965 | 0.973 | 0.980 | 0.996 | 1.005 | 1.023 | 1.042 |
| 1.30 | 0.96 | 0.965 | 0.965 | 0.965 | 0.973 | 0.980 | 0.996 | 1.014 | 1.023 | 1.042 |
| 1.50 | 0.97 | 0.973 | 0.973 | 0.980 | 0.980 | 0.988 | 1.005 | 1.014 | 1.033 | 1.042 |
| 1.70 | 0.97 | 0.980 | 0.988 | 0.988 | 0.988 | 0.996 | 1.014 | 1.023 | 1.033 | 1.052 |
| 2.00 | 0.98 | 0.996 | 0.996 | 0.996 | 1.005 | 1.005 | 1.023 | 1.033 | 1.042 | 1.052 |
| 2.50 | 0.98 | 1.014 | 1.014 | 1.014 | 1.014 | 1.023 | 1.033 | 1.042 | 1.052 | 1.070 |
| 3.00 | 0.98 | 1.023 | 1.023 | 1.023 | 1.033 | 1.033 | 1.042 | 1.052 | 1.061 | 1.080 |
| 4.00 | 0.99 | 1.042 | 1.042 | 1.042 | 1.042 | 1.052 | 1.061 | 1.070 | 1.080 | 1.089 |
| 6.00 | 0.99 | 1.061 | 1.061 | 1.061 | 1.061 | 1.070 | 1.080 | 1.089 | 1.098 | 1.108 |
| 8.00 | 0.99 | 1.070 | 1.070 | 1.070 | 1.070 | 1.080 | 1.089 | 1.098 | 1.108 | 1.117 |
| 10.00 | 1.00 | 1.070 | 1.070 | 1.070 | 1.080 | 1.080 | 1.089 | 1.098 | 1.108 | 1.117 |
| 25.00 | 1.00 | 1.089 | 1.089 | 1.089 | 1.089 | 1.098 | 1.108 | 1.117 | 1.127 | 1.136 |

GENERAL STABILITY OF A ROTOR ON AN ELASTIC FOUNDATION WITH INTERNAL FRICTION DAMPING

| DM = M1/M2 = 0. | | R = K2/KY = 1.00 | | | A = WCRO/D2 = 10.00 | | | WCY/WCRO = 0.707 | | D = D2/D1 |
|---|---|---|---|---|---|---|---|---|---|---|
| ALPHA | WCX/WCRO | D1=0.00 | D1=20.0 | D1=40.00 | D1=100 | D1=200 | D1=400 | D1=600 | D1=800 | D1=1000 |
| 0.04 | 0.20 | 9.577 | 28.625 | 28.625 | 28.625 | 28.625 | 28.625 | 28.625 | 28.625 | 28.625 |
| 0.10 | 0.30 | 8.938 | 28.625 | 28.625 | 28.625 | 28.625 | 28.625 | 28.625 | 28.625 | 28.625 |
| 0.20 | 0.41 | 7.839 | 28.625 | 28.625 | 28.625 | 28.625 | 28.625 | 28.625 | 28.625 | 28.625 |
| 0.40 | 0.53 | 5.375 | 28.625 | 28.625 | 28.625 | 28.625 | 28.625 | 28.625 | 28.625 | 28.625 |
| 0.50 | 0.58 | 4.178 | 6.874 | 10.131 | 7.839 | 8.175 | 28.625 | 28.625 | 28.625 | 28.625 |
| 0.60 | 0.61 | 3.102 | 3.666 | 3.996 | 4.330 | 5.023 | 8.480 | 28.625 | 28.625 | 28.625 |
| 0.70 | 0.64 | 2.153 | 2.367 | 2.497 | 2.872 | 3.600 | 5.827 | 28.625 | 28.625 | 28.625 |
| 0.80 | 0.67 | 1.403 | 1.528 | 1.642 | 2.040 | 2.797 | 4.718 | 7.905 | 28.625 | 28.625 |
| 0.90 | 0.69 | 0.887 | 1.023 | 1.155 | 1.585 | 2.346 | 4.065 | 6.297 | 28.625 | 28.625 |
| 1.00 | 0.71 | 0.709 | 0.848 | 0.988 | 1.415 | 2.134 | 3.699 | 5.476 | 7.706 | 28.625 |
| 1.10 | 0.72 | 0.848 | 0.965 | 1.080 | 1.453 | 2.096 | 3.446 | 4.936 | 6.585 | 7.971 |
| 1.20 | 0.74 | 1.098 | 1.188 | 1.285 | 1.585 | 2.134 | 3.331 | 4.596 | 5.927 | 6.989 |
| 1.30 | 0.75 | 1.353 | 1.428 | 1.515 | 1.774 | 2.228 | 3.245 | 4.368 | 5.476 | 6.355 |
| 1.50 | 0.77 | 1.774 | 1.872 | 1.954 | 2.153 | 2.497 | 3.245 | 4.065 | 4.849 | 5.476 |
| 1.70 | 0.79 | 2.115 | 2.228 | 2.324 | 2.519 | 2.772 | 3.303 | 3.897 | 4.482 | 4.936 |
| 2.00 | 0.82 | 2.476 | 2.627 | 2.747 | 2.972 | 3.131 | 3.418 | 3.765 | 4.140 | 4.444 |
| 2.50 | 0.85 | 2.872 | 3.102 | 3.274 | 3.567 | 3.666 | 3.633 | 3.699 | 3.798 | 3.930 |
| 3.00 | 0.87 | 3.131 | 3.389 | 3.633 | 4.029 | 4.065 | 3.798 | 3.666 | 3.666 | 3.666 |
| 4.00 | 0.89 | 3.418 | 3.765 | 4.065 | 4.674 | 4.633 | 4.029 | 3.699 | 3.504 | 3.389 |
| 6.00 | 0.93 | 3.699 | 4.140 | 4.558 | 5.476 | 5.328 | 4.330 | 3.765 | 3.446 | 3.217 |
| 8.00 | 0.94 | 3.831 | 4.330 | 4.805 | 5.927 | 5.726 | 4.482 | 3.831 | 3.446 | 3.188 |
| 10.00 | 0.95 | 3.897 | 4.406 | 4.936 | 6.297 | 5.977 | 4.558 | 3.864 | 3.446 | 3.159 |
| 25.00 | 0.98 | 4.102 | 4.674 | 5.285 | 7.374 | 6.643 | 4.849 | 4.029 | 3.567 | 3.217 |

GENERAL STABILITY OF A ROTOR ON AN ELASTIC FOUNDATION WITH INTERNAL FRICTION DAMPING

DM = M1/M2 = 0. R = K2/KY = 10.00 A = WCRO/D2 = 10.00 WCY/WCRO = 0.302 D = D2/D1

| ALPHA | WCX/WCRO | D1=0.00 | D1=20.0 | D1=40.00 | D1=100 | D1=200 | D1=400 | D1=600 | D1=800 | D1=1000 |
|---|---|---|---|---|---|---|---|---|---|---|
| 0.04 | 0.06 | 9.928 | 28.625 | 28.625 | 28.625 | 28.625 | 28.625 | 28.625 | 28.625 | 28.625 |
| 0.10 | 0.10 | 9.928 | 28.625 | 28.625 | 28.625 | 28.625 | 28.625 | 28.625 | 28.625 | 28.625 |
| 0.20 | 0.14 | 9.752 | 28.625 | 28.625 | 28.625 | 28.625 | 28.625 | 28.625 | 28.625 | 28.625 |
| 0.40 | 0.20 | 9.319 | 28.625 | 28.625 | 28.625 | 28.625 | 28.625 | 28.625 | 28.625 | 28.625 |
| 0.50 | 0.22 | 9.091 | 28.625 | 28.625 | 28.625 | 28.625 | 28.625 | 28.625 | 28.625 | 28.625 |
| 0.60 | 0.24 | 8.633 | 28.625 | 28.625 | 28.625 | 28.625 | 28.625 | 28.625 | 28.625 | 28.625 |
| 0.70 | 0.26 | 7.971 | 28.625 | 28.625 | 28.625 | 28.625 | 28.625 | 28.625 | 28.625 | 28.625 |
| 0.80 | 0.27 | 6.758 | 28.625 | 28.625 | 28.625 | 28.625 | 28.625 | 28.625 | 28.625 | 28.625 |
| 0.90 | 0.29 | 4.482 | 28.625 | 28.625 | 28.625 | 28.625 | 28.625 | 28.625 | 28.625 | 28.625 |
| 1.00 | 0.30 | 0.302 | 28.625 | 28.625 | 28.625 | 28.625 | 28.625 | 28.625 | 28.625 | 28.625 |
| 1.10 | 0.31 | 3.864 | 28.625 | 28.625 | 28.625 | 28.625 | 28.625 | 28.625 | 28.625 | 28.625 |
| 1.20 | 0.33 | 5.676 | 28.625 | 28.625 | 28.625 | 28.625 | 28.625 | 28.625 | 28.625 | 28.625 |
| 1.30 | 0.34 | 6.585 | 28.625 | 28.625 | 28.625 | 28.625 | 28.625 | 28.625 | 28.625 | 28.625 |
| 1.50 | 0.36 | 7.441 | 28.625 | 28.625 | 28.625 | 28.625 | 28.625 | 28.625 | 28.625 | 28.625 |
| 1.70 | 0.38 | 7.839 | 28.625 | 28.625 | 28.625 | 28.625 | 28.625 | 28.625 | 28.625 | 28.625 |
| 2.00 | 0.41 | 8.175 | 28.625 | 28.625 | 28.625 | 28.625 | 28.625 | 28.625 | 28.625 | 28.625 |
| 2.50 | 0.45 | 8.480 | 28.625 | 28.625 | 28.625 | 28.625 | 28.625 | 28.625 | 28.625 | 28.625 |
| 3.00 | 0.48 | 8.633 | 28.625 | 28.625 | 28.625 | 28.625 | 28.625 | 28.625 | 28.625 | 28.625 |
| 4.00 | 0.53 | 8.785 | 28.625 | 28.625 | 28.625 | 28.625 | 28.625 | 28.625 | 28.625 | 28.625 |
| 6.00 | 0.61 | 8.862 | 28.625 | 28.625 | 28.625 | 28.625 | 28.625 | 28.625 | 28.625 | 28.625 |
| 8.00 | 0.67 | 8.938 | 28.625 | 28.625 | 28.625 | 28.625 | 28.625 | 28.625 | 28.625 | 28.625 |
| 10.00 | 0.71 | 8.938 | 28.625 | 28.625 | 28.625 | 28.625 | 28.625 | 28.625 | 28.625 | 28.625 |
| 25.00 | 0.85 | 9.014 | 10.630 | 10.191 | 9.167 | 8.038 | 6.931 | 6.355 | 6.027 | 5.777 |

# Appendix D

# Hydrodynamic Bearing Equations

## D.1 DERIVATION OF THE GENERAL REYNOLDS EQUATION FOR AN ISOTHERMAL COMPRESSIBLE FLUID

Consider the forces acting on a small volume element $\tau$. The equations of motion of the volume will be

$$\iiint_V \rho \frac{D\vec{u}}{Dt} d\tau = \iint_S \vec{T}^{\nu_i} \cdot \vec{n}\, ds + \iiint_V \vec{F}\, d\tau \tag{D.1}$$

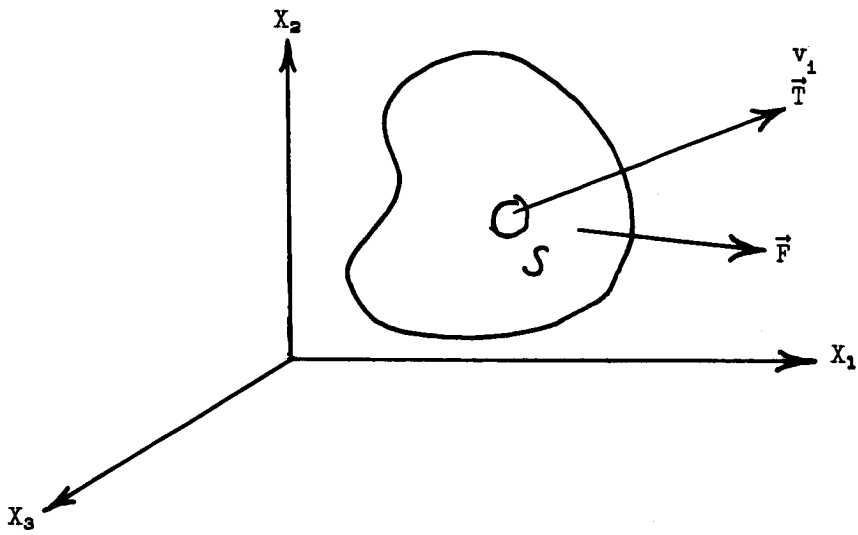


FIGURE D.1.–Forces acting on a small volume element.

Where

$\vec{F}$ = body force vector

$\vec{T}$ = traction vector = $\sigma_{ij} \nu_j \vec{n_i}$

By employing Gauss's theorem Eq. (D.1) becomes

$$\iiint_V \left[\rho \frac{Du_i}{Dt} - \frac{\partial \sigma_{ij}}{\partial X_j} - F_i\right] d\tau = 0 \tag{D.2}$$

Since the volume of integration is arbitrary, then

$$\rho \frac{Du_i}{Dt} = \frac{\partial \sigma_{ij}}{\partial X_j} + F_i; \qquad i = 1, 2, 3 \tag{D.3}$$

Let

$$\sigma_{ij} = -P\delta_{ij} + \tau_{ij} \tag{D.4}$$

where $\tau_{ij}$ = viscous shear stresses.

If the fluid is assumed to be Newtonian, then the viscous shear stresses are linearly related to the rate of shear strain. This is represented by

$$\tau_{ij} = C_{ijkl}\epsilon_{kl} \tag{D.5}$$

If the fluid is also isotropic, then the fourth-order tensor $C_{ijkl}$ is symmetric and invariant under coordinate transformation and is given by

$$C_{ijkl} = \lambda\delta_{ij}\delta_{kl} + \mu[\delta_{ik}\delta_{jl} + \delta_{il}\delta_{jk}] + \gamma[\delta_{ik}\delta_{jl} - \delta_{il}\delta_{jk}] \tag{D.6}$$

Hence the stress-strain rate for an isotropic Newtonian fluid is given by

$$\tau_{ij} = \lambda\delta_{ij}\Delta + 2\mu\epsilon_{ij} \tag{D.7}$$

Where

$\lambda, \mu$ = Lamé constants

$\epsilon_{ij}$ = symmetric strain rate tensor

$= \frac{1}{2}[u_{i,j} + u_{j,i}]$

$\Delta$ = dilatation $= \epsilon_{ii} = u_{i,i}$

Contraction of Eq. (D.7) results in

$$\tau_{ii} = [3\lambda + 2\mu]\Delta \tag{D.8}$$

In the case of an incompressible fluid where the dilatation $\Delta$ is zero, then the sum of the viscous normal stresses $\tau_{ii}$ is zero. If we assume that $\tau_{ii}$ will be zero even for a compressible mediam, then

$$3\lambda + 2\mu = 0 \tag{D.9}$$

or

$$\lambda = -2/3\mu$$

This is known as Stokes approximation and eliminates one of the Lamé constants from the governing equations of motion. This approximation has been shown to be true only for the case of a monatomic gas, but usually results in only higher order deviations for most gases at normal temperature and pressure. This assumption is invalid in regions where large pressure or velocity gradients exist. As an example, the assumption breaks down in the immediate vicinity of a supply orifice to an externally pressurized bearing if a shock wave occurs.

$$\tau_{ij} \underset{(D.7,\,9)}{=} \mu\left[-\frac{2}{3}\delta_{ij}u_{k,k} + u_{i,j} + u_{j,i}\right] \tag{D.10}$$

Therefore the equations of motion are:

$$\rho\frac{Du_i}{Dt} \underset{(D.3,\,4,\,10)}{=} -\frac{\partial P}{\partial X_i} + F_i + \frac{\partial}{\partial X_j}\left[\mu\left(-\frac{2}{3}\delta_{ij}u_{k,k} + u_{i,j} + u_{j,i}\right)\right] \tag{D.11}$$

If the viscosity $\mu$ is not a function of the coordinates $X$, then Eq. (D.11) reduces to

$$\frac{\rho Du_i}{Dt} = -\frac{\partial P}{\partial X_i} + F_i + \mu\left[\frac{1}{3}u_{j,ij} + u_{i,jj}\right] \tag{D.12}$$

If the body forces $F_i$ are zero, then Eq. (D.12) relates the inertia forces to the rates of change of the hydrostatic pressure and viscous shear stresses. The major assumption in the formulation of a lubrication problem is that the flow is laminar. This is possible only if the inertia terms of the left-hand side of Eq. (D.12) are small in comparison to the viscous shear forces. This is equivalent to the statement that the Reynolds number is less than 1

$$R_e^* = \frac{\text{Inertia forces}}{\text{Viscous forces}} \approx \frac{\rho\dfrac{U^2}{L}}{\mu\dfrac{U}{h^2}} = \frac{UL}{\nu}\left(\frac{h}{L}\right)^2$$

Where

$R_e^*$ = reduced Reynolds number
$U$ = velocity
$L$ = characteristic bearing length
$h$ = characteristic film thickness
$\nu$ = kinematic viscosity

If

$$R_e^* \ll 1$$

then

$$\frac{\partial P}{\partial X_i} = \mu\left[\frac{1}{3}u_{j,ij} + u_{i,jj}\right] \tag{D.13}$$

Assign for $X_i$ and $u_i$ the following orders of magnitude:

$$X_1 = L \qquad u_1 = U$$

$$X_2 = h \qquad u_2 = \delta U$$

$$X_3 = L \qquad u_3 = U$$

where

$$\left(\frac{h}{L}\right) \quad \text{and} \quad \left(\frac{\delta U}{U}\right) \ll 1$$

As an example, let $i = 1$, in Eq. (D.12)

$$\frac{\partial P}{\partial X_1} = \mu\left[\frac{1}{3}\left(\frac{\partial^2 u_1}{\partial X_1 \partial X_1} + \frac{\partial^2 u_2}{\partial X_1 \partial X_2} + \frac{\partial^2 u_3}{\partial X_1 \partial X_3}\right) + \frac{\partial^2 u_1}{\partial X_1^2} + \frac{\partial^2 u_1}{\partial X_2^2} + \frac{\partial^2 u_1}{\partial X_3^2}\right] \tag{D.14}$$

It is seen that the term $\partial^2 u_1/\partial X_2^2$ is an order of magnitude higher than the other terms. Hence, Eq. (D.13) reduces to:

$$\frac{\partial P}{\partial X_1} = \mu \frac{\partial^2 u_1}{\partial X_2^2} \tag{D.15}$$

Likewise for $i = 2$ and 3

$$\frac{\partial P}{\partial X_2} = 0 \tag{D.16}$$

$$\frac{\partial P}{\partial X_3} = \mu \frac{\partial^2 u_3}{\partial X_2^2} \tag{D.17}$$

For convenience let

$$X_1 = X; \qquad u_1 = u$$

$$X_2 = Y; \qquad u_2 = V$$

$$X_3 = Z; \qquad u_3 = W$$

Equations (D.14–D.16) may be written as

$$\frac{\partial P}{\partial X}=\mu\frac{\partial^2 u}{\partial Y^2} \tag{D.18}$$

$$\frac{\partial P}{\partial Y}=0 \tag{D.19}$$

$$\frac{\partial P}{\partial Z}=\mu\frac{\partial^2 W}{\partial Y^2} \tag{D.20}$$

Since $\partial P/\partial Y_{(D.18)}=0$, the fluid film pressure may be considered as uniform across the film thickness. Equations (D.17) and (D.19) may be integrated directly and upon application of the following boundary conditions:

$$y=0 \qquad u(0)=U_1; \qquad W(0)=W_1$$

$$y=h \qquad u(h)=U_2; \qquad W(h)=W_2$$

(where $h=h(X,z,t)$ is the film thickness distribution)

$$u=\frac{1}{2\mu}\left(\frac{\partial P}{\partial X}\right)(Y-h)\,Y+U_1\left[\frac{h-Y}{h}\right]+U_2\frac{Y}{h} \tag{D.21}$$

$$W=\frac{1}{2\mu}\left(\frac{\partial P}{\partial Z}\right)[Y-h]\,Y+W_1\left[\frac{h-Y}{h}\right]+\frac{W_2 Y}{h} \tag{D.22}$$

Equations (D.20) and (D.21) are insufficient to formulate the lubrication problem. Another relationship is required. This is the continuity equation which is the statement of the conservation of mass in an elemental volume and is given by

$$\frac{\partial \rho}{\partial t}+\frac{\partial(\rho u)}{\partial X}+\frac{\partial(\rho V)}{\partial Y}+\frac{\partial(\rho W)}{\partial Z}=0 \tag{D.23}$$

If we assume a compressible isothermal fluid film which obeys the perfect gas laws, then

$$P=\mathscr{K}\rho$$

and Eq. (D.23) becomes:

$$\frac{\partial(PV)}{\partial Y}=-\left[\frac{\partial P}{\partial t}+\frac{\partial(Pu)}{\partial X}+\frac{\partial(PW)}{\partial Z}\right] \tag{D.24}$$

Integrate Eq. (D.23) across the fluid film

$$PV\Big|_{y=0}^{y=h} = -\int_0^{h(x,z,t)} \left[\frac{\partial P}{\partial t} + \frac{\partial (Pu)}{\partial X} + \frac{\partial (PW)}{\partial Z}\right] dy \tag{D.25}$$

In order to perform the above integration, it is necessary to place the derivatives with respect to $X$ and $Z$ outside the integration sign. To accomplish this we will use the Leibniz rule for differentiating under the integral sign when the limits of integration are a function of the current variable itself. If

$$I(\beta(x), \alpha(x), X) = \int_{\alpha(x)}^{\beta(x)} f(x,y)\, dy$$

then

$$\frac{dI}{dX} = \frac{\partial I}{\partial X} + \frac{\partial I}{\partial \beta(x)}\left(\frac{\partial \beta}{\partial X}\right) + \frac{\partial I}{\partial \alpha}\left(\frac{\partial \alpha}{\partial X}\right)$$

Hence:

$$\frac{dI}{dX} = \int_{\alpha(x)}^{\beta(x)} \frac{\partial f}{\partial X}\, dy + f\Big|_{y=\beta(x)} \frac{\partial \beta}{\partial X} - f\Big|_{y=\alpha(x)} \frac{\partial \alpha}{\partial X} \tag{D.26}$$

Thus:

$$\left.\begin{aligned} \int_0^h \frac{\partial}{\partial X}(Pu)dy &= -\frac{\partial}{\partial X}\int_0^h Pu dy + Pu\Big|_{y=h}\frac{\partial h}{\partial X} \\ \text{and} \\ \int_0^h \frac{\partial}{\partial Z}(PW)dy &= -\frac{\partial}{\partial Z}\int_0^h PW dy + PW\Big|_{y=h}\frac{\partial h}{\partial Z} \end{aligned}\right\} \tag{D.27}$$

After integrating Eq. (D.25) using the velocity profiles and rearranging

$$\frac{1}{6\mu}\left[\frac{\partial}{\partial X}\left(Ph^3\frac{\partial P}{\partial X}\right) + \frac{\partial}{\partial Z}\left(Ph^3\frac{\partial P}{\partial Z}\right)\right] = 2P(V_2 - V_1) + 2\frac{\partial P}{\partial t}h$$

$$+ h\left\{\frac{\partial}{\partial X}[P(U_2 + U_1)] + \frac{\partial}{\partial Z}[P(W_2 + W_1)]\right\} + P(U_1 - U_2)\frac{\partial h}{\partial X}$$

$$+ P(W_1 - W_2)\frac{\partial h}{\partial Z} \tag{D.28}$$

The above equation represents the general three-dimensional Reynolds equation as applied to an isothermal compressible fluid film.

## D.2 DISCUSSION OF ASSUMPTIONS INVOLVED IN THE DERIVATION OF REYNOLDS EQUATION

The derivation of Reynolds equation as applied to a compressible isothermal fluid film proceeds from the consideration of the sum of the inertia, body forces, and tractions acting over a volume of fluid. By means of Gauss' theorem, the surface traction integral is converted to a volume integral to obtain the partial differential equations as applied to an infinitesimal element. The first assumption employed is:

(a) The fluid is Newtonian.

This implies that the fluid properties are invariant (isotropic) or unchanging in any direction and also that the stress tensor is linearly related to the strain rate tensor. (For fluids such as greases, the stress-strain rate is not linear at low shear rates and hence the media is non-Newtonian.)

By assuming a linear stress-strain, rate relationship, two Lamé constants are required to express the viscous shear stress in terms of shear strain rate (as an example, in solid mechanics these two constants are usually expressed in terms of $E$, Young's modulus, and $\nu$, Poisson's ratio, or $E$ and $G$ = the shear modulus). The constants appearing in Eq. (D.7) are $\lambda$ and $\mu$ the fluid viscosity. For the case of an incompressible fluid, the second Lamé constant $\lambda$ does not enter into the equations, since the dilatation is zero (see Eq. (D.8)). In order to remove $\lambda$, it is assumed that—

(b) The bulk modulus $(3\lambda + 2\mu) = 0$.

By this means we are able to express $\lambda$ in terms of $\mu$. This is known as Stokes approximation, and thus the pressure $P$ is independent of the dilatation. This assumption has shown to be valid only for a monatomic gas in which higher order molecular collisions are neglected and the gas is not an extreme pressure condition. In the normal gas bearing application, where the flow is laminar, the dilatation $\Delta$ is small and only secondary errors accrue. The assumption is invalid in regions where there are high velocity or pressure gradients. Such regions would be at the leading or trailing edge of a partial journal bearing where high-velocity gradients exist. Another region in which the assumption breaks down is in the immediate vicinity of a supply orifice for an externally pressurized bearing. In this case it is possible to have a local shock front formed downstream, and associated with it would be high-pressure gradients.

Equation (D.12) is usually referred to as the Navier-Stokes equations and represents three highly nonlinear partial differential equations. As such, no general solutions are available for Eq. (D.12) in its present

form. To reduce the complexity of Eq. (D.12), the following assumptions are made:

(c) The effect of the body forces $F_i$ are negligible.

For fluid film bearings with the body forces due to gravity only, this is true. In the case where the body forces are exerted by magnetic effects (magnetohydrodynamics), the forces $F_i$ can be sizable. The key assumption in reducing the complexity of the general Navier-Stokes equations in the derivation Reynolds equation is the assumption that the flow is laminar viscous and the inertia effects are small in comparison to the viscous shear forces.

This assumption is equivalent to the statement that

(d) The reduced Reynolds number $R_e^*$ is much less than unity.

This permits us to set the left-hand side of Eq. (D.12) equal to zero. To demonstrate the validity of statement (d), the reduced Reynolds number will be calculated for a typical gas bearing.

*Example*

The effective Reynolds number must be less than one for the Reynolds equation to be valid, or

$$R_e^* \ll 1$$

where

$$R_e^* = \frac{UL}{\nu}\left(\frac{h}{L}\right)^2$$

The effective Reynolds number will be calculated corresponding to typical operating conditions of a pivoted pad gas bearing experimental test rotor:

$N = 18\,000$ rpm
$R =$ radius of rotor $= 2$ in.
$U = \dfrac{2\pi R}{60} N = 3768$ in./sec
$\mu = 2.61 \times 10^{-9}$ lb-sec/in.$^2$
$P = 14.7$ psia
$T = 70°$ F
$\rho = \dfrac{P}{gRT} = 1.1 \times 10^{-7}$ lb-sec$^2$/in.$^4$
$h = 0.001$ in. = average shoe film thickness
$\nu = \dfrac{\mu}{\rho} = 2.38 \times 10^{-2}$

$$L = R\alpha = 3.3 \text{ in.}$$

$$R_e^* = \frac{(3.768)(3.3)}{2.38 \times 10^{-2}} \left( \frac{1 \times 10^{-3}}{3.3} \right)^2 = 4.72 \times 10^{-2}$$

or

$$R_e^* \approx 0.05$$

Thus the assumption that the inertia terms are small in comparison to the viscous shear forces is valid and hence may be neglected in the range of operation considered. It has been pointed out by Constantinescu and Gross that in cases where $R_e^*$ exceeds 1, the error induced by neglecting the contribution of the inertia terms is still small, acting so as to increase the bearing load capacity and friction losses.

## D.3 DERIVATION OF FILM THICKNESS BETWEEN JOURNAL AND BEARING

Consider the triangle $O_b$, $R$, $O_j$ of Fig. D.2

$$\cos \gamma = \frac{R - e_r}{R + C - h} \tag{D.29}$$

where

$e_r = e \cos (\theta - \phi - \gamma)$

$h$ = bearing film thickness

If $C/R \ll 1$, then:

(a) $\cos \gamma \approx 1.0$

(b) $e_r \approx e \cos (\theta - \phi)$

Equation (D.29) becomes

$$1.0 = \frac{R - e \cos (\theta - \phi)}{R + C - h(\theta)} \tag{D.30}$$

Solving for $h(\theta)$

$$h(\theta) = C [1 + \epsilon \cos (\theta - \phi)] \tag{D.31}$$

where

$\epsilon$ = eccentricity ratio $= e/C$

Let the eccentricity vector $\vec{e}$ be given by

$$\vec{e} = e\vec{e}_r = -X\vec{n}_x + Y\vec{n}_y \tag{D.32}$$

Taking the dot product of Eq. (D.32) with respect to $\vec{n}_x$ and $\vec{n}_y$

$$e\vec{e}_r = (-X\vec{n}_x + Y\vec{n}_y) \cdot (\vec{n}_x; \vec{n}_y)$$

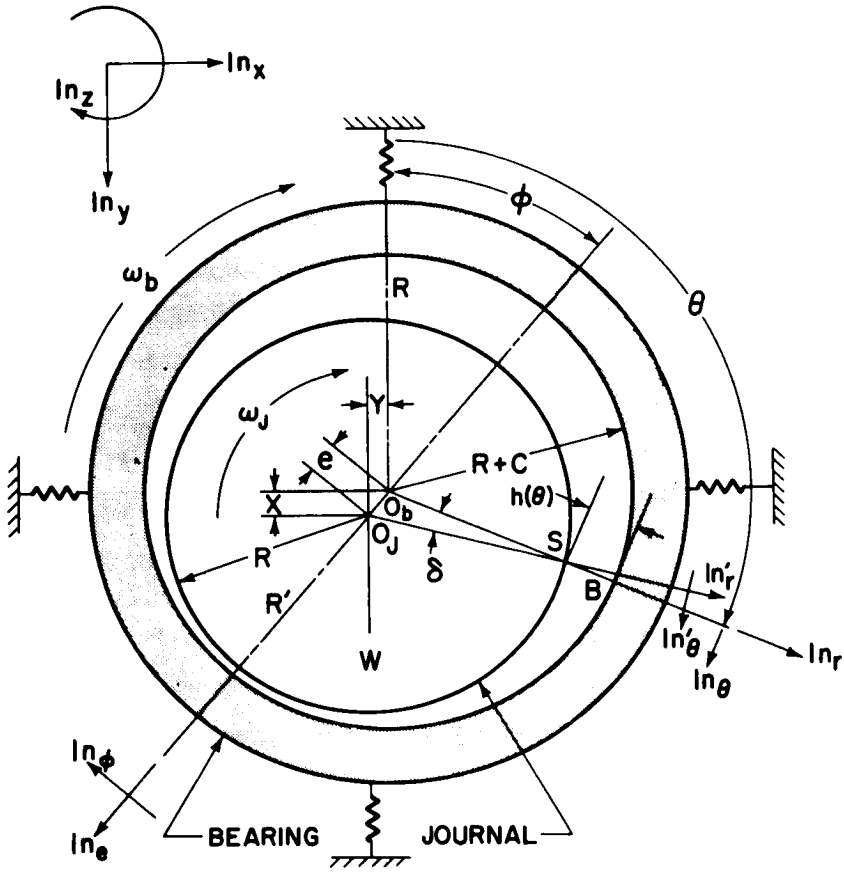


FIGURE D.2. – Bearing geometry.

yields

(a) $-e \sin \phi = X$

(b) $e \cos \phi = Y$ (D.33)

The film thickness in terms of Cartesian coordinates is given by

$$h(\theta) = C + Y \cos \theta + X \sin \theta \quad \text{(D.31, D.33)}$$

## D.4 KINEMATICS

### D.4.1 Journal Motion

The velocity of an arbitrary point $S$ on the journal surface in reference frame $R$ is given by

$$\overset{R\to S}{\mathbf{V}} = \overset{R\to O_j/O_B}{\mathbf{V}} + \overset{R\to S/O_j}{\mathbf{V}} \tag{D.34}$$

where

$R$ = reference frame fixed in bearing

$\overset{R\to O_j/O_B}{\mathbf{V}}$ = velocity of journal center $O_j$ relative to bearing $O_B$ in $R$

$\overset{R\to S/O_j}{\mathbf{V}}$ = velocity of point $S$ relative to the journal center $O_j$ in $R$

$$\overset{R\to O/O_B}{\mathbf{V}} = \frac{{}^R d}{dt}[e\vec{e}_r] = \dot{e}\vec{e}_r + {}^R\vec{\omega}^{R'} \times (e\vec{e}_r)$$

where

${}^R\vec{\omega}^{R'}$ = angular velocity of rotating reference frame $R'$ in $R$

$= \dot{\phi}\vec{n}_z$ = precession or whirl speed

$\overset{R\to O_j/O_B}{\mathbf{V}} = \dot{e}\vec{e}_r + e\dot{\phi}\vec{e}_\phi$

transforming to the $\vec{n}_r$, $\vec{n}_\theta$ vector set

$$\overset{R\to O_j/O_B}{\mathbf{V}} = -[\dot{e}\cos(\theta-\phi) + e\dot{\phi}\sin(\theta-\phi)]\vec{n}_r + [\dot{e}\sin(\theta-\phi) - e\dot{\phi}\cos(\theta-\phi)]\vec{n}_\theta \tag{D.35}$$

If the journal eccentricity is expressed in Cartesian coordinates, then the velocity of the journal center is

$$\overset{R\to O_j/O_B}{\mathbf{V}} = -[\dot{X}\sin\theta + \dot{Y}\cos\theta]\vec{n}_r + [\dot{Y}\sin\theta - \dot{X}\cos\theta]\vec{n}_\theta \tag{D.36}$$

The velocity of point $S$ relative to $O$ is given by

$$\overset{R\to S/O_j}{\mathbf{V}} = \overset{R'\to S/O_j}{\mathbf{V}} + {}^R\vec{\omega}^{R'} \times_{O_j} \vec{PS}$$

where

${}^R\omega^j$ = angular velocity of journal in rotating reference frame $R'$

$\overset{R'\to S/O_j}{\mathbf{V}} = {}^{R'}\omega^j\vec{n}_z \times (R\vec{n}_r)$

$= {}^{R'}\omega^j R\vec{n}'_\theta$

$\overset{R\to S/O_j}{\mathbf{V}} = (\dot{\phi} + {}^{R'}\omega^j)R\vec{n}'_\theta = {}^R\omega^j R\vec{n}'_\theta$ (D.37)

The total velocity of point $S$ in $R$ is given by

$$\left.\begin{aligned} {}^{R\to S}\vec{V} &= -[\dot{e}\cos(\theta-\phi)+e\dot{\phi}\sin(\theta-\phi)]\vec{n}_r \\ &\quad +[\dot{e}\sin(\theta-\phi)-e\dot{\phi}\cos(\theta-\phi)]\vec{n}_\theta + {}^R\omega^j R\vec{n}'_\theta \end{aligned}\right\} \quad (D.38)$$

or

$$\begin{aligned} {}^{R\to S}\vec{V} &= -[\dot{X}\sin\theta+\dot{Y}\cos\theta]\vec{n}_r+[\dot{Y}\sin\theta \\ &\quad -\dot{X}\cos\theta]\vec{n}_\theta+{}^R\omega^j R\vec{n}_\theta \end{aligned}$$

The $\vec{n}'_\theta$ unit vector is given by

$$\vec{n}'_\theta=\cos\gamma\,\vec{n}_\theta+\sin\gamma\,\vec{n}_r \quad (D.39)$$

now, consider triangle $O_j$, $O_b$, $S$

$$\sin\gamma=\frac{e\sin(\theta-\phi-\gamma)}{R+C-h}$$

if $C/R \ll 1.0$, then $\gamma \ll 1.0$

Hence

$$\sin\gamma=\gamma\approx\frac{e\sin(\theta-\phi)}{R}$$

Since

$$h=C+e\cos(\theta-\phi)$$

$$\frac{\partial h}{\partial\theta}=-e\sin(\theta-\phi)$$

hence

$$\gamma=\frac{1}{R}\frac{\partial h}{\partial\theta}$$

$$\vec{n}'_\theta=\vec{n}_\theta-\frac{1}{R}\frac{\partial h}{\partial\theta}\vec{n}_r \quad (D.40)$$

The total velocity of point $S$ in $R$ is given by

$${}^{R}\vec{V}^{S}\underset{(D.37,\,D.39)}{=}-\left[\dot{X}\sin\theta+\dot{Y}\cos\theta+{}^R\omega^j\frac{\partial h}{\partial\theta}\right]\vec{n}_r$$

$$+[\dot{Y}\sin\theta-\dot{X}\cos\theta+R\,{}^R\omega^j]\vec{n}_\theta \quad (D.41)$$

$$\overset{R\to S}{\mathbf{V}} \underset{(D.37,\ D.39)}{=} -\left[\dot{e}\cos(\theta-\phi)+e\dot{\phi}\sin(\theta-\phi)+{}^{R}\omega^{j}\frac{\partial h}{\partial\theta}\right]\vec{\mathbf{n}}_r$$

$$+[\dot{e}\sin(\theta-\phi)-e\dot{\phi}\cos(\theta-\phi)+R\omega]\vec{\mathbf{n}}_\theta$$

Differentiating Eq. (D.31)

$$\frac{dh}{dt}=\dot{e}\cos(\theta-\phi)+e\sin(\theta-\phi)\dot{\phi}$$

$$=\dot{e}\cos(\theta-\phi)-\dot{\phi}\frac{\partial h}{\partial\theta} \tag{D.42}$$

$$\therefore \overset{R\to S}{\mathbf{V}} \underset{(D.41,\ D.40)}{=} -\left[\frac{dh}{dt}+{}^{R}\omega^{j}\frac{\partial h}{\partial\theta}\right]\vec{\mathbf{n}}_r+\left[{}^{R}\omega^{j}R-\frac{d}{dt}\left(\frac{\partial h}{\partial\theta}\right)\right]\vec{\mathbf{n}}_\theta \tag{D.43}$$

The velocity of point $S$ in a Newtonian reference frame is given by

$$\overset{N\to S}{\mathbf{V}}=\overset{N\to S/O_b}{\mathbf{V}}+\overset{N\to O_b}{\mathbf{V}}$$

where

$\overset{N\to O_b}{\mathbf{V}}$ = velocity of bearing center

$$=\dot{X}_0\vec{\mathbf{n}}_x+\dot{Y}_0\vec{\mathbf{n}}_y$$

$$\overset{N\to S}{\mathbf{V}}=\overset{N\to O_b}{\mathbf{V}}+\overset{R\to S/O_b}{\mathbf{V}}+\overset{N\to R}{\boldsymbol{\omega}}\times\overset{O_b\to S}{\mathbf{P}}$$

where ${}^{N}\omega^{R}=\omega^{b}=$ bearing angular speed in Newtonian reference frame

$$\underset{(D.42)}{=}\dot{X}_0\vec{\mathbf{n}}_x+\dot{Y}_0\vec{\mathbf{n}}_y+\left[({}^{N}\omega^{R}+{}^{R}\omega^{j})R-\frac{d}{dt}\left(\frac{\partial h}{\partial\theta}\right)\right]\vec{\mathbf{n}}_\theta-\left[\frac{dh}{dt}+{}^{R}\omega^{j}\frac{\partial h}{\partial\theta}\right]\vec{\mathbf{n}}_r \tag{D.44}$$

$$\overset{N\to E}{\mathbf{V}}=\dot{X}_0\vec{\mathbf{n}}_x+\dot{Y}_0\vec{\mathbf{n}}_y+(R+C){}^{N}\omega^{R}\vec{\mathbf{n}}_\theta$$

$$=(\dot{X}_0\cos\theta+\dot{Y}_0\sin\theta)\vec{\mathbf{n}}_r$$

$$+(-\dot{X}_0\sin\theta+\dot{Y}_0\cos\theta+(R+C){}^{N}\omega^{R})\vec{\mathbf{n}}_\theta \tag{D.45}$$

The journal-bearing velocity components are given by

$$U_2=-\dot{X}_0\sin\theta+\dot{Y}_0\cos\theta+(R+C)\omega_b$$

$$U_1=-\dot{X}_0\sin\theta+\dot{X}_0\cos\theta+R\omega_j-\frac{d}{dt}\left(\frac{\partial h}{\partial\theta}\right)$$

$$V_2 = \dot{X}_0 \cos\theta + \dot{Y}_0 \sin\theta$$

$$V_1 = -\left[\frac{dh}{dt} + {}^R\omega^J \frac{\partial h}{\partial \theta}\right]$$

$$W_2 = W_1 = 0$$

Substituting the above velocity components into Eq. (D.28) and after eliminating higher order terms, $h/R$, $C/R$, $\dot{X}_0/R\omega$, $\dot{Y}_0/R\omega$ results in the following dimensionless Reynolds equation

$$\frac{\partial}{\partial\theta}\left(PH^3\frac{\partial P}{\partial\theta}\right) + \left(\frac{R}{L}\right)^2 \frac{\partial}{\partial\eta}\left(PH^3\frac{\partial P}{\partial\eta}\right) = \Lambda\frac{\partial}{\partial\theta}(PH) + \frac{\sigma\partial}{\partial\tau}(PH) \tag{D.46}$$

where

$P$ = dimensionless pressure $= p/P_a$

$P_a$ = ambient pressure

$\Lambda$ = compressibility parameter $= \dfrac{6\mu(\omega_j + \omega_b)}{P_a}\left(\dfrac{R}{C}\right)^2$

$H$ = dimensionless film thickness $= h/C$

$L$ = bearing width

$\eta$ = dimensionless width $= Z/L$

$\sigma$ = squeeze film number $= \dfrac{12\mu f}{Pa}\left(\dfrac{R}{C}\right)^2$

$\tau$ = dimensionless time $= tf$

$f$ = system characteristic frequency

To obtain the form of the Reynolds equation with respect to the rotating reference frame $R'$, we transform the time derivative of pressure as follows

$$\frac{{}^R\partial P}{\partial t} = \frac{{}^{R'}\partial P}{\partial t} + \dot{\phi}\frac{\partial P}{\partial\theta}$$

and substitute the above into Eq. (D.45) to obtain

$$\frac{\partial}{\partial\theta}\left(PH^3\frac{\partial P}{\partial\theta}\right) + \left(\frac{R}{L}\right)^2\frac{\partial}{\partial\eta}\left(PH^3\frac{\partial P}{\partial\eta}\right) = \Lambda\left[2\frac{{}^{R'}\partial}{\partial T'}(PH) + \left(1 - \frac{2\dot{\phi}}{\omega}\right)\frac{\partial(PH)}{\partial\theta}\right] \tag{D.47}$$

where

$H = 1 + \epsilon\cos\theta$

$\omega = \omega_j + \omega_b$

$T' = \omega t$

Examination of Eqs. (D.46) and (D.47) shows that the form of the pressure equation depends upon the system of coordinates used. For

example, if the rotor motion is stable synchronous precession in which $e$ is constant (vertical rotor), the time-transient term of Eq. (D.46) expressed in fixed coordinates is nonzero, but the transient pressure term of Eq. (D.47) expressed in the relative reference frame $R'$ is zero.

The influence of compressibility can be neglected only when both the compressibility number $\Lambda$ and squeeze film number $\sigma$ approach zero. In this case Eq. (D.47) reduces to

$$\frac{\partial}{\partial\theta}\left(H^3\frac{\partial P}{\partial\theta}\right)+\left(\frac{R}{L}\right)^2\frac{\partial}{\partial\eta}\left(H^3\frac{\partial P}{\partial\eta}\right)=\Lambda\left[\left(1-\frac{2\dot{\phi}}{\omega}\right)\frac{\partial H}{\partial\theta}+\frac{2}{\omega}\dot{H}\right] \quad \text{(D.48)}$$

which represents the governing Reynolds equation for an incompressible fluid.

## D.5 BEARING FRICTION

The friction shear stress acting on the rotating journal is given by

$$\tau=\mu\frac{\partial u}{\partial y}\bigg|_{y=h} \quad \text{(D.49)}$$

$$u(y)=\frac{1}{2\mu R}\frac{\partial P}{\partial\theta}\,y(y-h)+\frac{y}{h}\,(R\omega+\dot{e}\sin\theta-\dot{\phi}e\cos\theta)$$

$$\therefore\tau=\frac{h}{2R}\frac{\partial P}{\partial\theta}+\frac{\mu}{h}\,[R\omega-\dot{\phi}e\cos\theta+\dot{e}\sin\theta] \quad \text{(D.50)}$$

The first term in the above expression represents the shear stress contribution due to pressure profile drag and the second term represents the velocity drag. An order of magnitude analysis shows that the pressure profile drag may be neglected in comparison to the velocity drag:

$$\tau\approx\left(\frac{C}{R}\right)\left(\frac{W}{D}\right)+\mu\left(\frac{R}{C}\right)\omega$$

$$\approx\mu\left(\frac{R}{C}\right)\omega\left[1+\left(\frac{C}{R}\right)^2\left(\frac{W}{\mu R\omega}\right)\right]$$

Typical values for a gas bearing are

$D=2$ in. $\qquad \mu=2.51\times10^{-6}$ lb-sec/in.$^2$

$C=0.001$ in. $\qquad \omega=1000$ rad/sec

$W=50$ lb

$$\tau\approx\mu\left(\frac{R}{C}\right)\omega\left[1+\frac{(10^{-6})(50)}{(2.51\times10^{-6})1\times10^3}\right]$$

$$\approx f[1+0.02]$$

Reference 28 shows that neglecting the shear contribution of the pressure gradient term will cause at most only a 10-percent error in the friction force

$$\therefore \tau = \mu \frac{R}{C} \frac{\omega}{H} \left[ 1 + \left( \frac{C}{R} \right) (\dot{\epsilon} \sin \theta - \dot{\phi} \epsilon \cos \theta) \right]$$

Thus since $C/R \approx 1 \times 10^{-3}$, the journal friction is relatively independent of the precession rate. The net shear force component acting normal to the journal-bearing line of centers is given by

$$F_N = \int_0^L \int_0^{2\pi} \mu \frac{\partial u}{\partial y} \cos \theta R d\theta dz$$

$$= \frac{\mu R^2 L \omega}{C} \int_0^{2\pi} \frac{\cos \theta d\theta}{1 + \epsilon \cos \theta} \tag{D.51}$$

To integrate the above expression consider the following. Let

$$z = e^{i\theta} \qquad \cos \theta = \frac{z + z^{-1}}{2}$$

$$d\theta = -i dz/z$$

$$\int_0^{2\pi} \frac{d\theta}{1 + \epsilon \cos \theta} = i \oint \frac{2dz}{z[2 + \epsilon(z + z^{-1})]} = \frac{i2}{\epsilon} \oint \frac{dz}{(z - z_1)(z - z_2)}$$

where the roots $z_1$ and $z_2$ are given by

$$z_1 = -\frac{1}{\epsilon} \left[ 1 + \sqrt{1 - \epsilon^2} \right]$$

$$z_2 = -\frac{1}{\epsilon} \left[ 1 - \sqrt{1 - \epsilon^2} \right]$$

The root $z_1$ lies inside the unit circle and hence the integral is singular when $z = z_1$. The value of the integral is given by

$$\oint f(z) dz = 2\pi i \, \Sigma Res$$

Where the residue for a simple pole is given by

$$(Z - Z_1) f(z) \Big|_{z = z_2} = \frac{\epsilon}{2\sqrt{1 - \epsilon^2}}$$

$$\therefore \int_0^{2\pi} \frac{d\theta}{1 + \epsilon \cos \theta} = 2\pi i \left[ -\frac{i2}{\epsilon} \right] \left[ \frac{\epsilon}{2\sqrt{1 - \epsilon^2}} \right] = \frac{2\pi}{\sqrt{1 - \epsilon^2}} \tag{D.52}$$

The bearing normal friction force then is given by

$$F_N = \frac{\mu R^2 L \omega}{C} \int_0^{2\pi} \frac{1}{\epsilon} \left[ 1 - \frac{1}{1 + \epsilon \cos \theta} \right] d\theta$$

$$\underset{(D.51,52)}{=} \frac{\mu R^2 L \omega}{C} \frac{2\pi}{\epsilon} \left[ 1 - \frac{1}{(1-\epsilon^2)^{1/2}} \right] \tag{D.53}$$

Under normal steady-state conditions, the bearing friction force is neglected in comparison to the hydrodynamic bearing force in the determination of the journal equilibrium position. There are special circumstances in which the bearing friction force is not negligible, such as when $\epsilon$ approaches unity, then $F_N$ approaches infinity, and when the journal precession rate $\dot{\phi}$ approaches half the rotor speed. In this case the pressure forces approach zero as $\dot{\phi}$ approaches $\omega/2$. Hence the friction force can be of the same order of magnitude as the hydrodynamic forces under these circumstances.

# Appendix E

# Nomenclature

| *Symbol* | *Definition* |
|---|---|
| $A$ | Amplification factor, dim. |
| $A$ | $\omega_{CR_0}/D_2$, Internal rotor friction factor, dim. |
| $A$ | Complex amplitude of limit cycle, dim. |
| $A_b$ | Rotor amplification factor for backward synchronous precession, dim. |
| $A_f$ | Rotor amplification factor for forward synchronous precession, dim. |
| $B$ | Amplitude of half-frequency whirl component, dim. |
| $C$ | Damping coefficient, lb-sec/in |
| $C$ | Radial clearance, in. |
| $C_{ij}$ | Generalized damping coefficients, dim. |
| $C_{ijkl}$ | Fourth-order tensor |
| $C_xC_y$ | Foundation damping in $x$,$y$ direction, lb-sec/in |
| $C_1$ | Foundation damping coefficient, lb-sec/in |
| $C_2$ | Internal friction coefficient, lb-sec/in |
| $D$ | $1/A$ Inverse amplification factor, dim. |
| $D$ | $D_2/D_1$, Damping ratio, dim. |
| $D_1$ | $C_1/m_2$, External damping factor, rad/sec |
| $D_2$ | $C_2/m_2$, Internal damping factor, rad/sec |
| $E$ | Young's modulus, lb/in$^2$ |
| $e_\mu$ | Displacement of rotor mass center from shaft elastic centerline, in. |
| $F$ | Force, lbs |
| $F_{gr}$ | Generalized force |
| $\vec{\mathbf{F}}$ | Force vector, lbs |
| $f$ | $\omega/\omega_{CR}$, Frequency ratio, dim. |
| $f_r$ | Radial force per unit length, lbs/in |
| $f_\theta$ | Tangential force per unit length, lb/in |
| $g$ | Acceleration due to gravity, in/sec$^2$ |
| $g_r$ | Generalized coordinate |

| *Symbol* | *Definition* |
|---|---|
| $H$ | Film thickness, dim. |
| $h$ | Film thickness, in. |
| $I$ | Moment of inertia, lb-sec$^2$-in |
| $K$ | Stiffness coefficient, lb/in |
| $K_{ij}$ | Generalized stiffness coefficients, lb/in |
| $K_r$ | Rotor stiffness characteristic, lb/in |
| $K_s$ | $c/m$, Damping factor, rad/sec |
| $K_x$ | Foundation flexibility in $x$-direction, lb/in |
| $K_y$ | Foundation flexibility in $y$-direction, lb/in |
| $K_1$ | Foundation stiffness, lb/in |
| $K_2$ | Rotor stiffness, lb/in |
| $\mathscr{K}_{ij}$ | $K_{ij}$/m, rad$^2$/sec$^2$ |
| $k$ | Radius of gyration, in. |
| $k_f$ | $\omega_{CR}^2$, rad/sec$^2$ |
| $L$ | Rotor length, in. |
| $L$ | $T$–$V$, Lagrangian |
| $L$ | Bearing width, in. |
| $M,m$ | Rotor mass, lb-sec$^2$/in |
| $M_R$ | Bending moment, in-lbs |
| $M_1$ | Bearing housing mass, lb-sec$^2$/in |
| $M_2$ | Rotor mass, lb-sec$^2$/in |
| $n_1$ | $D_1\left(\frac{R}{1+R}\right)^2$, Stationary damping coefficient of bearing support |
| $n_2$ | $D_2\left(\frac{1}{1+R}\right)^2$, Rotating damping coefficient of shaft unit vector |
| $\vec{\mathrm{n}}$ | Unit vector |
| $_0$ | Subscript |
| $P$ | Real part of complex number, exponent governing system stability |
| $P$ | Pressure, dim. |
| $P_a$ | Ambient pressure, lb/in$^2$ |
| $P_{ij}$ | Potentiometer settings |
| $\vec{\mathrm{P}}$ | Position vector |
| $q_r$ | Generalized coordinate |
| $R'$ | Rotating reference frame with angular velocity $\omega$ |
| $R$ | Fixed reference frame |
| $R$ | $K_2/K_y$, stiffness ratio, dim. |
| $R$ | Radius of rotor, in. |
| $R_e$ | Reynolds number |
| $r$ | Displacement of rotor mass center from steady-state position, in. |

| Symbol | Definition |
|---|---|
| $r$ | Subscript |
| $r_0$ | Shaft radius, in. |
| $S$ | Imaginary root |
| $T$ | Kinetic energy, in-lbs |
| $T$ | Kinetic energy, in-lbs |
| $T$ | Rotor drive torque, in-lbs |
| $t$ | Time, sec |
| $U$ | Velocity, in/sec |
| $V$ | Potential energy, in-lbs |
| $V_m$ | Velocity of mass center, in/sec |
| $W$ | Rotor weight, lbs |
| $X$ | Horizontal coordinate |
| $X_0$ | Equilibrium coordinate |
| $X_1$ | Horizontal foundation deflection, in |
| $X_2$ | Horizontal shaft deflection, in |
| $Y$ | Vertical coordinate |
| $Y_0$ | Equilibrium coordinate |
| $Y_1$ | Vertical foundation deflection, in |
| $Y_2$ | Vertical shaft deflection, in |
| $Z$ | $X+iY$, Complex rotor deflection |
| $\alpha$ | $K_x/K_y$, Foundation flexibility ratio, dim. |
| $\alpha$ | Nonlinear stiffness coefficient |
| $\beta$ | Phase angle, deg |
| $\delta$ | Deflection of shaft centerline from bearing line of centers, in. |
| $\delta_b$ | Deflection of bearing center, in. |
| $\delta_m$ | $m_1/m_2$, Mass ratio, dim. |
| $\delta_r$ | Deflection of elastic center from bearing center, in. |
| $\delta_{st}$ | Rotor static deflection, in |
| $\epsilon,\epsilon_\mu$ | Displacement of rotor mass center from shaft elastic centerline, in |
| $\epsilon$ | Eccentricity ratio $e/c$, dim. |
| $\epsilon_{ij}$ | Strain tensor |
| $\eta$ | Bearing width, dim. |
| $\Phi$ | Moment of inertia, lb-sec$^2$-in |
| $\Lambda$ | $\frac{6\mu\omega}{p_a}(R/C)^2$, Compressibility parameter, dim |
| $\lambda$ | $P+i\Omega$, Complex root |
| $\mu$ | Absolute viscosity, lb-sec/in$^2$ |
| $\mu_x$ | $D_2\left(\frac{\alpha}{\alpha+R}\right)^2$, Coefficient, rad/sec |
| $\mu_y$ | $D_2\left(\frac{1}{1+R}\right)^2$, Coefficient, rad/sec |
| $\nu$ | Kinematic viscosity |

219-720 O-66—15

| *Symbol* | *Definition* |
|---|---|
| $\nu_x$ | $D_1\left(\frac{\alpha}{\alpha+R}\right)^2$, Coefficient, rad/sec |
| $\nu_y$ | $D_1\left(\frac{R}{1+R}\right)^2$, Coefficient, rad/sec |
| $\sigma$ | Squeeze film number |
| $\sigma_{ij}$ | Stress tensor |
| $\sigma_z$ | Stress, lb/in$^2$ |
| $\phi$ | Precession angle, deg |
| $\Omega$ | Angular velocity, rad/sec |
| $\omega$ | Rotor angular velocity, rad/sec |
| $\omega_{bf}$ | Critical speed for backward precession, rad/sec |
| $\omega_{cf}$ | Critical speed for forward precession, rad/sec |
| $\omega_{CR}$ | Rotor critical speed, rad/sec |
| $\omega_{CR_0}$ | Rotor natural resonance frequency on rigid supports, rad/sec |
| $\omega_{cx}$ | Natural system resonance frequency for $X$-direction, rad/sec |
| $\omega_{cy}$ | Natural system resonance frequency for $Y$-direction, rad/sec |
| $\omega_P$ | Rotor precession speed, rad/sec |
| $\omega_S$ | Rotor stability threshold speed, rad/sec |

# References


1. BAKER, J. G.: Self-Induced Vibrations. *Trans. ASME*, Vol. 55, 1933, pp. 5–13.
2. BISHOP, R. E. D.: The Vibration of Rotating Shafts. *J. Mech. Eng. Sci.*, Vol. 1, June 1959, pp. 50–65.
3. BISHOP, R. E. D.; AND JOHNSON, D. C.: Modes of Vibration of a Certain System Having a Number of Equal Frequencies. *J. Appl. Mech.*, 1956, p. 379.
4. BOEKER, G. F.; AND STERNLICHT, B.: Investigation of Translatory Fluid Whirl in Vertical Machines. *Trans. ASME*, Vol. 78, 1956, pp. 13–20.
5. CASTELLI, V.; AND ELROD, H. G.: Solution of the Stability Problem for 360° Self-Acting, Gas-Lubricated Bearings. ASME Paper No. 64–LUBS–10, 1964.
6. CHENG, H. S.: The Dynamics of the Infinitely Long, Self-Acting Gas Lubricated Journal Bearing Under a Steady Load. Ph. D. thesis, Univ. of Pennsylvania, 1961.
7. CHENG, H. S.; AND TRUMPLER, P. R.: Stability of the High Speed Journal Bearing Under Steady Load. *Trans. ASME, J. Eng. Ind.*, Vol. 85, 1963, p. 274.
8. CHENG, H. S.; AND PAN, C. H. T.: Stability Analysis of Gas-Lubricated, Self-Acting Plain, Cylindrical, Journal Bearings of Finite Length Using Galerkin's Method. ASME Paper No. 64–LUBS–5, 1964.
9. CHREE, C.: Whirling and Transverse Vibrations of Rotating Shafts. *Phil. Mag.*, Series 6, Vol. 37, 1904, p. 304.
10. COLE, J. A.; AND KERR, J.: Observations on the Performance of Air Lubricated Bearings. Paper 95, Hydrodynamic Lubrication Conference on Lubrication and Wear (London), Oct. 1957, The Inst. of Mech. Eng.
11. CONSTANTINESCU. V. N.: Dynamic Stability of Gas-Lubricated Bearings. *Rev. Mecan. Appl.*, Vol. 4, 1959, pp. 627–642.
12. DOWNHAM, E.: Theory of Shaft Whirling. *Engineer*, London, Vol. 204, 1957, pp. 518, 552, 588, 624, 660.
13. DUNKERLEY, S.: On the Whirling and Vibration of Shafts. *Phil. Trans. A*, Vol. 185, 1894, p. 279.
14. EHRICH, F. F.: Shaft Whirl Induced by Rotor Internal Damping. *J. Appl. Mech.*, June 1964, pp. 279–282.
15. ELROD, H. G., JR.; AND MALANOSKI, S. B.: Theory and Design Data for Continuous Film Self-Acting Journal Bearings of Finite Length. *The Franklin Institute Interim Report*, No. I–A2049–13, 1960.
16. ELWELL, R.: Energy Theory of Half-Frequency Whirl. Technical Brief, *Trans. ASME, J. Basic Eng.*, Sept. 1961, pp. 478–480.
17. FILON, C.; AND JESSOP: On the Stress-Optical Effect in Transparent Solids Strained Beyond the Elastic Limit. *Proc. Roy. Soc. A*, 1922, pp. 105–169.
18. FISCHER, G. K.; CHERUBIM, J. L.; AND DECKER, O.: Some Static and Dynamic Characteristics of High Speed Shaft Systems Operating With Gas-Lubricated Bearings. *Proceedings of First International Symposium on Gas-Lubricated Bearings*, ONR ACR–49, Washington, Oct. 26–28, 1959, pp. 383–417.
19. FISCHER, G. K.; CHERUBIM, J. L.; AND FULLER, D. D.: Some Instabilities and Operating Characteristics of High-Speed, Gas-Lubricated Journal Bearings. ASME Paper No. 58A–231.

20. FRITH, J.; AND BUCKINGHAM, F.: The Whirling of Shafts. *J. Inst. Elec. Engrs.*, Vol. 62, 1924, p. 107.
21. Gas Bearing Conference, Univ. of Southampton, England, 1963.
22. GREEN, R. B.: Gyroscopic Effects on the Critical Speed of Flexible Rotors. *J. Appl. Mech.*, Dec. 1948.
23. GROSS, W. A.: Investigation of Whirl in Externally Pressurized Air-Lubricated Journal Bearings. *Trans. ASME, J. Basic Eng.*, Mar. 1962, pp. 132–138.
24. GUENTHER, T. G.; AND LOVEJOY, D. C.: Analysis for Calculating Lateral Vibration Characteristics of Rotating Systems With Any Number of Flexible Supports. Part 2—Application of the Method of Analysis. *Trans. ASME, J. Appl. Mech.*, Vol. 83, pp. 591–600.
25. GUNTER, E. J.; HINKLE, J. G.; AND FULLER, D. D.: The Application of Gas-Lubricated Bearings to High Speed Turbo-Machinery. *The Franklin Institute Report*, No. Q–A2392–3–6, AT(30–1)–2512, Mod. No. 3, Aug. 1962.
26. GUNTER, E. J.; AND FULLER, D. D.: Recent Progress on the Development of Gas-Lubricated Bearings for High-Speed Rotating Machinery. *Proceedings of the USAF Aerospace Fluids and Lubricants Conference*, Sept. 1963, pp. 487–508.
27. GUNTER, E. J.; CASTELLI, V.; AND STEVENSON, C. H.: Steady-State Characteristics of Gas-Lubricated Self-Acting, Partial-Arc Journal Bearings of Finite Width. *Trans. ASLE*, Vol. 6, 1963.
28. GUNTER, E. J.; HINKLE, J. G.; AND FULLER, D. D.: The Effects of Speed, Load, and Film Thickness on the Performance of Gas-Lubricated, Tilting-Pad Journal Bearings. *Trans. ASLE*, Vol. 7, 1964, pp. 353–365.
29. HAGG, A. C.: The Influence of Oil Film Journal Bearings on the Stability of Rotating Machines. *J. Appl. Mech.*, Vol. 68, 1946, p. 211.
30. HAGG, A. C.; AND WARNER, P. C.: Oil Whip of Flexible Rotors. *Trans. ASME*, Oct. 1953, pp. 1339–1344.
31. HARRISON, W. J.: The Hydrodynamical Theory of Lubrication With Special Reference to Air As Lubricant. *Trans. Cambridge Phil. Soc.*, Vol. 22, 1913, p. 39.
32. HOMES, R.: Oil-Whirl Characteristics of a Rigid Rotor in 360° Journal Bearings. *Proc. Inst. Mech. Engrs.*, Vol. 177, No. 11, 1963, pp. 291–307.
33. HORI, Y.: Theory of Oil Whip. *J. Appl. Mech.*, Vol. 26, *Trans. ASME*, Series E, Vol. 81, 1959, p. 189.
34. HARVAY, G.; AND ARMONDROYD, J.: Appropriate Lumped Constants of Vibrating Shaft Systems. *Trans. ASME, J. Appl. Mech.*, Vol. 65, 1943, p. 220, and (Discussion), Vol. 67, 1945, p. 55.
35. HOWLAND, R. C. J.: The Vibrations of Revolving Shafts. *Phil. Mag.*, Series 7, Vol. 12, No. 76, Aug. 1931, pp. 297–311.
36. HULL, E. H.: Oil-Whip Resonance. *Trans. ASME*, Vol. 80, 1958, pp. 1490–1496.
37. HUMMEL, C. H.: Kritische Drehzahlen als Folge der Nachgiebigkeit des Schmiermittels im Lager. *Forschungsarbeiten*, V.D.I., 1926, No. 287.
38. HURWITZ, A.: Über die Bedingungen unter welchen Gleichung Nur Wurzeln mit negativen rellen Theilen besitzt. *Math. Ann.*, Vol. 46, 1895, pp. 273–284.
39. JACKSON, A. S.: Analog Computation. McGraw-Hill, 1960.
40. JEFFCOTT, H. H.: The Lateral Vibration of Loaded Shafts in the Neighbourhood of a Whirling Speed—The Effect of Want of Balance. *Phil. Mag.*, Series 6, Vol. 37, 1919, p. 304.
41. JOHNSON, D. C.: Forced Vibration of a Rotating Elastic Body. *Aircraft Eng.*, Vol. 24, 1952, p. 271.
42. JOHNSON, D. C.: Free Vibration of a Rotating Elastic Body. *Aircraft Eng.*, Vol. 24, 1952, p. 234.
43. JOHNSON, D. C.: Apparatus for Demonstrating Shaft Whirl. *Engineering*, London, Vol. 278, 1954, p. 266.

44. JOHNSON, D. C.: Synchronous Whirl of Vertical Shaft Having Clearance in One Bearing. *J. Mech. Eng. Sci.*, Vol. 4N1, Mar. 1962, pp. 85–93.
45. KANE, T. R.: An Addition to the Theory of Whirling. *Trans. ASME, J. Appl. Mech.*, Vol. 83, 1961, pp. 383–386.
46. KERR, J: Air Lubricated Journal Bearings at High Compressibility Numbers. *Inst. Mech. Engrs.*, Paper No. 5 of eight papers on nonconventional lubricants, 1962.
47. KIMBALL, A. T.: Internal Friction Theory of Shaft Whirling. *Gen. Elec. Rev.*, Vol. 27, 1924, p. 244.
48. KIMBALL, A. T.: Measurement of Internal Friction in a Revolving Deflected Shaft. *Gen. Elec. Rev.*, Vol. 28, 1925, p. 554.
49. KIMBALL, A. L.: Internal Friction as a Cause of Shaft Whirling. *Phil. Mag.*, Vol. 49, 1925, pp. 724–727.
50. KIMBALL, A. L.; AND HULL, E. H.: Vibration Phenomena of a Loaded Unbalanced Shaft While Passing Through Its Critical Speed. *Trans. ASME*, Vol. 47, 1925, pp. 673–698.
51. KIMBALL, A. L.; AND LOVELL, D. E.: Internal Friction in Solids. *Trans. ASME*, Vol. 48, 1926, p. 479.
52. KORN, G. A.; AND KORN, T. M.: Electric Analog Computers, 2d edition, McGraw-Hill, 1956.
53. KOROVCHINSKII, M. V.: Stability of Position of Equilibrium of a Journal on an Oil Film. *Friction and Wear in Machinery*, Vol. 11, 1956, pp. 248–305.
54. KUSHUL', M. Y.: The Self-Induced Oscillations of Rotors. (Trans. from Russian.) Consultants Bureau, New York, 1964.
55. LARSON, R. H.; AND RICHARDSON, H. H.: A Preliminary Study of Whirl Instability for Pressurized Gas Bearings. *Trans. ASME*, Paper No. 61–WA–67, 1962.
56. LEWIS, F. M.: Vibration During Acceleration Through a Critical Speed. *Trans. ASME*, Vol. 54, 1932, pp. 253–261.
57. LINN, F. C.; AND PROHL, M. A.: The Effect of Flexibility of Support Upon the Critical Speeds of High-Speed Rotors. *Trans. SNAME*, Vol. 59, 1951, pp. 536–553.
58. LUND, J. W.; AND STERNLICHT, B.: Rotor Bearing Dynamics With Emphasis on Attenuation. *Trans. ASME, J. Basic Eng.*, Dec. 1962, pp. 491–502.
59. MARTIN, F. A.: Steady-State Whirl in Journal Bearings for a Vertical Flexible Rotor System. ASME Paper No. 63–LUBS–8.
60. MATSCH, L. A.: Tilting Pad Gas Bearing Test Program Results. Program review of NASA Contract NAS 3–2778′ APS–5055–R2, AiResearch Co., Mar. 1964.
61. MCCANN, R. A.: Stability of Unloaded Gas-Lubricated Bearings. *Trans. ASME, J. Basic Eng.*, Vol. 85, 1963, pp. 513–518.
62. MORRIS, J.: Impact of Bearing Clearances on Shaft Stability. *Aircraft Eng.*, Vol. 29, 1957, p. 382.
63. NEWKIRK, B. L.: Shaft Whipping. *Gen. Elec. Rev.*, Vol. 27, 1924, p. 169.
64. NEWKIRK, B. L.: Varieties of Shaft Disturbances Due to Fluid Films in Journal Bearings. *Trans. ASME*, Vol. 78, 1956, pp. 985–988.
65. NEWKIRK, B. L., AND TAYLOR, H. D.: Shaft Whipping Due to Oil Action in Journal Bearing. *Gen. Elec. Rev.*, Vol. 28, 1925, pp. 559–568.
66. NEWKIRK, B. L.; AND GROBEL, L. P.: Oil Film Whirl—A Nonwhirling Bearing. *Trans. ASME*, Vol. 56, 1934.
67. NEWKIRK, B. L.; AND LEWIS, J. F.: Oil Film Whirl—An Investigation of Disturbances Due to Oil Films in Journal Bearings. *Trans. ASME*, Jan. 1956, pp. 21–27.
68. ORBECK, F.: Theory of Oil Whip for Vertical Rotors Supported by Plain Journal Bearing. *Trans. ASME*, Oct. 1958, pp. 1497–1502.
69. PAN, C. H. T.; AND STERNLICHT, B.: Comparison Between Theories and Experiment for the Threshold of Instability of Rigid Rotor in Self-Acting Plain-Cylindrical Journal Bearings. *Trans. ASME, J. Basic Eng.*, June 1964, pp. 321–327.

70. PARZEWSKI, J.; AND CAMERON, A.: Oil Whirl of Flexible Rotors. *Proc. Inst. Mech. Engrs.* (London), Vol. 176, 1962, p. 523.
71. PESTEL, VON E.: Beitrag Zur Ermittlung der Hydrodynamischen Dämpfungs und Federeigenschaften von Gleitlagern. *Ingenieur—Archiv* XXII Band Drittes Heft, 1954, pp. 147–155.
72. PINKUS, O.: A Note on Oil Whip. *Trans. ASME, J. Appl. Mech.*, Vol. 75, 1953, p. 450.
73. PINKUS, O.: Experimental Investigation of Resonant Whip. *Trans. ASME*, Vol. 78. 1956, pp. 975, 983.
74. PINKUS, O.; AND STERNLICHT, B.: Theory of Hydrodynamic Lubrication. McGraw-Hill, New York, 1961.
75. PORITSKY, H.: Contribution to the Theory of Oil Whip. *Trans. ASME*, Aug. 1953, pp. 1153–1161.
76. POWELL, J. W.: Unbalance Whirl of Rotors Supported in Gas Journal Bearings. *The Engineer*, July 26, 1963, pp. 145–146.
77. PROHL, M. A.: A General Method for Calculating Critical Speeds of Flexible Rotors. *Trans. ASME*, Vol. 67, 1945, *J. Appl. Mech.*, Vol. 12, p. A–142.
78. RANKINE, W. A.: On the Centrifugal Force of Rotating Shafts. *Engineer*, London, Vol. 27, 1869, p. 249.
79. REDDI, M. M.; AND TRUMPLER, P. R.: Stability of the High-Speed Journal Bearing Under Steady Load—I. The Incompressible Film. *Trans. ASME, J. Eng. Ind.*, Vol. 84, 1962, pp. 351–358.
80. RENTZEPIS, G. M.; AND STERNLICHT, B.: On the Stability of Rotors in Cylindrical Journal Bearings. *Trans. ASME, J. Basic Eng.*, Dec. 1962, pp. 521–532.
81. REYNOLDS, O.: On the Theory of Lubrication and Its Application to Mr. Towers' Experiments. *Phil. Trans. Soc. London*, Vol. 177, 1886, pp. 157–234.
82. ROBERTSON, D.: Whirling of a Journal in a Sleeve Bearing. *Phil. Mag.*, Series 7, Vol. 15, 1933, pp. 113–130.
83. ROBERTSON, DAVID: Whirling of a Shaft With Skew Stiffness. *Engineer*, Vol. 156, 1933, pp. 152, 179, 213.
84. ROBERTSON, D.: The Whirling of Shafts. *Engineer*, London, Vol. 158, 1934, pp. 216, 228.
85. ROBERTSON, D.: Transient Whirling of a Rotor. *Phil. Mag.*, Series 7. Vol. 20, 1935, p. 793.
86. ROBERTSON, D.: Hysteretic Influences on the Whirling of Rotors. *Proc. Inst. Mech. Engrs.* (London), Vol. 131, 1935, p. 513.
87. ROGERS, C.: On the Vibration and Critical Speeds of Rotors. *Phil. Mag.*, Series 6, Vol. 44, July 1922, No. 259.
88. ROUTH, E. J.: A Treatise on the Stability of a Given State of Motion. Macmillan Co.
89. SALJI, ERNST: Self-Excited Vibrations of Systems With Two Degrees of Freedom. *Trans. ASME*, 1956, p. 737.
90. SHAWKI, G. S. A.: Whirling of a Journal Bearing Experiment Under No Load Conditions. *Engineering*, Vol. 179, 1955, pp. 243–246.
91. SIMONS, E. M.: The Hydrodynamic Lubrication of Cyclically Loaded Bearings. *Trans. ASME*, Vol. 72, 1950, p. 805.
92. SIXSMITH, H.; AND WILSON, W. A.: The Theory of Stable High-Speed Externally Pressurized Gas-Lubricated Bearing. *J. Res. Natl. Bur. Std.—C. Eng. and Inst.*, Vol. 68C, No. 2, Apr.–June 1964.
93. SMITH, D. M.: The Motion of a Rotor Carried by a Flexible Shaft in Flexible Bearings. *Proc. Roy. Soc.* (London), Series A, Vol. 142, 1933, pp. 92–118.
94. SODERBERG, C. R.: On Subcritical Speeds of Rotating Shafts. *Trans. ASME, J. Appl. Mech.*, Vol. 54, No. 2, May 30, 1932, pp. 45–50 (and Discussion, pp. 50–52).

95. STAHLUTH, P. H.: Hybrid Gas Bearings for Better Stability. *Prod. Eng.*, Vol. 32, Apr. 10, 1961, pp. 56–59.
96. STERNLICHT, B.: Elastic and Damping Properties of Cylindrical Journal Bearings. *J. Basic Eng.*, June 1959, pp. 101–108.
97. STERNLICHT, B. H.; PORITSKY, H.; AND ARWAS, E.: Dynamic Stability Aspects of Compressible and Incompressible Cylindrical Journal Bearings. *First International Gas Bearings Symposium*, ONR ACR–49, Washington, D.C., Oct. 26–28, 1959, pp. 119–160.
98. STERNLICHT, B.; AND ELWELL, R. C.: Synchronous Whirl in Plain Journal Bearings. ASME Paper No. 62–LUBS–19.
99. STODOLA, A.: Kritische Wellenstörung infolge der Nachgiebigkeit des Olpolsters im Lager. *Schweiz. Bauzeitung*, 1925, Vol. 85, p. 265.
100. STODOLA, A.: Steam and Gas Turbines. McGraw-Hill, 1927.
101. STOKES, J. J.: Nonlinear Vibrations. Interscience Pub., Inc. 1957, pp. 202–222.
102. TANG, T. M.; AND TRUMPLER, P. R.: Dynamics of Synchronous-Precessing Turborotors With Particular Reference to Balancing, Part I—Theoretical Foundations. *Trans. ASME, J. Appl. Mech.*, Vol. 31, Mar. 1964, pp. 115–122.
103. TAYLOR, H. D.: Shaft Behaviour at Critical Speed. *Gen. Elec. Rev.*, Vol. 32, 1929, pp. 194–200.
104. TAYLOR, H. D.: Critical Speed Behavior of Unsymmetrical Shafts. *Trans. ASME, J. Appl. Mech.*, Vol. 62, 1940, p. 71, and (Discussion) Vol. 63, 1941, p. 181.
105. TIMOSHENKO, S.: Vibration Problems in Engineering. 3d edition, D. Van Nostrand Co., 1955, pp. 290–294.
106. TIPEI, N.: La Stabilite due Mouvement Dans Les Paliers A Charge Dynamique. *Revue de Mecanique Appliquee*, Tome 1, 1956, No. 2, pp. 115–122.
107. TONDL, A.: Experimental Investigations of Self-Excited Vibrations of Rotors Due to the Action of Lubrication Oil Film in Journal Bearings. *Wear*, 5, 1962, pp. 136–137. (The National Research Institute of Heat Engineering, Prague, Czech.)
108. TONDL, A.: The Motion of a Journal Bearing in the Unstable Region of Equilibrium Position of the Center of the Journal. Proceedings, Ninth International Congress for Appl. Mech., 1957, pp. 95–107.
109. TRUMPLER, P. R.: Problems in Engineering Design. Univ. of Pennsylvania, 1964.
110. WHITLEY, S.; AND BOWHILL, A. J.: The Load Capacity and Half-Speed of Hydrodynamic Gas Journal Bearings. UKAEA.DEG, Report 199 (CA), 1960.
111. WILDMANN, M.: Experiments on Gas-Lubricated Journal Bearings. ASME Paper No. 56–LUB–8, 1956.

# Index

U.S. GOVERNMENT PRINTING OFFICE : 1966 OL—219-720